

**GEOLOGY, ALTERATION, AND LITHOGEOCHEMISTRY OF THE HOOD DEPOSITS,  
NUNAVUT, CANADA**

by © Hannah Klara Mills, B.Sc. (Hons). A Thesis submitted to the  
School of Graduate Studies in partial fulfillment of the requirements for the degree of

**Master of Science Department of Earth Sciences**

Memorial University of Newfoundland

**May, 2014**

St. John's

Newfoundland

**ABSTRACT**  
(150 word maximum)

This study concerns the Hood volcanogenic massive sulfide (VMS) deposits that are hosted by the ~2.68 Ga Amooga Booga volcanic belt in the northwestern Slave Craton, Nunavut, Canada. The deposits comprise a cluster of bimodal-mafic VMS Cu-Zn-Pb lenses and mineral occurrences. On the basis of crustally contaminated felsic and mafic rocks, the volcanism is interpreted to have occurred in a tectonic environment comparable to a modern continental marginal back-arc basin.

Geochemical study of the Hood volcanic rocks indicates controls on felsic petrogenesis such as fractionation temperature and interaction with the sialic basement have important implications for mineral prospectivity. Evidence for seafloor replacement style mineralization includes remnant host rock clasts within mineralized intervals and alteration in both the footwall and the hanging wall to mineralization. Vectors to mineralization at the Hood deposits include Na<sub>2</sub>O loss, Fe<sub>2</sub>O<sub>3</sub>, MgO and base metal gains and high principal component 1 scores proximal to mineralization

## ACKNOWLEDGEMENTS

This thesis has benefited from the assistance and support of many people. First and foremost, I would like to thank my supervisor, Dr. Stephen Piercey for his constant support, guidance, and encouragement. His excitement and passion for geology is infectious. I also thank Toby Rivers for being on my committee and reviewing this manuscript and Pam King for her help with laboratory work.

This project was supported throughout by MMG Resources Ltd. who allowed me to study the Hood deposits and provided the logistical support and expertise that made it possible. In particular, I would like to thank Trish Toole whose mentorship and help has been invaluable. Field assistance from Rob Lyght, Conor Mckinley and Thomas Buckland is also greatly appreciated.

Financial assistance was provided by a NSERC Alexander Graham Bell Graduate Scholarship, a Society of Economic Geologists Graduate Fellowship, and the Dr. Alfred K. Snelgrove Graduate Scholarship to the author. Additional funding was provided to Dr. Steve Piercey by MMG Resources Ltd., a NSERC Discovery Grant, and NSERC-Altius Industrial Research Chair funding by NSERC, Altius Resources Inc., and the Research and Development Corporation of Newfoundland and Labrador (RDC).

My time at Memorial University would not have been the same without my friends and colleagues, so thank you for many lunch-time chats, soccer-watching afternoons, and trivia nights. It has been a wonderful few years. I also thank my parents, Catherine and Barry, and my brother, Fergil, for their unfailing support, understanding and patience during the course of my studies, for fostering my love of science and the

natural world from a young age, and for reading me many stories about dinosaurs when I was a kid.



## TABLE OF CONTENTS

Abstract.....	ii
Acknowledgements.....	iii
Table of Contents.....	v
List of Figures.....	viii
List of Tables.....	xiv
List of Symbols, Nomenclature or Abbreviations.....	xv
Chapter 1: Introduction to the Hood volcanogenic massive sulfide deposits, Nunavut, Canada.....	1
1.1 Introduction and Purpose of Study.....	1
1.2 Regional Geological Overview.....	2
1.3 VMS Overview.....	5
1.4 Previous Work.....	6
1.5 Location and Access.....	7
1.6 Objectives.....	8
1.7 Methodology.....	9
1.7.1 Drill Core Logging and Sampling.....	9
1.7.2 Petrography.....	9
1.7.3 Lithogeochemistry.....	9
1.7.4 Short-Wave-Infrared Spectroscopy.....	10
1.8 Thesis Presentation.....	10
References.....	12

Chapter 2: Geology, alteration, and lithogeochemistry of the Hood Deposits, Nunavut, Canada.....	18
2.1 Abstract.....	18
2.2 Introduction.....	19
2.3 Regional Geology.....	21
2.4 Local Geological Setting.....	22
2.5 Stratigraphy and Setting of the Hood VMS Deposits.....	24
2.5.1 Hood 10 Lens.....	24
2.5.2 Hood 41 Lens.....	28
2.5.3 Hood 41A Lens.....	31
2.5.4 Hood 46, Hood 461, and Hood 462 Occurrences.....	35
2.6 Mineralization.....	37
2.6.1 Hood 10 Lens.....	37
2.6.2 Hood 41 Lens.....	37
2.6.3 Hood 41A Lens.....	38
2.6.4 Hood 46, Hood 461, and Hood 462 Occurrences.....	39
2.7 Lithogeochemistry.....	39
2.7.1 Sampling and Analytical Methods.....	39
2.7.2 Primary Immobile Element Lithogeochemistry.....	41
2.7.3 Mobile Element Lithogeochemistry.....	46
2.7.4 Principal Component Analysis.....	51
2.8 Discussion .....	54
2.8.1 Petrogenesis of the Hood VMS Deposits Host Rocks.....	54

2.8.2 Hydrothermal Alteration.....	58
2.8.3 Tectonic Setting and the Slave Craton.....	62
2.9 Conclusions.....	65
References.....	67
Chapter 3: Summary and Directions of Future Research.....	100
3.1 Summary.....	100
3.2 Directions of Future Research.....	102
References.....	103
Combined References.....	104
Appendix 1: Drill Logs.....	114
Appendix 2: Lithogeochemistry, mass change, fractionation curves, principal components, and principal component scores.....	170
Appendix 3: Vertical cross-sections from Hood 10 and Hood 41A depicting SWIR- spectroscopy results, mass change, and principal component analysis.....	260

## LIST OF FIGURES

**Figure 1-1:** Simplified Slave Craton geology (Stubley, 2005) and selected VMS deposits (Bleeker and Hall, 2007). Labeled basement complexes are the Central Slave Basement complex (CSBC), the Northern Slave Basement Complex (NSBC), and the Acasta gneiss. Labeled greenstone belts are the Amooga Booga volcanic belt (ABVB), Izok Lake volcanic belt (ILVB), Point Lake volcanic belt (PLVB), Yellowknife volcanic belt (YVB), the Cameron River volcanic belt (CRVB), and the Beaulieu River volcanic belt (BRVB).....16

**Figure 1-2:** Geology of the Hanikahimajuk Lake area and locations of Hood deposit lenses and mineral occurrences (Gebert, 1995).....17

**Figure 2-1:** Simplified Slave Craton geology (Stubley, 2005) and selected VMS deposits (Bleeker and Hall, 2007). Labeled basement complexes are the Central Slave Basement complex (CSBC), the Northern Slave Basement Complex (NSBC), and the Acasta gneiss. Labeled greenstone belts are the Amooga Booga volcanic belt (ABVB), Izok Lake volcanic belt (ILVB), Point Lake volcanic belt (PLVB), Yellowknife volcanic belt (YVB), the Cameron River volcanic belt (CRVB), and the Beaulieu River volcanic belt (BRVB).....76

**Figure 2-2:** Geology of the Hanikahimajuk Lake area and locations of Hood deposit lenses and mineral occurrences (Gebert, 1995).....77

<b>Figure 2-3:</b> Schematic diagrams of the Hood deposits lenses and mineral occurrences demonstrating the different stratigraphic settings.....	78
<b>Figure 2-4:</b> Vertical cross-section through the southern part of the Hood 10 lens based on drill intersections from drill holes H10-01, H10-02, and H10-11. Drill hole width is exaggerated for clarity and contacts in drill logs are not shown with true dip.....	79
<b>Figure 2-5:</b> Common lithologies of the Hood deposits. A) Amygduloidal basalt. B) Sinuous chilled margin on basalt flow intruding into mafic tuff. C) Quartz-eye rhyolite. D) Porcelain rhyolite. E) Rim granite. F) Mixed intrusive rock.....	80
<b>Figure 2-6:</b> Representative samples of common alteration for the Hood deposits. A) Sericite alteration of rhyolite. B) Strong pervasive chlorite alteration near mineralization. C) Selective sericite + chlorite spider web alteration of andesite-basalt. D) Patchy quartz alteration of quartz-eye dacite. E) Black chlorite alteration along fractures in rhyolite. F) Selective quartz alteration along foliation creating banding in grey dacite .....	81
<b>Figure 2-7:</b> Vertical cross-section through the centre of the Hood 41 lens based on drill intersections from drill holes H41-05 and H41-17. Drill hole width is exaggerated for clarity and contacts in drill logs are not shown with true dip.....	82

**Figure 2-8:** Vertical cross-section through the southeast end of the Hood 41A lens demonstrating abundant mafic and mixed volcanoclastic rocks based on drill intersections from drill holes H41A-01, H41A-02, and H41A-15. Drill hole width is exaggerated for clarity and contacts in the drill logs are not shown with true dip.....83

**Figure 2-9:** Vertical drill logs from the Hood 46, Hood 461, and Hood 462 occurrences with large packages of coherent felsic volcanic rocks but limited mineralization. Lateral distribution and drill log width are not to scale.....84

**Figure 2-10:** Mineralization types of the Hood deposits. A) Chalcopyrite stringers. B) Chalcopyrite in pyrrhotite with chlorite altered remnant host rock clasts. C) Fine pyrite bands in argillite. D) Buckshot pyrite in massive pyrrhotite, typically with interstitial sphalerite visible in thin section. E) Sphalerite and pyrite banding. F) Pyrite replacement within clasts and the matrix of a volcanic breccia.....85

**Figure 2-11:** Magmatic discrimination diagrams for the Hood deposits magmatic rock data. A) Zr/TiO<sub>2</sub> vs Nb/Y diagram (Pearce, 1996). B) La vs Yb diagram from Barrett and MacLean (1999).....86

**Figure 2-12:** Immobile element plots for the Hood deposits felsic magmatic rocks. A) Nb vs Y discrimination diagram (Pearce et al., 1984). B) Nb/Ta vs Zr/TiO<sub>2</sub>. C) (La/Yb)<sub>CN</sub> vs Yb<sub>CN</sub> plot for outlining felsic groupings (Hart et al., 2004, modified after Leshner et al., 1986). D) Zr/Ga vs Zr/TiO<sub>2</sub>. E) Zr/Y vs Al<sub>2</sub>O<sub>3</sub>/Zr. F) Zr/TiO<sub>2</sub> vs Al<sub>2</sub>O<sub>3</sub>/TiO<sub>2</sub>. .....87

**Figure 2-13:** Primitive mantle normalized extended multi-element plots of the felsic rocks of the Hood deposit (Sun and McDonough, 1989). A) Felsic suite A. B) Felsic suite B. C) Felsic suite C. D) Felsic and mixed tuff suite. E) Anomalous felsic signatures (altered). F) Granite core samples compared to outcrop samples from this study and Yamashita et al., (2000). Symbols as in Figure 2-12.....88

**Figure 2-14:** Tectonomagmatic discrimination diagrams for the Hood deposits mafic rocks. ARC-Arc-related basalts; BABB- Back-arc basin basalt; BON- Boninite; E-MORB- Enriched mid-ocean ridge basalt; IAT- Island-arc tholeiite; LOTI-Low-Ti tholeiite; OIB-Ocean island basalt; N-MORB-normal mid-ocean ridge basalt. A) Ti-V diagram (Shervais, 1982). B) Th-Zr-Nb plot (Wood, 1980). C) Zr/Yb vs Nb/Yb diagram discriminating depleted- to enriched-mantle derived rocks (Pearce and Peate, 1995) with global values of OIB, N-MORB, and E-MORB (Sun and McDonough, 1989). D) Nb/Th vs La/Sm.....89

**Figure 2-15:** Primitive mantle normalized extended multi-element plots of the mafic rocks of the Hood deposit (Sun and McDonough, 1989). A) Type I mafic rocks. B) Type II mafic rocks. C) Type III mafic rocks. D) Type IV mafic rocks. Symbols as in Figure 2-14..... 90

**Figure 2-16:** Alteration box plot of the chlorite-carbonate-pyrite index vs the Hashimoto alteration index (AI) for the rocks of the Hood deposits (Large et al., 2001b).....91

**Figure 2-17:** A)  $\text{Al}_2\text{O}_3$  vs Th plot with the least altered fractionation curve and mass loss and gain trends for Hood samples. B) Exponential fit fractionation line for Zr of least altered samples demonstrating two Zr vs Th trends. C) Exponential fit fractionation line for  $\text{SiO}_2$  of least altered samples. D) Exponential fit fractionation line for MgO of least altered samples. Symbols as in Figure 2-11.....92

**Figure 2-18:** Mass change plots for Hood deposits. A)  $\Delta\text{K}_2\text{O}$  vs  $\Delta\text{Na}_2\text{O} + \Delta\text{CaO}$ . B)  $\Delta\text{SiO}_2$  vs  $\Delta\text{Fe}_2\text{O}_3 + \Delta\text{MgO}$ . C) Data array with selected element mass change plotted against  $\Delta\text{K}_2\text{O}$ . D) Data array with selected element mass change plotted against  $\Delta\text{Fe}_2\text{O}_3 + \Delta\text{MgO}$ . Symbols as in Figure 2-11.....93

**Figure 2-19:** Hood 41A cross-sections comparing A) interpreted stratigraphy based on drill logs to B) 3-D gridding of Zn mass change, C) 3-D gridding of  $\text{Na}_2\text{O}$  mass change and D) 3-D gridding of principal component 1 scores.....95

**Figure 2-20:** Principal component scores for Hood samples with interpreted trends. A) PC 4 vs PC 1 accounts for 66.5% of the total variation in the dataset. B) PC 5 vs PC 2 accounts for 13.5% of the total variation in the dataset. Symbols as in Figure 2-11.....96

**Figure A1-1:** Hood deposits drill logs recording lithology and alteration.....116



<b>Figure A3-1:</b> Hood 10 cross-section through the southern end of the lens demonstrating the distribution of alteration minerals based on SWIR spectroscopy.....	261
--	-----

<b>Figure A3-2:</b> Hood 41A cross-section through the southeast end of the lens demonstrating the distribution of alteration minerals based on SWIR spectroscopy.....	262
--	-----

<b>Figure A3-3:</b> Hood 10 cross-section comparing stratigraphy to 2-D slices of modelled element mass change.....	263
---	-----

<b>Figure A3-4:</b> Hood 41A cross-sections comparing stratigraphy to 2-D slices of modelled element mass change.....	271
---	-----

## LIST OF TABLES

<b>Table 2-1:</b> Lithology, alteration, and mineralization summary table.....	97
<b>Table 2-2:</b> Mass change summary table divided by felsic and mafic rock types and deposits; if only a single sample of a rock type occurred no range is given.....	98
<b>Table A2-1:</b> Geochemical data for the rocks of the Hood deposits.....	171
<b>Table A2-2:</b> Major element mass change based on the MacLean (1990) multiple precursor method, SWIR mineralogy, and alteration indexes.....	234
<b>Table A2-3:</b> Calculated best fit fractionation curves for least altered elements on element vs Th plots.....	250
<b>Table A2-4:</b> Principal Component Analysis eigenvalues and rescaled eigenvectors.....	251
<b>Table A2-5:</b> Principal component scores for samples and elements.....	253

## **LIST OF SYMBOLS, NOMENCLATURE, AND ABBREVIATIONS**

ABVB – Amooga Booga volcanic belt

BABB – back-arc basin basalt

BIF – banded iron formation

BRVB – Beaulieu River volcanic belt

CR-BR – Cameron River- Beaulieu River volcanic belt

CRVB – Cameron River volcanic belt

CSBC – Central Slave Basement Complex

CSCG – Central Slave Cover Group

E-MORB – enriched mid-ocean ridge basalt

EM/MAG – electromagnetic/magnetic

HFSE – high field strength elements

HREE – heavy rare earth elements

ICP-AES – inductively coupled plasma atomic emission spectrometry

ICP-MS – inductively coupled plasma mass spectrometry

ILVB – Izok Lake volcanic belt

LFSE – low field strength elements

LREE – light rare earth elements

MORB – mid-ocean ridge basalt

NSBC – Northern Slave Basement Complex

OIB – ocean island basalt

PC – principal component

PCA – principal component analysis

PLVB – Point Lake volcanic belt

REE – rare earth elements

SWIR spectroscopy – short-wave-infrared spectroscopy

VMS – volcanogenic massive sulfide

YVB – Yellowknife volcanic belt

# **Chapter 1: Introduction to the Hood volcanogenic massive sulfide deposits, Nunavut, Canada**

## **1.1 INTRODUCTION AND PURPOSE OF STUDY**

The Hood volcanogenic massive sulfide (VMS) deposits are located 425 km north of Yellowknife, Northwest Territories, in the Hanikahimajuk Lake area, Nunavut. The Hood deposits (total resource of all lenses in the deposits – 3.2Mt @ 2.6% Cu and 3.6% Zn; not NI 43-101 compliant) are bimodal-mafic Cu-Zn VMS deposits that remain poorly understood despite intermittent exploration for the past 40 years. The deposits consist of a cluster of lenses over a ~10 km<sup>2</sup> area hosted by the late Archean Amooga Booga volcanic belt (ABVB) in the west-central part of the Slave craton (Gebert, 1995).

Study of the Hood deposits since the 1970s has been limited and largely confined to internal company reports. This thesis was undertaken in part because our better understanding of VMS systems since exploration in the 1980s and 1990s, and the use of high quality lithogeochemical data allows for a more refined reassessment of the Hood deposits, and also will provide general information and insight into this type of deposit elsewhere. Furthermore, studies of the ABVB and other greenstone belts within the Slave Craton have provided information relevant to the tectonic environment in which the VMS deposits formed and can be evaluated in this study. This thesis provides a characterization of the volcanic stratigraphy, lithogeochemistry, and hydrothermal alteration of the host rocks of the Hood deposits, and attempts to place them in a stratigraphic and tectonic framework within the Slave Craton.

## 1.2 REGIONAL GEOLOGICAL OVERVIEW

The Slave Craton in the northern Canada consists of supracrustal rocks, principally linear greenstone belts composed of mafic and felsic metavolcanic rocks, and associated metasedimentary sequences, and granitoid rocks that include both basement gneisses to the supracrustal rocks and younger granitoid batholiths and intrusions (Fig. 1-1) (Mortensen et al., 1988; Padgham and Fyson, 1992; Isachsen and Bowring, 1994; Bleeker and Hall, 2007; Helmstaedt and Pehrsson, 2012). Bleeker and Hall (2007) and Helmstaedt and Pehrsson (2012) summarize much of the previous work in the Slave Craton. The basement gneisses of the Slave craton belong to the 4.0-2.9 Ga Central and Northern Slave Basement Complex (CSBC and NSBC; Fig. 1), which underlies the western, central, and northern parts of the craton and have a long and complex geological history (Bleeker et al., 1999a; Bleeker et al., 1999b; Davis et al., 2003; Ketchum et al., 2004; Helmstaedt and Pehrsson, 2012). The CSBC and NSBC are included in the Central Slave Superterrane (CSST) of Helmstaedt and Pehrsson (2012), however, the former terminology will be maintained in this thesis. The CSBC includes the Acasta gneiss which, like much of the CSBC, is primarily composed of dioritic and tonalitic gneisses (Bleeker et al., 1999b).

In the southern and central Slave Craton, the CSBC is overlain by the Yellowknife Supergroup, a thick package of supracrustal rocks deposited unconformably on the CSBC at ~2.9 Ga with sedimentation continuing episodically until cratonization ca. 2.59 Ga (Bleeker and Hall, 2007). In the text that follows, metavolcanic and metasedimentary rocks metamorphosed to greenschist and amphibolite facies are described by their

inferred protoliths. The base of the Yellowknife Supergroup is marked by the Central Slave Cover Group (CSCG), a thin sequence (of a few hundred metres), principally consisting of quartzite, banded iron formations (BIF) and mafic volcanic rocks, that lies with angular unconformity on the CSBC (Bleeker et al., 1999b). Overlying the CSCG is a thick package (up to 8 km thick) of ca. 2.73-2.70 Ga tholeiitic basalts, with minor komatiite and rhyolite, known as the Kam Group in the Yellowknife volcanic belt (Helmstaedt and Padgham, 1986; Fyson and Helmstaedt, 1988; Bleeker et al., 1999b; Cousens, 2000; Bleeker and Hall, 2007). The Kam Group is overlain by the transitional to calc-alkalic rocks of the Banting Group, which consists of basalt with abundant felsic and intermediate volcanic rocks ranging in age from 2687 to 2660 Ma (Mortensen et al., 1988; Isachsen and Bowring, 1994; Cousens et al., 2002; Bleeker and Hall, 2007).

Overlying the volcanic sequences are turbiditic greywackes and mudstones of the Burwash Basin that extend across the entire Slave Craton (Bleeker and Hall, 2007). The deposition of these rocks has been dated between ca. 2.68 Ga (oldest detrital zircons) to ca. 2.66 Ga (Bleeker and Hall, 2007). A second, younger, turbidite sequence in the western and north-western part of the Slave is distinguished from the Burwash turbidites by the presence of 2.63 Ga detrital zircons from the Defeat Suite plutons (see below; Bleeker and Hall, 2007).

Craton-wide plutonism post-dated the sedimentary rocks of the Burwash Basin and occurred in two phases: the 2.63-2.61 Ga Defeat Suite plutonism and the 2.59-2.58 Ga plutonism. The Defeat Suite represents the earlier phase of plutonism and is diachronous across the Slave Craton (Davis and Bleeker, 1999; Davis et al., 2003). Defeat suite-type plutons in the western, central and northern parts of the province are 15-25

m.y. younger than the plutons of the southeast corner of the craton (Davis and Bleeker, 1999; Davis et al., 2003). Davis and Bleeker (1999) suggested this diachronous pattern may be related to the NW migration of a subduction-related arc. The younger phase of plutonic activity occurred ca. 2.59 to 2.58 Ga and is inferred to represent the final cratonization period of the Slave Craton (Bleeker and Hall, 2007). The timing of intrusion of the two-mica granites and K-feldspar granites of this event are synchronous across the craton (Davis and Bleeker, 1999; Davis et al., 2003).

Characterization of the regional stratigraphy of the Slave Craton greenstone belts is largely based on the Yellowknife volcanic belt (YVB) and the Cameron River volcanic belt (CRVB) at the southern edge of the Slave Craton (Fig. 1-1) (Helmstaedt and Padgham, 1986; Fyson and Helmstaedt, 1988; Bleeker et al., 1999b). However, questions remain as to the suitability of the YVB as a model for regional Slave Craton stratigraphy as there are significant differences between it and other Slave Craton belts (MacLachlan and Helmstaedt, 1995; Cousens et al., 2002, Helmstaedt and Pehrsson, 2012). Felsic volcanic rocks belonging to Banting Group correlatives in these greenstone belts host VMS mineralization including the Izok Lake, Hackett River, Sunrise, Gondor, Kennedy Lake and High Lake deposits (Fig. 1-1) (Bleeker and Hall, 2007).

The ABVB is a northeast trending felsic-dominated extension of the mafic-dominated Point Lake volcanic belt (PLVB) (Fig.1-1) a N-S trending belt running along the western margin of the Slave Craton (Gebert, 1995). The Izok Lake volcanic belt (ILVB) is also an extension off of the PLVB (Gebert, 1995). The ABVB has also been referred to as the Takiyuak metavolcanic belt, and the south segment of the Takijuq supracrustal belt in older reports (Gill, 1977; Rockingham, 1979; Gebert, 1995).



In the Hanikahimajuk Lake area several localities of >3.0 Ga basement have been identified (Fig. 1-2) and the overlying ABVB supracrustal package is up to 10 km thick (Gebert, 1995; Jensen, 1995). The volcanic package in the area consists of tholeiitic mafic volcanic rocks grading into calc-alkaline felsic to intermediate volcanic rocks overlain by calc-alkaline mafic volcanic rocks (Jensen, 1995).

Development of a tectonic model for both the ABVB and the Slave Craton in general has been problematic. Neither an accretionary-collisional model nor an intracratonic rifting model can account for the geochemical characteristics of the ABVB (Jensen, 1995; Yamashita et al., 2000). The most recent model applied to the ABVB placed the formation of the greenstone belt in a modified back-arc basin tectonic setting after the model of MacLachlan and Helmstaedt (1995) (Yamashita et al., 2000). The MacLachlan and Helmstaedt (1995) model was developed for the Yellowknife and Cameron River volcanic belts and involves the rifting of the old gneissic basement resulting in the formation of oceanic crust followed by a reduction in extension which reduced the input of the juvenile depleted mantle and triggered calc-alkaline felsic to intermediate magmatism (MacLachlan and Helmstaedt, 1995). Nearby subduction subsequently produced the overlying calc-alkaline arc-like volcanism (MacLachlan and Helmstaedt, 1995; Yamashita et al., 2000).

### **1.3 VMS OVERVIEW**

Volcanogenic massive sulfide deposits are polymetallic sulfide lenses associated with contemporaneous submarine volcanism (Franklin et al., 1981; Ohmoto and Skinner, 1983; Franklin et al., 2005). The sulfide lenses form from the discharge of metal laden

hydrothermal fluids at or near the seafloor (Franklin et al., 2005; Galley et al., 2007). Hydrothermal cells are driven by the heat from subvolcanic intrusions and form when heated seawater rises along synvolcanic structures that focus the discharge, and cold seawater is drawn down to recharge the system through the surrounding rock (Franklin et al., 2005; Galley et al., 2007). Volcanogenic massive sulfide deposits have been extensively studied to understand the tectonic setting of the deposits and their genesis, and to understand secondary hydrothermal fluid-rock interactions effects (Leshner et al., 1986; Barrie et al., 1993; Hart et al., 2004; Piercey, 2011). The primary geochemistry of the volcanic rocks associated with VMS deposits helps identify the tectonic environment in which they formed (Leshner et al., 1986; Barrie et al., 1993; Barrett and MacLean, 1999; Hart et al., 2001; Piercey, 2011 and references therein). Alteration mineralogy and geochemistry identifies the consequences of fluid-rock interactions within the hydrothermal cell and can indicate proximity to mineralization (the centre of the system), making it particularly useful as a vectoring tool for VMS mineralization (Franklin et al., 1981; Gemmell and Large, 1992; Large et al., 2001; Doyle and Allen, 2003; Franklin et al., 2005).

#### **1.4 PREVIOUS WORK**

Prior to the discovery of the Hood deposits in the 1970s, the area had been mapped at a reconnaissance scale by the Geological Survey of Canada (GSC) in the late 1950s and was interpreted to be largely underlain by metasedimentary rocks (Fraser, 1960). The Hood 10 gossan was identified in 1972 by Bernard Laplante during exploration for Texasgulf (Heslop, 1973). Subsequent exploration included drilling,

surface mapping, soil geochemistry and electromagnetic/magnetic (EM-MAG) geophysical surveys until the late 1970s. During this period a Ph.D. and a M.Sc. thesis on the Hood deposits were completed (Gill, 1977; Rockingham, 1979).

Additional drilling and metallurgical testing were completed by Kidd Creek Mines Ltd. (formerly Texasgulf Canada Inc.) in 1981 and 1982 (Bruce, 1991). Falconbridge obtained the properties in the mid-1980s and did lithogeochemical surveys, re-logging of drill core, remapping and additional geophysical surveys in 1989 and 1990 (Bruce, 1991). The Hood deposits were purchased from Falconbridge Ltd. by Minnova in 1991 who, in conjunction with Metall Mining Corp., completed additional drilling in 1992 and 1993 (Thomas and Glenn, 1992, 1994).

Gebert (1995), Jensen (1995) and Yamashita et al. (2000) completed regional geological studies in the Hanikahimajuk Lake area. Geochronology of the area is based on U-Pb dating of zircon by Mortensen et al. (1988), Bowring (unpublished) and Yamashita et al. (2000). Samples from Hood 10 were included in the Slave Craton-wide lead isotopic study of Thorpe et al. (1992).

The property is currently held by MMG Resources Limited who completed a 2012 summer exploration program. This program included drilling of the Hood-10 lens, extensive lithogeochemical sampling of the core, downhole and surface geophysical surveys, and the collection of structural geological data.

## **1.5 LOCATION AND ACCESS**

The Hood deposits are located on the south side of the Hanikahimajuk Lake (Fig. 1-2). The deposit and the former Hood camp site are accessed by helicopter from the Izok

lake camp, ~45 km south of Hood. All historical drill core is stored in and around a metal building at the Hood Camp site on the north side of the lake. The area has widespread exposure of lichen-covered bedrock with vegetation and glacial sediment largely confined to creek gullies.

## 1.6 OBJECTIVES

Apart from internal company reports, studies of the Hood deposits and the surrounding area are few (e.g., Gill, 1977; Rockingham, 1979; Gebert, 1995; Jensen, 1995; Yamashita et al., 2000). The deposit itself has not been closely studied since the late 1970s. Application of modern lithogeochemistry tools and updated VMS deposit models allow for the deposit to be re-evaluated. In that context, the main research goals of this study are:

- clarification of the volcanic, plutonic, and hydrothermal facies and their stratigraphic relationships on a deposit scale through detailed core logging;
- characterization of lithological setting through petrography and lithogeochemistry;
- characterization of alteration assemblages through petrography, lithogeochemistry, and short-wave infrared (SWIR) spectroscopy; and
- assessment of the tectonic setting of the ABVB during the formation of the Hood deposits and how the ABVB relates to other greenstone belts of the Slave craton.

## **1.7 METHODOLOGY**

### **1.7.1 Drill Core Logging and Sampling**

Drill core logging and geochemical sampling of historically drilled diamond drill core were carried out over two summer field seasons in 2011 and 2012. Drill core logging was done at 1:500 scale. A total of 249 drill core samples were collected. The majority of these samples (229 samples) were cut in half, with half sent for geochemical analysis and half retained as reference hand samples. Samples of four ~1.5m sections of drill core and a single outcrop location were collected for U-Pb geochronology. Samples of sulfide mineralization were selected for thin sectioning and as reference hand samples.

### **1.7.2 Petrography**

Polished thin sections of 30 samples were made by Vancouver Petrographics. These samples were selected as representative of lithologies, alteration and sulfide mineralization. Petrographic analysis was done under transmitted, polarized, and reflected light to identify textures, mineralogy, and mineralization.

### **1.7.3 Lithogeochemistry**

A total of 229 drill core samples and one outcrop sample were analyzed for a 60 element suite of major and trace elements at ALS Minerals Laboratories (Vancouver, B.C.). Samples were chosen from throughout each drill hole to characterize primary geochemistry and secondary alteration geochemistry in a 3D framework. The samples were crushed in jaw crushers and pulverized in low chrome steel bowls. The samples were analysed for major elements ( $\text{SiO}_2$ ,  $\text{Al}_2\text{O}_3$ ,  $\text{Fe}_2\text{O}_3$ ,  $\text{CaO}$ ,  $\text{MgO}$ ,  $\text{Na}_2\text{O}$ ,  $\text{K}_2\text{O}$ ,  $\text{TiO}_2$ ,

MnO), base metals (Ag, Cu, Cd, Mo, Ni, Pb, Sc, Zn), C and S, for trace elements and REEs, and volatile elements (As, Bi, Hg, Sb, Se, Te). Major elements were determined by inductively coupled plasma atomic emission spectrometry (ICP-AES) following a lithium metaborate fusion and acid dissolution. Base metals were analyzed by ICP-AES after 4-acid digestion. Trace elements and REEs were analyzed by inductively coupled plasma mass spectrometry (ICP-MS) following lithium borate fusion and dissolution in acid. Carbon and sulfur were characterized by combustion furnace. The volatile elements were determined by ICP-MS after *aqua regia* dissolution.

#### **1.7.4 Short-Wave-Infrared Spectroscopy**

Short-wave-infrared (SWIR) spectroscopy was used to identify fine-grained alteration minerals such as sericite, chlorite and biotite, and variations in their respective compositions and relative abundances (Thompson et al., 1999). A TerraSpec<sup>TM</sup> mineral spectrometer with Hi-Brite Muglight was used to analyze the representative samples. RS<sup>3</sup> Spectral Acquisition software was used to calibrate the instrument and collect spectral data from each sample. Every twenty analyses optimization of the instrument was completed, a white reference was taken, and the spectra of two mineral standards were collected. Each sample was analyzed until the spectral reading stabilized (~2 to 4 minutes).

### **1.8 THESIS PRESENTATION**

This thesis consists of three chapters and supplemental appendices. Chapter 1 is an introductory chapter that presents the purpose and format of the thesis, the regional

geology, previous work in the thesis area, the location of the field area and description of the methods used during the study.

Chapter 2, the main body of the thesis, is a research manuscript intended for publication in a scientific journal. This chapter presents the stratigraphic reconstruction, the primary lithogeochemistry and the alteration geochemistry of the Hood deposits and frames these characteristics in both a regional and craton-wide tectonic setting.

Chapter 3 is a summary chapter that presents conclusions drawn from Chapter 2 and from additional evidence presented in the appendices, and directions for future research.

The appendices provide supplementary data including digitized drill logs of the re-logged holes and the complete set of geochemical data from sampling.

## References

- Barrett, T. J., and MacLean, W. H., 1999, Volcanic sequences, lithogeochemistry, and hydrothermal alteration in some bimodal volcanic-associated massive sulfide systems: *Reviews in Economic Geology*, v. 8, p. 101-131.
- Barrie, C. T., Ludden, J. N., and Green, T. H., 1993, Geochemistry of volcanic rocks associated with Cu-Zn and Ni-Cu deposits in the Abitibi Subprovince: *Economic Geology*, v. 88, p. 1341 – 1358.
- Bleeker, W., and Hall, B., 2007, The Slave craton: geological and metallogenic evolution, *in* Goodfellow, W. D., ed., *Mineral Deposits of Canada: A Synthesis of Major Deposit-types, District Metallogeny, the Evolution of Geological Provinces, and Exploration Methods*, Special Publication 5, Mineral Deposits Division, Geological Association of Canada, p. 849-879.
- Bleeker, W., Ketchum, J., and Davis, W., 1999a, The Central Slave Basement Complex, Part II: age and tectonic significance of high-strain zones along the basement-cover contact: *Canadian Journal of Earth Sciences*, v. 36, p. 1111-1130.
- Bleeker, W., Ketchum, J., Jackson, V., and Villeneuve, M., 1999b, The Central Slave Basement Complex, Part I: its structural topology and autochthonous cover: *Canadian Journal of Earth Sciences*, v. 36, p. 1083-1109.
- Bruce, C. S., 1991, Hood River Project # 708 - Report on the 1990 Field Program: Falconbridge Limited Company Report, p. 1-59.
- Cousens, B., Facey, K., and Falck, H., 2002, Geochemistry of the late Archean Banting Group, Yellowknife greenstone belt, Slave Province, Canada; simultaneous melting of the upper mantle and juvenile mafic crust: *Canadian Journal of Earth Sciences* v. 39, p. 1635-1656.
- Davis, W., and Bleeker, W., 1999, Timing of plutonism, deformation, and metamorphism in the Yellowknife Domain, Slave Province, Canada: *Canadian Journal of Earth Sciences*, v. 36, p. 1169-1187.
- Davis, W. J., Jones, A. G., Bleeker, W., and Grutter, H., 2003, Lithosphere development in the Slave craton: a linked crustal and mantle perspective: *Lithos*, v. 71, p. 575-589.
- Doyle, M. G., and Allen, R. L., 2003, Subsea-floor replacement in volcanic-hosted massive sulfide deposits: *Ore Geology Reviews*, v. 23, p. 183-222.



Fraser, J. A., 1960, North-central District of Mackenzie, Northwest Territories, Preliminary Map 18-1960, Geological Survey of Canada.

Franklin, J. M., Lydon, J. W., and Sangster, D. F., 1981, Volcanic-associated massive sulfide deposits, in Skinner, B. J., ed., Economic Geology 75th Anniversary Volume, p. 485-627.

Franklin, J. M., Gibson, H. L., Galley, A. G., and Jonasson, I. R., 2005, Volcanogenic Massive Sulfide Deposits, in Hedenquist, J. W., Thompson, J. F. H., Goldfarb, R. J., and Richards, J. P., eds., Economic Geology 100th Anniversary Volume: Littleton, CO, Society of Economic Geologists, p. 523-560.

Galley, A. G., Hannington, M., and Jonasson, I., 2007, Volcanogenic massive sulphide deposits, in Goodfellow, W. D., ed., Mineral Deposits of Canada: A Synthesis of Major Deposit-types, District Metallogeny, the Evolution of Geological Provinces, and Exploration Methods, Special Publication 5, Mineral Deposits Division, Geological Association of Canada, p. 141-161.

Gebert, J. S., 1995, Archean Geology of the Hanikahimajuk Lake Area, Northern Point Lake Volcanic Belt, West-Central Slave Structural Province, District of Mackenzie, N.W.T.: NWT EGS Open File p. 27.

Gill, J. W., 1977, The Takiyuak metavolcanic belt: Geology, geochemistry, and mineralization: Unpub. Ph.D. thesis, Carleton University, Ottawa, Ontario, Canada, 210 p.

Gemmell, J.B., Large, R.R., 1992, Stringer system and alteration zones underlying the Hellyer volcanic-hosted massive sulfide deposit, Tasmania, Australia: Economic Geology, v. 87, p. 620-649.

Hart, T.R., Gibson, H.L., Leshner, C.M., 2004, Trace element geochemistry and petrogenesis of felsic volcanic rocks associated with volcanogenic massive Cu-Zn-Pb sulfide deposits: Economic Geology, v. 99, p. 1003-1013.

Helmstaedt, H., and Padgham, W. A., 1986, A new look at the stratigraphy of the Yellowknife Supergroup at Yellowknife, N.W.T. – implications for the age of gold-bearing shear zones and Archean basin evolution: Canadian Journal of Earth Sciences, v. 23, p. 454-475.

Helmstaedt, H. H., and Pehrsson, S. J., 2012, Geology and Tectonic Evolution of the Slave Province – A Post-Lithoprobe Perspective in Percival, J. A., Cook, F. A., and Clowes, R. M., eds., Tectonic Styles in Canada: The Lithoprobe Perspective. Special Paper, Geological Association of Canada, p. 379-466.

Heslop, J. B., 1973, Hood River Project #94 - Report H-2: Geology of Area #46 - Grid "C": Private Report, p. 111.

Isachsen, C. E., and Bowring, S. A., 1994, Evolution of the Slave Craton: *Geology*, v. 22, p. 917-920.

Jensen, J. E., 1995, Geology, geochemistry and Nd isotopic study of the Hanikahimajuk Lake area, Slave Province, NWT: Unpub. M.Sc. Thesis, University of Alberta, Edmonton, Alberta.

Ketchum, J. W. F., Bleeker, W., and Stern, R. A., 2004, Evolution of an Archean basement complex and its autochthonous cover, southern Slave Province, Canada: *Precambrian Research*, v. 135, p. 149-176.

Large, R.R., Gemmell, J.B., Paulick, H., and Huston, D.L., 2001, The alteration box plot: a simple approach to understanding the relationships between alteration mineralogy and lithogeochemistry associated with VHMS deposits: *Economic Geology*, v. 96, p. 957-971.

Leshner, C. M., Goodwin, A. M., Campbell, I. H., and Gorton, M.P., 1986, Trace element geochemistry of ore-associated and barren felsic metavolcanic rocks in the Superior province, Canada: *Canadian Journal of Earth Sciences*, v. 23, p. 222-237.

MacLachlan, K., and Helmstaedt, H., 1995, Geology and geochemistry of an Archean mafic dyke complex in the Chan formation-basis for a revised plate-tectonic model of the Yellowknife greenstone-belt: *Canadian Journal of Earth Sciences*, v. 32, p. 614-630.

Mortensen, J. K., Thorpe, R. I., Padgham, W. A., King, J. E., and Davis, W. J., 1988, U-Pb zircon ages for felsic volcanism in the Slave Province, N.W.T., *Radiogenic Age and Isotope Studies: Report 2, Paper 88-2*, Geological Survey of Canada, p. 85-95.

Ohmoto, H., Skinner, B.J., 1983, The Kuroko and Related Volcanogenic Massive Sulfide Deposits: Introduction and Summary of New Findings In: Ohmoto H, Skinner BJ (eds) *The Kuroko and Related Volcanogenic Massive Sulfide Deposits*. pp 604.

Padgham, W. A., and Fyson, W. K., 1992, The Slave Province - A distinct Archean craton: *Canadian Journal of Earth Sciences*, v. 29, p. 2072-2086.

Piercey, S., 2011, The setting, style, and role of magmatism in the formation of volcanogenic massive sulfide deposits: *Mineralium Deposita*, p. 1-23.

Rockingham, C. J., 1979, Metamorphism and metal zoning of the Hood River-41 massive sulfide deposits, Slave Structural Province, N.W.T.: Unpub. M.Sc. thesis, University of Western Ontario, 125 p.

Thomas, D. A., and Glenn, D. G., 1992, 1992 Summary Report: Geology, Whole Rock Chemistry, Pulse EM, and Diamond Drilling, Hood Project - PN 420, Minnova Inc Company Report, p. 136.

Thomas, D. A., and Glenn, D. G., 1994, 1993 Summary Report: Diamond Drilling and Pulse EM, Hood Project - PN 420 Minnova Inc Company Report, p. 110.

Thompson, A. J., Hauff, B., and Robitaille, P. L., 1999, Alteration mapping in exploration: Application of short-wave infrared (SWIR) spectroscopy: Society of Economic Geology Newsletter, v. 39.

Yamashita, K., Creaser, R. A., Jensen, J. E., and Heaman, L. M., 2000, Origin and evolution of mid- to late-Archean crust in the Hanikahimajuk Lake area, Slave Province, Canada; evidence from U-Pb geochronological, geochemical and Nd-Pb isotopic data: Precambrian Research, v. 99, p. 197-224.

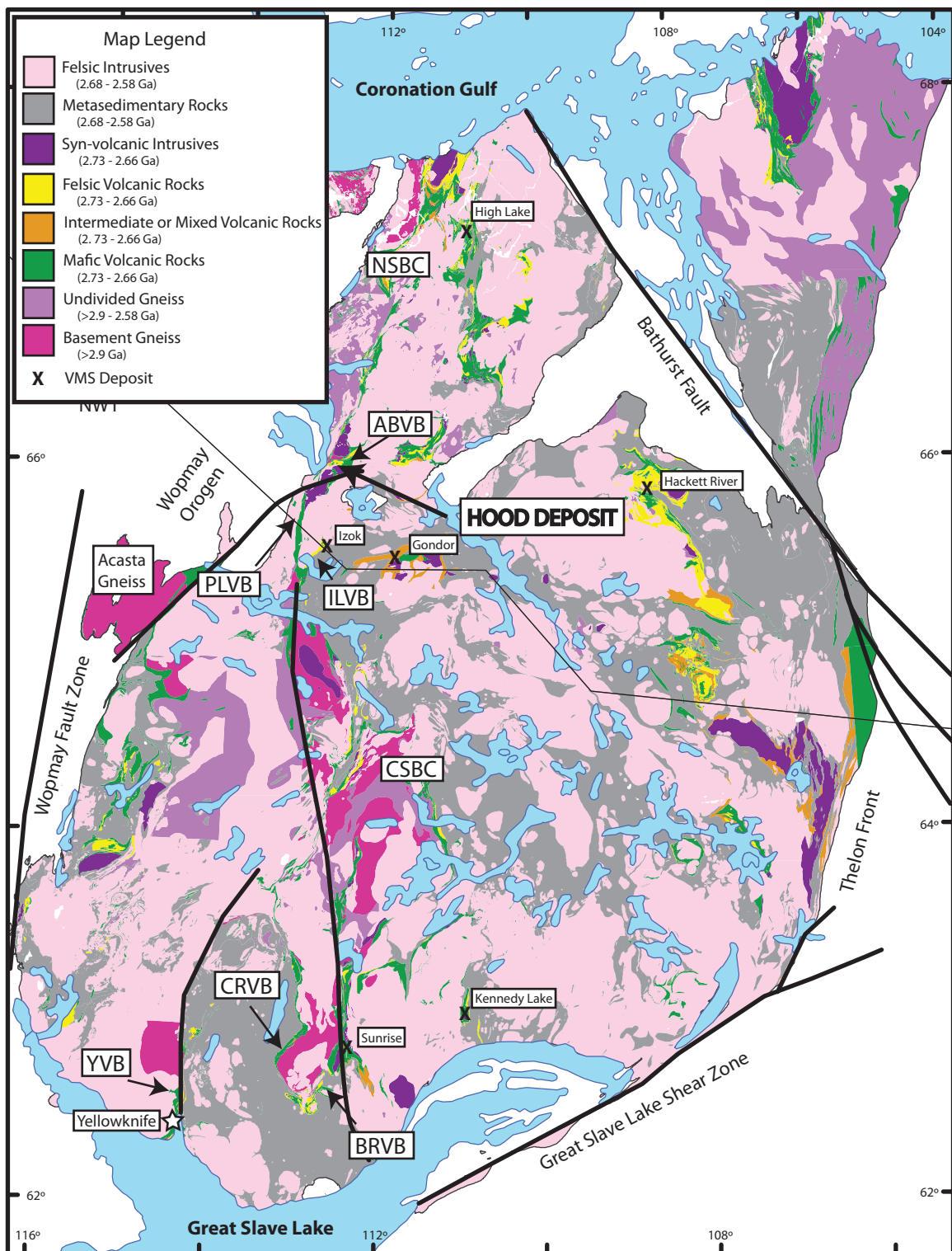


Figure 1-1: Simplified Slave Craton geology (Stubley, 2005) and selected VMS deposits (Bleeker and Hall, 2007). Labeled greenstone belts are the Amooga Booga volcanic belt (ABVB), Izok Lake volcanic belt (ILVB), Point Lake volcanic belt (PLVB), Yellowknife volcanic belt (YVB), Cameron River volcanic belt (CRVB), and the Beaulieu River volcanic belt (BRVB).

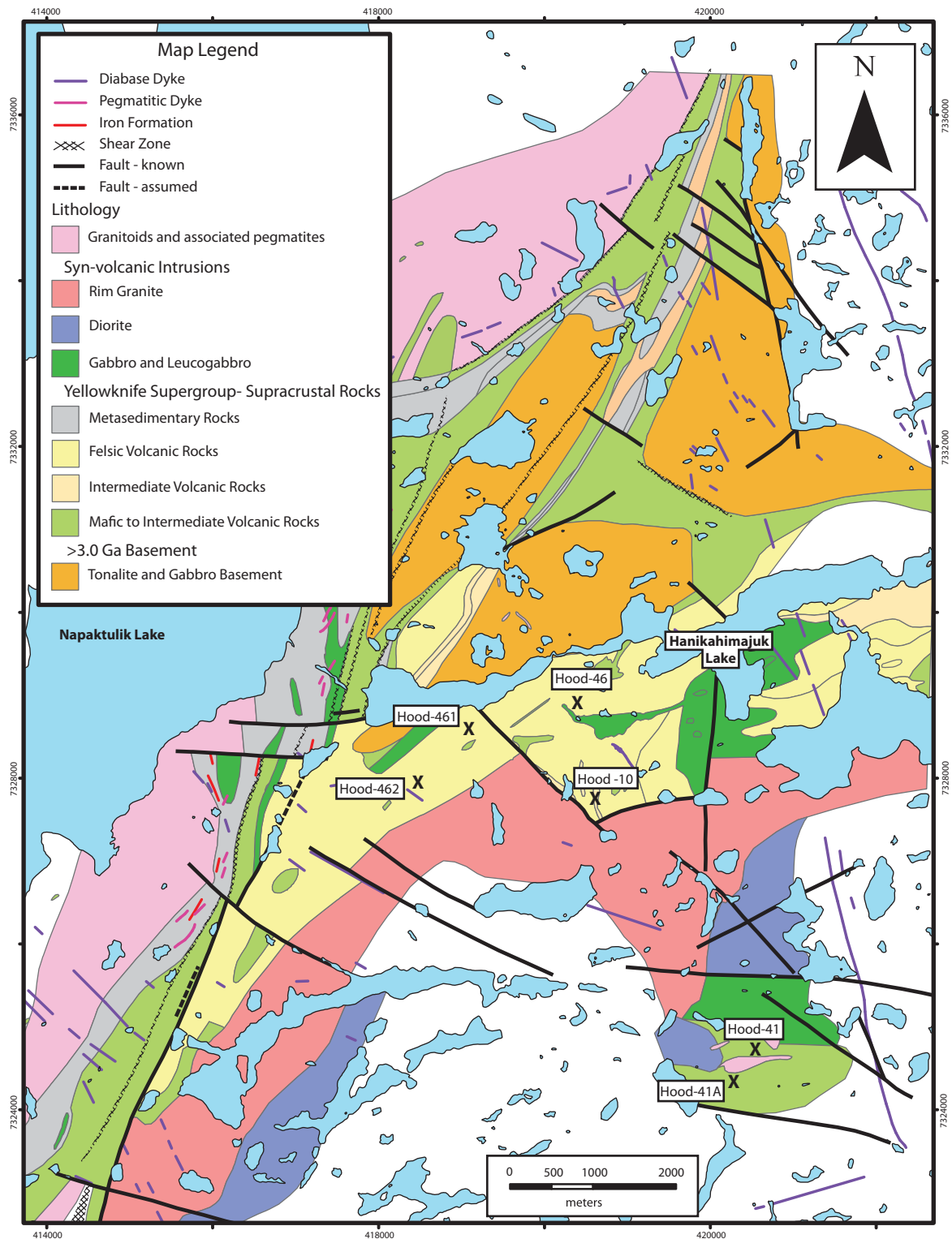


Figure 1-2: Geology of the Hanikahimajuk Lake area and locations of Hood deposit lenses and mineral occurrences (Gebert, 1995).

## **Chapter 2: Geology, alteration, and lithogeochemistry of the Hood Deposits, Nunavut, Canada.**

### **2.1 ABSTRACT**

The Hood volcanogenic massive sulfide (VMS) deposits are hosted by the ~2.68 Ga Amooga Booga volcanic belt (ABVB) in the northwestern Slave Craton. The deposits consist of three massive to semi-massive sulfide lenses (Hood 10, 41 and 41A) and three smaller mineral occurrences (Hood 46, 461 and 462). The mineralization consists of massive to semi-massive pyrrhotite, pyrite, chalcopyrite, sphalerite, and galena and is hosted predominantly by coherent felsic volcanic flows with subordinate felsic to mafic volcanoclastic units within the predominantly mafic ABVB. The mineralized lenses occur at different stratigraphic levels, do not appear to be a single mineralized horizon, and have textural, alteration, and stratigraphic features consistent with formation via seafloor replacement. Sericite and chlorite are the dominant alteration minerals associated with the VMS mineralization at Hood. Alteration occurs in both the footwalls and the hanging walls to the lenses, with the strongest chlorite alteration occurring within mineralized intervals and the footwalls immediately below mineralized horizons.

The felsic volcanic rocks in the Hood deposit can be subdivided into four volcanic suites based on immobile trace element geochemistry. The main felsic suites, suites A and B, are petrographically indistinguishable. Suite A has higher Zr/Ga and Zr/TiO<sub>2</sub> and lower Al<sub>2</sub>O<sub>3</sub>/Zr ratios, and in addition has greater high field strength element (HSFE) and rare earth element (REE) contents than suite B, which suggests a hotter fractionation

temperature for suite A. Suite A also has higher Nb/Ta values indicative of lesser crustal contamination and greater mantle input compared to suite B rocks. Mineralization is more closely associated with suite A than suite B.

The two mafic volcanic rock types previously identified in the ABVB both occur within the Hood deposits. Type I mafic rocks have enriched-mid-ocean ridge basalt (E-MORB) -like signatures. Type II mafic rocks have similar HFSE composition to type I mafic rocks but have weak negative Nb anomalies and higher Zr and Hf. The type II mafic suite is interpreted to be the result of variable crustal contamination of type I magma. The volcanic rocks of the ABVB are interpreted to have formed in a marginal continental arc/back-arc setting. The similarities of the ABVB to other Slave Craton greenstone belts further highlights the overall potential for greenstone-hosted VMS mineralization in the Slave Craton.

## **2.2 INTRODUCTION**

The Hood volcanogenic massive sulfide (VMS) deposits in the northwestern Slave Craton, Canada, consist of several Cu-Zn-Pb mineral occurrences in a ~9km<sup>2</sup> area hosted by the ~2.68 Ga Amooga Booga volcanic belt (ABVB). Exploration of the Hood deposit has identified three main lenses (Hood 10, 41, and 41A) with a total resource of 3.2 Mt @ 3.2% Zn and 2.6% Cu (this is a historical resource estimate and not NI-43-101 compliant; MMG Resources Ltd.); and several small mineral occurrences (Hood 46, 461 and 462). The deposits were discovered in 1972 during regional exploration by Texasgulf. Intermittent shallow (<200 m) drilling was undertaken on the deposit in the 1970s and early 1980s. Deeper drilling in 1992 and 1993 by Minnova Inc. extended the known depth



of mineralization (Thomas and Glenn, 1994). The property is currently being explored by MMG Resources Ltd.

Studies of the area surrounding the Hood deposits are limited. Prior to 1990, studies characterized the volcanic facies, mineralization and metal zonation, and major element lithogeochemistry (Gill, 1977; Rockingham, 1979; Hassard, 1983). Several studies in the mid-1990s to early 2000s refined the regional geological map, provided analyses of trace element lithogeochemistry and  $\epsilon\text{Nd}$  signatures of the volcanic and plutonic rocks, and determined the geochronology of the gneissic basement and volcanic rocks (Gebert, 1995; Jensen, 1995; Yamashita et al., 2000). These latter studies proposed a continental marginal back-arc basin environment of formation (Jensen, 1995; Yamashita et al., 2000).

Despite these previous regional and deposit-scale studies, fundamental work remains to be done, including: 1) documentation of the stratigraphy, lithofacies, alteration, and emplacement mechanisms for the deposits in light of improved understanding of VMS deposits; 2) expanded primary and secondary lithogeochemistry; 3) assessment of tectonic setting; and 4) relationships of the above to ore formation and exploration. In addressing these questions we have utilized detailed lithofacies and stratigraphic mapping of vintage diamond drill core for the various lenses and occurrences within the Hood deposits. This has been augmented by lithogeochemistry, near infrared-short wave infrared (NIR-SWIR) spectroscopy, and mineralogy, coupled with elemental mass change calculations and principal component analysis. These results are integrated to provide answers to the above questions and to enhance understanding of this poorly understood Archean VMS deposit.



## 2.3 REGIONAL GEOLOGY

The Archean Slave Craton is dominated by late (2.63-2.62 and 2.59-2.58 Ga) plutonic suites and large (2.66-2.61 Ga) sedimentary basins with subordinate older (2.73-2.66 Ga) greenstone belts making up a small proportion of the craton (Fig. 2-1) (Mortensen et al., 1988; Davis and Bleeker, 1999; Bleeker and Hall, 2007; Ootes et al., 2009). It is bounded on the west by the Wopmay Orogen and bounded on the east by the Taltson-Thelon Orogen (Fig. 2-1) (Hoffman, 1988). The craton also consists of a >3.0 Ga crystalline basement, the Central Slave Basement Complex (CSBC), overlain by the supracrustal (2.9-2.58 Ga) Yellowknife Supergroup (Bleeker et al., 1999). The base of the Yellowknife Supergroup is the Central Slave Cover Group (CSCG), a thin package of volcanic rocks, quartzite, conglomerate, and banded iron formation (BIF) (Bleeker et al., 1999). The CSCG is overlain by two major (2.73-2.70 and 2.70- 2.66 Ga ) volcanic sequences with minor sedimentary packages and the (2.68- 2.63 Ga) Duncan Lake Group, Burwash basin turbiditic rocks (Bleeker et al., 1999). The basement and supracrustal rocks of the Slave Craton are cut by several (2.63-2.62 and 2.59-2.58 Ga) granitic plutonic phases and affected by several phases of deformation from 2.66-2.63 Ga and 2.61-2.59 Ga (Relf, 1992; Davis et al., 1994; Isachsen and Bowring, 1994; Davis and Bleeker, 1999; Bleeker and Hall, 2007). The greenstone belts consist of the (2.73-2.66 Ga) volcanic and subordinate sedimentary sequences of the Yellowknife Supergroup that underlie the (2.68-2.63 Ga) Duncan Lake Group turbiditic rocks (Fig. 2-1) (Isachsen et al., 1991; Isachsen and Bowring, 1997; Ootes et al., 2009). The lower volcanic sequence is a dominantly tholeiitic mafic volcanic rocks defined as the >2.7 Ga Kam Group in the

Yellowknife area (Helmstaedt and Padgham, 1986, Fyson and Helmstaedt, 1988; Isachsen and Bowring, 1994, 1997; Cousens, 2000; Bleeker and Hall, 2007). The Kam Group is overlain by the <2.7 Ga Banting Group, which is calc-alkaline and has a greater proportion of felsic volcanic rocks (Isachsen et al., 1991; Cousens et al., 2002). Volcanic packages in other greenstone belts of the Slave Craton have typically been interpreted as Kam Group or Banting Group correlatives; however, in the Hood area the volcanic rocks do not have characteristics that truly match either the Kam or the Banting groups and this regional subdivision may not be applicable (Jensen, 1995; Yamashita et al., 2000).

## **2.4 LOCAL GEOLOGICAL SETTING**

The ABVB is a north-east trending volcanic belt in the west-central part of the Slave Craton that hosts the Hood deposits (Fig. 2-1) (Gebert, 1995; Jensen, 1995). It is geographically continuous with the Point Lake volcanic belt (PLVB) to the south and the Napaktulik Lake volcanic belt to the north (Gebert, 1995; Jensen, 1995). Old (>3.0 Ga) tonalitic and gabbroic basement occurs in three locations in the Hanikahimajuk Lake area (Fig. 2-2) (Gebert, 1995; Jensen, 1995). The overlying supracrustal rocks of the ABVB are a 10 km package with poorly understood stratigraphy as a result of limited lateral continuity of units (Gebert, 1995). The overall stratigraphy is thought to young to the northwest, however, there are local variations in younging direction (Gebert, 1995). Geographically, the ABVB forms a central area of felsic volcanism surrounded by mafic flows and mafic and felsic volcanoclastic rocks (Gill, 1977).

Mafic and intermediate volcanic rocks include pillowed mafic flows, laminated mafic volcanoclastic rocks, quartz-filled amygdule-bearing mafic rocks, and intermediate

volcaniclastic rocks (Gebert, 1995). Mafic rocks have two REE signatures (type I and type II) that represent variable crustal contamination of MORB-like magmas in an ensialic back-arc basin setting (Gebert, 1995; Jensen, 1995; Yamashita et al., 2000). Both type I and type II pillowed mafic flows occur within close proximity (10s of metres) (Gebert, 1995).

Sedimentary rocks of the ABVB form thin layers between flows including discontinuous Fe-formation, pelite, psammite, quartzwacke, and conglomerate (Gebert, 1995). Synvolcanic gabbro and diorite and post-volcanic granitoids intrude the ABVB (Gebert, 1995). The term “mixed rock” has been given to amphibolite grade rocks that are likely supracrustal in origin but have been extensively intruded by diorite and granitoid intrusive rocks (Gebert, 1995). Four different sets of diabase dykes and a single type of pegmatite intrude rocks in the Hanikahimajuk Lake area (Jensen, 1995).

Neodymium isotopic signatures ( $\epsilon\text{Nd}_t$ ) of the ABVB volcanic rocks range from -1.2 to +2.5 (Jensen, 1995). Although the mafic rocks have mostly positive  $\epsilon\text{Nd}_t$ , they have trends in  $\epsilon\text{Nd}$ - $^{147}\text{Sm}/^{144}\text{Nd}$  space consistent with mantle melts contaminated by sialic crust (Jensen, 1995; Yamashita et al., 2000). All felsic and some intermediate rocks have lower  $\epsilon\text{Nd}_t$  signatures indicating a crustal component in their genesis (Jensen, 1995). There is no correlation between geochemical type of mafic rock, type I or type II, and its  $\epsilon\text{Nd}_t$  signature (Jensen, 1995). Granitoid rocks have  $\epsilon\text{Nd}_t$  signatures that falls within the western granitoid field for the Slave Craton (Davis and Hegner, 1992).

In the vicinity of the Hood deposits, calc-alkaline felsic rocks make up 25% of the volcanic rocks (Bruce, 1991). Felsic volcanic rocks consist primarily of rhyolitic and dacitic felsic and fragmental volcaniclastic rocks (Jensen, 1995). Units are subdivided and

variously named in exploration company reports, but are essentially similar to regionally described units throughout the ABVB. The detailed structural setting of the deposits is uncertain; however, Hood 41, and Hood 41A are only very gently folded but overturned, and Hood 10 has previously been interpreted as being isoclinally folded (Hassard, 1983).

Regional metamorphic grade in unaltered mafic rocks in the Hood area is greenschist facies (chlorite-actinolite-epidote-plagioclase-calcite) (Thomas and Glenn, 1994). Hydrothermally altered rocks often have chlorite-sericite-quartz and Na<sub>2</sub>O depletions compared to the volcanic rocks surrounding the Hood deposits (Bruce, 1991), typical of volcanic rocks associated with VMS deposits (Spitz and Darling, 1978).

## **2.5 STRATIGRAPHY AND SETTING OF THE HOOD VMS DEPOSITS**

The Hood deposits consists of three lenses, Hood 10, 41, and 41A, and three occurrences, Hood 46, 461, and 462 (Fig. 2-2), each having distinct stratigraphy (Table 2-1; Fig. 2-3). The three lenses (Hood 10, 41, and 41A) host bulk of the mineralization and compose the entirety of the geological resource. The mineral occurrences (Hood 46, 461, and 462) have limited mineralization and a single drill hole from each was logged during this study to determine stratigraphy along the northern edge of the deposit area. Individual drill logs are compiled in Figure A1-1.

### **2.5.1 Hood 10 Lens**

The Hood 10 lens is hosted by massive to brecciated dacite and rhyolite flows with minor basalt and andesite volcanic units (Table 2-1; Fig. 2-4 and 2-5). Fine-grained mafic to felsic dykes cross-cut the volcanic rocks. Hood 10 is the most structurally

complex of the three lenses. Way-up indicators are ambiguous making identification of the hanging wall vs. footwall uncertain. Sulfide horizons are the most obvious marker horizons. Previous workers have interpreted the deposit as a single isoclinally folded horizon of mineralization (Hassard, 1983); however, the absence of repeating stratigraphic units on either side of the mineralization support an alternative interpretation, that there are two closely spaced mineralized horizons in the deposits occurring in the nose of larger fold. The stratigraphy youngs overall to the east (Fig. 2-4). Outlined below are the main lithofacies and alteration lithologies within the Hood 10 lens.

#### ***2.5.1.1 Lithofacies***

##### *2.5.1.1.1 Felsic Flows*

Rhyolite flows are light cream to tan coloured (Fig. 2-5), siliceous and porcelain-like with black chlorite-filled fractures. They commonly display jigsaw-fit breccia, breccia, or banded textures. Massive fine-grained rhyodacite with up to 10% blue-grey quartz eyes is abundant in the northern end of the Hood 10 lens (Fig. 2-5C). Fine-grained massive, uniformly grey dacite and dark grey-black and white mottled dacite are common and commonly contain chlorite-altered angular breccia clasts.

##### *2.5.1.1.2 Mafic to Intermediate Flows*

Mafic flows are fine-grained, and range from pillowed with brecciated tops to massive basalt with minor amygdules (Fig. 2-5A). Carbonate veins and pervasive carbonate alteration are common in mafic flows. There are minor sections of grey-green

andesite (Fig. 2-4), which are typically massive and fine-grained with chlorite alteration that form green spots.

#### *2.5.1.1.3 Mafic to Intermediate Tuffs*

Mafic to intermediate tuff and lapilli tuff are a minor unit in Hood-10. The tuffs are fine- to very fine-grained, dark to light green with weakly to moderately developed laminations, and in some cases contain fine lapilli and/or crystals.

#### *2.5.1.1.4 Dykes*

There are several types of fine-grained mafic dykes that cross-cut the Hood-10 lens including: aphanitic, dark grey, massive, non-magnetic dykes; aphanitic, dark grey, magnetic dykes; fine-grained, light green, carbonate veined dykes; fine-grained tan, banded dyke; and light green brown, fine-grained chlorite speckled dykes. Dyke margins are typically straight with narrow chilled margins, unlike massive flows, which do not have chilled margins.

#### *2.5.1.2 Alteration*

Alteration in the Hood 10 lens consists predominantly of quartz, sericite and chlorite (Table 2-1; Fig. 2-6). Quartz  $\pm$  sericite is the most widespread alteration assemblage and is the predominant alteration in felsic rocks. Quartz alteration is pervasive to mottled in brecciated and massive rocks, and is extremely common in dacite resulting in a typical grey-with-white-mottled appearance. In laminated tuffs and in rocks with flow banding, quartz and sericite alteration intensity is variable between individual

laminated layers and flow bands. Weak to strong quartz and sericite alteration occurs throughout the entire hanging wall and footwall.

Chlorite alteration is pervasive to spotty in the mafic and intermediate rocks and of variable intensity (Fig. 2-6). Wispy selective chlorite alteration of mafic rocks results in the appearance of pseudoclasts. In felsic rocks, chlorite commonly occurs along fractures or partially replaces angular clasts in breccias (Fig. 2-6). Chlorite alteration, along with quartz alteration, is strongest immediately adjacent (within ~1m) to the mineralization. Within the mineralization host-rock fragments are pervasively replaced by quartz and chlorite alteration and surrounded by sulfide.

The alteration intensity above and below mineralization is variable which makes it difficult to identify hanging wall and footwall based on alteration intensity alone. In some sections chlorite alteration is stronger above the mineralization; in other sections chlorite alteration is stronger below the sulfide mineralization. Chlorite alteration occurs throughout the entire hanging wall and footwall. Sericite alteration intensity has similar variations and extent.

Pervasive calcite alteration, calcite veining, and Fe-carbonate veins cross-cut mineralization, host rocks, and VMS-related alteration, and are interpreted to be related to regional metamorphism and deformation. Calcite alteration and veining is hosted predominantly within the mafic volcanic and intrusive rocks, although calcite veins do occur in the mafic and intermediate tuff, throughout the footwall and hangingwall of the Hood 10 lens. Orange, Fe-carbonate veins, if present in a drill core, tend to occur in all volcanic rock units sampled by that core. In some drill holes finely banded dacite is orange due to pervasive Fe-carbonate staining.

### 2.5.2 Hood 41 Lens

The Hood 41 lens is dominated by massive mafic flows overlain by dacite (Table 2-1; Fig. 2-7). Stratigraphy is sub-vertical to slightly overturned with a SSW-NNE strike direction. Strong chlorite alteration up hole (stratigraphically below) from the sulfide mineralization indicates that the deposit faces upwards towards the southeast. Dacite is a minor lithology and is almost exclusively located down hole (stratigraphically above) from sulfide mineralization. All units have been extensively intruded by pink fine- to coarse-grained granite and undergone patchy quartz and K-feldspar alteration. Outlined below are the lithofacies and alteration in the Hood 41 lens.

#### 2.5.2.1 *Lithofacies*

##### 2.5.2.1.1 *Mafic and Intermediate Volcanic Rocks*

Dark green, massive, basalt flows dominate the Hood 41 lens. They are typically fine-grained with zones of rare white amygdules (Fig. 2-5), and have been extensively altered by the intrusion of large granite dykes. The resulting intrusion and alteration of the massive basalts results in 1-2 cm dykes cutting the basalts coupled with patches of medium-grained quartz crystals and the growth of actinolite crystals up to 1 cm in size in the basalt. This alteration is typically strongest adjacent to granite dykes but zones of it also occur 10s of metres away from intersected pink granite dykes.

Andesite is a very minor unit in the Hood 41 lens. It is massive to weakly banded, grey-green with moderate quartz and chlorite alteration. It locally grades into more felsic units.

##### 2.5.2.1.2 *Felsic Volcanic Rocks*



Dacite flows are within the hanging wall to mineralization (below sulfide mineralization in drill core). Dacite occurs proximal to mineralization, either directly hosting sulfide or present < 20 m stratigraphically above the sulfide. The dacite is medium-grey, fine-grained and massive to banded with weak chlorite alteration is weak. Quartz alteration is typically moderate and produces a mottled grey and white appearance.

#### *2.5.2.1.3 Mafic Dykes*

The most common mafic dykes are green, fine-grained, and cut mafic and felsic volcanic rocks. They have sharp contacts, but are otherwise very similar to the fine-grained mafic coherent volcanic rocks described above, indicating they may be synvolcanic dykes (Fig. 2-5). Two other less common mafic dyke types cross cut the volcanic rocks, these are olive-brown, fine-grained, mafic dykes, and a medium-grey, aphanitic, mafic dyke.

#### *2.5.2.1.4 Granite*

Granite is pink to pale pink to cream, fine- to coarse-grained, and is the most common intrusion in the Hood-41 lens (Fig. 2-5). It intrudes all units including the sulfide mineralization. It is typically massive, though it commonly displays fractures that are parallel to the foliation found in adjacent rocks. Granite occurs as thick intrusions (10s of metres) down to cm-wide dykes. This granite is petrographically similar to the Rim granite, which forms the large central batholith to the northwest of Hood 41 (Fig. 2-2)

#### *2.5.2.1.5 Diorite*

Syn-volcanic diorite dykes have a fine- to medium- grained “salt and pepper” textures with quartz and amphibole crystals. They have sharp contacts with surrounding rocks, and range from massive to foliated and locally cut sulfide mineralization. Syn-VMS hydrothermal chlorite alteration of mafic minerals causes the diorite to have green and white colouration. Diorite is more altered than the granite and is intruded by granite as well.

#### ***2.5.2.2 Alteration***

The Hood 41 lens has chlorite, quartz, and sericite alteration. The mafic volcanic rocks that dominate the stratigraphy typically have moderate intensity, pervasive chlorite alteration (Table 2-1; Fig. 2-6). Chlorite is distinctively stronger footwall alteration (uphole from the mineralization) than hanging wall alteration (downhole), indicating that the footwall is to the northwest and the hanging wall is to the southeast; however, this is a tentative conclusion as there has been limited drilling below the sulfide bodies. Strong chlorite alteration and moderate quartz alteration occurs within, and up to 10 m into the footwall of the mineralized zones. Chlorite alteration of mafic or felsic volcanic clasts within the mineralized zone is also common. Weak to moderate quartz and sericite alteration are also present in both the hanging wall and the footwall. In the footwall the quartz-sericite alteration is sporadic to continuous and extends for at least 150 m (extent of drilling). Quartz-sericite alteration is common in the felsic flows of the hanging wall, extending for at least 40 m (extent of drilling into hanging wall).

Significant quartz and K-feldspar alteration of all lithologies is inferred to have occurred as a result of intrusion of granite. This alteration occurs up to approximated 1 m

from the granite dykes, and consists of fine to coarse quartz crystals ( $\pm$  pink K-feldspar crystals) in the volcanic rocks with the appearance of grey-blue spots. Quartz and K-feldspar alteration is commonly accompanied by coarse actinolite crystals up to 1cm in size, both in bands and as porphyroblasts in the mafic volcanic rocks. The abundance of the quartz alteration in the mafic volcanic rocks makes it difficult to distinguish any quartz  $\pm$  sericite alteration related to VMS mineralization. Based on the spatial relations of quartz alteration to granite dykes most of the quartz present in the mafic volcanic rocks is likely related to the granite intrusions and not the hydrothermal alteration associated with VMS mineralization.

### **2.5.3 Hood 41A Lens**

Mixed felsic and mafic volcanoclastic rocks (tuff to lapilli tuff) are the dominant lithologies in Hood 41A lens with lesser, but significant volumes of volcanic flows (Table 2-1; Fig. 2-8). There are several varieties of intrusive rocks that cut the stratigraphy including synvolcanic and post-volcanic mafic dykes, diorite-gabbro dykes, and granite dykes. In agreement with observations by previous workers, stronger alteration up hole from the sulfides and downhole graded bedding in volcanoclastic units indicates the lens is overturned. Stratigraphy and mineralization dip moderately to the southwest. Outlined below are the main lithofacies and alteration within the Hood 41A lens.

#### ***2.5.3.1 Lithofacies***

##### ***2.5.3.1.1 Mafic, Mixed, and Felsic Tuff, Lapilli Tuff***

Volcaniclastic units are the most common lithology in Hood 41A. They are dark green to grey, and despite being affected by alteration, colour is useful as a crude proxy to estimate geochemical composition of the tuff. Mafic tuff is dark to medium green with faint to strong colour banding that can range from finely laminated up to 2 cm in width (Fig. 2-5). Lapilli tuff contains 0-10% rounded white quartz lapilli typically <2 mm in size. Felsic tuff is similar to mafic tuff, but more grey in colour; mixed tuff have alternating light and dark bands of mafic and felsic composition, and often containing lapilli. Chlorite and sericite alteration of the tuff units are common and affect tuff colour.

#### *2.5.3.1.2 Coherent Mafic Volcanic Rocks*

The coherent massive mafic volcanic rocks are dark grey to green flows. They commonly exhibit a cobweb pattern of thin green chlorite veins that often form pseudoclasts (Fig. 2-6C). Mafic (flow) breccias are a similar colour to coherent flows with dark green clasts in a slightly lighter green matrix. Clasts are angular, 5-10 mm and densely packed. In both breccias and massive mafic volcanic rocks, alteration (chlorite  $\pm$  sericite) highlights the foliation of the volcanic rocks. Chlorite alteration is pervasive and common. Small carbonate veins and clots are also common.

#### *2.5.3.1.3 Coherent Felsic Volcanic Rocks*

Rhyolite and dacite are similar to those in Hood 10, but are minor lithologies. Siliceous, light coloured rhyolite is the most easily identified of the felsic rocks (Fig. 2-5). It exhibits poor to well-defined flow banding. Dacite is typically grey, massive, and fine-grained.

#### 2.5.3.1.4 *Mafic Dykes*

There are several types of mafic dykes that cut the volcanic rocks of the Hood 41A deposit. Grey, aphanitic mafic dykes are common proximal to mineralization in holes H-41A-01 and H-41A-02. Their contacts are occasionally rounded and finger into the volcanoclastic material indicating the tuffs were not solidified and the dykes are syn-volcanic (Fig. 2-5B). The other distinctive mafic dyke is a fine-grained porphyritic brown dyke with 2-3 mm pyroxene crystals. The pyroxene-bearing dykes lack the calcite alteration common in other lithologies and are not intruded by granite.

#### 2.5.3.1.5 *Diorite/Mixed Intrusive Rocks*

A significant component of the stratigraphy in Hood 41A consists of a mixed intrusive unit composed of diorite and gabbro (Fig. 2-5F). This unit has many variants and is very heterogeneous, ranging in colour from white-pink and black zones consisting of more felsic material to dark black and green zones consisting of more gabbroic material. Crystal size is also highly variable, ranging from very fine- to coarse-grained and containing crystals of pyroxene and hornblende. This unit has considerable graded variation in colour, composition and crystal size.

#### 2.5.3.1.6 *Granite*

Bright pink granite with coarse K-feldspar and quartz crystals intrude all units except the above-mentioned brown, porphyritic mafic dyke (Fig. 2-5). The intrusive contacts can be sharp or obscured by quartz-K-feldspar alteration of the surrounding rock.

Where granite cuts mineralization it locally contains chalcopyrite and pyrite stringers and blebs.

#### ***2.5.3.2 Alteration***

Alteration of Hood 41A includes quartz, chlorite, and sericite. Strong footwall alteration is up hole from the sulfides indicating the deposit is overturned but there is still significant chlorite alteration in the hanging wall (downhole) to mineralization. Chlorite alteration is very common in mafic volcanic rocks and felsic tuff, as well as along fractures in coherent felsic rocks (Table 2-1; Fig. 2-6). In both felsic and mafic tuff, chlorite alteration is generally pervasive, though it is stronger in the mafic tuff than in the felsic tuff. Weak to moderate chlorite alteration is common for several 100 metres in the footwall with strong chlorite alteration within the mineralization. Chlorite alteration in the hanging wall (downhole) the sulfide mineralization is typically weaker than immediately in the footwall of the sulfide mineralization.

Intensities of quartz and sericite alteration are variable, but alteration occurs throughout the entire lens in both the hanging wall and the footwall. Quartz and sericite alteration are often quite strong in the felsic flow units where there is selective replacement along flow bands (Fig. 2-6). It is also stronger and more widespread in the western side of the Hood 41A compared to the eastern side of the deposit. Carbonate veining and clots are common throughout the hanging wall and footwall of the Hood 41A lens, particularly in the mafic and felsic tuff and mafic flows. There is no zonation of the carbonate alteration.

#### **2.5.4 Hood 46, Hood 461, and Hood 462 Occurrences**

The three mineral prospects Hood 46, 461 and 462 are small zones of minor mineralization that lie to the north and west of the Hood 10 lens (Fig. 2-2). As none of the occurrences has significant mineralization, a drill hole was selected from each to characterize the general stratigraphy in the area (Table 2-1; Fig. 2-9). Hood 46 and Hood 461 are dominated by thick packages of aphyric and quartz-phyric rhyodacite. The rhyodacite package of Hood 461 is underlain by a package of fine-grained coherent mafic volcanic rocks. Hood 462 is characterized by quartz-phyric rhyodacite overlying mafic to intermediate volcanic rock. There has been significant faulting at Hood 462 and the deposit has been strongly affected by shearing. Outlined below are the lithofacies and alteration in the Hood 46, 461 and 462 occurrences.

##### ***2.5.4.1 Lithofacies***

###### ***2.5.4.1.1 Felsic Rocks***

All three prospects have thick packages of coherent felsic rocks. Felsic rocks consist of three main lithologies: quartz-phyric rhyolite, aphanitic rhyolite and a quartz- and feldspar-phyric unit (Fig. 2-5). Quartz eyes vary from fine, distinct grey crystals to more subtle cloudy white crystals. They are interpreted to be felsic flows, although the occurrences of sharp contacts suggest there may be some shallow level synvolcanic intrusions within the units.

###### ***2.5.4.1.2 Intermediate and Mafic Rocks***

Intermediate and mafic rocks are limited to the Hood 461 and 462 occurrences. Intermediate to dacitic rocks are fine-grained, brown-grey, coherent volcanic rocks with chlorite and sericite alteration. Andesite and basalt are fine-grained and finely foliated; foliation is strong in Hood 462. Both drill holes from Hood 461 and Hood 462 end in a slightly grainy mafic rock that is possibly a very fine-grained gabbro.

#### *2.5.4.1.3 Mafic Dykes*

Numerous fine-grained mafic dykes cross-cut the host volcanic rocks. Mafic dykes are typically light to dark green fine-grained intrusive rocks with rare biotite, amphibole and pyrite porphyroblasts. Pervasive carbonate alteration and calcite veining through these dykes are common. Medium grained Fe-carbonate stained diorite dykes and light coloured fine-grained brown-green intermediate dykes also intrude the volcanic rocks.

#### *2.5.4.2 Alteration*

Chlorite, quartz, and sericite alteration are the dominant alteration types in the Hood 46, 461 and 462 occurrences. Quartz and sericite alterations are more prevalent in the felsic rocks and chlorite alteration in felsic rocks is typically confined to fractures (Table 2-1; Fig. 2-6). Chlorite alteration of mafic and intermediate rocks is typically weak to moderate with very strong chlorite alteration confined to zones of less than 10 meters. The rocks from Hood 462 have undergone more significant strain than the rocks from Hood 461 and Hood 46; this is likely due to proximity to a major regional N-S running fault. Hood 462 is also characterized by common Fe-carbonate veining and hematite lenses.



## **2.6 MINERALIZATION**

### **2.6.1 Hood 10 Lens**

Mineralization is hosted by rhyolite and dacite. Most drill holes intersect two mineralized horizons with the lower horizon typically the thicker of the two (up to 25 m). Mineralization ranges from Cu-rich to Zn-rich and consists of stringers to massive sulfide (Table 2-1; Fig. 2-10). Copper-rich zones consist of disseminated chalcopyrite stringers to massive sulfide consisting of chalcopyrite and pyrrhotite with lesser pyrite (Fig. 2-10). Zinc-rich mineralization consists of semi-massive to massive fine-grained sphalerite and pyrite, locally occurring as distinct bands or semi-massive to massive pyrrhotite  $\pm$  fine sphalerite with cubic buckshot pyrite, and clasts of chlorite altered host rock (Fig. 2-10). Zoning between the mineralization types occurs with abrupt transitions. The Hood 10 lens is laterally and longitudinally zoned, changing from Cu-rich to Zn-rich west to east and north to south (Hassard, 1983; Thomas and Glenn, 1994).

### **2.6.2 Hood 41 Lens**

Sulfide mineralization at Hood 41 occurs as either semi-massive to massive sulfide zones or stringer sulfide zones (Table 2-1). Massive sulfide is composed of variable amounts of fine-grained pyrite, pyrrhotite, and sphalerite. Cubic buckshot pyrite crystals, up to 3mm in size, are commonly present within a fine-grained massive pyrrhotite  $\pm$  pyrite  $\pm$  sphalerite matrix (Fig. 2-10). This type of mineralization also contains irregularly shaped chlorite-altered volcanic clasts. Stringer sulfides zones contain chalcopyrite and/or pyrite stringers and blebs with minor sphalerite or pyrrhotite (Fig.

2-10). Generally the chalcopyrite and pyrite stringers occur separately, in distinct sections within a single stringer sulfide zone. Where granite has intruded into the sulfide, chalcopyrite and pyrite have been remobilized to form veins and stringers in the granite; pyrrhotite and sphalerite do not occur in the granite. Metal zoning in Hood 41 consists of alternating zones of Cu-rich and Zn-rich mineralization (Rockingham, 1979).

### **2.6.3 Hood 41A Lens**

Sulfide mineralization in Hood 41A consists of massive to semi-massive sulfide and stringer sulfide zones, although there is no distinct zonation between the mineralization types (Table 2-1). Mineralization occurs in well-defined horizons within tuffs with interlayering of massive sulfide and barren zones up to several meters thick. The contacts between mineralized and non-mineralized zones are abrupt, and the intersections of sulfide mineralization vary between massive sulfide, semi-massive sulfide, and stringer sulfide. The massive sulfide consists of fine pyrrhotite with buckshot, cubic pyrite crystals and chlorite-altered clasts (Fig. 2-10D). Fine sphalerite commonly occurs with the pyrrhotite but the similarity in colour of the pyrrhotite and sphalerite makes the sphalerite difficult to distinguish in hand specimen; chalcopyrite is also present in these sulfides as stringers. Semi-massive sulfide consists of the pyrrhotite with buckshot pyrite, but with more abundant chlorite altered clasts when compared to massive sulfide; chalcopyrite is also present as stringers. Sulfide stringers zones consist predominantly of chalcopyrite and pyrite stringers within the host rocks (Fig. 2-10).

#### **2.6.4 Hood 46, Hood 461, and Hood 462 Occurrences**

The mineralization at Hood 46 and Hood 461 is near surface and was not intersected in drillholes. Surface mineralization in Hood 46 consists of pyrite stringers and disseminations with limited base metal intersected by drilling (Table 2-1) (Thomas and Glenn, 1994). Surface mineralization in Hood 461 consists of chalcopyrite stringers (Thomas and Glenn, 1994). Mineralization intersected in the Hood 462 prospect differs significantly from the mineralization of the Hood 10, 41 or 41A deposits. It is characterized by fine-grained pyrite layers interbedded with hematite and chloritic argillite or volcanic ash layers. The mineralization also occurs in a fault zone with extensive fracturing and fault gouge. Trace pyrite and chalcopyrite stringers and blebs occur rarely throughout Hood 46, Hood 461 and Hood 462.

### **2.7 LITHOGEOCHEMISTRY**

#### **2.7.1 Sampling and Analytical Methods**

A total of 228 drill core samples and an outcrop sample were collected for geochemical analysis. Samples were cut in half with one half retained for archiving and the other half analyzed. The samples were analyzed at ALS Minerals Laboratory in Vancouver, Canada. The samples were crushed in jaw crushers and pulverized in low chrome steel bowls. The 229 samples were analysed for major elements ( $\text{SiO}_2$ ,  $\text{Al}_2\text{O}_3$ ,  $\text{Fe}_2\text{O}_3$ ,  $\text{CaO}$ ,  $\text{MgO}$ ,  $\text{Na}_2\text{O}$ ,  $\text{K}_2\text{O}$ ,  $\text{TiO}_2$ ,  $\text{MnO}$ ,  $\text{P}_2\text{O}_5$ ,  $\text{SrO}$ ,  $\text{BaO}$ ), base metals (Ag, Cu, Cd, Mo, Ni, Pb, Sc, Zn), C and S, for high field strength elements (HFSE), low field strength elements (LFSE) and REE, and volatiles (As, Bi, Hg, Sb, Se, Te). Major elements were

determined by inductively coupled plasma atomic emission spectrometry (ICP-AES) following a lithium metaborate fusion and acid dissolution. Base metals were analyzed by ICP-AES after 4-acid digestion. Trace elements and REE were analyzed by inductively coupled plasma mass spectrometry (ICP-MS) following lithium borate fusion and dissolution in acid. Carbon and sulfur were characterized by combustion furnace. The volatiles elements were determined by ICP-MS after aqua regia dissolution. The full results of sample geochemistry are compiled in Table A2-1. A series of duplicate core samples were included along with laboratory duplicates and standards to ensure the accuracy and precision of the lithogeochemical analysis. Results from laboratory duplicates and standards analyses fell within the expected and acceptable range of results. Results for duplicate core samples fell within  $2\sigma$  of the mean value for all major and trace elements.

Short-wave infrared (SWIR) spectroscopy was used to study hydrous mineral phases and their compositions (e.g. sericite, chlorite) (Thompson, 1999; Cudahy et al., 2001; Herrmann et al., 2001). Spectral data from representative samples of the Hood deposits were collected using a TerraSpec<sup>TM</sup> mineral spectrometer with Hi-Brite Muglight and optimization and white balance undertaken using a Spectralon<sup>®</sup> calibration puck at the Department of Earth Sciences at Memorial University of Newfoundland. Each sample was analyzed for 2-4 minutes until spectral readings stabilized. RS<sup>3</sup> Spectral Acquisition software was used to collect the cumulative spectra for each sample and to calibrate the instrument. The instrument was recalibrated after twenty analyses and the internal reference samples (pure pyrophyllite and talc) were utilized to monitor instrument performance. ViewSpec Pro<sup>TM</sup> v.6.0 software was used to process a splice correction for

the data and The Spectral Geologist<sup>TM</sup> software was used to identify mineral spectra. The two dominant alteration minerals for each sample are presented in Table A2-2.

### **2.7.2 Primary Immobile Element Lithogeochemistry**

The Hood deposit volcanic rocks have been affected by hydrothermal alteration, alteration related to the intrusion of granite, and subsequent regional metamorphism. Due to variable element mobility of most major elements and LFSE during hydrothermal alteration, immobile elements, including  $\text{Al}_2\text{O}_3$  and  $\text{TiO}_2$ , HFSE, and REE, were used to determine magma affinities, rock classification, and primary geochemical signatures of the volcanic rocks (Barrett and MacLean, 1999). The samples were classified using a standard Winchester and Floyd (1977) plot (modified by Pearce, 1996) and are predominantly basalt, andesite/basalt, or rhyolite/dacite (Fig. 2-11A). Rock samples from Hood are bimodal with samples clustering within the rhyolite/dacite field and at the boundary between the andesite/basalt-basalt fields. Mixed tuffs plot in between these two clusters (Fig. 2-11A). Hood volcanic rocks are generally subalkaline with Nb/Y ratios  $<0.7$  and have La/Yb, Th/Yb and Zr/Y values typical for rocks with calc-alkaline to transitional affinities (Fig. 2-11) (Winchester and Floyd, 1977; Barrett and MacLean, 1999; Ross and Bédard, 2009).

#### ***2.7.2.1 Geochemistry of Felsic Rocks***

Felsic rocks are subdivided into numerous groups based on their trace element geochemistry. Felsic volcanic rocks are subdivided into two main groups (suite A and suite B), and a third minor group (suite C). These groups are indistinguishable based on petrology alone but do have different spatial distributions (explained below). A fourth

group is composed of mixed and felsic tuffs from Hood 10 and 41A as well as quartz-phyric dacite from Hood 46, and 461. Granite is sub-divided into two groups corresponding to samples of granite dykes from Hood 41A and an outcrop sample from the central granite batholith. A final group consists of three anomalous dacite samples that are not geochemically similar to any of the previously mentioned groups, nor to each other.

The majority of the felsic rock samples belong to suite A. Suite A has HFSE contents similar to rocks with volcanic arc I-type to within plate magmatic affinities (Fig. 2-12A). Suite A samples have Nb/Ta values ranging from 8.9-17.1 with an average value of 12.9 (Fig. 2-12B). The suite A felsic rocks have  $(La/Yb)_{CN}$  vs  $(Yb)_{CN}$  ratios that are typical of FII-rhyolites (Fig. 2-12C). Primitive mantle-normalized multi-element plots for suite A samples demonstrate LREE-enrichment, flat HREE, strong negative Nb and Ti anomalies, weak negative Eu anomalies, and very weak positive Zr and Hf anomalies (Fig. 2-13A). A sample of Rim granite taken from the central granitic batholith in the area is geochemically indistinguishable from the suite A volcanic rocks (Figs. 2-12 and 2-13).

The suite B felsic suite is similar in many respects to suite A, but is characterized by lower  $Zr/TiO_2$ , and  $Zr/Ga$  and a higher  $Al_2O_3/TiO_2$  and  $Al_2O_3/Zr$  ratios (Fig. 2-12). In addition, suite B has lower Nb/Ta values than suite A, and has FI signatures in  $(La/Yb)_{CN}$  vs  $Yb_{CN}$  space (Fig. 2-12). Primitive mantle-normalized multi-element plots of suite B samples are similar to suite A but with less variability (Fig. 2-13B). Suite B felsic rocks are present in the Hood 46, 461, 462 occurrences and in the Hood 10 lens but are absent from Hood 41 and 41A lenses.

The suite C felsic suite is also similar in composition to the A and B suites, but has higher  $\text{TiO}_2$  contents, and lower  $\text{Zr/TiO}_2$  and  $\text{Al}_2\text{O}_3/\text{TiO}_2$  than suites A and B yet has Nb/Ta values between those of suite A and suite B (Fig. 2-12).

The core granite samples from Hood 41A have distinctively lower  $\text{Zr/TiO}_2$  and Nb/Ta values and higher  $\text{Al}_2\text{O}_3/\text{TiO}_2$  values than the other felsic rock groups (Fig. 2-12). The primitive mantle normalized multi-element plot for these samples has a similar pattern to suite A samples but with lower absolute abundances of trace elements (Fig. 2-13F). The granite sampled from core has lower Zr/Hf values than the outcrop granite sample (Table A2-1). The Hood 41A granite samples do not have the same geochemistry as the outcrop sample of Rim granite that is geochemically indistinguishable from the suite A felsic suite.

The fourth group of felsic rocks, which is volumetrically minor, consists of volcanoclastic felsic and mixed tuff samples from Hood 10 and 41A and quartz-phyric dacite from Hood 46 and 461. This group has a more andesitic composition, potentially due to contamination from mafic detritus (Fig. 2-11). The trace element composition of these samples is not unlike suite A, but with higher  $\text{TiO}_2$  contents. An additional group is made up of three anomalously altered samples (Figs. 2-12 and 2-13E). These two groups are not considered significant to the genesis of the ABVB and are not investigated further.

#### ***2.7.2.2 Geochemistry of Mafic Rocks***

There are four geochemically distinct suites of mafic rocks among the Hood samples: two main groups of basalts and related subvolcanic rocks; and two geochemically distinctive groups of dykes. The two main groups of basalts correspond to

type I and type II mafic rocks of Jensen (1995) and Yamashita et al. (2000) and this nomenclature has been maintained.

Type I mafic rocks are less abundant than type II mafic rocks and have sub-alkalic Nb/Y and Zr/TiO<sub>2</sub> ratios and a transitional to calc-alkaline magmatic affinity (Fig. 2-11). Their Ti-V ratios are similar to those of mid-ocean ridge basalts and back-arc basin basalts (Fig. 2-14). Type I mafic rocks have geochemical characteristics similar to enriched mid-ocean ridge basalts (E-MORB) except for little to no positive Nb anomaly (Figs. 2-14 and 2-15A). Primitive mantle-normalized plots of type I mafic rocks have downward sloping profiles with flat to positive Nb anomalies, LREE enrichment and HREE depletion (Fig. 2-15A). Both extrusive and fine grained intrusive mafic rocks have type I signatures. Type I mafic volcanics are present in Hood 10, 41 and 41A. Mafic dykes with type I signatures are interpreted to be syn-volcanic based on similarity in appearance to basalts and faint dyke margins without evidence of contact metamorphism. Type I mafic dykes occur in Hood 10, 41, 41A, 46 and 461.

Type II mafic rocks have a transitional to calc-alkaline magmatic affinity (Fig. 2-11). Type II mafic rocks are more LREE-, and in particular Th-, enriched than type I mafic rocks (Fig. 2-15B). They also have moderate negative Nb anomalies, weak positive Zr and Hf anomalies, and weak negative Ti anomalies (Figs. 2-14 and 2-15). Type I and II mafic rocks have very similar Zr/Yb and Nb/Yb values and the data array of type I and II rocks on a Nb/Th vs La/Sm diagram is consistent with crustal contamination (Fig. 2-14). Type II signatures are associated with a variety of lithologies including mafic flows, tuffs, and dykes. Type II dykes are interpreted to be syn-volcanic based on soft sediment deformation of mafic tuffs along their sinuous margins (Fig. 2-5B).



Type III mafic rocks are dykes with OIB to E-MORB signatures and Nb/Y values near the alkaline/subalkaline boundary (Fig. 2-11A). This suite is Nb- enriched compared to type I and II mafic rocks and have BAAB/MORB to alkalic affinities (Fig. 2-14).

Two dyke samples are type IV mafic rocks. These rocks have E-MORB with negative Nb anomalies signatures (Fig. 2-15D). They are less enriched in HFSE and REE than type II mafic rocks. They plot in the alkalic field in the Ti vs. V plot but have a subalkaline Nb/Y ratio (Fig. 2-14). This paradox is likely the result of weak positive Ti anomalies paired with moderate negative Nb anomalies for the type IV mafic rocks (Fig. 2-15).

#### ***2.7.2.3 Chemostratigraphic and Spatial Distributions of Geochemical Suites***

Within the individual lenses there is no strong spatial relationship between lithology or stratigraphic position and lithogeochemistry. The different rock suites are interlayered and show poor lateral continuity between drill holes. There is however, a notable geographical distribution of the geochemical suites. Type A felsic rocks occur in Hood 10, 41, 41A, 461 and 462. Type B felsic rocks are common only in the smaller northern mineral occurrences Hood 46, 461 and 462, are a minor component of Hood 10 and do not occur at all in Hood 41 and 41A. Overall felsic rocks are more voluminous in the north (Hood 10, 46, 461 and 462) than in the south (Hood 41 and 41A). Type I and II mafic rocks both occur in Hood 10 and 41A and are interlayered throughout those deposits. Only type I mafic rocks occur in Hood 41.

### **2.7.3 Mobile Element Lithogeochemistry**

#### ***2.7.3.1 Element Plots***

Geological and petrographic studies from the Hood deposit indicate that the rocks have variable quartz, sericite, and chlorite alteration (Fig. 2-4, Fig. 2-7, Fig. 2-8, Fig. 2-9 and Fig. 2-16). The alteration box plot for the Hood deposit samples indicates that felsic rocks have undergone both chlorite-pyrite and sericite alteration (Fig. 2-16). Suite B felsic rocks are more sericite altered than chlorite altered, whereas suite A felsic rocks are more chlorite-pyrite altered (Fig. 2-16). The majority of the intermediate and mafic rocks are chlorite-pyrite altered with lesser ankerite alteration (Fig. 2-16).

#### ***2.7.3.2 SWIR Spectroscopy***

The lithogeochemical indicators for chlorite and sericite alteration are supported by SWIR-spectroscopy. FeMg-chlorite and sericite were overwhelmingly the most commonly detected alteration minerals (Table A2-1). Downhole profiles of the alteration minerals detected by SWIR-spectroscopy do not demonstrate zoning; FeMg-chlorite and sericite occur throughout the deposits (Figs. A3-1 and A3-2). Minor alteration minerals, in order of decreasing abundance, include: phengite, Mg-chlorite, hornblende, illitic muscovite, Fe-chlorite, phlogopite, ankerite, epidote, and Fe-tourmaline.

#### ***2.7.3.3 Alteration Mass Change***

To quantify the elements lost and gained during alteration the multiple precursor method of MacLean (1990) has been utilized. MacLean's (1990) method allows chemical mass changes of altered rocks derived from multiple precursors to be determined,

assuming they are related by magmatic fractionation. While this assumption is often not the case for bimodal volcanic belts (Piercey, 2011), the method provides the best available method for areas with rocks having multiple magmatic affinities and compositions. A total of 18 samples are classified as “least altered” samples based on visual assessment of the degree of alteration, low volatile element content (low LOI), low metal contents (Cu, Zn, Pb, Ag, or Cd), SiO<sub>2</sub> content (<72 wt%), Al<sub>2</sub>O<sub>3</sub> content (11-16 wt%), and Na<sub>2</sub>O content (2-5 wt%) (Table A2-2).

The multiple precursor method uses the plotting of immobile compatible elements (e.g. Al<sub>2</sub>O<sub>3</sub>, TiO<sub>2</sub>) against immobile incompatible elements (e.g., Th, Zr) to determine the precursor composition of the immobile incompatible element for each sample (MacLean, 1990). The best fit line of the least altered samples is the magmatic fractionation line (Fig. 2-17A) (MacLean, 1990). The spread of data from the magmatic fractionation defines the alteration lines due to mass loss (sample falls above the fractionation line) and mass gain (sample falls below the fractionation line) that project through the origin (Fig. 2-17) (MacLean, 1990). The intersection of the alteration line and the fractionation line represents the precursor immobile element content (in this study Th) of a given sample (MacLean, 1990). Thorium was selected as the precursor immobile incompatible element instead of Zr because the least altered samples identified two different Zr vs Th trends (Fig. 2-17B). The enriched Zr trend is interpreted to be due to winnowing of tuffs before burial and Zr enrichments due to zircon accumulation.

The precursor Th content is used to compare the Th content in the altered rocks to calculate an enrichment factor ( $EF = Th_{\text{precursor}}/Th_{\text{altered}}$ ), which is used to correct for the

absolute mass change in the rock and obtain the reconstituted element concentration (RC) of the sample (MacLean, 1990):

$$RC = EF \times (\text{element in altered sample}) \quad \text{Eq. 1}$$

At the same time, using the least altered suite of samples, various elements are plotted against Th to obtain a precursor compositional equation (Fig. 2-17). This equation is then used to calculate the precursor elemental composition (PEC) of the samples (Table A2-3), and the difference between the precursor composition and the reconstituted composition represents the absolute mass change (MC) (MacLean, 1990):

$$MC = RC - PEC \quad \text{Eq. 2}$$

The ranges and average major element mass changes for each felsic and mafic suite type and deposit are presented in Table 2-2 and mass change of notable major elements for each sample is presented in (Table A2-2). Notable results are presented below.

#### 2.7.3.3.1 Major Element Mass Change

The calculated mass changes for  $\text{Al}_2\text{O}_3$  and  $\text{TiO}_2$  are typically low (~ 1-2 wt %) with a narrow range of values regardless of rock type or mineral occurrence (Tables 2-1 and A1-2), suggesting these elements are immobile and the MacLean (1990) multiple precursor method has provided reasonable results for mass change. Felsic rocks exhibit stronger mass gains of MgO in the sulfide lenses (Hood 10, 41 and 41A) compared to the smaller mineral occurrences (Hood 46, 461 and 462) (Table 2-2). Within an individual lens felsic suite A has typically gained more MgO than the other felsic suites (Table 2-2). Mass change of  $\text{Fe}_2\text{O}_3$  behaves similarly with more substantial gains at Hood 10, 41 and

41A compared to Hood 46, 461 and 462. Within lenses and occurrences suite A rocks exhibit greater  $\text{Fe}_2\text{O}_3$  mass gains than the other felsic suites (Table 2-2). Mafic rocks generally exhibit mass gains of  $\text{MgO}$  and  $\text{Fe}_2\text{O}_3$  (Table 2-2 and A1-2). Felsic rocks typically exhibit loss of  $\text{Na}_2\text{O}$  and gains of  $\text{K}_2\text{O}$ , whereas mafic rocks typically exhibit losses of both  $\text{Na}_2\text{O}$  and  $\text{K}_2\text{O}$  (Fig. 2-18A)

#### *2.7.3.3.2 Trace Element Mass Change*

Hood rocks have typically undergone small base metal gains with a few outlier samples having large base metal gains (Fig. 2-18D). High base metal gains are associated with mass gains in  $\text{MgO} + \text{Fe}_2\text{O}_3$  (Fig. 2-18D). Mass change in Pb is a minor component of the total base metal mass change (Table A2-1). Mass changes for Zr and Nb are variable with felsic rocks generally gaining more HFSE compared to the mafic rocks. (Fig. 2-18D; Table A2-1). Barium and Rb show significant variability in mass loss and gain with Ba and Rb gain associated with gains in  $\text{K}_2\text{O}$  (Fig. 2-18C). Hood rocks exhibit little loss or gain of Cs (Fig. 2-18C; Table A2-1). There is again an overall trend of mafic rocks losing LFSE and felsic rocks gaining LFSE (Figure 2-18D). Lanthanum and Sm show more mass loss and gain variability than Yb (Fig. 2-18D; Table A2-2). Most samples exhibit a mass loss of Yb (Fig. 2-18D). The REE do not show a strong relationship between rock composition and overall REE mass loss or gain (Fig. 2-18D).

#### *2.7.3.3.3 Spatial Distribution of Mass Change.*

To investigate the spatial distribution of element mass change, 3-D voxels were created using Geosoft Target<sup>TM</sup> extension for ESRI's ARCmap<sup>TM</sup> software. Kriging of core sample point data was done using a cell size of 8 m to create 3-D voxels of mass

change of selected elements. Two dimensional cross-section slices of the voxels are compared to stratigraphic sections for the Hood 10 and 41A deposits and presented in Figures 2-19, A3-3, and A3-4.

Areas of known mineralization correlate strongly to the zones of greatest gains in base metals (e.g., Cu and Zn) for both Hood 10 and 41A (Fig. 2-19) (Figure A3-3 and A3-4). Mass change plots for Hood 41A show a distinctive gain in  $\text{Fe}_2\text{O}_3$  and MgO as well as strong depletion of  $\text{Na}_2\text{O}$  for ~100 m in the stratigraphic footwall of the mineralization (Figure A3-4). In Hood 10 strong depletion of  $\text{Na}_2\text{O}$  and gains of  $\text{Fe}_2\text{O}_3$  and MgO occur within mineralized horizons and for ~100m below mineralization in the footwall (Figure A3-3). Mass change plots of the Hood 10 and 41A lenses demonstrate that their respective hanging walls also have undergone  $\text{Na}_2\text{O}$  mass loss and  $\text{Fe}_2\text{O}_3$  mass gains, albeit not as dramatically as in their footwalls, or immediately surrounding the mineralization. Hood 10 also has a zone of pronounced  $\text{SiO}_2$  gain immediately above mineralization (Figure A3-3I).

The spatial distribution of  $\text{K}_2\text{O}$  mass change does not show a distinctive zonation in relation to mineralization for Hood 41A; however, the distribution of the LFSE (Ba, Rb, Cs) mimics the mass gain and loss of  $\text{K}_2\text{O}$  (Figure A3-3 and A3-4). Strong mass loss of  $\text{K}_2\text{O}$  (and the LFSE) generally corresponds to mineralized areas in Hood 10 (Figure A3-3F, M, N, and O). Spatial distribution of REE (La, Sm, Yb) and HFSE (Zr, Nb) do not show distinctive zonation in relation to mineralization, suggesting that they are essentially immobile during the mineralizing process (Figure A3-3 and A3-4).

## **2.7.4 Principal Component Analysis**

### ***2.7.4.1 Method***

Principal component analysis (PCA) reduces the variables necessary to describe variation within a dataset and is useful when dealing with multi-element geochemical datasets (Grunsky, 2010). Principal components are the eigenvectors that describe the variance-covariance, or correlation matrix of a dataset (Davis, 2002). The corresponding eigenvalue for each eigenvector is proportional to the total variance that eigenvector represents (Davis, 2002). Eigenvectors that describe an insignificant amount of the variation in a dataset can be ignored, reducing the number of variables that have to be considered (Davis, 2002). Matrix multiplication of the original dataset with a matrix whose columns are the important eigenvectors creates a new matrix of principal component scores for each sample. When principal component scores for each sample are plotted against each other and against selected elements various geochemical processes, for example, fractionation, contamination and alteration trends, can be identified (Grunsky and Kjarsgaard, 2008; Grunsky, 2010). These plots also describe significant and quantifiable amounts of the total variation within a dataset (Davis, 2002; Grunsky, 2010).

The PCA analysis of the 60 element geochemical data set for the Hood deposit reduces the number of variables required to describe the variation to six. The following procedure was done. Because geochemical data are not typically normally distributed (Grunsky, 2010), and have orders of magnitude variation in concentrations, the data were normalized with the method outlined below. First, weight percent data were converted to parts per million and then the entire dataset was normalized using the following equation:

$$x_{nm} = \frac{x_i}{\sum_{i=1}^n x_i} \quad \text{Eq 3}$$

where  $x_{nm}$  is the normalized element value for a sample,

$x_i$  is the reported element value, and

$n$  is the number of samples in the population.

A symmetrical 60 x 60 variance-covariance matrix for all the elements in the data set is defined using the following equations:

$$\sigma^2 = \frac{\sum_{i=1}^n (x_i - \mu)^2}{n} \quad \text{Eq 4}$$

where  $\sigma^2$  is the variance or the square of the standard deviation of the values for element  $i$ ,

$n$  is number of samples in the population,

$x_i$  is the normalized element value for a given sample ( $i$ ), and

$\mu$  is the normalized population mean of the element;

and

$$cov_{jk} = \frac{n \sum_{i=1}^n x_{ij} x_{ik} - \sum_{i=1}^n x_{ij} \sum_{i=1}^n x_{ik}}{n(n-1)} \quad \text{Eq 5}$$

where  $cov_{jk}$  is the covariance of any two elements ( $j$  and  $k$ ),

$x_{ij}$  is the  $i^{\text{th}}$  measurement of the element denoted by  $j$ ,

$x_{ik}$  is the  $i^{\text{th}}$  measurement of the element denoted by  $k$ .

The principal components of the variance-covariance table were determined using IBM SPSS Statistics<sup>TM</sup> software. The same software was used for the matrix multiplication of the of principal components against the original dataset and additional



samples representing pure elements to calculate principal component scores for each sample and element.

#### **2.7.4.2 Results**

The six most significant eigenvectors for the variance-covariance matrix account for 89.7% of the total variance within the dataset (Table A2-4). Matrix multiplication of the normalized data matrix with the eigenvector matrix produced six principal component scores for each rock sample. Principal component scores were also calculated for all 60 individual elements.

Plots of principal component (PC) scores are shown in Figure 2-20. Principal component 1 accounts for 60% of the variation in the Hood sample dataset (Table A2-4) and the elements associated with PC1 are those associated with mineralization (Cu, Pb, Zn, Ag, S, Se, Bi, Hg, Cd) (Fig. 2-20) (Table A2-5). Other elements that have a positive, moderate PC1 scores (MgO, Fe<sub>2</sub>O<sub>3</sub>, MnO, As, and Co) are those associated with chlorite alteration and mineralization. Immobile elements such as HFSE, REE and Y have PC1 scores close to zero (Fig. 2-20; Table A2-5). Those associated with quartz-sericite alteration (K<sub>2</sub>O, SiO<sub>2</sub> and Na<sub>2</sub>O) have negative scores, or scores close to zero (Fig. 2-20; Table A2-5). The second principal component score has notable negative values for Cu, Cd, Se, Sn, and Zn and positive values for Bi, Te and Pb (Fig. 2-20; Table A2-5). The third principal component has negative scores for Te, Ag, Cu, Sn, Pb and Co and positive scores for Zn, S and Hg (Table A2-5). The fourth principal component produces the greatest spread in major elements, ranging from negative scores for elements such as CaO, MnO, Fe<sub>2</sub>O<sub>3</sub>, MgO and TiO<sub>2</sub> to positive scores for K<sub>2</sub>O, SiO<sub>2</sub>, Zr and the REE (Fig.

2-20; Table A2-5). Principal component 5 and PC6 are roughly inversely proportional with a few exceptions. Both PC5 and PC6 separate SiO<sub>2</sub> and K<sub>2</sub>O from Al<sub>2</sub>O<sub>3</sub>, Fe<sub>2</sub>O<sub>3</sub>, MnO, TiO<sub>2</sub>, Na<sub>2</sub>O, and CaO (Table A2-5).

## 2.8 DISCUSSION

### 2.8.1 Petrogenesis of the Hood VMS Deposits Host Rocks

Previous geochemical and isotopic studies of the felsic rocks of the ABVB indicate they are likely the result of low pressure (<1.0 GPa), dehydration melting of hydrated mafic rocks, accompanied by variable basement contamination (Jensen, 1995; Yamashita et al., 2000). Similar models have been proposed for rhyolitic rocks in greenstone belts globally (Leshner et al., 1986; Barrie et al., 1993; Hart et al., 2004; Piercey, 2011), and also for rhyolitic rocks in modern bimodal mafic environments (Shukuno et al., 2006; Bindeman et al., 2012). Inasmuch as the geochemistry of rhyolite in the study area is comparable to those of the models, the results herein are consistent with variations between volcanic suites being explained by slightly different petrogenetic histories. Although felsic suites A and B have broadly similar geochemical characteristics, felsic suite A is enriched in HFSE and REE, and has higher Zr/Ga and Zr/TiO<sub>2</sub> in comparison to suite B, which can be explained if suite A formed at higher temperatures than suite B (Fig. 2-12) (Watson and Harrison, 1983; Lentz, 1998; Hanchar and van Westrenen, 2007; Piercey et al., 2008). In particular, Watson and Harrison (1983), Hanchar and van Westrenen (2007), Lentz (2008), and Piercey et al. (2001, 2008) illustrated that with increasing temperature of melting, the magmas generated will have greater HFSE and REE contents, features consistent with their concentrations in suite A

versus suite B. This hypothesis is also supported by Nb/Ta values. Felsic suite A has slightly higher Nb/Ta ratios (mean =12.9) compared to suite B felsic rocks (mean =10.3) and both are closer to values for the upper continental crust (Nb/Ta =~11-12) than for the mantle (Nb/Ta = ~17.5) (Green, 1995; Kamber and Collerson, 2000; Rudnick et al., 2000). This suggests an important role for continental crustal contamination of felsic rocks in both suites A and B; however, the slightly higher Nb/Ta in suite A is consistent with these felsic rocks having a greater mantle component in their genesis, and is indirectly indicative of formation at a higher temperature.

There are important spatial and metallogenic associations of the various felsic suites. Felsic suite B is confined to the northern end of the Hood deposits area, hosting the minor Hood 46, Hood 461 and Hood 462 mineral occurrences and occurring as a minor component of Hood 10, whereas felsic suite A is associated with the bulk of the more mineralized areas including Hood 10, 41 and 41A. These relationships imply that the more prospective stratigraphic packages were associated with rhyolitic rocks that had higher temperatures of emplacement, whereas less prospective areas were associated with cooler temperatures of emplacement, and likely a less thermally anomalous environment of formation. This is also supported by felsic suite A having primarily of FII-type affinities, whereas suite B have unfavourable FI-type signatures (Fig.2-12C) (Leshner et al., 1986; Hart et al., 2004).

The two main mafic magmatic suites (I and II) are consistent with derivation from moderately enriched mantle source based on Zr, Nb, and Yb systematics (Fig. 2-14). Zr/Yb and Nb/Yb ratios are useful for determining magmatic sources because Zr, Yb and Nb are incompatible elements and are resistant to the effects of partial melting and

fractionation (Pearce and Peate, 1995). The most pronounced difference between the two suites is Nb/Th<sub>pnn</sub> ratios, with type I mafic rocks having flat to positive Nb anomalies (Nb/Th<sub>pnn</sub> ≥ 1) and the type II mafic rocks exhibiting negative Nb anomalies (Nb/Th<sub>pnn</sub> < 1). Negative Nb anomalies in basalts have been interpreted as both the results of subduction-related metasomatism (Pearce and Peate, 1995) and/or the contamination of mafic magma by continental crust (Kerrick and Wyman, 1997; Piercey et al., 2004). In this case, type II mafic rocks are interpreted to be crustally contaminated type I rocks on the basis of their strong negative Nb anomalies, higher La/Sm compared to type I mafic rocks, and the distribution of type I and type II along a single continuous trend on a Nb/Th vs La/Sm plot (Figs. 2-14 and 2-15). This conclusion is compatible with geochemical and Nd isotopic work by Yamashita et al. (2000), who concluded that both mafic suites were contaminated by continental crust in a sialic back-arc basin setting. The interlayering of type I mafic rocks with type II mafic rocks at Hood 10 and Hood 41A suggests variable contamination of a MORB-type magma by continental basement.

The other two mafic suites (III and IV) occur in the cross-cutting dykes only and postdate VMS mineralization. They illustrate broadly similar signatures and hence are interpreted as indicative of a similar tectonic environment of formation for the later magmatic events after the formation of mineralization.

The presence of FII rhyolitic rocks associated with E-MORB-type signatures, is consistent with the Hood deposits forming within an environment comparable to a modern extensional back-arc basin environment (Yamashita et al., 2000), and is a petrochemical assemblage commonly found in VMS environments (Piercey, 2011). In this chemostratigraphic and geodynamic scenario, it has been frequently inferred that the

felsic rocks formed from the melting of a mafic to felsic substrate by the upwelling of MORB-type magmas during extension (Lentz, 1998; Piercey et al., 2001; Piercey et al., 2008; Piercey, 2011). This type of setting allows for abundant heat to be transferred to the near-surface environment, thus creating a thermally anomalous environment that could drive and sustain hydrothermal activity (Piercey, 2011). Furthermore, it is compatible with the observed lithologies and the formation of extensional structures that allow recharge, focusing and discharge of VMS-forming hydrothermal fluids (Piercey, 2011).

This model, along with the general VMS model, is compatible with the occurrence of high level sub-volcanic intrusive complexes that act as the “heat pump” to drive hydrothermal circulation (Galley, 1993, 2003; Franklin et al., 2005; Galley et al., 2007). The large ca. 2676 Ma synvolcanic (Yamashita et al., 2000) Rim granite may have acted as the heat source to drive the hydrothermal circulation that formed the Hood VMS deposits. The synvolcanic emplacement and its similar composition to felsic suite A, support a petrogenetic link (Figs. 2-12 and 2-13). The geochemical differences between the Rim granite and the petrologically identical offshoot granite dykes that crosscut the Hood 41A deposit (Figs. 2-12 and 2-13) can be explained by effective fractionation and segregation of REE-rich accessory phases, such as zircon. In particular, zircon fractionation results in a low Zr/Hf ratio in derivative liquids (Claiborne et al., 2006), a feature present in the granite dykes but lacking in the main body of the Rim granite (Table A2-1). Furthermore, the lower REE in the dykes compared to the granite is also consistent with REE sequestering in early crystallizing REE-phases during fractionation (Mittlefehldt and Miller, 1983).

### 2.8.2 Hydrothermal Alteration

Volcanogenic massive sulfide deposits commonly have distinctive footwall alteration assemblages, typically with chlorite proximal to mineralization and with sericite (+/- quartz) distal from mineralization (Franklin et al., 1981; Gemmell and Large, 1992; Large et al., 2001a; Franklin et al., 2005). In some cases, where deposits were rapidly covered by hanging wall strata, or formed by subseafloor replacement, there is distinctive hanging wall alteration (Gemmell and Fulton, 2001; Doyle and Allen, 2003). The results of mapping, lithogeochemistry, and SWIR spectroscopy show that the Hood deposits contain alteration similar to many VMS deposits (Figs. 2-6, 2-18, A3-1, and A3-2). Hood 41 and 41A exhibit notably stronger chlorite alteration in the footwall than in the hanging wall. Unlike many VMS deposits, however, the Hood deposits, particularly the Hood 10 deposits, do not show a pronounced difference in footwall vs hanging-wall alteration intensity. The hanging walls of the Hood deposits contain moderate chlorite and sericite (+/- quartz) alteration, resulting in less distinctive alteration mineral zonation in the Hood deposits than in other VMS deposits. This may be due in part to the limited depth of drilling below mineralization and our sample suite being proximal to mineralization. This alteration distribution, coupled with textural evidence of abundant clasts in mineralization, suggest the Hood 10 deposit likely formed from sub-seafloor replacement rather than exhalation (Doyle and Allen, 2003).

Short-wave infrared spectroscopy supports the above assertions and indicates that FeMg-chlorite and sericite (muscovite) are the dominant alteration minerals within the

Hood deposit (Table A2-2). Spatial distribution of SWIR-spectroscopy results, however, did not identify any zoning of the alteration minerals (Figure A3-1 and A3-2).

#### ***2.8.2.1 Element Mass Changes Associated with Alteration and Mineralization***

There are notable differences in major element mass changes between rock types and deposits in the Hood deposits. Type A felsic rocks have typically gained more  $\text{Fe}_2\text{O}_3$  and  $\text{MgO}$  and lower  $\text{Na}_2\text{O}$  than type B and C felsic rocks, particularly at the three deposits Hood 10, Hood 41, and Hood 41A (Table 2-2). As previously discussed, type A felsic rocks are the more favourable host rock for mineralization and this increase in  $\text{Fe}_2\text{O}_3$  and  $\text{MgO}$  and losses in  $\text{Na}_2\text{O}$  is likely because of the stronger development of FeMg-chlorite associated with mineralization. The gain of  $\text{K}_2\text{O}$  in felsic rocks as opposed to the  $\text{K}_2\text{O}$  loss in mafic rocks, and the general gain of  $\text{Fe}_2\text{O}_3$  and  $\text{MgO}$  in mafic suites, is the result of the development of sericite and chlorite in felsic and mafic rocks, respectively, and indicates that the reactivity of the lithology is an important control on alteration mineral development (Riverin and Hodgson, 1980; Hajash and Chandler, 1981; Barrett and MacLean, 1994; Large et al., 2001b).

Base metal mass gains are associated with strong chlorite development (larger gains in  $\text{Fe}_2\text{O}_3$  and  $\text{MgO}$ ) (Table A2-2). The samples with anomalously high base metal gains are directly adjacent to mineralized horizons (Fig. A3-3 and A3-4). Mass changes of low field strength elements correlate strongly with mass loss and gain of  $\text{K}_2\text{O}$ , indicating that LFSE mass change is related to the development sericite alteration (Table A2-2). Rare earth elements have low mass loss and gains with unclear relationships to

chlorite or sericite alteration, suggesting that they had minimal mobility and were essentially immobile.

High field strength elements (Zr and Nb) show moderate mass loss and gain; however, there is a distinctive trend of HFSE mass loss in mafic rocks to HFSE mass gain in felsic rocks (Fig. 2-18D). Given that both empirical and experimental evidence suggests that these elements are immobile in most cases except in the presence of F or C (Winchester and Floyd, 1977; Barrett and MacLean, 1994; Jenner, 1996), except for extreme alteration or in the presence of complexing ligands (Campbell et al., 1984; Rubin et al., 1993; Bau and Dulski, 1995), the data indicate that the multiple precursor method does not completely account for compositional variation related to magma fractionation and the actual mass change in HFSE is likely less than calculated (Table A2-2).

#### ***2.8.2.2 Spatial Distribution of Element Mass Change and Principal Component Analysis***

Spatial distribution of element mass change and principal component analysis for Hood 10 and 41A illustrates the relationships between mass change, principal component analysis, mineralization, hanging wall alteration, and footwall alteration (Fig. 2-19). These relationships can be useful for vectoring to mineralization and identifying areas of high mineral potential.

The data in this study show that principal component analysis is extremely useful in delineating elemental groupings associated with various geochemical processes associated with rock formation, alteration, and mineralization within the Hood River deposit. Principal component 1 (PC1) represents the majority of variation within dataset



and clearly identifies metallic elements associated with mineralization (Cu, Pb, Zn, Ag), as well as those associated with chlorite alteration (e.g.  $\text{Fe}_2\text{O}_3$ , MgO and MnO), albeit with lower scores (Table 2-4; Fig. 2-19). Contouring and kriging of the PC1 scores indicates zones of the highest PC1 scores broadly correspond with the areas of known mineralization (Fig. 2-19). In spite of all the samples being taken within ~300m of mineralization and sampling being limited to non-mineralized host rock, the principal component analysis was successful at determining the areas of highest mineral potential.

The greater gain of  $\text{Fe}_2\text{O}_3$  and MgO downhole from mineralization in Hood 10 and uphole from mineralization in Hood 41A supports the interpretation that the Hood 10 is right way up and youngs to the northeast and that Hood 41A is overturned and youngs to the northeast (Figs. A3-3 and A3-4). The lesser but still overall mass gain of MgO and  $\text{Fe}_2\text{O}_3$  in the hanging wall to mineralization compared to the footwall in both deposits supports the interpretation of replacement-type mineralization as chlorite is developed in both the footwall and the hanging wall (Figs. A3-3 and A3-4)(Doyle and Allen, 2003).

The general depletion of  $\text{Na}_2\text{O}$  throughout the footwall and the hanging wall is likely a reflection of the destruction of albite by hydrothermal fluids (Figs. 2-19 and A3-3) (Riverin and Hodgson, 1980; Date et al., 1983; Barrett and MacLean, 1994; Large et al., 2001b). At Hood 10 the mass loss of  $\text{Na}_2\text{O}$  away from the mineralized zone is accompanied by a gain of  $\text{K}_2\text{O}$ , reflective of the feldspar replacement by sericite (Figs. 2-19, A3-3, and A3-4) (Riverin and Hodgson, 1980; Hajash and Chandler, 1981; Date et al., 1983; Large et al., 2001b). However, closer to the mineralization (~20 m) the mass loss of  $\text{Na}_2\text{O}$  is accompanied by a mass loss of  $\text{K}_2\text{O}$ , likely the result of the further alteration of sericite into chlorite (Riverin and Hodgson, 1980; Large et al., 2001b). The similarity

between the mass loss and gain distribution of K<sub>2</sub>O and that of the LFSE (Ba, Rb, Cs) indicates the similar behaviour of those elements to K (Figs. A3-3 and A3-4).

The absence of distinctive patterns related to mineralization for the HFSE and the REE suggest that their behaviour is not strongly controlled by alteration and is controlled to a greater extent by the initial host rock type and magmatic suite, and that these elements were essentially immobile during fluid-rock interaction.

### **2.8.3 Tectonic Setting and the Slave Craton**

Understanding the tectonic setting of VMS deposits is important for assessing the mineral potential of similar environments (e.g. Leshner et al., 1986; Swinden, 1991; Lentz, 1998; Hart et al., 2004; Piercey, 2011). The tectonic origin of the Slave greenstone belts remains a subject of considerable debate (Hamilton, 1998; Kusky and Polat, 1999; Bleeker, 2002; Helmstaedt and Pehrsson, 2012). The greenstone belts of the Slave Craton have previously been divided based on geochemistry, geographic distribution, and geochronology largely based on studies of the southern Slave Craton, particularly of the Yellowknife volcanic belt (YVB) (Fig. 2-1). (Fyson and Helmstaedt, 1988; Padgham, 1992; Padgham and Fyson, 1992; Isachsen and Bowring, 1994; Jensen, 1995; Villeneuve et al., 1997; Cousens, 2000; Cousens et al., 2002). This has resulted in an evolving terminology to describe these belts from Yellowknife-belt-type vs Hackett River-type greenstone belts (Padgham, 1992) to Kam Group and correlatives (2.73-2.70 Ga) vs Banting Group and correlatives (2.69-2.66 Ga) (Cousens et al., 2002; Bleeker and Hall, 2007; Helmstaedt and Pehrsson, 2012). Similarly, multiple tectonic origins for the Slave Craton greenstone belts have been proposed including accretion of island arcs (Kusky,

1991), back-arc or modified back-arc settings (Northrup et al., 1999; Yamashita et al., 2000; Goodwin et al., 2006), continental rifts, and marginal continental rift settings (Cousens, 2000) with subsequent arc-related volcanism (MacLachlan and Helmstaedt, 1995).

Studies of the ABVB (in the northwestern part of the Slave Craton) offer an opportunity to test a “pan-Slave” tectonic model by comparing the ABVB to greenstone belts of similar age in the Slave Craton and the various tectonic models. Although the 2662 Ma Banting Group of the YVB is younger than the ABVB, the Banting Group is nonetheless frequently compared with all  $< 2.7$  Ga volcanic rocks of the Slave craton (Mortensen et al., 1988; Isachsen et al., 1991; Yamashita et al., 2000). The volcanic rocks of the Banting Group differ from the Hood deposit volcanic rocks in that they have an adakitic composition with high Sr, and depleted HREE absent from the Hood volcanic rocks (Cousens et al., 2002; Goodwin et al., 2006). Instead, the Hood volcanic rocks have similar minor and trace element geochemical characteristics to the bimodal calc-alkaline volcanic rocks in the Tumpline Lake area of the Cameron River-Beaulieu River volcanic belt (CR-BR) in the south of the Slave craton (Goodwin et al., 2006). Though the timing of volcanism in the Tumpline Lake area is poorly constrained, it is interpreted to be part of the younger 2.68-2.66 Ga volcanic package in the CR-BR (Goodwin et al., 2006). In the central Slave Craton, the volcanic rocks in 2.69-2.67 Ga Point Lake volcanic belt (PLVB) are coeval with the ABVB. Though the PLVB is dominated by the tholeiitic basalts of the Peltier formation, those rocks are overlain by the bimodal calc-alkaline rocks of the Samandre and Beuparlant formation (Corcoran and Dostal, 2001). However,

the calc-alkaline volcanics are depleted in HREE unlike the ABVB volcanic rocks (Corcoran and Dostal, 2001).

In spite of some differences in geochemistry and timing, the proposed models for the genesis of the CR-BR and the PLVB both invoke continental marginal back-arc basin settings, which account for the para-autochthonous nature of many Slave greenstone belts (Corcoran and Dostal, 2001; Goodwin et al., 2006). Given that the ABVB has stronger geochemical similarities to the Tumpline Lake volcanics of the CR-BR and is more similar timing of volcanism to the PLVB than the Banting Group, using the petrogenetic history and geochemistry of the Banting Group as the type location for all 2.69-2.66 Ga greenstone belts of the Slave Craton is flawed. Thus, tectonic models for the development of greenstone belts in the Slave craton should be based on volcanic belts other than the Yellowknife greenstone belts, particularly for the 2.69-2.67 Ga era of volcanism.

Previous geochemical and isotopic studies of the ABVB suggested that it formed in an Archean environment comparable to a modern back-arc basin marginal to pre-existing continental crust where sialic crust interacted with primitive magmas (Jensen, 1995; Yamashita et al., 2000). This tectonic setting is similar to the model proposed for the Point Lake volcanic belt (Corcoran and Dostal, 2001). Such an environment is consistent with the variable crustal contamination of MORB-like and MORB-derived mafic and felsic rock suites identified in this study, and the felsic volcanic rocks of the belt having variable mantle and continental signatures. The similarity in tectonic setting between the ABVB, PLVB and CR-BR suggests that tectonic models developed based on greenstone belts other than the YVB can be applied to greenstone belts further north.

Marginal continental arcs and associated back-basins are a favourable environment for the formation of VMS systems (e.g. Lentz, 1999; Piercey et al., 2004; Whalen et al., 2004; Piercey, 2011 and references therein). The extensional tectonic environment of formation for the belt, the association of mineralization with high temperature felsic magmatism, and the presence of large syn-volcanic plutons, such as the Rim granite, suggest that high heat flow and extension were critical to driving and localizing hydrothermal circulation, leading to the formation of the VMS deposits in the ABVB. The presence of known VMS mineralization in the ABVB, the common field alteration and petrological associations to global VMS environments, and the similarity of the ABVB to other Slave greenstone belts further indicate the high potential for VMS deposits throughout the Slave craton.

## **2.9 CONCLUSIONS**

The Hood deposit is a series of sub-seafloor replacement mineralized lenses hosted by felsic volcanic rocks with minor mafic flows and volcanoclastic rocks. Mineralization is zoned, varying from massive to semi-massive chalcopyrite-rich zones to massive to semi-massive sphalerite-rich zones to chalcopyrite stringer zones. Immobile element lithogeochemistry is useful for the determination of chemostratigraphic units identifying two main felsic volcanic suites (suites A and B), a third minor felsic volcanic suite (suite C) in addition to confirming the existence of two main mafic volcanic suites (types I and II) previously identified in the ABVB area.

The most important conclusion from this study concerns the slight differences in petrogenesis on mineralization potential. Trace element geochemistry is key to detecting

subtle differences in felsic rock geochemistry that have important ramifications for localized VMS mineralization potential. The felsic suite A contains the large majority of the mineralization whereas felsic suite B is largely barren. As suite A rocks have higher HFSE and REE contents and Nb/Ta ratios and lower  $\text{Al}_2\text{O}_3$  ratios than suite B it is suggested that they represent melts that had hotter temperatures of emplacement and less crustal contamination leading to more favourable conditions for VMS formation. The associated large coeval pluton in the area is geochemically identical to the felsic suite A and may have acted as a subvolcanic intrusive complex that provided the heat source and drove the mineralizing hydrothermal system.

Hydrothermal alteration is associated with VMS mineralization at Hood. Chlorite and sericite (+/- quartz) alteration are predominant and associated with elemental mass gains in  $\text{Fe}_2\text{O}_3$  and MgO in both the footwall and hanging walls of the mineralized lenses supporting the interpretation of replacement-style mineralization. Further mass change results indicate that suite A felsic rocks have undergone the largest losses of  $\text{Na}_2\text{O}$  and the greatest gains of MgO and  $\text{Fe}_2\text{O}_3$ , of all felsic rocks, supporting their higher prospectivity for mineralization.

The Hood VMS deposit is interpreted to have formed in an environment comparable to modern continental marginal back-arc basin. The eruption of magma through the pre-existing sialic basement resulted in the contamination of the felsic and mafic magmas. This type of extensional environment associated with high heat flow is similar to global VMS environments proximal to continental margins (e.g., Sturgeon Lake, Bathurst, Finlayson Lake). The ABVB is similar to other ca. 2.68 Ga belts of the Slave Craton supporting the VMS potential of many Slave Craton greenstone belts.

## References

- Barrett, T. J., and MacLean, W. H., 1994, Mass changes in hydrothermal alteration zones associated with VMS deposits of the Noranda area: *Exploration and Mining Geology*, v. 3, p. 131-160.
- Barrett, T. J., and MacLean, W. H., 1999, Volcanic sequences, lithogeochemistry, and hydrothermal alteration in some bimodal volcanic-associated massive sulfide systems, *in* Barrie, C. T., and Hannington, M. D., eds., *Volcanic-Associated Massive Sulfide Deposits: Processes and Examples in Modern and Ancient Environments*, *Reviews in Economic Geology* 8, Society of Economic Geologists, p. 101-131.
- Barrie, C. T., Ludden, J. N., and Green, T. H., 1993, Geochemistry of volcanic rocks associated with Cu-Zn and Ni-Cu deposits in the Abitibi Subprovince: *Economic Geology*, v. 88, p. 1341-1358.
- Bau, M., and Dulski, P., 1995, Comparative study of yttrium and rare-earth element behaviours in fluorine-rich hydrothermal fluids: *Contributions to Mineralogy and Petrology*, v. 119, p. 213-223.
- Bindeman, I., Gurenko, A., Carley, T., Miller, C., Martin, E., and Sigmarsson, O., 2012, Silicic magma petrogenesis in Iceland by remelting of hydrothermally altered crust based on oxygen isotope diversity and disequilibria between zircon and magma with implications for MORB: *Terra Nova*, v. 24, p. 227-232.
- Bleeker, W., 2002, Archaean tectonics: a review, with illustrations from the Slave craton, *in* Fowler, C. M. R., Ebinger, C. J., and Hawkesworth, C. J., eds., *The Early Earth: Physical, Chemical and Biological Development*, Special Publication: London, Geological Society, p. 151-181.
- Bleeker, W., and Hall, B., 2007, The Slave craton: geological and metallogenic evolution, *in* Goodfellow, W. D., ed., *Mineral Deposits of Canada: A Synthesis of Major Deposit-types, District Metallogeny, the Evolution of Geological Provinces, and Exploration Methods*, Special Publication 5, Mineral Deposits Division, Geological Association of Canada, p. 849-879.
- Bleeker, W., Ketchum, J., Jackson, V., and Villeneuve, M., 1999, The Central Slave Basement Complex, Part I: its structural topology and autochthonous cover: *Canadian Journal of Earth Sciences*, v. 36, p. 1083-1109.
- Bruce, C. S., 1991, Hood River Project # 708 - Report on the 1990 Field Program: Falconbridge Limited Company Report, p. 1-59.

Campbell, I. H., Leshar, C. M., Coad, P., Franklin, J. M., Gorton, M. P., and Thurston, P. C., 1984, Rare-earth element mobility in alteration pipes below massive Cu-Zn sulfide deposits: *Chemical Geology*, v. 45, p. 181-202.

Claiborne, L. L., Miller, C. F., Walker, B. A., Wooden, J. L., Mazdab, F. K., and Bea, F., 2006, Tracking magmatic processes through Zr/Hf ratios in rocks and Hf and Ti zoning in zircons: An example from the Spirit Mountain batholith, Nevada: *Mineralogical Magazine*, v. 70, p. 517-543.

Corcoran, P.L., and Dostal, J., 2001, Development of an ancient back-arc basin overlying continental crust: the archean Peltier Formation, Northwest Territories, Canada: *The Journal of Geology*, v. 109, p. 329-348.

Cousens, B. L., 2000, Geochemistry of the Archean Kam Group, Yellowknife Greenstone Belt, Slave Province, Canada: *Journal of Geology*, v. 108, p. 181-197.

Cousens, B., Facey, K., and Falck, H., 2002, Geochemistry of the late Archean Banting Group, Yellowknife greenstone belt, Slave Province, Canada; simultaneous melting of the upper mantle and juvenile mafic crust: *Canadian Journal of Earth Sciences* v. 39, p. 1635-1656.

Cudahy, T. J., Okada, K., Yamato, Y., Yoshizawa, K., Wilson, J., and Brauhart, C., 2001, Archean VMS Hydrothermal alteration systems at Panorama, WA, revealed through airborne VNIR-SWIR spectrometry: *Contributions of the Economic Geology Research Unit*, v. 59, p. 40-41.

Date, J., Watanabe, Y., and Saeki, Y., 1983, Zonal alteration around the Fukazawa Kuroko deposits, Akita Prefecture, northern Japan., *in* Ohmoto, H., and Skinner, B. J., eds., *Kuroko and Related Volcanogenic Massive Sulfide Deposits*, *Economic Geology Monograph* 5, p. 365-386.

Davis, J. C., 2002, *Statistics and Data Analysis in Geology*, Third Edition: New York, John Wiley and Sons, 638 p.

Davis, W., and Bleeker, W., 1999, Timing of plutonism, deformation, and metamorphism in the Yellowknife Domain, Slave Province, Canada: *Canadian Journal of Earth Sciences*, v. 36, p. 1169-1187.

Davis, W., and Hegner, E., 1992, Neodymium isotopic evidence for the tectonic assembly of the Late Archean crust in the Slave Province, northwest Canada: *Contributions to Mineralogy and Petrology*, v. 111, p. 493-504.

Davis, W. J., Fryer, B. J., and King, J. E., 1994, Geochemistry and evolution of Late Archean plutonism and its significance to the tectonic development of the Slave craton: *Precambrian Research*, v. 67, p. 207-241.



Doyle, M. G., and Allen, R. L., 2003, Subsea-floor replacement in volcanic-hosted massive sulfide deposits: *Ore Geology Reviews*, v. 23, p. 183-222.

Franklin, J. M., Lydon, J. W., and Sangster, D. F., 1981, Volcanic-associated massive sulfide deposits, *in* Skinner, B. J., ed., *Economic Geology 75th Anniversary Volume*, p. 485-627.

Franklin, J. M., Gibson, H. L., Galley, A. G., and Jonasson, I. R., 2005, Volcanogenic Massive Sulfide Deposits, *in* Hedenquist, J. W., Thompson, J. F. H., Goldfarb, R. J., and Richards, J. P., eds., *Economic Geology 100th Anniversary Volume*: Littleton, CO, Society of Economic Geologists, p. 523-560.

Fyson, W. K., and Helmstaedt, H., 1988, Structural patterns and tectonic evolution of supracrustal domains in the Archean Slave Province, Canada: *Canadian Journal of Earth Sciences*, v. 25, p. 301-315.

Galley, A. G., 1993, Characteristics of semi-conformable alteration zones associated with volcanogenic massive sulphide districts: *Journal of Geochemical Exploration*, v. 48, p. 175-200.

Galley, A. G., 2003, Composite synvolcanic intrusions associated with Precambrian VMS-related hydrothermal systems: *Mineralium Deposita*, v. 38, p. 443 - 473.

Galley, A. G., Hannington, M., and Jonasson, I., 2007, Volcanogenic massive sulphide deposits, *in* Goodfellow, W. D., ed., *Mineral Deposits of Canada: A Synthesis of Major Deposit-types, District Metallogeny, the Evolution of Geological Provinces, and Exploration Methods*, Special Publication 5, Mineral Deposits Division, Geological Association of Canada, p. 141-161.

Gebert, J. S., 1995, Archean Geology of the Hanikahimajuk Lake Area, Northern Point Lake Volcanic Belt, West-Central Slave Structural Province, District of Mackenzie, N.W.T.: NWT EGS Open File p. 27.

Gemmell, J. B., and Fulton, R., 2001, Geology, genesis, and exploration implications of the footwall and hanging-wall alteration associated with the Hellyer volcanic-hosted massive sulphide deposit, Tasmania, Australia.: *Economic Geology*, v. 96, p. 1003-1036.

Gemmell, J. B., and Large, R. R., 1992, Stringer system and alteration zones underlying the Hellyer volcanic-hosted massive sulfide deposit, Tasmania, Australia: *Economic Geology*, v. 87, p. 620-649.

Gill, J. W., 1977, The Takiyuak metavolcanic belt: Geology, geochemistry, and mineralization: Unpub. Ph.D. thesis, Carleton University, Ottawa, Ontario, Canada, 210 p.

Goodwin, A. M., Lambert, M. B., and Ujike, O., 2006, Geochemical and metallogenic relations in volcanic rocks of the southern Slave Province: implications for late Neoproterozoic tectonics: Canadian Journal of Earth Sciences, v. 43, p. 1835-1857.

Green, T. H., 1995, Significance of Nb/Ta as an indicator of geochemical processes in the crust-mantle system: Chemical Geology, v. 120, p. 347-359.

Grunsky, E. C., 2010, The interpretation of geochemical survey data: Geochemistry: Exploration, Environment, Analysis, v. 10, p. 27-74.

Grunsky, E. C., and Kjarsgaard, B. A., 2008, Classification of distinct eruptive phases of the diamondiferous Star kimberlite, Saskatchewan, Canada based on statistical treatment of whole rock geochemical analyses: Applied Geochemistry, v. 23, p. 3321-3336.

Hajash, A., and Chandler, G. W., 1981, An experimental investigation of high-temperature interactions between seawater and rhyolite, andesite, basalt and peridotite: Contributions to Mineralogy and Petrology, v. 78, p. 240-254.

Hamilton, W. B., 1998, Archean magmatism and deformation were not products of plate tectonics: Precambrian Research, v. 91, p. 143-179.

Hanchar, J. M., and van Westrenen, W., 2007, Rare Earth Element Behavior in Zircon-Melt Systems: ELEMENTS, v. 3, p. 37-42.

Hart, T. R., Gibson, H. L., and Leshner, C. M., 2004, Trace element geochemistry and petrogenesis of felsic volcanic rocks associated with volcanogenic massive Cu-Zn-Pb sulfide deposits: Economic Geology, v. 99, p. 1003-1013.

Hassard, F. R., 1983, Hood River- No. 10 Deposit, Diamond Drilling, Geological and Geophysical Exploration and Compilation: Kidd Creek Mines Ltd. - Company Report, p. 42.

Helmstaedt, H., and Padgham, W. A., 1986, A new look at the stratigraphy of the Yellowknife Supergroup at Yellowknife, N.W.T. – implications for the age of gold-bearing shear zones and Archean basin evolution: Canadian Journal of Earth Sciences, v. 23, p. 454-475.

Helmstaedt, H. H., and Pehrsson, S. J., 2012, Geology and Tectonic Evolution of the Slave Province - A Post-Lithoprobe Perspective, in Percival, J. A., Cook, F. A., and

Clowes, R. M., eds., Tectonic Styles in Canada: The Lithoprobe Perspective. Special Paper, Geological Association of Canada, p. 379-466.

Herrmann, W., Blake, M., Doyle, M., Huston, D., Kamprad, J., Merry, N., and Pontual, S., 2001, Short Wavelength Infrared (SWIR) Spectral Analysis of Hydrothermal Alteration Zones Associated with Base Metal Sulfide Deposits at Rosebery and Western Tharsis, Tasmania, and Highway-Reward, Queensland: *Economic Geology*, v. 96, p. 939-955.

Hoffman, P. F., 1988, United plates of America, the birth of a craton: Early Proterozoic assembly and growth of Laurentia: *Annual Reviews of Earth and Planetary Science*, v. 16, p. 543-603.

Isachsen, C. E., and Bowring, S. A., 1994, Evolution of the Slave Craton: *Geology*, v. 22, p. 917-920.

Isachsen, C.E., and Bowring, S. A., 1997, The Bell Lake group and Anton Complex: a basement – cover sequence beneath the Archean Yellowknife greenstone belt revealed and implicated in greenstone belt formation: *Canadian Journal of Earth Sciences*, v. 34, p. 169-189.

Isachsen, C. E., Bowring, S. A., and Padgham, W. A., 1991, U-Pb Zircon Geochronology of the Yellowknife Volcanic Belt, NWT, Canada: New Constraints on the Timing and Duration of Greenstone Belt Magmatism: *The Journal of Geology*, v. 99, p. 55-67.

Jenner, G. A., 1996, Trace element geochemistry of igneous rocks: Geochemical nomenclature and analytical geochemistry, *in* Wyman, D. A., ed., *Trace Element Geochemistry of Volcanic Rocks: Applications for Massive Sulfide Exploration*, Short Course Notes Volume 12., Geological Association of Canada, p. 51-77.

Jensen, J. E., 1995, Geology, geochemistry and Nd isotopic study of the Hanikahimajuk Lake area, Slave Province, NWT: Unpub. M.Sc. Thesis, University of Alberta, Edmonton, Alberta.

Kamber, B. S., and Collerson, K. D., 2000, Role of 'hidden' deeply subducted slabs in mantle depletion: *Chemical Geology*, v. 166, p. 241-254.

Kerrick, R., and Wyman, D. A., 1997, Review of developments in trace-element fingerprinting of geodynamic settings and their implications for mineral exploration: *Australian Journal of Earth Sciences*, v. 44, p. 465-487.

Kusky, T. M., 1991, Structural development of an archaean orogen, western Point Lake, Northwest Territories: *Tectonics*, v. 10, p. 820-841.

Kusky, T. M., and Polat, A., 1999, Growth of granite-greenstone terranes at convergent margins, and stabilization of Archean cratons: *Tectonophysics*, v. 305, p. 43-73.

Large, R. R., Allen, R. L., Blake, M. D., and Herrmann, W., 2001a, Hydrothermal alteration and volatile element haloes for the Rosebery K Lens volcanic-hosted massive sulfide deposit, western Tasmania: *Economic Geology*, v. 96, p. 1055-1072.

Large, R. R., Gemmell, J. B., Paulick, H., and Huston, D. L., 2001b, The alteration box plot: a simple approach to understanding the relationships between alteration mineralogy and lithogeochemistry associated with VHMS deposits: *Economic Geology*, v. 96, p. 957-971.

Lentz, D. R., 1998, Petrogenetic evolution of felsic volcanic sequences associated with Phanerozoic volcanic-hosted massive sulfide systems: the role of extensional geodynamics: *Ore Geology Reviews*, v. 12, p. 289-327.

Lentz, D. R., 1999, Petrology, geochemistry and oxygen isotopic interpretation of felsic volcanic and related rocks hosting the Brunswick 6 and 12 massive sulfide deposits (Brunswick Belt), Bathurst Mining Camp, New Brunswick, Canada: *Economic Geology*, v. 94, p. 57-86.

Leshner, C. M., Goodwin, A. M., Campbell, I. H., and Gorton, M. P., 1986, Trace element geochemistry of ore-associated and barren felsic metavolcanic rocks in the Superior province, Canada: *Canadian Journal of Earth Sciences*, v. 23, p. 222-237.

MacLachlan, K., and Helmstaedt, H., 1995, Geology and geochemistry of an Archean mafic dyke complex in the Chan formation-basis for a revised plate-tectonic model of the Yellowknife greenstone-belt: *Canadian Journal of Earth Sciences*, v. 32, p. 614-630.

MacLean, W. H., 1990, Mass change calculations in altered rock series: *Mineralium Deposita*, v. 25, p. 44-49.

Mittlefehldt, D. W., and Miller, C. F., 1983, Geochemistry of the Sweetwater Wash Pluton, California: Implications for "anomalous" trace element behavior during differentiation of felsic magmas: *Geochimica Et Cosmochimica Acta*, v. 47, p. 109-124.

Mortensen, J. K., Thorpe, R. I., Padgham, W. A., King, J. E., and Davis, W. J., 1988, U-Pb zircon ages for felsic volcanism in the Slave Province, N.W.T., *Radiogenic Age and Isotope Studies: Report 2, Paper 88-2*, Geological Survey of Canada, p. 85-95.

Northrup, C. J., Isachsen, C., and Bowring, S. A., 1999, Field relations, U-Pb geochronology, and Sm-Nd isotope geochemistry of the Point Lake greenstone belt and

adjacent gneisses, central Slave craton, N.W.T., Canada: Canadian Journal of Earth Sciences, v. 36, p. 1043-1059.

Ootes, L., Davis, W. J., Bleeker, W., and Jackson, V. A., 2009, Two Distinct Ages of Neoarchean Turbidites in the Western Slave Craton: Further Evidence and Implications for a Possible Back-Arc Model: The Journal of Geology, v. 117, p. 15-36.

Padgham, W. A., 1992, Mineral deposits in the archaic slave structural province; lithological and tectonic setting: Precambrian Research, v. 58, p. 1-24.

Padgham, W. A., and Fyson, W. K., 1992, The Slave Province - A distinct Archean craton: Canadian Journal of Earth Sciences, v. 29, p. 2072-2086.

Pearce, J.A., 1996, A user's guide to basalt discrimination diagrams, *in* Wyman, D. A., ed., Trace element geochemistry of volcanic rocks: Applications for massive sulphide exploration, Short Course Notes, Volume 12, Geological Association of Canada, p. 79-113.

Pearce, J. A., and Peate, D. W., 1995, Tectonic implications of the composition of volcanic arc magmas: Annual Review of Earth and Planetary Sciences, v. 23, p. 251-285.

Piercey, S., 2011, The setting, style, and role of magmatism in the formation of volcanogenic massive sulfide deposits: Mineralium Deposita, p. 1-23.

Piercey, S. J., Paradis, S., Murphy, D. C., and Mortensen, J. K., 2001, Geochemistry and paleotectonic setting of felsic volcanic rocks in the Finlayson Lake volcanic-hosted massive sulfide (VHMS) district, Yukon, Canada: Economic Geology, v. 96, p. 1877-1905.

Piercey, S. J., Murphy, D. C., Mortensen, J. K., and Creaser, R. A., 2004, Mid-Paleozoic initiation of the northern Cordilleran marginal backarc basin; geologic, geochemical, and neodymium isotope evidence from the oldest mafic magmatic rocks in the Yukon-Tanana Terrane, Finlayson Lake District, southeast Yukon,: Geological Society of America Bulletin, v. 116, p. 1087-1106.

Piercey, S. J., Peter, J. M., Mortensen, J. K., Paradis, S., Murphy, D. C., and Tucker, T. L., 2008, Petrology and U-Pb Geochronology of Footwall Porphyritic Rhyolites from the Wolverine Volcanogenic Massive Sulfide Deposit, Yukon, Canada: Implications for the Genesis of Massive Sulfide Deposits in Continental Margin Environments: Economic Geology, v. 103, p. 5-33.

Relf, C., 1992, 2 distinct shortening events during Late Archean orogeny in the west-central Slave Province, Northwest Territories, Canada: Canadian Journal of Earth Sciences, v. 29, p. 2104-2117.

Riverin, G., and Hodgson, C. J., 1980, Wall-rock alteration at the Millenbach Cu-Zn mine, Noranda, Quebec: *Economic Geology*, v. 75, p. 424-444.

Rockingham, C. J., 1979, Metamorphism and metal zoning of the Hood River-41 massive sulfide deposits, Slave Structural Province, N.W.T.: Unpub. M.Sc. thesis, University of Western Ontario, 125 p.

Ross, P.-S., and Bédard, J. H., 2009, Magmatic affinity of modern and ancient subalkaline volcanic rocks determined from trace-element discriminant diagrams: *Canadian Journal of Earth Sciences*, v. 46, p. 823-839.

Rubin, J. N., Henry, C. D., and Price, J. G., 1993, The mobility of zirconium and other "immobile" elements during hydrothermal alteration: *Chemical Geology*, v. 110, p. 29-47.

Rudnick, R. L., Barth, M. G., Horn, I., and McDonough, W. F., 2000, Rutile-bearing refractory eclogites: Missing link between continents and depleted mantle: *Science*, v. 287, p. 278-281.

Shukuno, H., Tamura, Y., Tani, K., Chang, Q., Suzuki, T., and Fiske, R. S., 2006, Origin of silicic magmas and the compositional gap at Sumisu submarine caldera, Izu-Bonin arc, Japan: *Journal of Volcanology and Geothermal Research*, v. 156, p. 187-216.

Spitz, G., and Darling, R., 1978, Major and minor element lithogeochemical anomalies surrounding the Louvem copper deposit, Val d'Or, Quebec: *Canadian Journal of Earth Sciences*, v. 15, p. 1161-1169.

Stubley, M. P., 2005, Slave Craton: Interpretive bedrock compilation, NWT-NU Open File 2005-01.

Sun, S.-s., and McDonough, W. F., 1989, Chemical and isotopic systematics of oceanic basalts: implications for mantle composition and processes, *in* Saunders, A. D., and Norry, M. J., eds., *Magmatism in the Ocean Basins*, Geological Society Special Publication 42, p. 313-345.

Swinden, H. S., 1991, Paleotectonic settings of volcanogenic massive sulphide deposits in the Dunnage Zone, Newfoundland Appalachians: *Canadian Institute of Mining and Metallurgy Bulletin*, v. 84, p. 59-89.

Thomas, D. A., and Glenn, D. G., 1994, 1993 Summary Report: Diamond Drilling and Pulse EM, Hood Project - PN 420 Minnova Inc Company Report, p. 110.

Thompson, A. J. B., 1999, Alteration mapping in exploration; application of short-wave infrared (SWIR) spectroscopy, *in* Hauff, P. L., and Robitaille, J. A., eds., *SEG*

Newsletter, 39: United States, Society of Economic Geologists : Littleton, CO, United States, p. 1.

Villeneuve, M. E., Henderson, J. R., Hrabi, R. B., Jackson, V. A., and Relf, C., 1997, 2.70-2.58 Ga plutonism and volcanism in the Slave Province, District of Mackenzie, Northwest Territories: Radiogenic Age and Isotopic Studies, Geological Survey of Canada Current Research 1997-F, v. 10.

Watson, E. B., and Harrison, T. M., 1983, Zircon saturation revisited: temperature and composition effects in a variety of crustal magma types: Earth and Planetary Science Letters, v. 64, p. 295-304.

Whalen, J. B., McNicoll, V. J., Galley, A. G., Longstaffe, F. J., and Percival, J. A., 2004, Tectonic and metallogenic importance of an Archean composite high- and low-Al tonalite suite, western Superior Province, Canada: Precambrian Research, v. 132, p. 275-301.

Winchester, J. A., and Floyd, P. A., 1977, Geochemical discrimination of different magma series and their differentiation products using immobile elements: Chemical Geology, v. 20, p. 325-343.

Yamashita, K., Creaser, R. A., Jensen, J. E., and Heaman, L. M., 2000, Origin and evolution of mid- to late-Archean crust in the Hanikahimajuk Lake area, Slave Province, Canada; evidence from U-Pb geochronological, geochemical and Nd-Pb isotopic data: Precambrian Research, v. 99, p. 197-224.



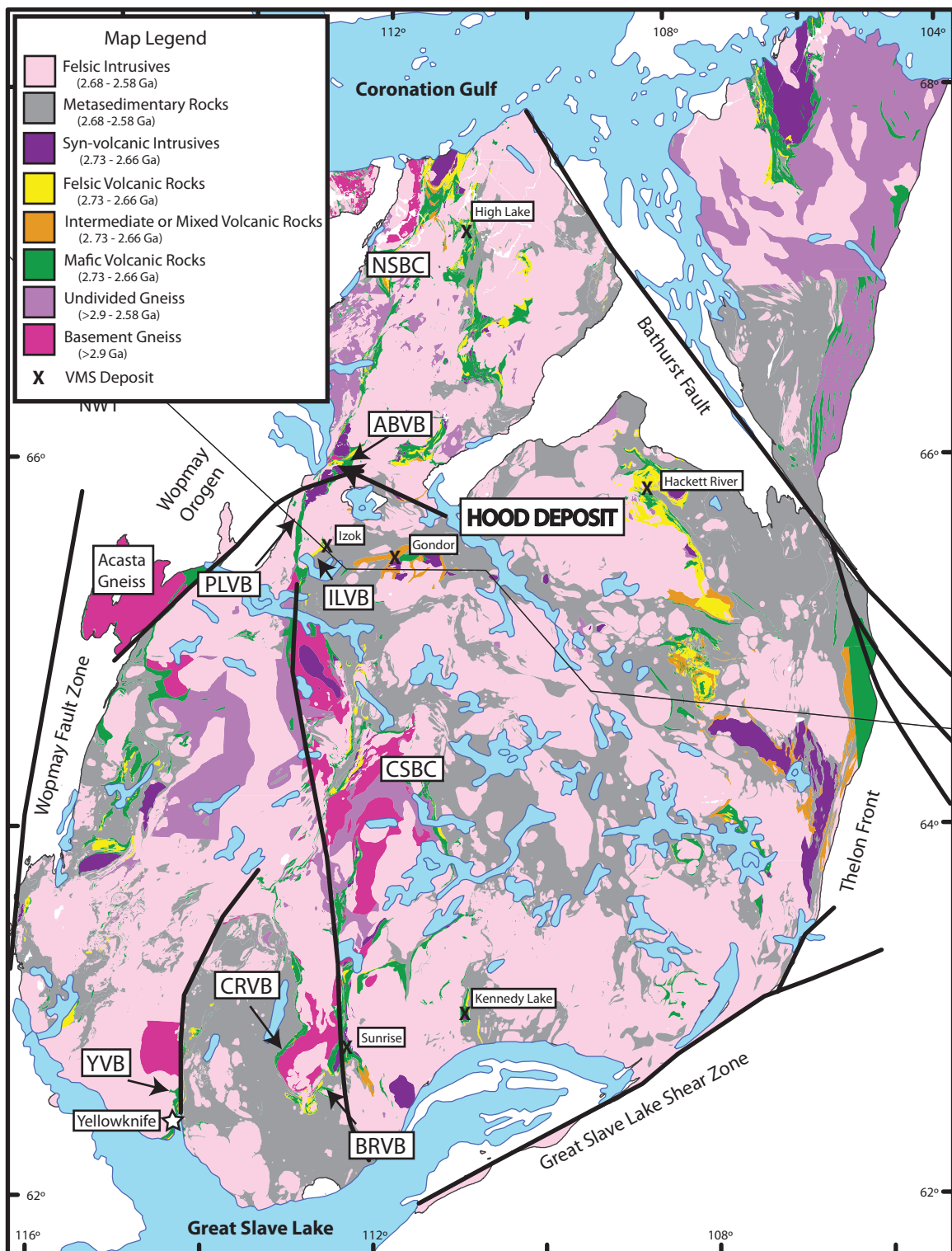


Figure 2-1: Simplified Slave Craton geology (Stubley, 2005) and selected VMS deposits (Bleeker and Hall, 2007). Labeled greenstone belts are the Amooga Booga volcanic belt (ABVB), Izok Lake volcanic belt (ILVB), Point Lake volcanic belt (PLVB), Yellowknife volcanic belt (YVB), Cameron River volcanic belt (CRVB), and the Beaulieu River volcanic belt (BRVB).



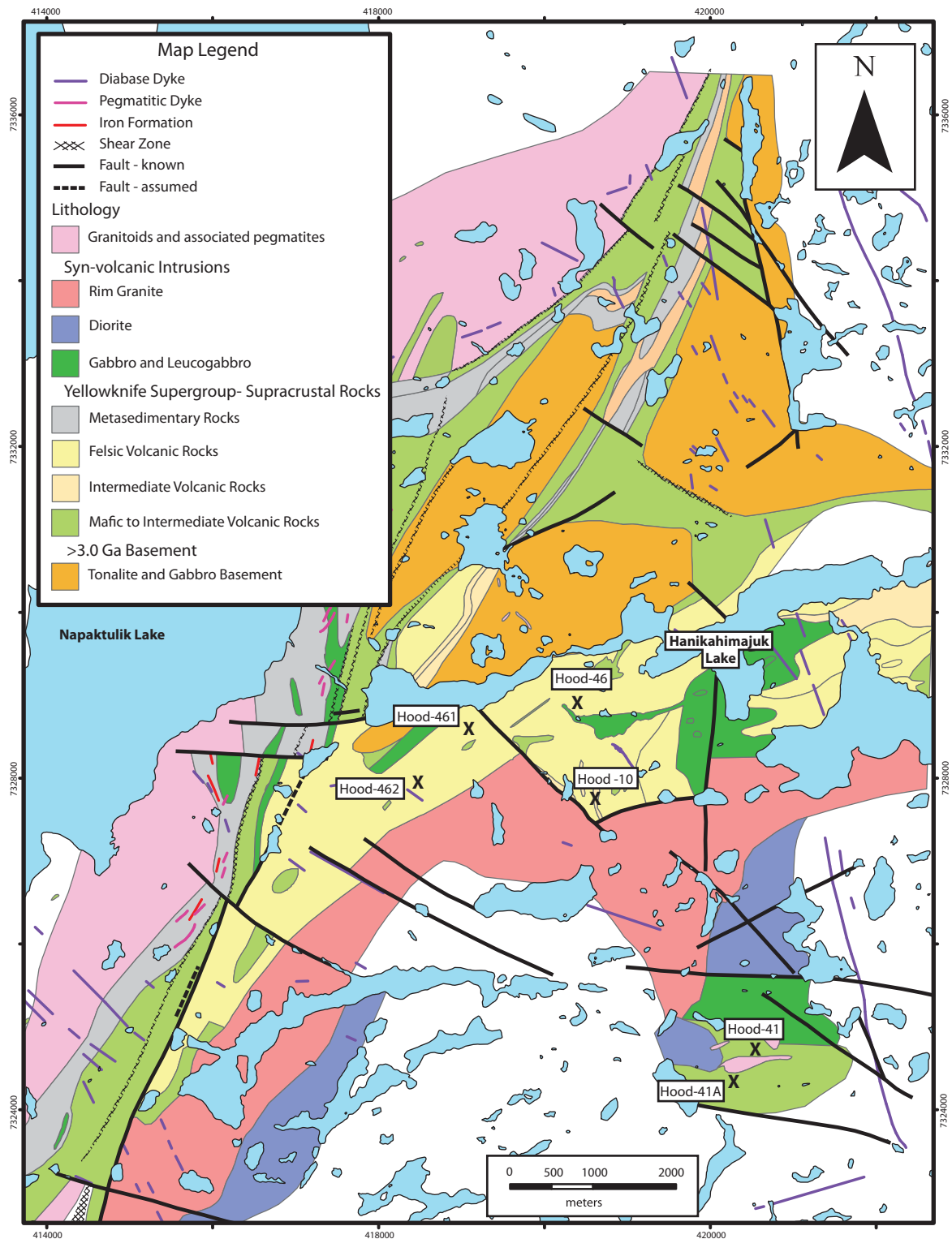


Figure 2-2: Geology of the Hanikahimajuk Lake area and locations of Hood deposit lenses and mineral occurrences (Gebert, 1995).

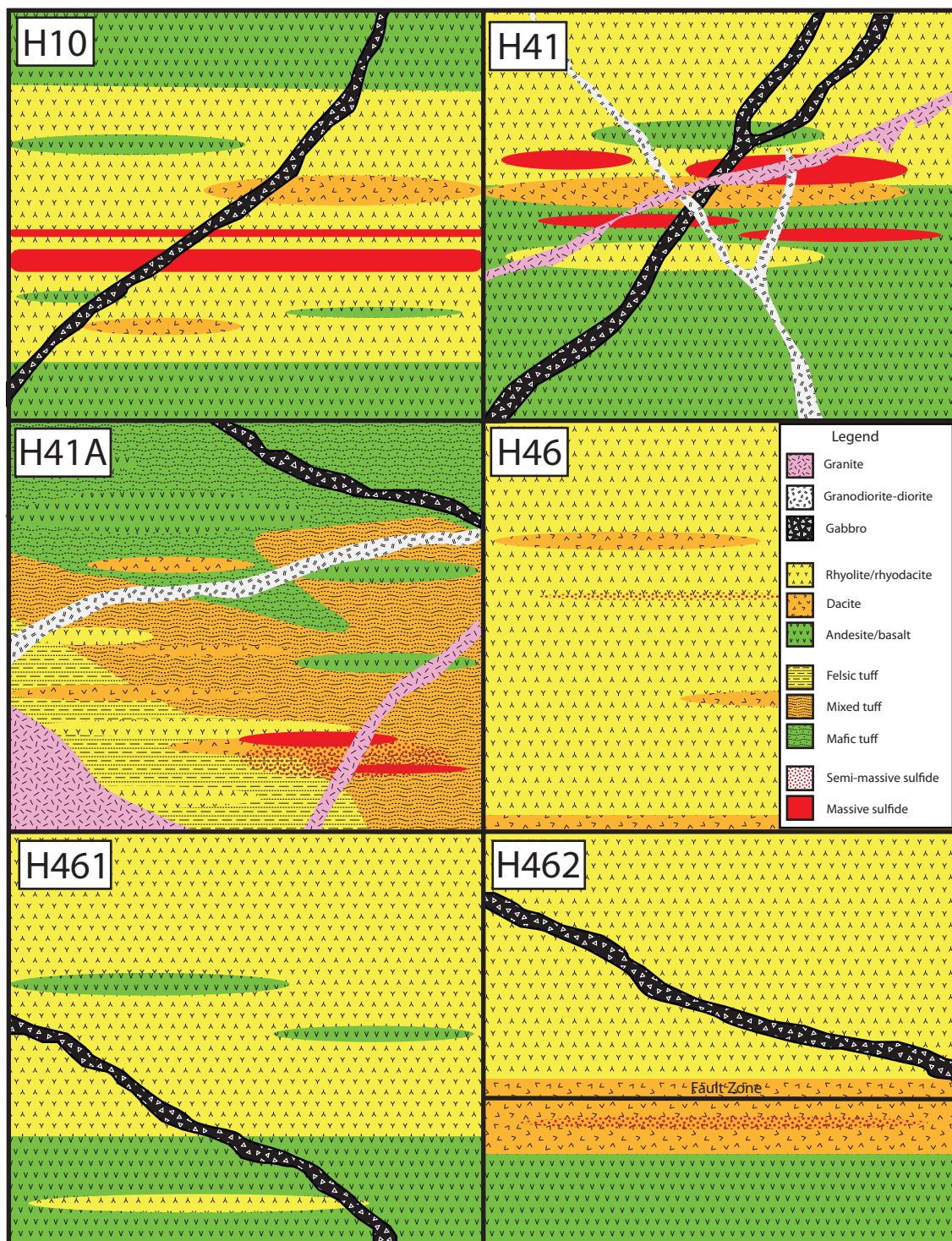


Figure 2-3: Schematic diagrams of the Hood deposits lenses and mineral occurrences demonstrating the different stratigraphic settings. Diagrams not to scale.

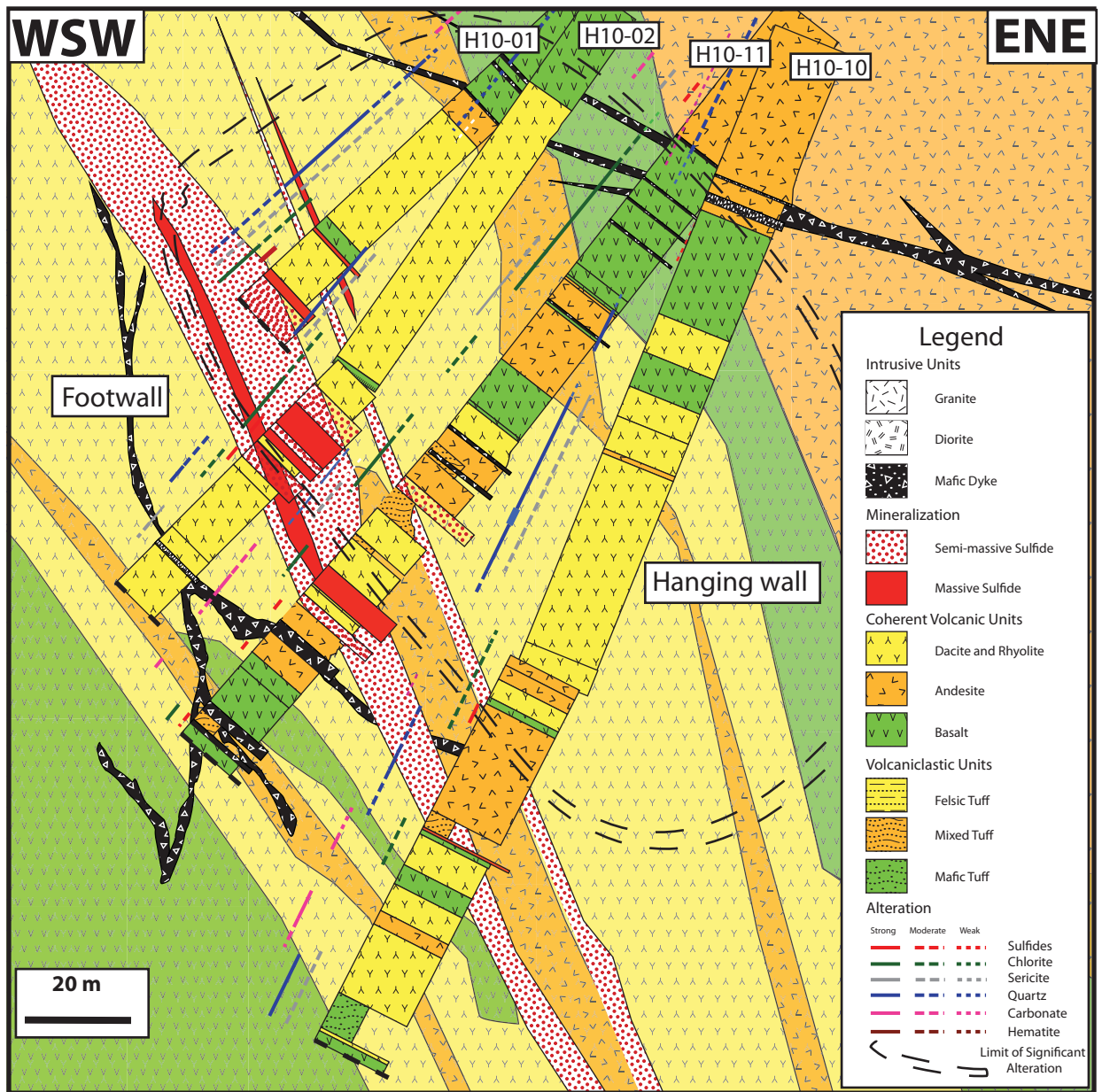


Figure 2-4: Vertical cross-section through the southern part of the Hood 10 lens based on drill intersections from drill holes H10-01, H10-02, H10-10, and H10-11. Drill hole width is exaggerated for clarity and contacts in drill logs are not shown with true dip.



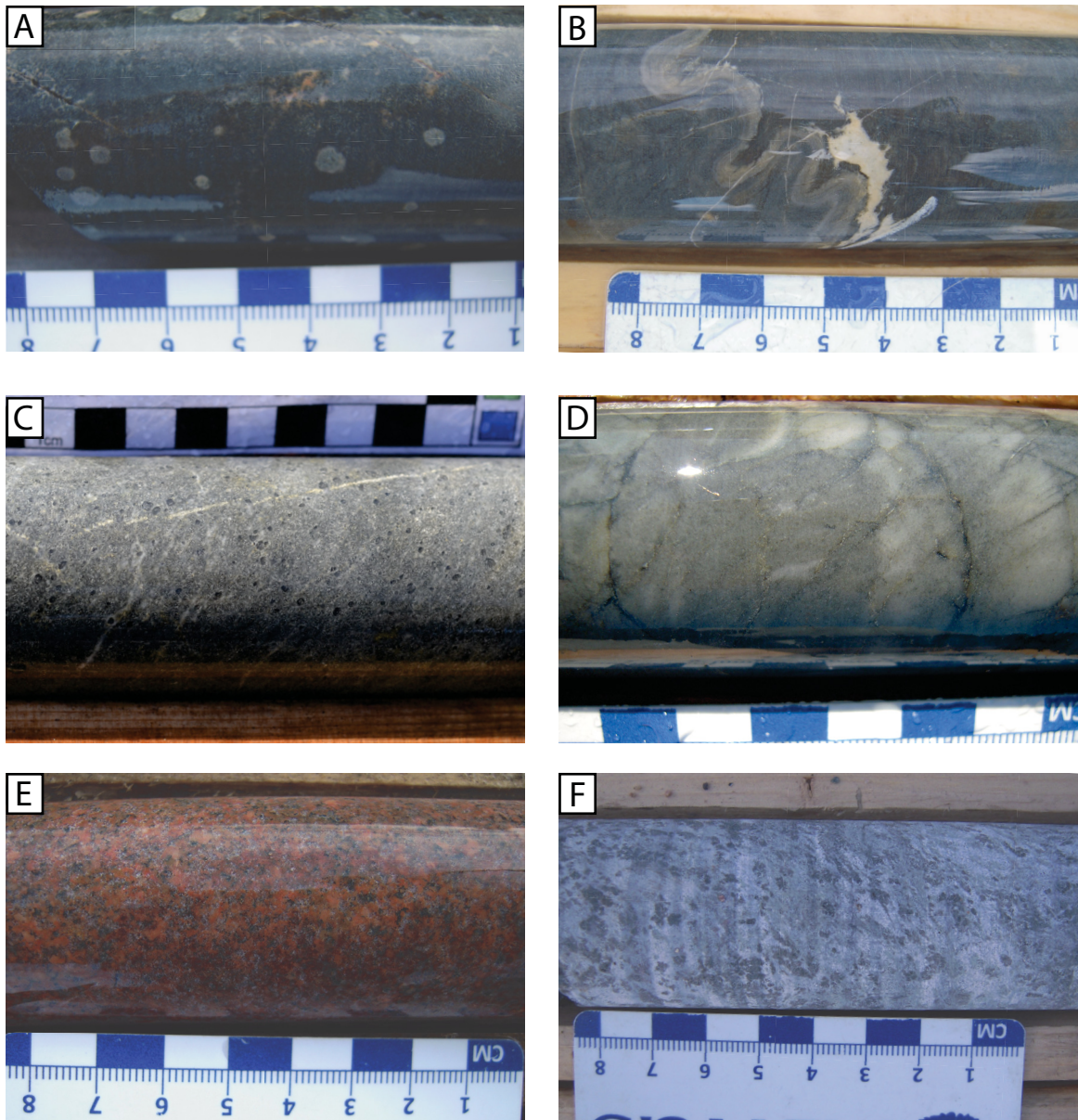


Figure 2-5: Common lithologies of the Hood deposits. A) Amygduloidal basalt. B) Sinuous chilled margin on basalt flow intruding into mafic tuff. C) Quartz-eye rhyolite. D) Porcelain rhyolite. E) Rim granite. F) Mixed intrusive rock.

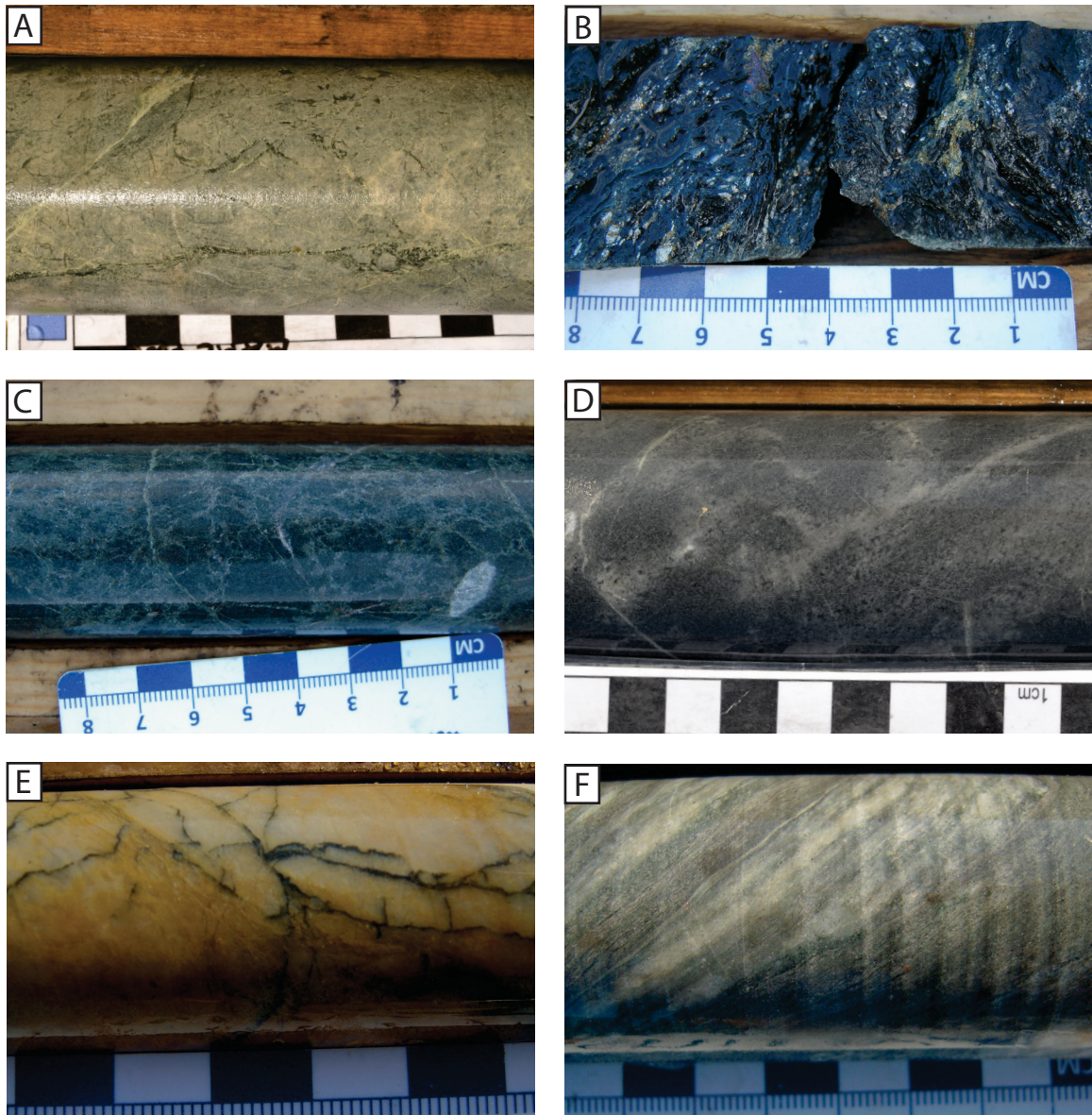


Figure 2-6: Representative samples of common alteration for the Hood deposits. A) Sericite alteration of rhyolite. B) Strong pervasive chlorite alteration near mineralization. C) Selective sericite + chlorite spider web alteration of andesite-basalt. D) Patchy quartz alteration of quartz-eye dacite. E) Black chlorite alteration along fractures in rhyolite. F) Selective quartz alteration along foliation creating banding in grey dacite.



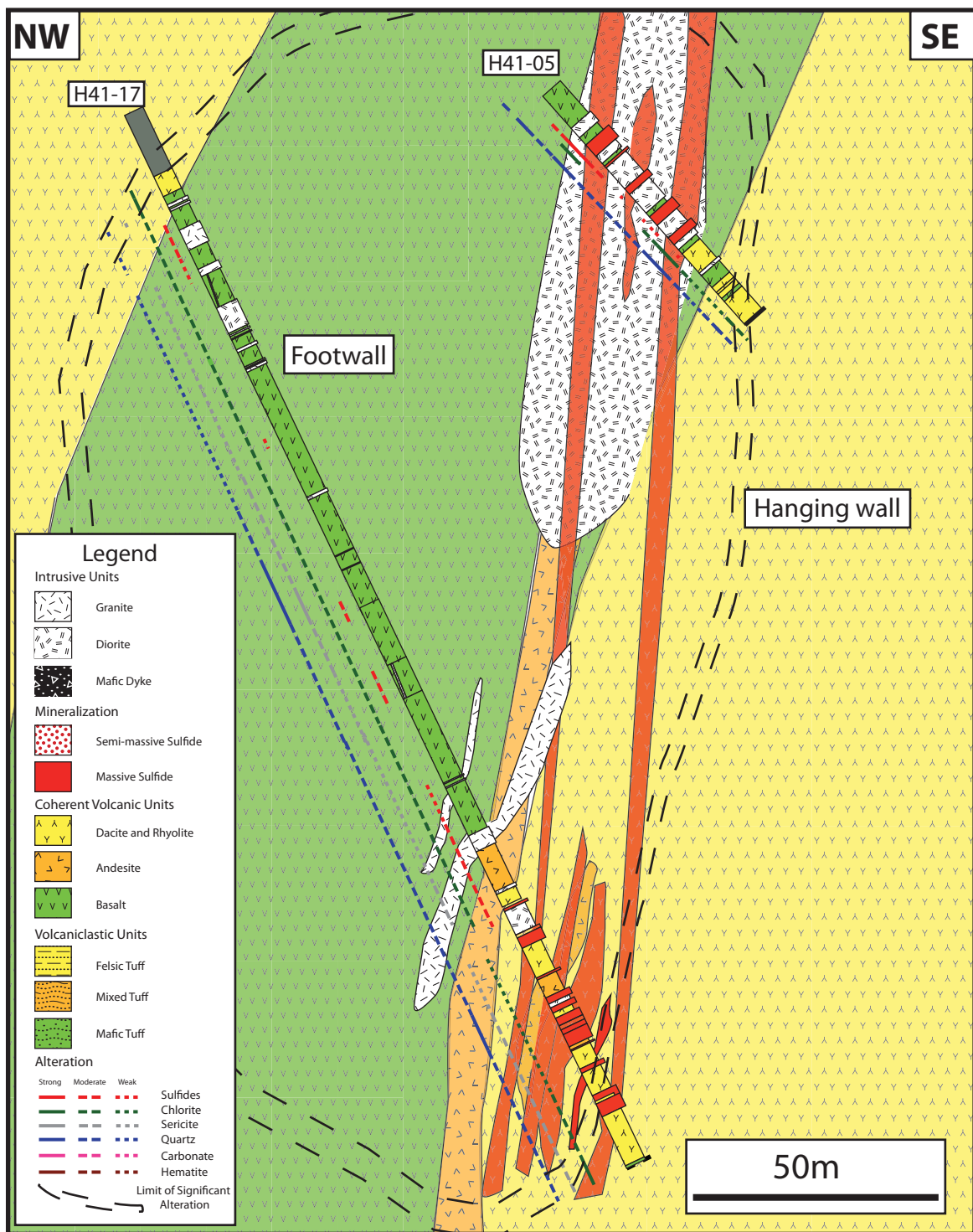


Figure 2-7: Vertical cross-section through the centre of the Hood 41 lens based on drill intersections from drill holes H41-05 and H41-17. Drill hole width is exaggerated for clarity and contacts in drill logs are not shown with true dip.

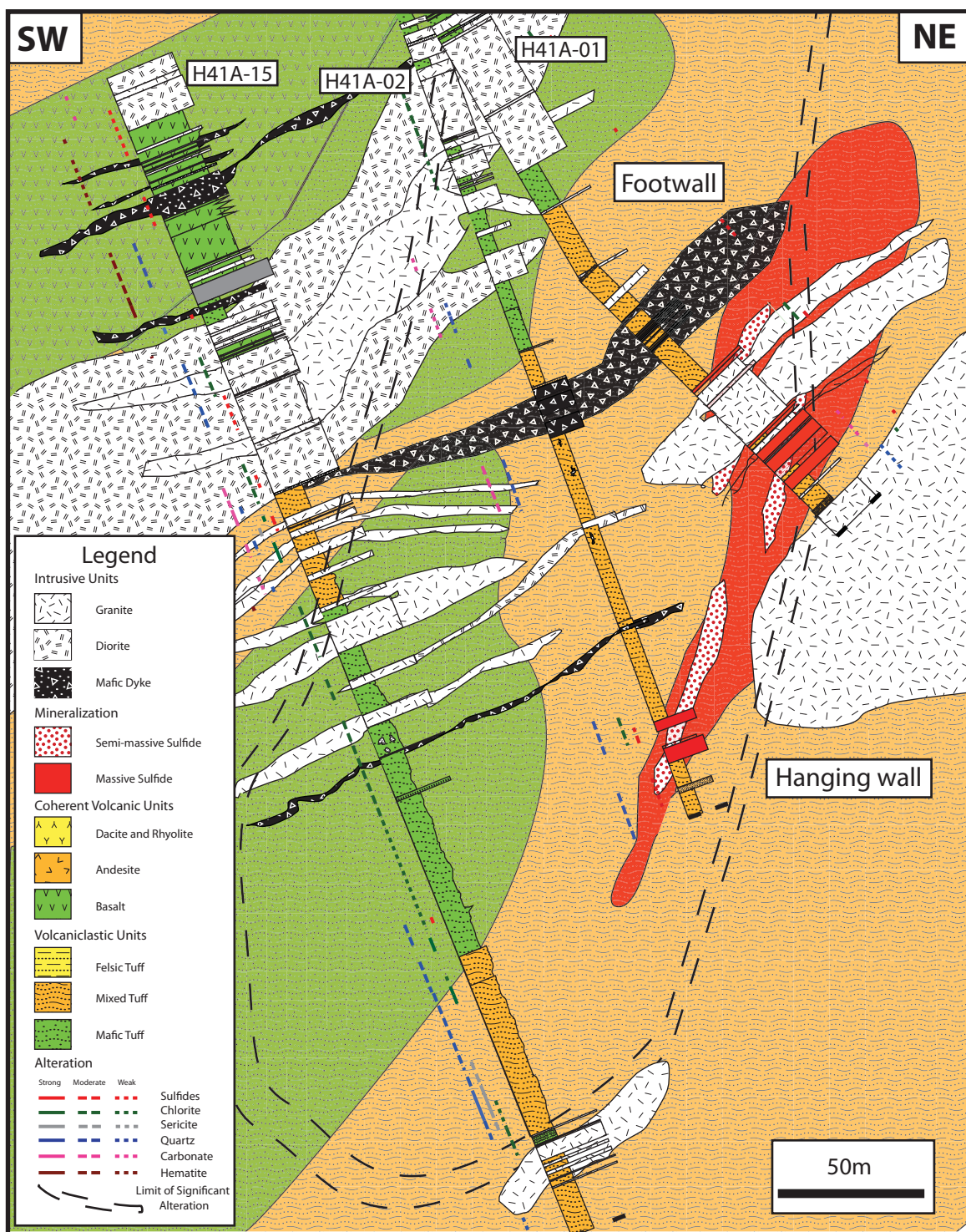


Figure 2-8: Vertical cross-section through the southeast end of the Hood 41A lens demonstrating abundant mafic and mixed volcaniclastic rocks based on drill intersections from drill holes H41A-01, H41A-02, and H41A-15. Drill hole width is exaggerated for clarity and contacts in drill logs are not shown with true dip. .

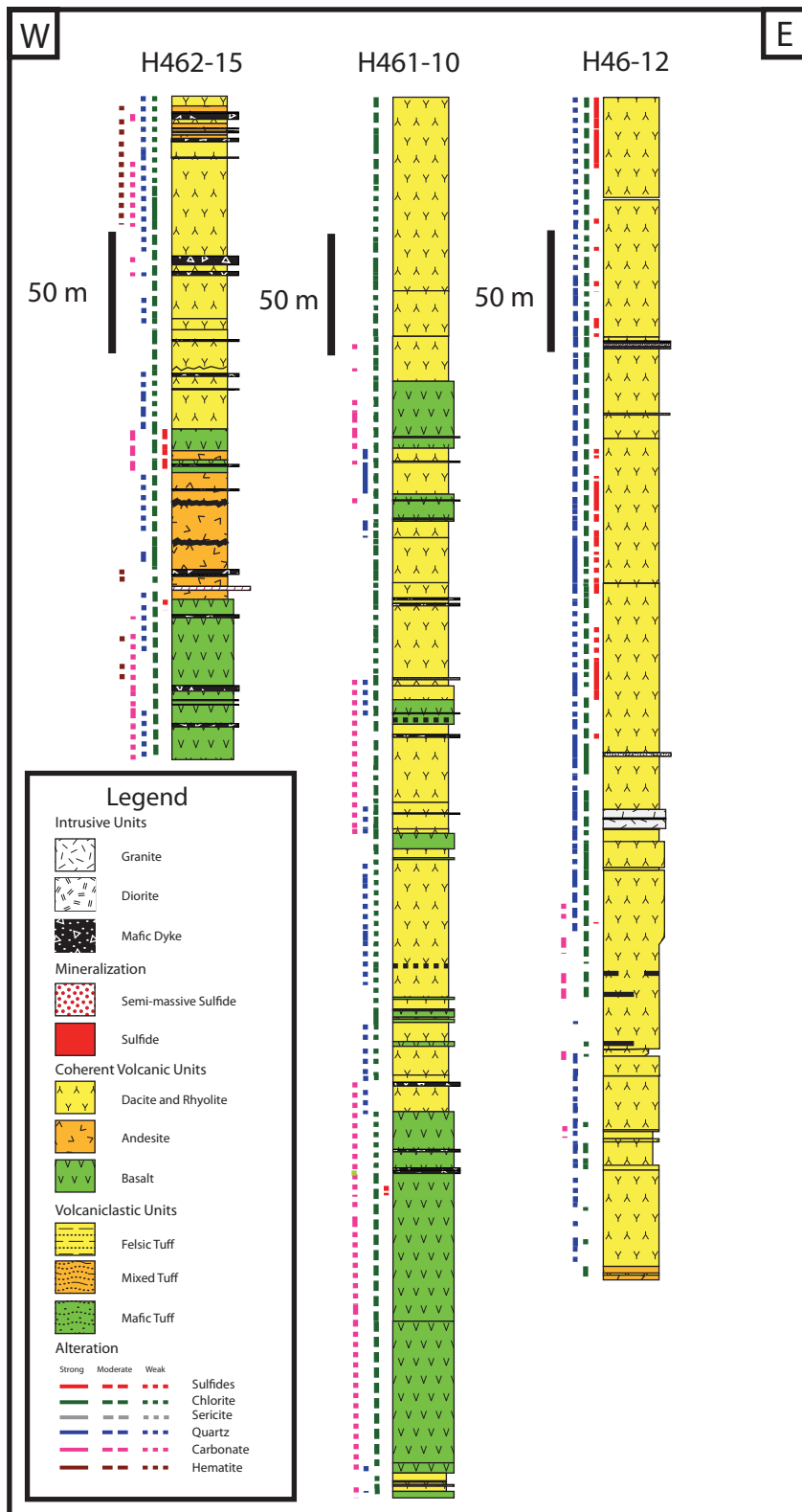


Figure 2-9: Vertical drill logs from the Hood 46, Hood 461, Hood 462 occurrences with large packages of coherent felsic volcanic rocks but limited mineralization. Lateral distribution and drill log width are not to scale.



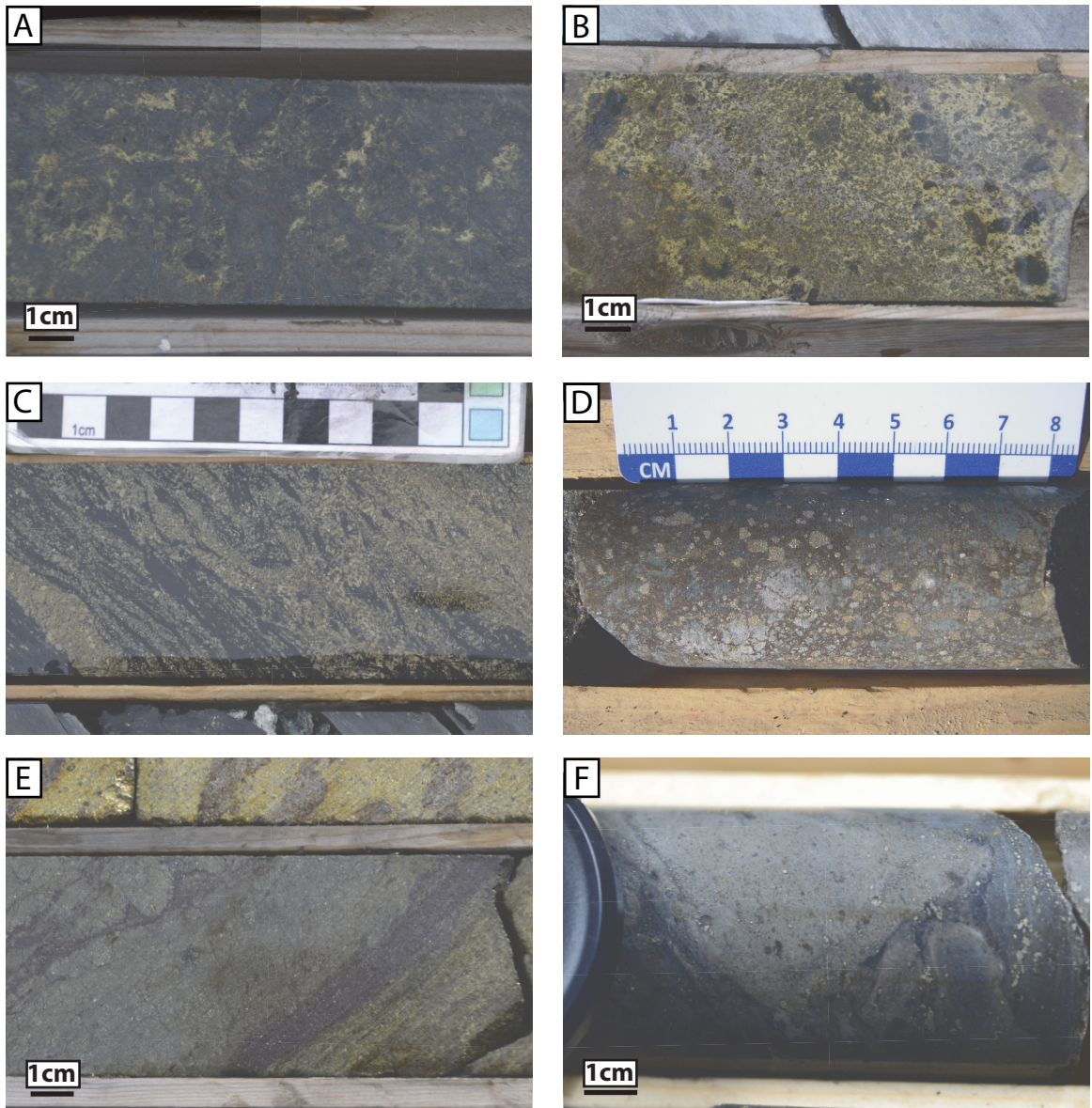


Figure 2-10: Mineralization types of the Hood deposits. A) Chalcopyrite stringers. B) Chalcopyrite in pyrrhotite with chlorite altered remnant host rock clasts. C) Fine pyrite bands in argillite. D) Buckshot pyrite in massive pyrrhotite, typically with interstitial sphalerite visible in thin section. E) Sphalerite and pyrite banding. F) Pyrite replacement within clasts and the matrix of a volcanic breccia.

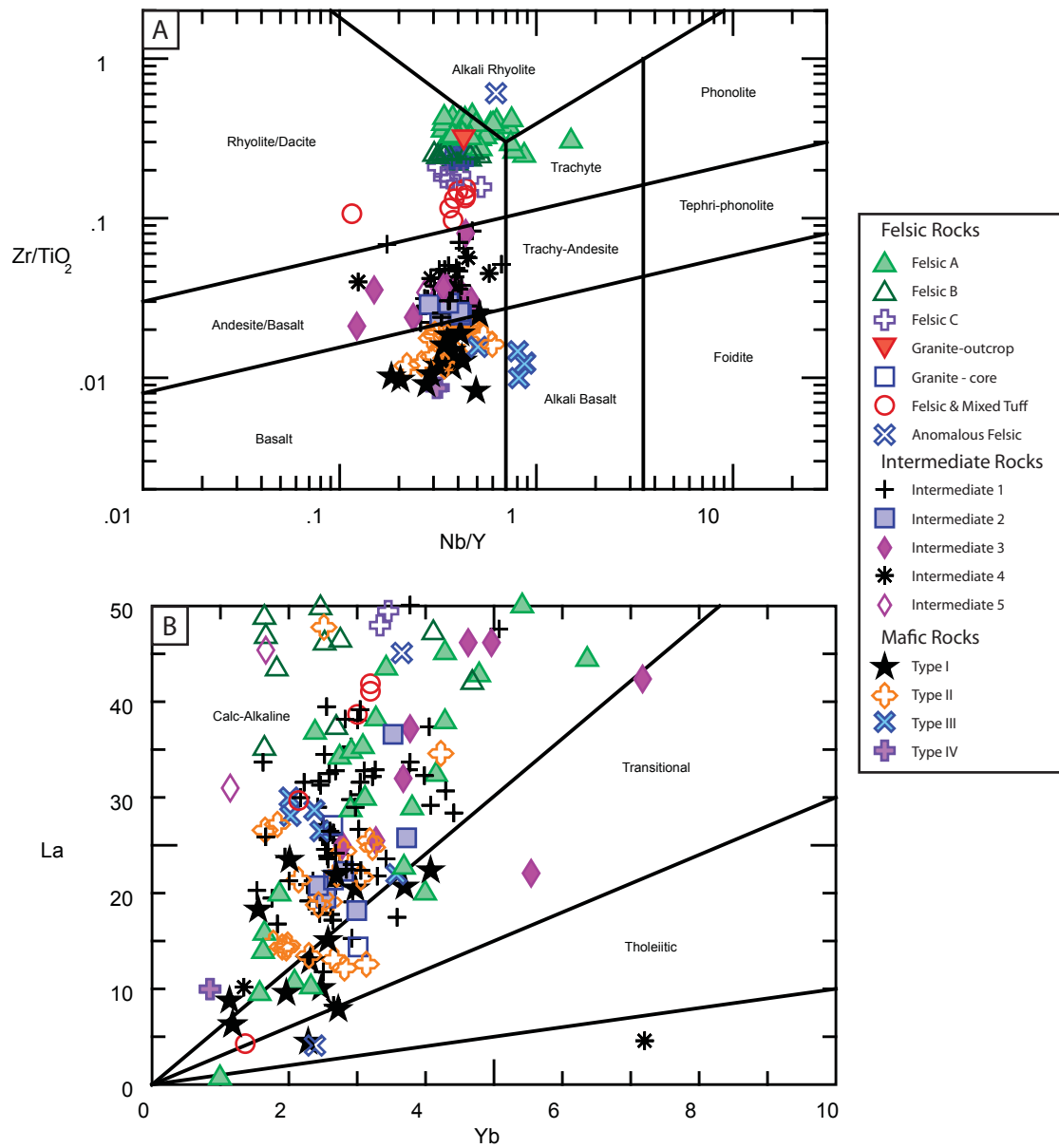


Figure 2-11: Magmatic discrimination diagrams for the Hood deposits magmatic rock data. A) Zr/TiO<sub>2</sub> vs Nb/Y diagram (Pearce, 1996). B) La vs Yb diagram from Barrett and MacLean (1999).

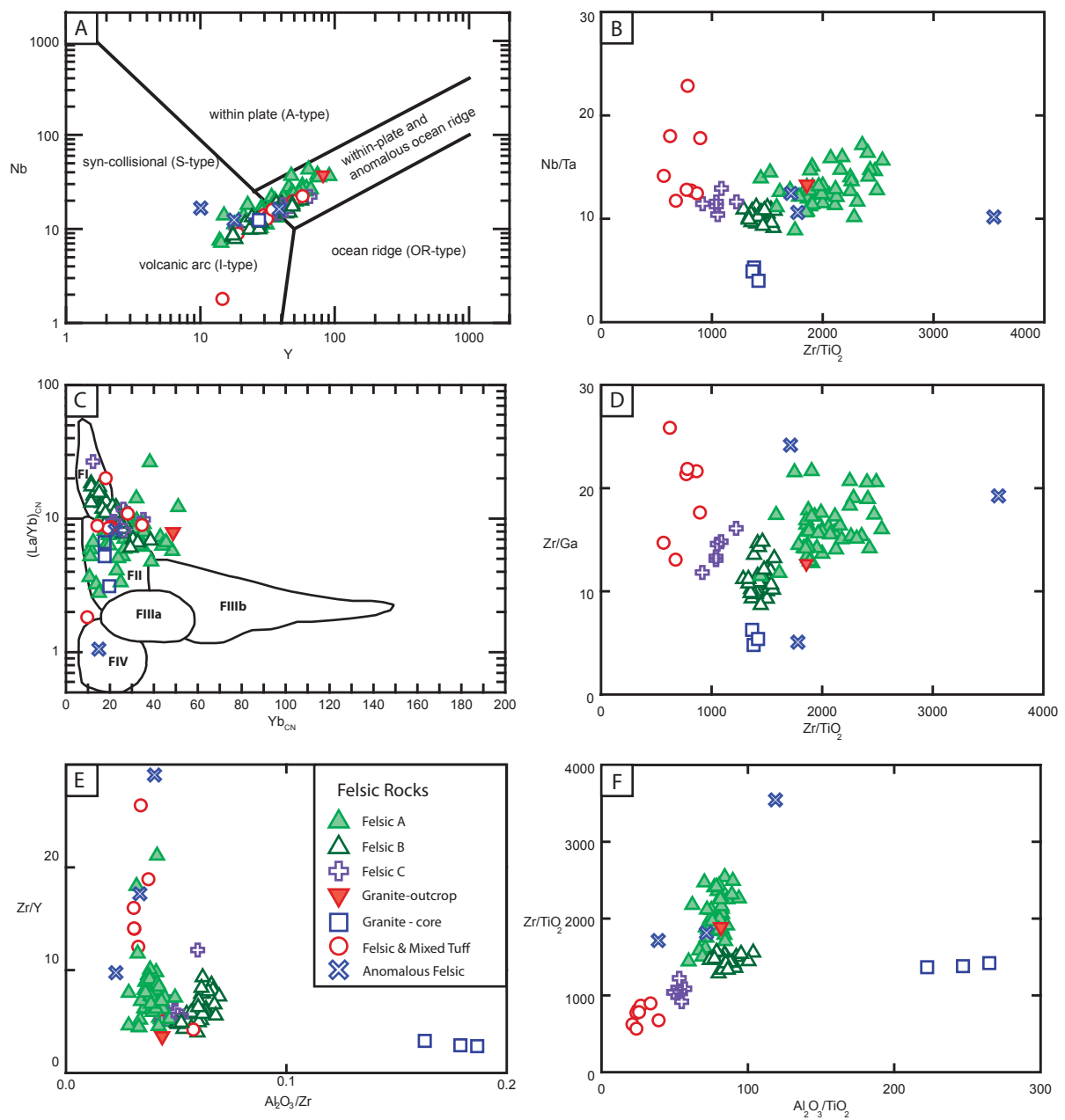


Figure 2-12: Immobility element plots for the Hood deposits felsic magmatic rocks. A) Nb vs Y discrimination diagram (Pearce et al., 1984). B) Nb/Ta vs Zr/TiO<sub>2</sub>. C) La/Yb)<sub>CN</sub> vs Yb<sub>CN</sub> plot for outlining felsic groupings (Hart et al., 2004, modified after (Leshner et al., 1986). D) Zr/Ga vs Zr/TiO<sub>2</sub>. E) Zr/Y vs Al<sub>2</sub>O<sub>3</sub>/Zr. F) Zr/TiO<sub>2</sub> vs Al<sub>2</sub>O<sub>3</sub>/TiO<sub>2</sub>.

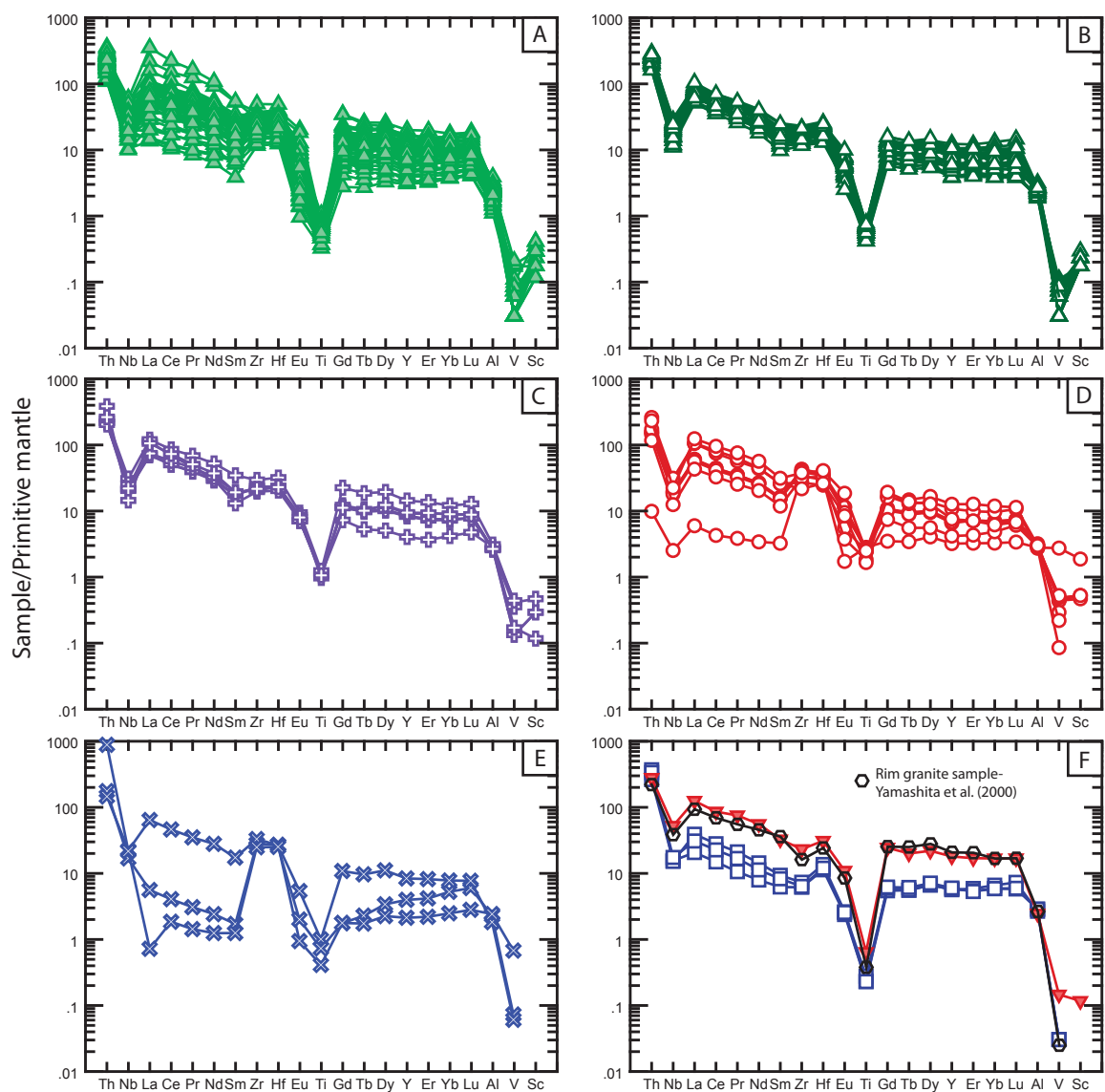


Figure 2-13: Primitive mantle normalized extended multi-element plots of the felsic rocks of the Hood deposits (Sun and McDonough, 1989). A) Felsic suite A. B) Felsic suite B. C) Felsic suite C. D) Felsic and mixed tuff signature suite. E) Anomalous felsic signatures (altered). F) Granite core samples compared to outcrop samples from this study and Yamashita et al. (2000). Symbols as in Figure 2-12.

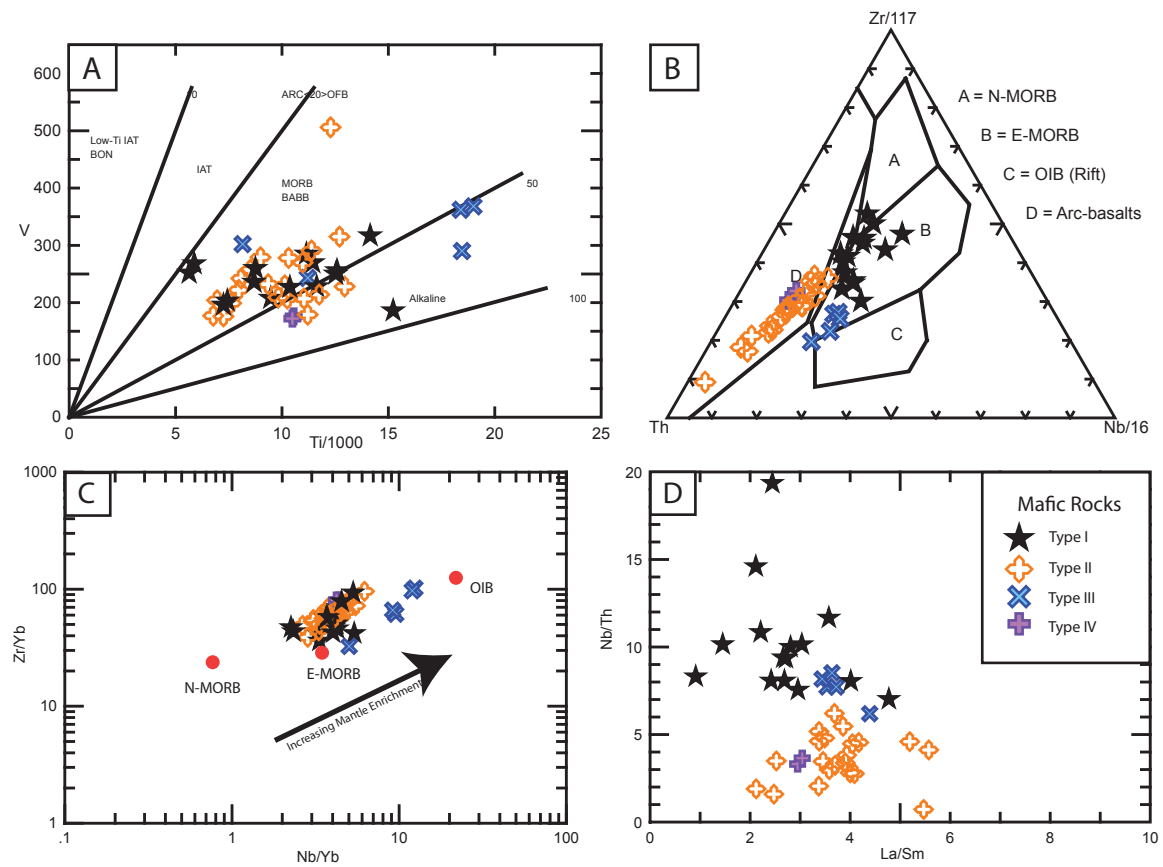


Figure 2-14: Tectonomagmatic discrimination diagrams for the Hood deposits mafic rocks. ARC-Arc-related basalts; BABB-back-arc basin basalt; BON-boninite; E-MORB-enriched mid-ocean ridge basalt; IAT-island-arc tholeiite; LOTI-low-Ti tholeiite; OIB-ocean island basalt; N-MORB-normal mid-ocean ridge basalt. A) Ti vs V diagram (Shervais, 1982); B) Th-Zr-Nb plot (Wood, 1980); C) Zr/Yb vs Nb/Yb diagram discriminating depleted- to enriched-mantle derived rocks (Pearce and Peate, 1995) with global values of OIB, N-MORB, and E-MORB (Sun and McDonough, 1989). D) Nb/Th vs La/Sm.

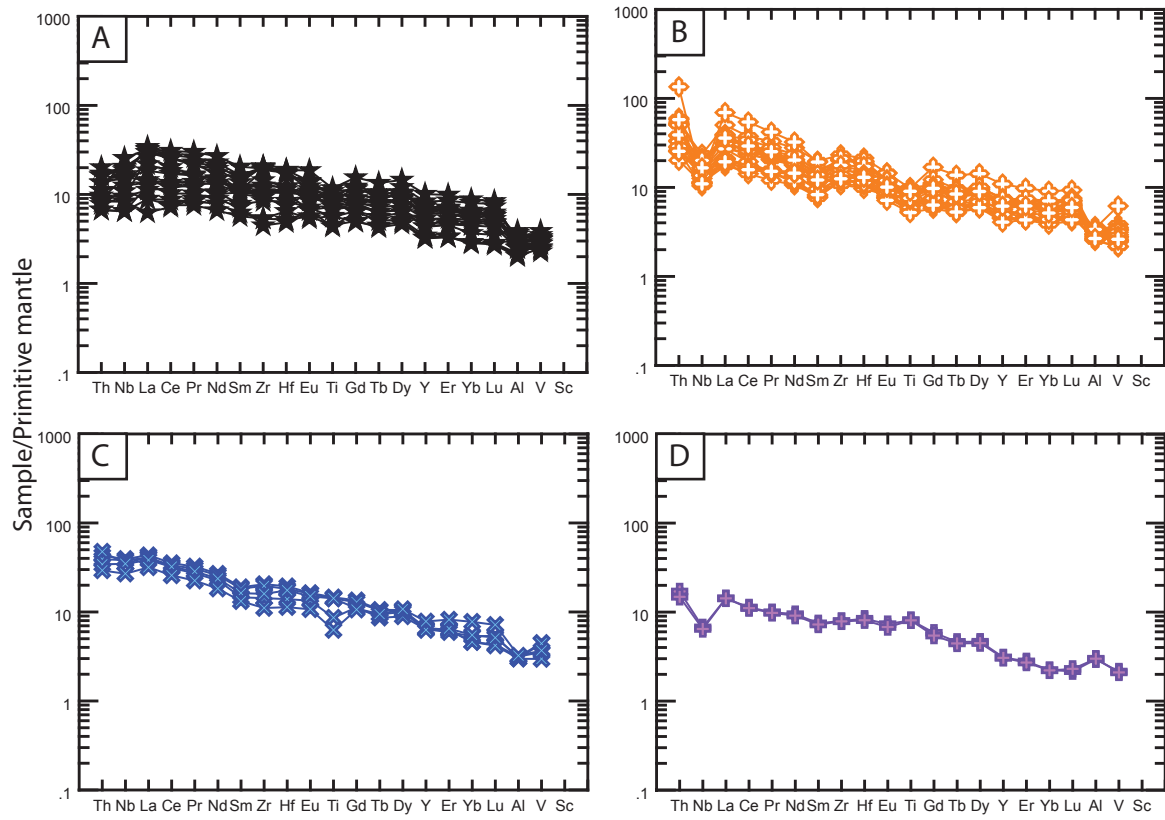


Figure 2-15: Primitive mantle normalized extended multi-element plots of the mafic rocks of the Hood deposits (Sun and McDonough, 1989). A) Type I mafic rocks. B) Type II mafic rocks. C) Type III mafic rocks. D) Type IV mafic rocks. Symbols as in Figure 2-14.

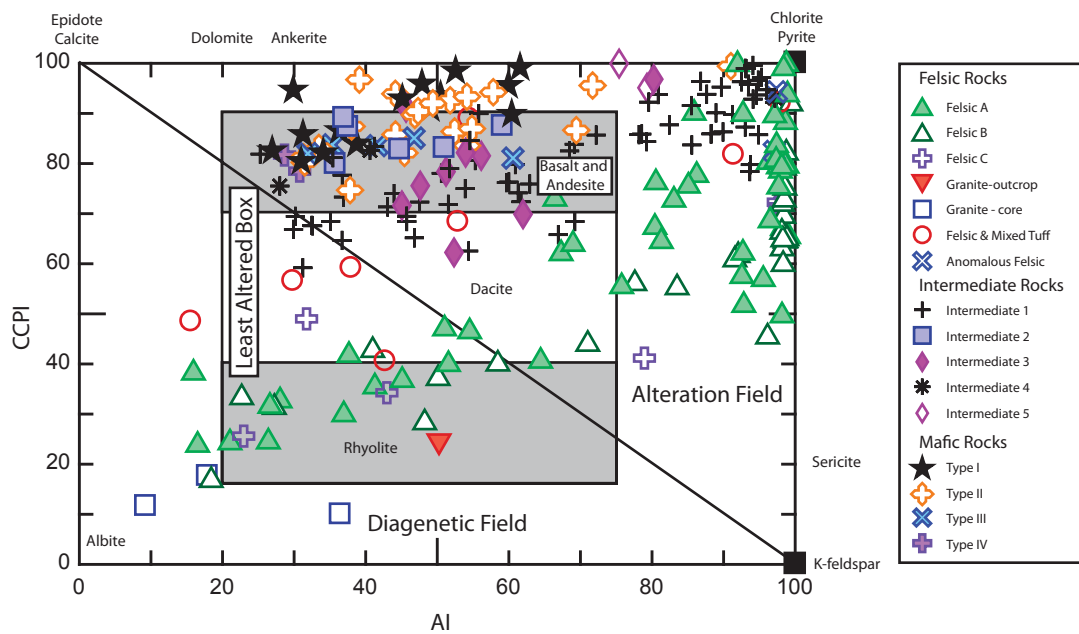


Figure 2-16: Alteration box plot of the chlorite-carbonate-pyrite index vs the Hashimoto alteration index (AI) for the rocks of the Hood deposits (Large et al., 2001b).

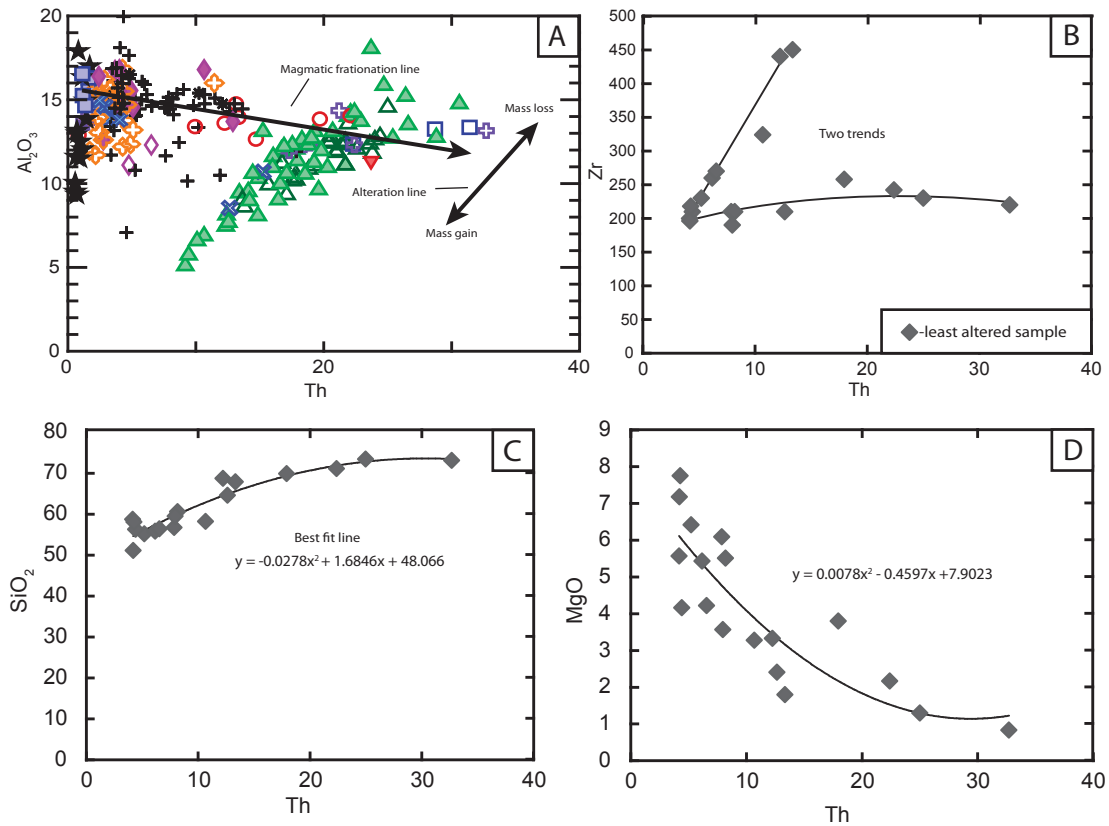


Figure 2-17 : A)  $\text{Al}_2\text{O}_3$  vs Th plot with the least altered fractionation curve and mass loss and gain trends for Hood samples. B) Exponential fit fractionation line for Zr of least altered samples demonstrating two Zr vs Th trends. C) Exponential fit fractionation line for  $\text{SiO}_2$  of least altered samples. D) Exponential fit fractionation line for MgO of least altered samples. Symbols as in Figure 2-11.



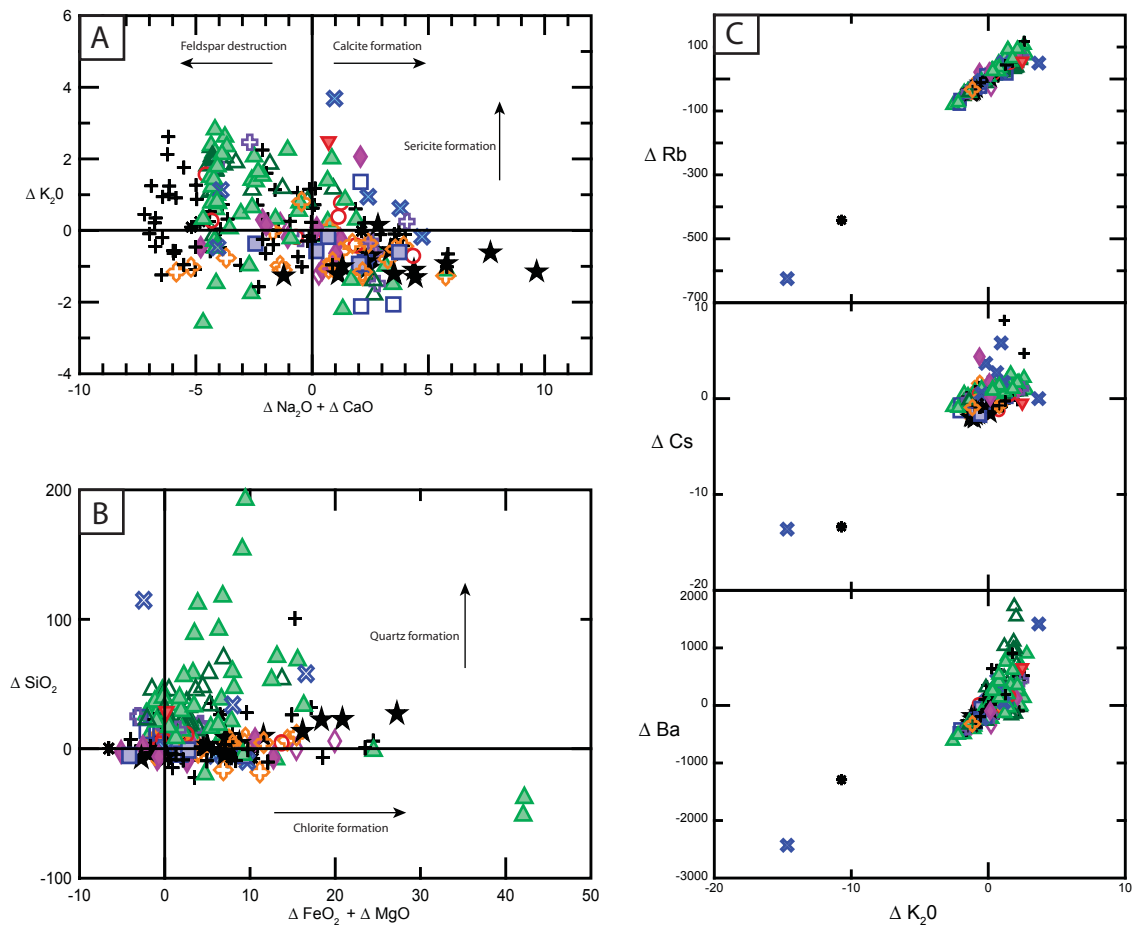


Figure 2-18: Mass change plots for Hood deposits. A)  $\Delta K_2O$  vs  $\Delta Na_2O + \Delta CaO$ . B)  $\Delta SiO_2$  vs  $\Delta Fe_2O_3 + \Delta MgO$ . C) Data array with selected element mass change plotted against  $\Delta K_2O$ . D) Data array with selected element mass change plotted against  $\Delta Fe_2O + \Delta MgO$ . Symbols as in Figure 2-11.

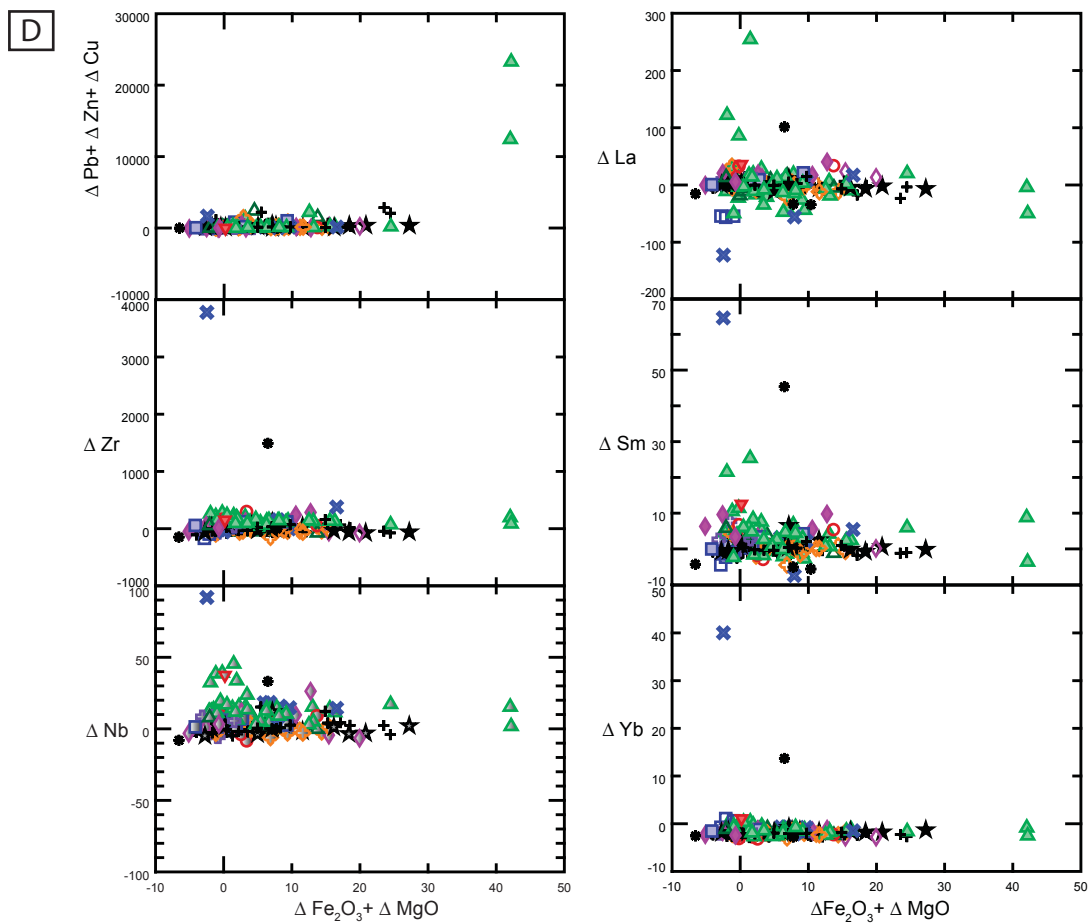


Figure 2-18 (continued): Mass change plots for Hood deposits. A)  $\Delta \text{K}_2\text{O}$  vs  $\Delta \text{Na}_2\text{O} + \Delta \text{CaO}$ . B)  $\Delta \text{SiO}_2$  vs  $\Delta \text{Fe}_2\text{O}_3 + \Delta \text{MgO}$ . C) Data array with selected element mass change plotted against  $\Delta \text{K}_2\text{O}$ . D) Data array with selected element mass change plotted against  $\Delta \text{Fe}_2\text{O}_3 + \Delta \text{MgO}$ . Symbols as in Figure 2-11.

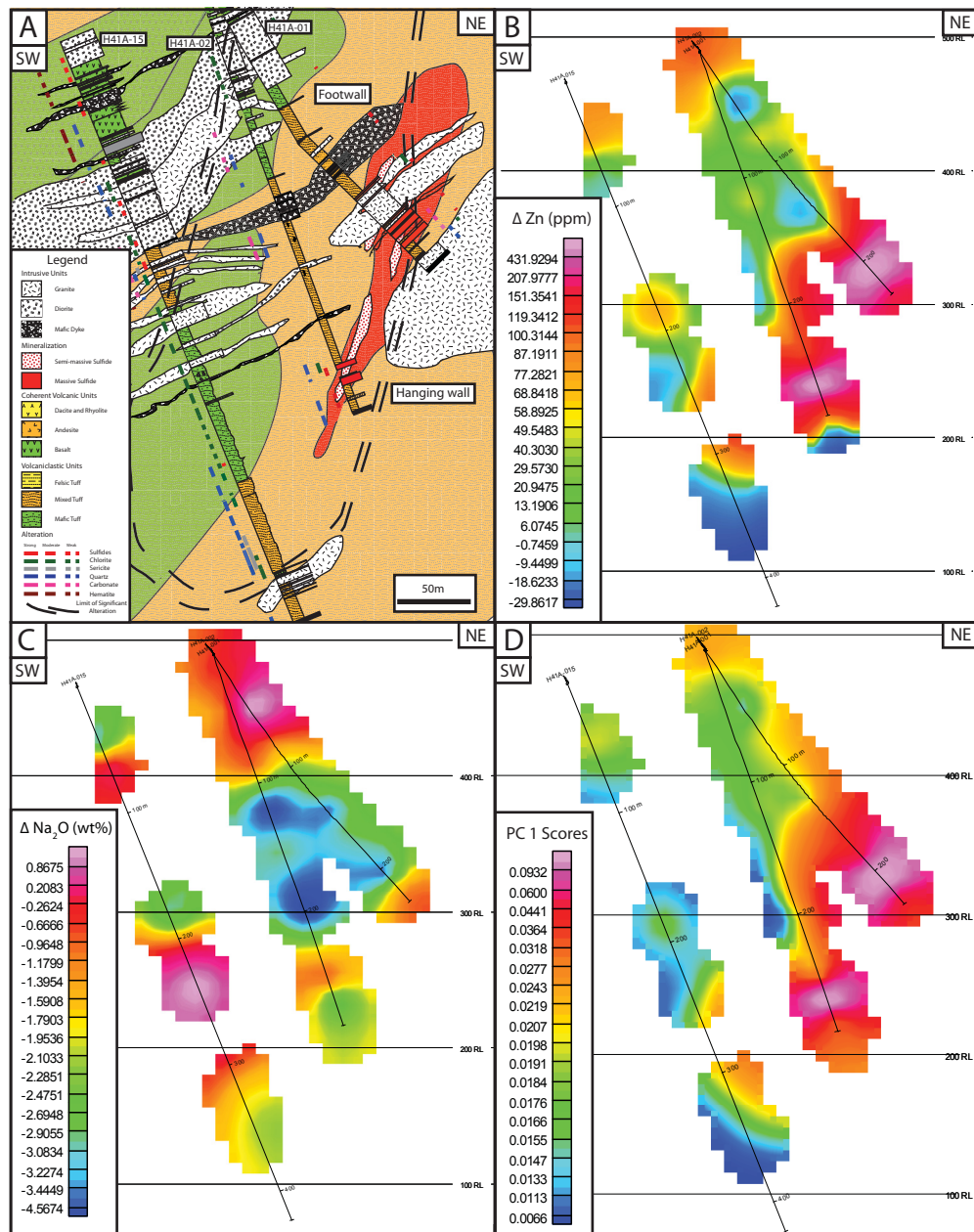


Figure 2-19: Hood 41A cross-sections comparing A) interpreted stratigraphy based on drill logs to B) 3-D gridding of Zn mass change, C) 3-D gridding of Na<sub>2</sub>O mass change and D) 3-D gridding of principal component 1 scores.

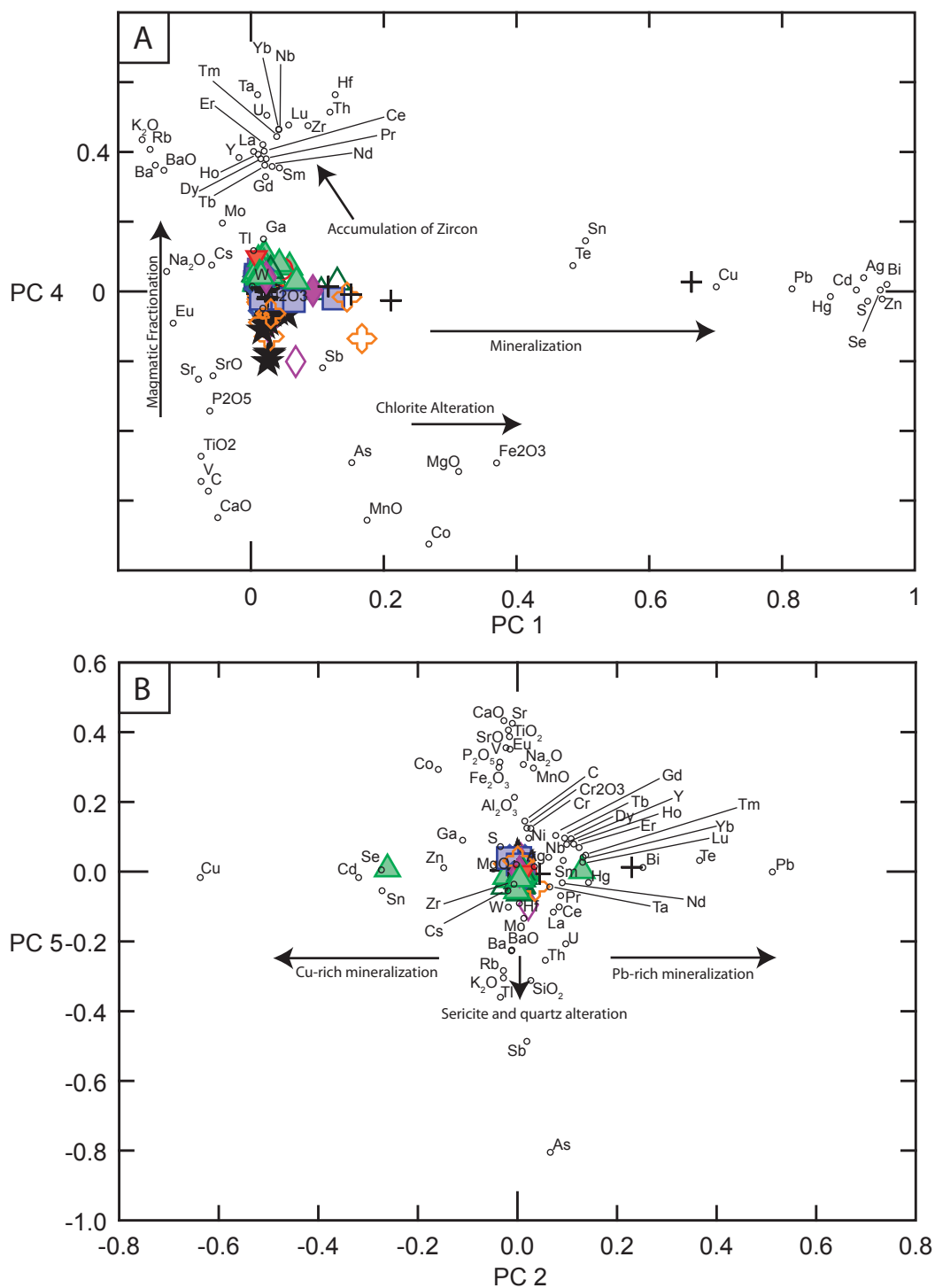


Figure 2-20: Principal component scores for Hood samples with interpreted trends. A) PC4 vs PC1 accounts for 66.5% of the total variation in the dataset. B) PC5 vs PC2 represents 13.5% of the total variation in the dataset. Symbols as in Figure 2-11.

Table 2-1: Lithology, alteration, and mineralization summary table

	Hood 10	Hood 41	Hood 41A	Hood 46, 461, 462
Lithology	Rhyolite and dacite flows with minor mafic and intermediate flows in both the footwall and hanging wall.	Thick basalt flows in footwall and felsic flows in hanging wall. Extensively intruded by Rim granite.	Dominantly mafic, mixed and felsic tuff, and lapilli tuff with minor mafic, intermediate and felsic flows.	Thick packages of quartz-eye rhyolite and dacite in Hood 46 and 461. Felsic flows at Hood 462 underlain by andesite and basalt flows with moderate to strong shearing and faulting.
Alteration	Variable intensity chlorite, sericite and quartz alteration throughout footwall and hanging wall. Strong chlorite alteration immediately adjacent to (~1 m) and within mineralized horizons.	Chlorite, sericite and quartz alteration throughout the hanging and footwalls. Chlorite alteration is stronger in the footwall compared to the hanging wall. Significant quartz and K-feldspar alteration of all lithologies is inferred to be due to extensive intrusion of granite.	Variable intensity chlorite, sericite and quartz alteration throughout footwall and hanging wall. Chlorite alteration in the hanging wall is typically weaker than in the footwall.	Strong chlorite alteration typically confined to zones of <10 metres (relationship to mineralization unclear). Moderate quartz and sericite alteration in felsic rocks with chlorite alteration confined to fractures. Common Fe-carbonate veining and alteration in Hood 462.
Mineralization	Two mineralized horizons; the lower horizon is typically the thicker of the two. Mineralization varies from Cu-rich to Zn-rich and consists of stringer to massive sulfide. Cubic buckshot pyrite surrounded by pyrrhotite and chlorite altered remnant clasts are common in massive sulfide.	Mineralization consists of stringer to massive sulfide zones. Massive sulfide typically consists of fine grained pyrrhotite + pyrite + sphalerite matrix with buckshot pyrite cubes and chlorite altered host rock clasts. Stringer sulfide zones consist of pyrite and chalcopyrite stringers. Pyrite and chalcopyrite have been remobilized to form veins and stringers in granite intrusions.	Mineralization consists of stringer to massive sulfide zones. Massive sulfide zones consist of fine grained pyrrhotite + pyrite + sphalerite with buckshot pyrite cubes, chalcopyrite stringers and chlorite altered host rock clasts. Stringer sulfide zone consist of pyrite and chalcopyrite stringers.	Limited mineralization; predominantly chalcopyrite stringers hosted by felsic flows in Hood 46 and 461. Mineralization at Hood 462 consists of pyrite layers interbedded with chloritic argillite or ash layers and hematite lenses.

Table 2-2: Mass change summary table divided by felsic and mafic rock types and deposit; if only a single sample of a rock type occurred no range is given.

Deposit	Element Mass Change	Felsic																					
		Type A				Type B				Type C				Core-granite				Tuff signature				All Felsic	
		Range	Average			Range	Average			Range	Average			Range	Average			Range	Average	Range	Average		
Hood 10	Al <sub>2</sub> O <sub>3</sub>	-29.96-2.26	1.05		2.2-1.1	2.06		2.17-2.24	2.21		-		2.26-2.26	2.26		-		-29.96-2.26	1.76				
	TiO <sub>2</sub>	-8.95-0.08	-0.34		0.04-0.05	0.05		0.04-0.13	0.08		-		0.18-0.18	0.18		-		-8.95-0.33	-0.11				
	CaO	-7.31-1.49	-0.90		-0.13--0.04	-0.10		-0.96-1.44	0.24		-		0.21-0.21	0.21		-		-7.31-2.73	-0.66				
	MgO	-5.37-11.2	3.22		-0.43-0.35	0.08		0.41-1.53	0.97		-		0.46-0.46	0.46		-		-5.37-17.96	2.70				
	SiO <sub>2</sub>	-8.17-192.35	47.86		22.69-30.99	25.62		5.18-14.53	9.85		-		3.48-3.48	3.48		-		-51.63-192.35	30.62				
	Fe <sub>2</sub> O <sub>3</sub>	-2.17-15.3	1.97		-1.63-0.16	-0.62		-1.88-0.02	-0.93		-		-0.99-0.99	-0.99		-		-2.17-25.84	2.05				
Hood 41	Na <sub>2</sub> O	-44.17-4.3	-2.77		2.42-2.79	2.63		-1.72-1.36	-0.18		-		0.92-0.92	0.92		-		-44.17-4.3	-1.87				
	K <sub>2</sub> O	-14.68-2.82	-0.06		-1.79--1.27	-1.49		-1.48-2.46	0.49		-		0.39-0.39	0.39		-		-14.68-2.82	0.36				
	Al <sub>2</sub> O <sub>3</sub>	2.04-2.26	2.19		-	-		-	-		-		-	-		-		2.04-2.26	2.19				
	TiO <sub>2</sub>	-0.22-0.03	-0.07		-	-		-	-		-		-	-		-		-0.22-0.03	-0.07				
	CaO	-1.6--0.45	-1.07		-	-		-	-		-		-	-		-		-1.6--0.45	-1.07				
	MgO	1.87-7.2	3.71		-	-		-	-		-		-	-		-		1.87-7.2	3.71				
Hood 41A	SiO <sub>2</sub>	-19.7-70.92	31.32		-	-		-	-		-		-	-		-		-19.7-70.92	31.32				
	Fe <sub>2</sub> O <sub>3</sub>	0.17-6.03	3.63		-	-		-	-		-		-	-		-		0.17-6.03	3.63				
	Na <sub>2</sub> O	-3.53--2.78	-3.08		-	-		-	-		-		-	-		-		-3.53--2.78	-3.08				
	K <sub>2</sub> O	-0.29-1.49	0.84		-	-		-	-		-		-	-		-		-0.29-1.49	0.84				
	Al <sub>2</sub> O <sub>3</sub>	1.93-2.26	2.13		-	-		1.18-2.24	1.71		1.47-2.18	1.82		1.34-2.23	1.87		-	1.18-2.26	2.12				
	TiO <sub>2</sub>	0.01-0.05	0.03		-	-		0.0-0.1	0.01		-0.15--0.1	-0.12		-0.32-0.33	0.07		-	-0.32-0.33	0.00				
Hood 46,461,462	CaO	-0.61-0.51	0.01		-	-		0.35-2.25	1.30		-0.22-2.73	0.97		-1.52-2.56	-0.15		-	-1.52-2.73	-0.46				
	MgO	0.08-17.96	11.42		-	-		-0.99-0.69	-0.84		-1.08-0.81	-0.94		-0.97-6.07	2.68		-	-1.08-17.96	2.48				
	SiO <sub>2</sub>	-51.63--2.57	-30.76		-	-		11.92-24.98	18.45		12.22-24.07	16.77		4.57-11	7.58		-	-51.63-24.98	25.22				
	Fe <sub>2</sub> O <sub>3</sub>	-0.55-25.84	16.51		-	-		-2.15-2.24	0.04		-1.89-0.15	-1.03		-0.38-7.64	2.68		-	-2.15-25.84	2.18				
	Na <sub>2</sub> O	-4.07--0.67	-2.62		-	-		-0.84-1.83	0.49		0.76-2.31	1.59		-3.05-1.78	-1.37		-	-4.07-2.31	-0.93				
	K <sub>2</sub> O	-2.58-0.77	-1.19		-	-		-0.23-0.25	0.01		-2.12-1.36	-0.94		-0.71-1.56	0.38		-	-2.58-1.56	0.40				
All Deposits	Al <sub>2</sub> O <sub>3</sub>	2.05-2.25	2.20		2.11-2.26	2.22		2.25-2.25	2.25		-		-0.8-1.76	1.07		-		-0.8-2.26	2.10				
	TiO <sub>2</sub>	-0.09-0.08	-0.02		-0.08-0.04	-0.01		0.07-0.08	0.08		-		-0.98-0.02	-0.25		-		-0.98-0.08	-0.03				
	CaO	-1.11-1.88	-0.04		-1.21-0.68	-0.78		-1.09-1.07	-1.08		-		-1.64-5.47	0.56		-		-1.64-5.47	-0.47				
	MgO	-0.22-2.26	1.00		-0.04-8.47	2.07		2.64-2.73	2.68		-		-0.86-1.92	0.27		-		-0.86-8.47	1.64				
	SiO <sub>2</sub>	9.23-58.16	31.15		3.7-69.83	30.66		17.59-18.99	18.29		-		3.69-11.47	6.98		-		3.69-69.83	27.88				
	Fe <sub>2</sub> O <sub>3</sub>	-1.91-1.37	-0.69		-2.03-5.29	1.09		1.33-1.48	1.41		-		0.1-46	0.71		-		-2.03-5.29	0.59				
All Deposits	Na <sub>2</sub> O	-3.71-3.74	-0.49		-3.7-1.18	-2.53		-3.06--3.04	-3.05		-		-4.22-2.35	0.20		-		-4.22-3.74	-1.74				
	K <sub>2</sub> O	-1.05-2.61	1.21		-0.17-2.32	1.45		1.82-1.82	1.82		-		-0.42-0.78	0.00		-		-1.05-2.61	1.26				
	Al <sub>2</sub> O <sub>3</sub>	-29.96-2.26	1.55		2.2-2.26	2.20		1.18-2.25	2.06		1.47-2.18	1.82		-0.8-2.26	1.52			-29.96-2.26	2.26				
	TiO <sub>2</sub>	-8.95-0.08	-0.20		-0.08-0.05	0.00		0.0-13	0.06		-0.15--0.1	-0.12		-0.98-0.33	-0.07			-8.95-0.33	-0.11				
All Deposits	CaO	-7.31-1.88	-0.69		-1.21-0.68	-0.71		-1.09-2.25	0.15		-0.22-2.73	0.97		-1.64-5.47	0.25			-7.31-5.47	-0.51				
	MgO	-5.37-17.96	3.30		-0.43-8.47	1.85		-0.99-2.73	0.94		-1.08-0.81	-0.94		-0.97-6.07	1.20			-5.37-17.96	2.50				
	SiO <sub>2</sub>	-51.63-192.35	36.82		3.7-69.83	30.10		5.18-24.98	15.53		12.22-24.07	16.77		3.48-11.47	6.77			-51.63-192.35	30.64				
	Fe <sub>2</sub> O <sub>3</sub>	-2.17-25.84	2.52		-2.03-5.29	0.90		-2.15-2.24	0.17		-1.89-0.15	-1.03		-0.99-7.64	1.24			-2.17-25.84	1.73				
All Deposits	Na <sub>2</sub> O	-44.17-4.3	-2.31		-3.7-2.79	-1.95		-3.06-1.83	-0.91		0.76-2.31	1.59		-4.22-2.35	-0.30			-44.17-4.3	-1.82				
	K <sub>2</sub> O	-14.68-2.82	0.29		-1.79-2.32	1.13		-1.48-2.46	0.78		-2.12-1.36	-0.94		-0.71-1.56	0.19			-14.68-2.82	0.53				

Table 2-2 (continued): Mass change summary table divided by felsic and mafic rock types and deposit; if only a single sample of a rock type occurred no range is given.

Deposit	Element Mass Change	Type I			Type II			Type III			Type IV			All Mafic		
		Range	Average		Range	Average		Range	Average		Range	Average		Range	Average	
Hood 10	Al <sub>2</sub> O <sub>3</sub>	-0.84 - -0.67	-0.79		-0.49 - 0.41	-0.10		-	-0.27		-	-		-0.84 - 0.41	-0.37	
	TiO <sub>2</sub>	0.37 - 1.42	0.73		-0.18 - 1.46	0.56		-	1.77		-	-		-0.18 - 1.77	0.73	
	CaO	4.91 - 7.38	6.61		-2.04 - 8.5	3.55		-	4.36		-	-		-2.04 - 8.5	4.74	
	MgO	0.13 - 3.36	2.32		-0.52 - 3.86	2.39		-	0.07		-	-		-0.52 - 3.86	2.16	
	SiO <sub>2</sub>	2.77 - 9.67	5.14		-1.12 - 8.22	5.27		-	-9.72		-	-		-9.72 - 9.67	3.86	
	Fe <sub>2</sub> O <sub>3</sub>	4.85 - 8.21	5.92		-0.7 - 10.7	5.23		-	9.62		-	-		-0.7 - 10.7	5.88	
	Na <sub>2</sub> O	-3.55 - -1.61	-2.56		-2.75 - 0.3	-1.56		-	-1.95		-	-		-3.55 - 0.3	-1.96	
Hood 41	K <sub>2</sub> O	-1.31 - -0.92	-1.12		-1.26 - -0.61	-0.98		-	0.94		-	-		-1.31 - 0.94	-0.86	
	Al <sub>2</sub> O <sub>3</sub>	-0.88 - -0.65	-0.75		-	-		-	-		-	-		-0.88 - -0.65	-0.75	
	TiO <sub>2</sub>	-0.48 - 0.28	-0.10		-	-		-	-		-	-		-0.48 - 0.28	-0.10	
	CaO	2.42 - 4.51	3.17		-	-		-	-		-	-		2.42 - 4.51	3.17	
	MgO	-3.56 - 0.46	-2.17		-	-		-	-		-	-		-3.56 - 0.46	-2.17	
	SiO <sub>2</sub>	-7.16 - -3.33	-5.14		-	-		-	-		-	-		-7.16 - -3.33	-5.14	
	Fe <sub>2</sub> O <sub>3</sub>	0.78 - 6.61	2.87		-	-		-	-		-	-		0.78 - 6.61	2.87	
Hood 41A	Na <sub>2</sub> O	-4.26 - -1.29	-2.28		-	-		-	-		-	-		-4.26 - -1.29	-2.28	
	K <sub>2</sub> O	-1.26 - -0.86	-1.09		-	-		-	-		-	-		-1.26 - -0.86	-1.09	
	Al <sub>2</sub> O <sub>3</sub>	-0.76 - -0.64	-0.71		-0.5 - 1.28	-0.11		-	-0.40		-0.63 - -0.69	-0.66		-0.76 - 1.28	-0.31	
	TiO <sub>2</sub>	-0.05 - 1.45	0.55		-0.21 - 1.16	0.25		-	-0.14		0.35 - 0.29	0.32		-0.21 - 1.45	0.31	
	CaO	4.03 - 10.95	6.23		-1.81 - 5.67	2.43		-	3.34		4.31 - 3.57	3.94		-1.81 - 10.95	3.47	
	MgO	-3.96 - 15.89	3.39		-3.31 - 9.81	0.62		-	-2.33		-3.49 - 3.54	-3.52		-3.96 - 15.89	0.74	
	SiO <sub>2</sub>	2.08 - 27.15	11.43		-18.13 - 10.45	-1.75		-	-0.03		9.15 - 8.01	8.58		-18.13 - 27.15	2.26	
Hood 46,461,462	Fe <sub>2</sub> O <sub>3</sub>	3.48 - 11.36	8.04		0.58 - 9.12	4.93		-	2.34		2.78 - 2.54	2.66		0.58 - 11.36	5.31	
	Na <sub>2</sub> O	-3.36 - -0.66	-2.25		-4.05 - -0.29	-2.32		-	-1.03		-1.06 - -1.56	-1.31		-4.05 - -0.29	-2.15	
	K <sub>2</sub> O	-1.21 - 0.15	-0.59		-1.16 - 0.81	-0.54		-	-1.00		-0.3 - -0.65	-0.48		-1.21 - 0.81	-0.56	
	Al <sub>2</sub> O <sub>3</sub>	-0.83 - -0.82	-0.83		-	0.16		-0.12 - 0.06	-0.05		-	-		-0.83 - 0.16	-0.27	
	TiO <sub>2</sub>	-0.21 - -0.19	-0.20		-	1.07		0.74 - 1.98	1.57		-	-		-0.21 - 1.98	0.89	
	CaO	8.98 - 12.05	10.51		-	-0.81		4.46 - 5.75	5.21		-	-		-0.81 - 12.05	5.97	
	MgO	10.73 - 12.82	11.78		-	0.43		-0.71 - 1.66	0.26		-	-		-0.71 - 12.82	4.13	
All Deposits	SiO <sub>2</sub>	22.35 - 22.69	22.52		-	2.08		-6.02 - -4.82	-5.33		-	-		-6.02 - 22.69	5.19	
	Fe <sub>2</sub> O <sub>3</sub>	7.67 - 8.03	7.85		-	7.58		6.6 - 6.95	6.74		-	-		6.6 - 8.03	7.25	
	Na <sub>2</sub> O	-4.59 - -2.39	-3.49		-	-0.48		-3.5 - -1.02	-2.04		-	-		-4.59 - -0.48	-2.27	
	K <sub>2</sub> O	-1.15 - -1.1	-1.13		-	-1.10		-0.18 - 3.68	1.38		-	-		-1.15 - 3.68	0.13	
	Al <sub>2</sub> O <sub>3</sub>	-0.88 - -0.64	-0.76		-0.5 - 1.28	-0.10		-0.4 - 0.06	-0.16		-0.69 - -0.63	-0.66		-0.88 - 1.28	-0.36	
	TiO <sub>2</sub>	-0.48 - 1.45	0.32		-0.21 - 1.46	0.38		-0.14 - 1.98	1.27		0.29 - 0.35	0.32		-0.48 - 1.98	0.46	
	CaO	2.42 - 12.05	6.08		-2.04 - 8.5	2.60		3.34 - 5.75	4.66		3.57 - 4.31	3.94		-2.04 - 12.05	4.12	
All Deposits	MgO	-3.96 - 15.89	2.74		-3.31 - 9.81	1.12		-2.33 - 1.66	-0.30		-3.54 - -3.49	-3.52		-3.96 - 15.89	1.31	
	SiO <sub>2</sub>	-7.16 - 27.15	6.81		-18.13 - 10.45	0.44		-9.72 - -0.03	-5.15		8.01 - 9.15	8.58		-18.13 - 27.15	2.39	
	Fe <sub>2</sub> O <sub>3</sub>	0.78 - 11.36	6.07		-0.7 - 10.7	5.14		2.34 - 9.62	6.43		2.54 - 2.78	2.66		-0.7 - 11.36	5.50	
	Na <sub>2</sub> O	-4.59 - -0.66	-2.51		-4.05 - 0.3	-2.01		-3.5 - -1.02	-1.82		-1.56 - -1.06	-1.31		-4.59 - 0.3	-2.13	
	K <sub>2</sub> O	-1.31 - 0.15	-0.94		-1.26 - 0.81	-0.69		-1 - 3.68	0.81		-0.65 - -0.3	-0.48		-1.31 - 3.68	-0.59	

## Chapter 3: **Summary and Directions of Future Research**

### 3.1 SUMMARY

This study has yielded field and geochemical results that characterize the Hood VMS deposits. The general conclusions of this study are:

1) The Hood VMS deposits are a group of three mineral lenses and three smaller mineral occurrences that are hosted by bimodal mafic and felsic volcanic flows and volcanoclastic rocks in the Amooga Booga volcanic belt of the Slave craton. Hood deposit stratigraphy, mineral textures, and alteration are consistent with subseafloor-replacement style mineralization. These features include mineralized lenses that cut across volcanic lithologies, remnant chlorite altered clasts indicative of sulfides replacing the host rocks around them and hydrothermal alteration continuing into the hanging walls of the mineral lenses.

2) The felsic volcanic rocks of the ABVB are derived from the partial melting of hydrated mafic rocks (Yamashita et al., 2000). Variability in fractionation temperature and crustal contamination resulted in the formation of two main felsic suites (suites A and B), and this contrasting petrogenesis has important implications for mineralization potential. Suite A has higher HFSE, REE and higher Nb/Ta ratios than suite B and is interpreted to have had a higher emplacement temperatures and less crustal contamination than suite B. Suite A is more closely associated with the bulk of the mineralization indicating that localized controls play an important role in the formation of VMS deposits. Suite A also has FII-type signatures compared to the FI-type signatures of suite



and therefore they are considered more prospective for VMS mineralization (Leshner et al., 1986; Hart et al., 2004).

3) The Rim granite is geochemically similar to suite A felsic rocks and is interpreted to have acted as the subvolcanic heat source that drove the hydrothermal circulation system that formed the Hood VMS deposits (Chapter 2).

4) The two main mafic volcanic suites of the ABVB were derived from moderately enriched mantle sources (Jensen, 1995; Yamashita et al., 2000). The two types are crustally contaminated with type I being weakly contaminated and type II being strongly contaminated, resulting in negative Nb anomalies,  $\text{Nb}/\text{Th}_{\text{pmn}} < 1$ , and elevated LREE for type II compared to type I. The two types of mafic volcanic rocks are interlayered in the Hood deposits lenses and can also occur as synvolcanic dykes.

5) Three dimensional reconstructions of the Hood deposits for element mass change, distribution of alteration minerals determined by SWIR spectroscopy, and principal component analysis is useful to identify areas of high sulfide mineral potential, and the effect of alteration in the footwall and hanging wall to the mineral lenses.

6) The geochemistry of the volcanic rocks of the Hood deposits is similar to that of rocks formed in modern continental marginal back-arc basin in which erupting magmas interacted with the pre-existing sialic basement. Such a tectonic environment is consistent with interpretations of similar aged greenstone belts in the Slave craton such as the Point Lake volcanic belt (Corcoran and Dostal, 2001). This type of extensional environment is favourable for VMS mineralization (Lentz, 1998; Piercey et al., 2008; Piercey, 2011).

### 3.2 DIRECTIONS OF FUTURE RESEARCH

This thesis contributes to the fundamental knowledge base for the Hood deposits, but many potential avenues for future research remain in both the ABVB and throughout the Slave craton. Over the course of field work for this study, samples were collected for future geochronological dating. Additional U-Pb dating is necessary to refine the geochronological relationship between volcanism, the plutonism of the Rim granite, and mineralization. Understanding the geochronology of greenstone belt tectonic events will also be useful for constraining tectonic models for the Slave craton and allows for volcanic belt correlations.

Sulfide samples were also collected for future research into the mineralization. Additional research is required on the sequence of sulfide mineral precipitation at the Hood deposits as well as isotopic work to understand the provenance of the metals. This is particularly relevant in the Slave craton where a Pb isotopic boundary is inferred to reflect the architecture of the craton basement (Thorpe, 1992).

The importance of felsic magma petrogenesis to mineral potential can be tested by detailed geochemistry of felsic volcanic rocks in other Slave greenstone belts that host VMS mineralization. Exploration in the ABVB should focus on felsic rocks with suite A affinities rather than suite B geochemical characteristics.

Further stratigraphic and geochemical studies of other 2.69-2.66 Ga greenstone belts of the Slave craton are required to refine a tectonic model for the evolution of the Slave craton.

## References

- Goodwin, A. M., Lambert, M. B., and Ujike, O., 2006, Geochemical and metallogenic relations in volcanic rocks of the southern Slave Province: implications for late Neoproterozoic tectonics: *Canadian Journal of Earth Sciences*, v. 43, p. 1835-1857.
- Hart, T. R., Gibson, H. L., and Leshner, C. M., 2004, Trace element geochemistry and petrogenesis of felsic volcanic rocks associated with volcanogenic massive Cu-Zn-Pb sulfide deposits: *Economic Geology*, v. 99, p. 1003-1013.
- Jensen, J. E., 1995, *Geology, geochemistry and Nd isotopic study of the Hanikahimajuk Lake area, Slave Province, NWT*, University of Alberta, Edmonton, Alberta.
- Lentz, D. R., 1998, Petrogenetic evolution of felsic volcanic sequences associated with Phanerozoic volcanic-hosted massive sulfide systems: the role of extensional geodynamics: *Ore Geology Reviews*, v. 12, p. 289-327.
- Leshner, C. M., Goodwin, A. M., Campbell, I. H., and Gorton, M. P., 1986, Trace element geochemistry of ore-associated and barren felsic metavolcanic rocks in the Superior province, Canada: *Canadian Journal of Earth Sciences*, v. 23, p. 222-237.
- Piercey, S., 2011, The setting, style, and role of magmatism in the formation of volcanogenic massive sulfide deposits: *Mineralium Deposita*, p. 1-23.
- Piercey, S. J., Peter, J. M., and Mortensen, J. K., 2008, A Special Issue Devoted to Continental Margin Massive Sulfide Deposits and Their Geodynamic Environments: *Economic Geology*, v. 103, p. 1-4.
- Thorpe, R. I., Cumming, G.L. and Mortensen, J.K., 1992, A major Pb-isotopic boundary in the Slave Province and its probable relation to ancient basement in the Slave Province and its probable relation to ancient basement in the western Slave, Canada - NWT MDA summary volume, Geological Survey of Canada, Open File 2484, p. 179 - 184.
- Yamashita, K., Creaser, R. A., Jensen, J. E., and Heaman, L. M., 2000, Origin and evolution of mid- to late-Archean crust in the Hanikahimajuk Lake area, Slave Province, Canada; evidence from U-Pb geochronological, geochemical and Nd-Pb isotopic data: *Precambrian Research*, v. 99, p. 197-224.

## References

- Barrett, T. J., and MacLean, W. H., 1994, Mass changes in hydrothermal alteration zones associated with VMS deposits of the Noranda area: *Exploration and Mining Geology*, v. 3, p. 131-160.
- Barrett, T. J., and MacLean, W. H., 1999, Volcanic sequences, lithogeochemistry, and hydrothermal alteration in some bimodal volcanic-associated massive sulfide systems, *in* Barrie, C. T., and Hannington, M. D., eds., *Volcanic-Associated Massive Sulfide Deposits: Processes and Examples in Modern and Ancient Environments*, *Reviews in Economic Geology* 8, Society of Economic Geologists, p. 101-131.
- Barrie, C. T., Ludden, J. N., and Green, T. H., 1993, Geochemistry of volcanic rocks associated with Cu-Zn and Ni-Cu deposits in the Abitibi Subprovince: *Economic Geology*, v. 88, p. 1341-1358.
- Bau, M., and Dulski, P., 1995, Comparative study of yttrium and rare-earth element behaviours in fluorine-rich hydrothermal fluids: *Contributions to Mineralogy and Petrology*, v. 119, p. 213-223.
- Bindeman, I., Gurenko, A., Carley, T., Miller, C., Martin, E., and Sigmarsson, O., 2012, Silicic magma petrogenesis in Iceland by remelting of hydrothermally altered crust based on oxygen isotope diversity and disequilibria between zircon and magma with implications for MORB: *Terra Nova*, v. 24, p. 227-232.
- Bleeker, W., 2002, Archaean tectonics: a review, with illustrations from the Slave craton, *in* Fowler, C. M. R., Ebinger, C. J., and Hawkesworth, C. J., eds., *The Early Earth: Physical, Chemical and Biological Development*, Special Publication: London, Geological Society, p. 151-181.
- Bleeker, W., and Hall, B., 2007, The Slave craton: geological and metallogenic evolution, *in* Goodfellow, W. D., ed., *Mineral Deposits of Canada: A Synthesis of Major Deposit-types, District Metallogeny, the Evolution of Geological Provinces, and Exploration Methods*, Special Publication 5, Mineral Deposits Division, Geological Association of Canada, p. 849-879.
- Bleeker, W., Ketchum, J., and Davis, W., 1999a, The Central Slave Basement Complex, Part II: age and tectonic significance of high-strain zones along the basement-cover contact: *Canadian Journal of Earth Sciences*, v. 36, p. 1111-1130.

Bleeker, W., Ketchum, J., Jackson, V., and Villeneuve, M., 1999b, The Central Slave Basement Complex, Part I: its structural topology and autochthonous cover: *Canadian Journal of Earth Sciences*, v. 36, p. 1083-1109.

Bruce, C. S., 1991, Hood River Project # 708 - Report on the 1990 Field Program: Falconbridge Limited Company Report, p. 1-59.

Campbell, I. H., Leshner, C. M., Coad, P., Franklin, J. M., Gorton, M. P., and Thurston, P. C., 1984, Rare-earth element mobility in alteration pipes below massive Cu-Zn sulfide deposits: *Chemical Geology*, v. 45, p. 181-202.

Claiborne, L. L., Miller, C. F., Walker, B. A., Wooden, J. L., Mazdab, F. K., and Bea, F., 2006, Tracking magmatic processes through Zr/Hf ratios in rocks and Hf and Ti zoning in zircons: An example from the Spirit Mountain batholith, Nevada: *Mineralogical Magazine*, v. 70, p. 517-543.

Corcoran, P.L., and Dostal, J., 2001, Development of an ancient back-arc basin overlying continental crust: the archaean Peltier Formation, Northwest Territories, Canada: *The Journal of Geology*, v. 109, p. 329-348.

Cousens, B. L., 2000, Geochemistry of the Archean Kam Group, Yellowknife Greenstone Belt, Slave Province, Canada: *Journal of Geology*, v. 108, p. 181-197.

Cousens, B., Facey, K., and Falck, H., 2002, Geochemistry of the late Archean Banting Group, Yellowknife greenstone belt, Slave Province, Canada; simultaneous melting of the upper mantle and juvenile mafic crust: *Canadian Journal of Earth Sciences* v. 39, p. 1635-1656.

Cudahy, T. J., Okada, K., Yamato, Y., Yoshizawa, K., Wilson, J., and Brauhart, C., 2001, Archaean VMS Hydrothermal alteration systems at Panorama, WA, revealed through airborne VNIR-SWIR spectrometry: *Contributions of the Economic Geology Research Unit*, v. 59, p. 40-41.

Date, J., Watanabe, Y., and Saeki, Y., 1983, Zonal alteration around the Fukazawa Kuroko deposits, Akita Prefecture, northern Japan., *in* Ohmoto, H., and Skinner, B. J., eds., *Kuroko and Related Volcanogenic Massive Sulfide Deposits*, *Economic Geology Monograph* 5, p. 365-386.

Davis, J. C., 2002, *Statistics and Data Analysis in Geology*, Third Edition: New York, John Wiley and Sons, 638 p.

Davis, W., and Bleeker, W., 1999, Timing of plutonism, deformation, and metamorphism in the Yellowknife Domain, Slave Province, Canada: *Canadian Journal of Earth Sciences*, v. 36, p. 1169-1187.

Davis, W., and Hegner, E., 1992, Neodymium isotopic evidence for the tectonic assembly of the Late Archean crust in the Slave Province, northwest Canada: *Contributions to Mineralogy and Petrology*, v. 111, p. 493-504.

Davis, W. J., Fryer, B. J., and King, J. E., 1994, Geochemistry and evolution of Late Archean plutonism and its significance to the tectonic development of the Slave craton: *Precambrian Research*, v. 67, p. 207-241.

Davis, W. J., Jones, A. G., Bleeker, W., and Grutter, H., 2003, Lithosphere development in the Slave craton: a linked crustal and mantle perspective: *Lithos*, v. 71, p. 575-589.

Doyle, M. G., and Allen, R. L., 2003, Subsea-floor replacement in volcanic-hosted massive sulfide deposits: *Ore Geology Reviews*, v. 23, p. 183-222.

Franklin, J. M., Lydon, J. W., and Sangster, D. F., 1981, Volcanic-associated massive sulfide deposits, *in* Skinner, B. J., ed., *Economic Geology 75th Anniversary Volume*, p. 485-627.

Franklin, J. M., Gibson, H. L., Galley, A. G., and Jonasson, I. R., 2005, Volcanogenic Massive Sulfide Deposits, *in* Hedenquist, J. W., Thompson, J. F. H., Goldfarb, R. J., and Richards, J. P., eds., *Economic Geology 100th Anniversary Volume*: Littleton, CO, Society of Economic Geologists, p. 523-560.

Fraser, J. A., 1960, North-central District of Mackenzie, Northwest Territories, Preliminary Map 18-1960, Geological Survey of Canada.

Fyson, W. K., and Helmstaedt, H., 1988, Structural patterns and tectonic evolution of supracrustal domains in the Archean Slave Province, Canada: *Canadian Journal of Earth Sciences*, v. 25, p. 301-315.

Galley, A. G., 1993, Characteristics of semi-conformable alteration zones associated with volcanogenic massive sulphide districts: *Journal of Geochemical Exploration*, v. 48, p. 175-200.

Galley, A. G., 2003, Composite synvolcanic intrusions associated with Precambrian VMS-related hydrothermal systems: *Mineralium Deposita*, v. 38, p. 443 - 473.

Galley, A. G., Hannington, M., and Jonasson, I., 2007, Volcanogenic massive sulphide deposits, *in* Goodfellow, W. D., ed., *Mineral Deposits of Canada: A Synthesis of Major Deposit-types, District Metallogeny, the Evolution of Geological Provinces, and Exploration Methods*, Special Publication 5, Mineral Deposits Division, Geological Association of Canada, p. 141-161.

Gebert, J. S., 1995, Archean Geology of the Hanikahimajuk Lake Area, Northern Point Lake Volcanic Belt, West-Central Slave Structural Province, District of Mackenzie, N.W.T.: NWT EGS Open File p. 27.

Gemmell, J. B., and Fulton, R., 2001, Geology, genesis, and exploration implications of the footwall and hanging-wall alteration associated with the Hellyer volcanic-hosted massive sulphide deposit, Tasmania, Australia.: *Economic Geology*, v. 96, p. 1003-1036.

Gemmell, J. B., and Large, R. R., 1992, Stringer system and alteration zones underlying the Hellyer volcanic-hosted massive sulfide deposit, Tasmania, Australia: *Economic Geology*, v. 87, p. 620-649.

Gill, J. W., 1977, The Takiyuak metavolcanic belt: Geology, geochemistry, and mineralization: Unpub. Ph.D. thesis, Carleton University, Ottawa, Ontario, Canada, 210 p.

Goodwin, A. M., Lambert, M. B., and Ujike, O., 2006, Geochemical and metallogenic relations in volcanic rocks of the southern Slave Province: implications for late Neoproterozoic tectonics: *Canadian Journal of Earth Sciences*, v. 43, p. 1835-1857.

Green, T. H., 1995, Significance of Nb/Ta as an indicator of geochemical processes in the crust-mantle system: *Chemical Geology*, v. 120, p. 347-359.

Grunsky, E. C., 2010, The interpretation of geochemical survey data: *Geochemistry: Exploration, Environment, Analysis*, v. 10, p. 27-74.

Grunsky, E. C., and Kjarsgaard, B. A., 2008, Classification of distinct eruptive phases of the diamondiferous Star kimberlite, Saskatchewan, Canada based on statistical treatment of whole rock geochemical analyses: *Applied Geochemistry*, v. 23, p. 3321-3336.

Hajash, A., and Chandler, G. W., 1981, An experimental investigation of high-temperature interactions between seawater and rhyolite, andesite, basalt and peridotite: *Contributions to Mineralogy and Petrology*, v. 78, p. 240-254.

Hamilton, W. B., 1998, Archean magmatism and deformation were not products of plate tectonics: *Precambrian Research*, v. 91, p. 143-179.

Hanchar, J. M., and van Westrenen, W., 2007, Rare Earth Element Behavior in Zircon-Melt Systems: *ELEMENTS*, v. 3, p. 37-42.

Hart, T. R., Gibson, H. L., and Leshner, C. M., 2004, Trace element geochemistry and petrogenesis of felsic volcanic rocks associated with volcanogenic massive Cu-Zn-Pb sulfide deposits: *Economic Geology*, v. 99, p. 1003-1013.

Hassard, F. R., 1983, Hood River- No. 10 Deposit, Diamond Drilling, Geological and Geophysical Exploration and Compilation: Kidd Creek Mines Ltd. - Company Report, p. 42.

Helmstaedt, H., and Padgham, W. A., 1986, A new look at the stratigraphy of the Yellowknife Supergroup at Yellowknife, N.W.T. – implications for the age of gold-bearing shear zones and Archean basin evolution: *Canadian Journal of Earth Sciences*, v. 23, p. 454-475.

Helmstaedt, H. H., and Pehrsson, S. J., 2012, Geology and Tectonic Evolution of the Slave Province - A Post-Lithoprobe Perspective, in Percival, J. A., Cook, F. A., and Clowes, R. M., eds., *Tectonic Styles in Canada: The Lithoprobe Perspective*. Special Paper, Geological Association of Canada, p. 379-466.

Herrmann, W., Blake, M., Doyle, M., Huston, D., Kamprad, J., Merry, N., and Pontual, S., 2001, Short Wavelength Infrared (SWIR) Spectral Analysis of Hydrothermal Alteration Zones Associated with Base Metal Sulfide Deposits at Rosebery and Western Tharsis, Tasmania, and Highway-Reward, Queensland: *Economic Geology*, v. 96, p. 939-955.

Heslop, J. B., 1973, Hood River Project #94 - Report H-2: Geology of Area #46 - Grid "C": Private Report, p. 111.

Hoffman, P. F., 1988, United plates of America, the birth of a craton: Early Proterozoic assembly and growth of Laurentia: *Annual Reviews of Earth and Planetary Science*, v. 16, p. 543-603.

Isachsen, C. E., and Bowring, S. A., 1994, Evolution of the Slave Craton: *Geology*, v. 22, p. 917-920.

Isachsen, C.E., and Bowring, S. A., 1997, The Bell Lake group and Anton Complex: a basement – cover sequence beneath the Archean Yellowknife greenstone belt revealed and implicated in greenstone belt formation: *Canadian Journal of Earth Sciences*, v. 34, p. 169-189.

Isachsen, C. E., Bowring, S. A., and Padgham, W. A., 1991, U-Pb Zircon Geochronology of the Yellowknife Volcanic Belt, NWT, Canada: New Constraints on the Timing and Duration of Greenstone Belt Magmatism: *The Journal of Geology*, v. 99, p. 55-67.



Jenner, G. A., 1996, Trace element geochemistry of igneous rocks: Geochemical nomenclature and analytical geochemistry, *in* Wyman, D. A., ed., Trace Element Geochemistry of Volcanic Rocks: Applications for Massive Sulfide Exploration, Short Course Notes Volume 12., Geological Association of Canada, p. 51-77.

Jensen, J. E., 1995, Geology, geochemistry and Nd isotopic study of the Hanikahimajuk Lake area, Slave Province, NWT: Unpub. M.S.c. Thesis, University of Alberta, Edmonton, Alberta.

Kamber, B. S., and Collerson, K. D., 2000, Role of 'hidden' deeply subducted slabs in mantle depletion: Chemical Geology, v. 166, p. 241-254.

Kerrick, R., and Wyman, D. A., 1997, Review of developments in trace-element fingerprinting of geodynamic settings and their implications for mineral exploration: Australian Journal of Earth Sciences, v. 44, p. 465-487.

Ketchum, J. W. F., Bleeker, W., and Stern, R. A., 2004, Evolution of an Archean basement complex and its autochthonous cover, southern Slave Province, Canada: Precambrian Research, v. 135, p. 149-176.

Kusky, T. M., 1991, Structural development of an archean orogen, western Point Lake, Northwest Territories: Tectonics, v. 10, p. 820-841.

Kusky, T. M., and Polat, A., 1999, Growth of granite-greenstone terranes at convergent margins, and stabilization of Archean cratons: Tectonophysics, v. 305, p. 43-73.

Large, R. R., Allen, R. L., Blake, M. D., and Herrmann, W., 2001a, Hydrothermal alteration and volatile element haloes for the Rosebery K Lens volcanic-hosted massive sulfide deposit, western Tasmania: Economic Geology, v. 96, p. 1055-1072.

Large, R. R., Gemmell, J. B., Paulick, H., and Huston, D. L., 2001b, The alteration box plot: a simple approach to understanding the relationships between alteration mineralogy and lithogeochemistry associated with VHMS deposits: Economic Geology, v. 96, p. 957-971.

Lentz, D. R., 1998, Petrogenetic evolution of felsic volcanic sequences associated with Phanerozoic volcanic-hosted massive sulfide systems: the role of extensional geodynamics: Ore Geology Reviews, v. 12, p. 289-327.

Lentz, D. R., 1999, Petrology, geochemistry and oxygen isotopic interpretation of felsic volcanic and related rocks hosting the Brunswick 6 and 12

massive sulfide deposits (Brunswick Belt), Bathurst Mining Camp, New Brunswick, Canada: *Economic Geology*, v. 94, p. 57-86.

Leshner, C. M., Goodwin, A. M., Campbell, I. H., and Gorton, M. P., 1986, Trace element geochemistry of ore-associated and barren felsic metavolcanic rocks in the Superior province, Canada: *Canadian Journal of Earth Sciences*, v. 23, p. 222-237.

MacLachlan, K., and Helmstaedt, H., 1995, Geology and geochemistry of an Archean mafic dyke complex in the Chan formation-basis for a revised plate-tectonic model of the Yellowknife greenstone-belt: *Canadian Journal of Earth Sciences*, v. 32, p. 614-630.

MacLean, W. H., 1990, Mass change calculations in altered rock series: *Mineralium Deposita*, v. 25, p. 44-49.

Mittlefehldt, D. W., and Miller, C. F., 1983, Geochemistry of the Sweetwater Wash Pluton, California: Implications for "anomalous" trace element behavior during differentiation of felsic magmas: *Geochimica Et Cosmochimica Acta*, v. 47, p. 109-124.

Mortensen, J. K., Thorpe, R. I., Padgham, W. A., King, J. E., and Davis, W. J., 1988, U-Pb zircon ages for felsic volcanism in the Slave Province, N.W.T., Radiogenic Age and Isotope Studies: Report 2, Paper 88-2, Geological Survey of Canada, p. 85-95.

Northrup, C. J., Isachsen, C., and Bowring, S. A., 1999, Field relations, U-Pb geochronology, and Sm-Nd isotope geochemistry of the Point Lake greenstone belt and adjacent gneisses, central Slave craton, N.W.T., Canada: *Canadian Journal of Earth Sciences*, v. 36, p. 1043-1059.

Ohmoto, H., Skinner, B.J., 1983, The Kuroko and Related Volcanogenic Massive Sulfide Deposits: Introduction and Summary of New Findings In: Ohmoto H, Skinner BJ (eds) *The Kuroko and Related Volcanogenic Massive Sulfide Deposits*. pp 604.

Ootes, L., Davis, W. J., Bleeker, W., and Jackson, V. A., 2009, Two Distinct Ages of Neoproterozoic Turbidites in the Western Slave Craton: Further Evidence and Implications for a Possible Back-Arc Model: *The Journal of Geology*, v. 117, p. 15-36.

Padgham, W. A., 1992, Mineral deposits in the Archean Slave structural province; lithological and tectonic setting: *Precambrian Research*, v. 58, p. 1-24.

Padgham, W. A., and Fyson, W. K., 1992, The Slave Province - A distinct Archean craton: *Canadian Journal of Earth Sciences*, v. 29, p. 2072-2086.

Pearce, J. A., 1996, A user's guide to basalt discrimination diagrams, *in* Wyman, D. A., ed., Trace element geochemistry of volcanic rocks: Applications for massive sulphide exploration, Short Course Notes, Volume 12, Geological Association of Canada, p. 79-113.

Pearce, J. A., Harris, N. B. W., and Tindle, A. G., 1984, Trace element discrimination diagrams for the tectonic interpretation of granitic rocks: *Journal of Petrology*, v. 25, p. 956-983.

Pearce, J. A., and Peate, D. W., 1995, Tectonic implications of the composition of volcanic arc magmas: *Annual Review of Earth and Planetary Sciences*, v. 23, p. 251-285.

Piercey, S., 2011, The setting, style, and role of magmatism in the formation of volcanogenic massive sulfide deposits: *Mineralium Deposita*, p. 1-23.

Piercey, S. J., Paradis, S., Murphy, D. C., and Mortensen, J. K., 2001, Geochemistry and paleotectonic setting of felsic volcanic rocks in the Finlayson Lake volcanic-hosted massive sulfide (VHMS) district, Yukon, Canada: *Economic Geology*, v. 96, p. 1877-1905.

Piercey, S. J., Murphy, D. C., Mortensen, J. K., and Creaser, R. A., 2004, Mid-Paleozoic initiation of the northern Cordilleran marginal backarc basin; geologic, geochemical, and neodymium isotope evidence from the oldest mafic magmatic rocks in the Yukon-Tanana Terrane, Finlayson Lake District, southeast Yukon,: *Geological Society of America Bulletin*, v. 116, p. 1087-1106.

Piercey, S. J., Peter, J. M., and Mortensen, J. K., 2008a, A Special Issue Devoted to Continental Margin Massive Sulfide Deposits and Their Geodynamic Environments: *Economic Geology*, v. 103, p. 1-4.

Piercey, S. J., Peter, J. M., Mortensen, J. K., Paradis, S., Murphy, D. C., and Tucker, T. L., 2008b, Petrology and U-Pb Geochronology of Footwall Porphyritic Rhyolites from the Wolverine Volcanogenic Massive Sulfide Deposit, Yukon, Canada: Implications for the Genesis of Massive Sulfide Deposits in Continental Margin Environments: *Economic Geology*, v. 103, p. 5-33.

Relf, C., 1992, 2 distinct shortening events during Late Archean orogeny in the west-central Slave Province, Northwest Territories, Canada: *Canadian Journal of Earth Sciences*, v. 29, p. 2104-2117.

Riverin, G., and Hodgson, C. J., 1980, Wall-rock alteration at the Millenbach Cu-Zn mine, Noranda, Quebec: *Economic Geology*, v. 75, p. 424-444.

Rockingham, C. J., 1979, Metamorphism and metal zoning of the Hood River-41 massive sulfide deposits, Slave Structural Province, N.W.T.: Unpub. M.Sc. thesis, University of Western Ontario, 125 p.

Ross, P.-S., and Bédard, J. H., 2009, Magmatic affinity of modern and ancient subalkaline volcanic rocks determined from trace-element discriminant diagrams: *Canadian Journal of Earth Sciences*, v. 46, p. 823-839.

Rubin, J. N., Henry, C. D., and Price, J. G., 1993, The mobility of zirconium and other "immobile" elements during hydrothermal alteration: *Chemical Geology*, v. 110, p. 29-47.

Rudnick, R. L., Barth, M. G., Horn, I., and McDonough, W. F., 2000, Rutile-bearing refractory eclogites: Missing link between continents and depleted mantle: *Science*, v. 287, p. 278-281.

Shervais, J. W., 1982, Ti-V plots and the petrogenesis of modern and ophiolitic lavas: *Earth and Planetary Science Letters*, v. 59, p. 101-118.

Shukuno, H., Tamura, Y., Tani, K., Chang, Q., Suzuki, T., and Fiske, R. S., 2006, Origin of silicic magmas and the compositional gap at Sumisu submarine caldera, Izu-Bonin arc, Japan: *Journal of Volcanology and Geothermal Research*, v. 156, p. 187-216.

Spitz, G., and Darling, R., 1978, Major and minor element lithogeochemical anomalies surrounding the Louvem copper deposit, Val d'Or, Quebec: *Canadian Journal of Earth Sciences*, v. 15, p. 1161-1169.

Stubbley, M. P., 2005, Slave Craton: Interpretive bedrock compilation, NWT-NU Open File 2005-01.

Sun, S.-s., and McDonough, W. F., 1989, Chemical and isotopic systematics of oceanic basalts: implications for mantle composition and processes, *in* Saunders, A. D., and Norry, M. J., eds., *Magmatism in the Ocean Basins*, Geological Society Special Publication 42, p. 313-345.

Swinden, H. S., 1991, Paleotectonic settings of volcanogenic massive sulphide deposits in the Dunnage Zone, Newfoundland Appalachians: *Canadian Institute of Mining and Metallurgy Bulletin*, v. 84, p. 59-89.

Thomas, D. A., and Glenn, D. G., 1992, 1992 Summary Report: Geology, Whole Rock Chemistry, Pulse EM, and Diamond Drilling, Hood Project - PN 420, Minnova Inc Company Report, p. 136.

Thomas, D. A., and Glenn, D. G., 1994, 1993 Summary Report: Diamond Drilling and Pulse EM, Hood Project - PN 420 Minnova Inc Company Report, p. 110.

Thompson, A. J., Hauff, B., and Robitaille, P. L., 1999, Alteration mapping in exploration: Application of short-wave infrared (SWIR) spectroscopy: Society of Economic Geology Newsletter, v. 39.

Thompson, A. J. B., 1999, Alteration mapping in exploration; application of short-wave infrared (SWIR) spectroscopy, *in* Hauff, P. L., and Robitaille, J. A., eds., SEG Newsletter, 39: United States, Society of Economic Geologists : Littleton, CO, United States, p. 1.

Thorpe, R. I., Cumming, G.L. and Mortensen, J.K., 1992, A major Pb-isotopic boundary in the Slave Province and its probably relation to ancient basement in the Slave Province and its probable relation to ancient basement in the western Slave, Canada - NWT MDA summary volume, Geological Survey of Canada, Open File 2484, p. 179 - 184.

Villeneuve, M. E., Henderson, J. R., Hrabi, R. B., Jackson, V. A., and Relf, C., 1997, 2.70-2.58 Ga plutonism and volcanism in the Slave Province, District of Mackenzie, Northwest Territories: Radiogenic Age and Isotopic Studies, Geological Survey of Canada Current Research 1997-F, v. 10.

Watson, E. B., and Harrison, T. M., 1983, Zircon saturation revisited: temperature and composition effects in a variety of crustal magma types: Earth and Planetary Science Letters, v. 64, p. 295-304.

Whalen, J. B., McNicoll, V. J., Galley, A. G., Longstaffe, F. J., and Percival, J. A., 2004, Tectonic and metallogenic importance of an Archean composite high- and low-Al tonalite suite, western Superior Province, Canada: Precambrian Research, v. 132, p. 275-301.

Winchester, J. A., and Floyd, P. A., 1977, Geochemical discrimination of different magma series and their differentiation products using immobile elements: Chemical Geology, v. 20, p. 325-343.

Wood, D. A., 1980, The application of a Th-Hf-Ta diagram to problems of tectonomagmatic classification and to establishing the nature of crustal contamination of basaltic lavas of the British Tertiary volcanic province: Earth and Planetary Science Letters, v. 50, p. 11-30.

Yamashita, K., Creaser, R. A., Jensen, J. E., and Heaman, L. M., 2000, Origin and evolution of mid- to late-Archean crust in the Hanikahimajuk Lake area, Slave Province, Canada; evidence from U-Pb geochronological, geochemical and Nd-Pb isotopic data: Precambrian Research, v. 99, p. 197-224.



## **Appendix 1: Drill Logs**

Legend




Intrusive Units

-  Granite
-  Diorite
-  Mafic Dyke


Mineralization

-  Semi-massive Sulfide
-  Massive Sulfide

Coherent Volcanic Units

-  Dacite and Rhyolite
-  Andesite
-  Basalt

Volcaniclastic Units

-  Felsic Tuff
-  Mixed Tuff
-  Mafic Tuff

Alteration

Strong Moderate Weak  
   Alteration Strength

D1411636  Sample location and number

### Figure A1-1: Drill Logs

[illegible]



Figure A1-1: Drill Logs

Prospect: Hood 10		Drillhole: H-10-02														
Location: 420673 E 7327395 N																
Photo	Alteration						Depth (m)	Lithology							Date Logged: July 1, 2011	
	Hematite	Epидote	Carbonate	Quartz	Sericite	Chlorite		Sulphide	Argillite	Tuff	Lapilli	Tuff Breccia	Flow	Intrusion	Sulphide	Notes
2772 2712																Fine-grained grey-green massive basalt with <10% quartz filled amygdules (~5mm)
																Mild carbonate alteration
2773																Grey-pink fine-grained felsic unit
																At 22.6m Fe-carbonate veins start to appear and calcite veins become more abundant
2774																Intensely silicified zones (often look like possible jigsaw breccias interbedded with more granular, fine grained layers)
2775																
2776																At 55.7m bleaching becomes more intense, rock is grey to cream coloured
2777																
2778																Grey green to white-cream colour variability
2779																
2780																Massive amygduloidal basalt layer
2781																
2782																Semi-massive sulfide: chalcopyrite stringers in intensely chlorite-altered rock
																Massive sulfide: buckshot pyrite crystals in pyrrhotite and chalcopyrite matrix with chlorite-altered clasts
2783																Intense chlorite alteration
																Semi-massive sulfide: some pyrite associated with pyrrhotite and chalcopyrite stringers
2784																Massive, light grey, felsic volcanic rock
2785																Strongly silicified zones with breccia textures
2786																Fine grained chlorite rich layer with patches of silicified rock

Figure A1-1: Drill Logs

Prospect: Hood 10		Drillhole: H-10-02												
Location:420673 E 7327395 N														
Photo	Alteration						Depth (m)	Lithology						Date Logged: July 1, 2011
	Hematite	Epidote	Carbonate	Quartz	Sericite	Chlorite		Sulphide	Argillite	Tuff	Lapilli	Tuff Breccia	Flow	Intrusion
2786	<div>D/411633</div> <div><div></div></div>							120	<div><div></div><div></div><div></div><div></div><div></div><div></div><div></div><div></div><div></div><div></div><div></div><div></div><div></div><div></div><div></div><div></div><div></div><div></div><div></div><div></div><div></div><div></div><div></div><div></div><div></div><div></div><div></div><div></div><div></div><div></div><div></div><div></div><div></div><div></div><div></div><div></div><div></div><div></div><div></div><div></div><div></div><div></div><div></div><div></div><div></div><div></div><div></div><div></div><div></div><div></div><div></div><div></div><div></div><div></div><div></div><div></div><div></div><div></div><div></div><div></div><div></div><div></div><div></div><div></div><div></div><div></div><div></div><div></div><div></div><div></div><div></div><div></div><div></div><div></div><div></div><div></div><div></div><div></div><div></div><div></div><div></div><div></div><div></div><div></div><div></div><div></div><div></div><div></div><div></div><div></div><div></div><div></div><div></div><div></div><div></div><div></div><div></div><div></div><div></div><div></div><div></div><div></div><div></div><div></div><div></div><div></div><div></div><div></div><div></div><div></div><div></div><div></div><div></div><div></div><div></div><div></div><div></div><div></div><div></div><div></div><div></div><div></div><div></div><div></div><div></div><div></div><div></div><div></div><div></div><div></div><div></div><div></div><div></div><div></div><div></div><div></div><div></div><div></div><div></div><div></div><div></div><div></div><div></div><div></div><div></div><div></div><div></div><div></div><div></div><div></div><div></div><div></div><div></div><div></div><div></div><div></div><div></div><div></div><div></div><div></div><div></div><div></div><div></div><div></div><div></div><div></div><div></div><div></div><div></div><div></div><div></div><div></div><div></div><div></div><div></div><div></div><div></div><div></div><div></div><div></div><div></div><div></div><div></div><div></div><div></div><div></div><div></div><div></div><div></div><div></div><div></div><div></div><div></div><div></div><div></div><div></div><div></div><div></div><div></div><div></div><div></div><div></div><div></div><div></div><div></div><div></div><div></div><div></div><div></div><div></div><div></div><div></div><div></div><div></div><div></div><div></div><div></div><div></div><div></div><div></div><div></div><div></div><div></div><div></div><div></div><div></div><div></div><div></div><div></div><div></div><div></div><div></div><div></div><div></div><div></div><div></div><div></div><div></div><div></div><div></div><div></div><div></div><div></div><div></div><div></div><div></div><div></div><div></div><div></div><div></div><div></div><div></div><div></div><div></div><div></div><div></div><div></div><div></div><div></div><div></div><div></div><div></div><div></div><div></div><div></div><div></div><div></div><div></div><div></div><div></div><div></div><div></div><div></div><div></div><div></div><div></div><div></div><div></div><div></div><div></div><div></div><div></div><div></div><div></div><div></div><div></div><div></div><div></div><div></div><div></div><div></div><div></div><div></div><div></div><div></div><div></div><div></div><div></div><div></div><div></div><div></div><div></div><div></div><div></div><div></div><div></div><div></div><div></div><div></div><div></div><div></div><div></div><div></div><div></div><div></div><div></div><div></div><div></div><div></div><div></div><div></div><div></div><div></div><div></div><div></div><div></div><div></div><div></div><div></div><div></div><div></div><div></div><div></div><div></div><div></div><div></div><div></div><div></div><div></div><div></div><div></div><div></div><div></div><div></div><div></div><div></div><div></div><div></div><div></div><div></div><div></div><div></div><div></div><div></div><div></div><div></div><div></div><div></div><div></div><div></div><div></div><div></div><div></div><div></div><div></div><div></div><div></div><div></div><div></div><div></div><div></div><div></div><div></div><div></div><div></div><div></div><div></div><div></div><div></div><div></div><div></div><div></div><div></div><div></div><div></div><div></div><div></div><div></div><div></div><div></div><div></div><div></div><div></div><div></div><div></div><div></div><div></div><div></div><div></div><div></div><div></div><div></div><div></div><div></div><div></div><div></div><div></div><div></div><div></div><div></div><div></div><div></div><div></div><div></div><div></div><div></div><div></div><div></div><div></div><div></div><div></div><div></div><div></div><div></div><div></div><div></div><div></div><div></div><div></div><div></div><div></div><div></div><div></div><div></div><div></div><div></div><div></div><div></div><div></div><div></div><div></div><div></div><div></div><div></div><div></div><div></div><div></div><div></div><div></div><div></div><div></div><div></div><div></div><div></div><div></div><div></div><div></div><div></div><div></div><div></div><div></div><div></div><div></div><div></div><div></div><div></div><div></div><div></div><div></div><div></div><div></div><div></div><div></div><div></div><div></div><div></div><div></div><div></div><div></div><div></div><div></div><div></div><div></div><div></div><div></div><div></div><div></div><div></div><div></div><div></div><div></div><div></div><div></div><div></div><div></div><div></div><div></div><div></div><div></div><div></div><div></div><div></div><div></div><div></div><div></div><div></div><div></div><div></div><div></div><div></div><div></div><div></div><div></div><div></div><div></div><div></div><div></div><div></div><div></div><div></div><div></div><div></div><div></div><div></div><div></div><div></div><div></div><div></div><div></div><div></div><div></div><div></div><div></div><div></div><div></div><div></div><div></div><div></div><div></div><div></div><div></div><div></div><div></div><div></div><div></div><div></div><div></div><div></div><div></div><div></div><div></div><div></div><div></div><div></div><div></div><div></div><div></div><div></div><div></div><div></div><div></div><div></div><div></div><div></div><div></div><div></div><div></div><div></div><div></div><div></div><div></div><div></div><div></div><div></div><div></div><div></div><div></div><div></div><div></div><div></div><div></div><div></div><div></div><div></div><div></div><div></div><div></div><div></div><div></div><div></div><div></div><div></div><div></div><div></div><div></div><div></div><div></div><div></div><div></div><div></div><div></div><div></div><div></div><div></div><div></div><div></div><div></div><div></div><div></div><div></div><div></div><div></div><div></div><div></div><div></div><div></div><div></div><div></div><div></div><div></div><div></div><div></div><div></div><div></div><div></div><div></div><div></div><div></div><div></div><div></div><div></div><div></div><div></div><div></div><div></div><div></div><div></div><div></div><div></div><div></div><div></div><div></div><div></div><div></div><div></div><div></div><div></div><div></div><div></div><div></div><div></div><div></div><div></div><div></div><div></div><div></div><div></div><div></div><div></div><div></div><div></div><div></div><div></div><div></div><div></div><div></div><div></div><div></div><div></div><div></div><div></div><div></div><div></div><div></div><div></div><div></div><div></div><div></div><div></div><div></div><div></div><div></div><div></div><div></div><div></div><div></div><div></div><div></div><div></div><div></div><div></div><div></div><div></div><div></div><div></div><div></div><div></div><div></div><div></div><div></div><div></div><div></div><div></div><div></div><div></div><div></div><div></div><div></div><div></div><div></div><div></div><div></div><div></div><div></div><div></div><div></div><div></div><div></div><div></div><div></div><div></div><div></div><div></div><div></div><div></div><div></div><div></div><div></div><div></div><div></div><div></div><div></div><div></div><div></div><div></div><div></div><div></div><div></div><div></div><div></div><div></div><div></div><div></div><div></div><div></div><div></div><div></div><div></div><div></div><div></div><div></div><div></div><div></div><div></div><div></div><div></div><div></div><div></div><div></div><div></div><div></div><div></div><div></div><div></div><div></div><div></div><div></div><div></div><div></div><div></div><div></div><div></div><div></div><div></div><div></div><div></div><div></div><div></div><div></div><div></div><div></div><div></div><div></div><div></div><div></div><div></div><div></div><div></div><div></div><div></div><div></div><div></div><div></div><div></div><div></div><div></div><div></div><div></div><div></div><div></div><div></div><div></div><div></div><div></div><div></div><div></div><div></div><div></div><div></div><div></div><div></div><div></div><div></div><div></div><div></div><div></div><div></div><div></div><div></div><div></div><div></div><div></div><div></div><div></div><div></div><div></div><div></div><div></div><div></div><div></div><div></div><div></div><div></div><div></div><div></div><div></div><div></div><div></div><div></div><div></div><div></div><div></div><div></div><div></div><div></div><div></div><div></div><div></div><div></div><div></div><div></div><div></div><div></div><div></div><div></div><div></div><div></div><div></div><div></div><div></div><div></div><div></div><div></div><div></div><div></div><div></div><div></div><div></div><div></div><div></div><div></div><div></div><div></div><div></div><div></div><div></div><div></div><div></div><div></div><div></div><div></div><div></div><div></div><div></div><div></div><div></div><div></div><div></div><div></div><div></div><div></div><div></div><div></div><div></div><div></div><div></div><div></div><div></div><div></div><div></div><div></div><div></div><div></div><div></div><div></div><div></div><div></div><div></div><div></div><div></div><div></div><div></div><div></div><div></div><div></div><div></div><div></div><div></div><div></div><div></div><div></div><div></div><div></div><div></div><div></div><div></div><div></div><div></div><div></div><div></div><div></div><div></div><div></div><div></div><div></div><div></div><div></div><div></div><div></div><div></div><div></div><div></div><div></div><div></div><div></div><div></div><div></div><div></div><div></div><div></div><div></div><div></div><div></div><div></div><div></div><div></div><div></div><div></div><div></div><div></div><div></div><div></div><div></div><div></div><div></div><div></div><div></div><div></div><div></div><div></div><div></div><div></div><div></div><div></div><div></div><div></div><div></div><div></div><div></div><div></div><div></div><div></div><div></div><div></div><div></div><div></div><div></div><div></div><div></div><div></div><div></div><div></div><div></div><div></div><div></div><div></div><div></div><div></div><div></div><div></div><div></div><div></div><div></div><div></div><div></div><div></div><div></div><div></div><div></div><div></div><div></div><div></div><div></div><div></div><div></div><div></div><div></div><div></div><div></div><div></div><div></div><div></div><div></div><div></div><div></div><div></div><div></div><div></div><div></div><div></div><div></div><div></div><div></div><div></div><div></div><div></div><div></div><div></div><div></div><div></div><div></div><div></div><div></div><div></div><div></div><div></div><div></div><div></div><div></div><div></div><div></div><div></div><div></div><div></div><div></div><div></div><div></div><div></div><div></div><div></div><div></div><div></div><div></div><div></div><div></div><div></div><div></div><div></div><div></div><div></div><div></div><div></div><div></div><div></div><div></div><div></div><div></div><div></div><div></div><div></div><div></div><div></div><div></div><div></div><div></div><div></div><div></div><div></div><div></div><div></div><div></div><div></div><div></div><div></div><div></div><div></div><div></div><div></div><div></div><div></div><div></div><div></div><div></div><div></div><div></div><div></div><div></div><div></div><div></div><div></div><div></div><div></div><div></div><div></div><div></div><div></div><div></div><div></div><div></div><div></div><div></div><div></div><div></div><div></div><div></div><div></div><div></div><div></div><div></div><div></div><div></div><div></div><div></div><div></div><div></div><div></div><div></div><div></div><div></div><div></div><div></div><div></div><div></div><div></div><div></div><div></div><div></div><div></div><div></div><div></div><div></div><div></div><div></div><div></div><div></div><div></div><div></div><div></div><div></div><div></div><div></div><div></div><div></div><div></div><div></div><div></div><div></div><div></div><div></div><div></div><div></div><div></div><div></div><div></div><div></div><div></div><div></div><div></div><div></div><div></div><div></div><div></div><div></div><div></div><div></div><div></div><div></div><div></div><div></div><div></div><div></div><div></div><div></div><div></div><div></div><div></div><div></div><div></div><div></div><div></div><div></div><div></div><div></div><div></div><div></div><div></div><div></div><div></div><div></div><div></div><div></div><div></div><div></div><div></div><div></div><div></div><div></div><div></div><div></div><div></div><div></div><div></div><div></div><div></div><div></div><div></div><div></div><div></div><div></div><div></div><div></div><div></div><div></div><div></div><div></div><div></div><div></div><div></div><div></div><div></div><div></div><div></div><div></div><div></div><div></div><div></div><div></div><div></div><div></div><div></div><div></div><div></div><div></div><div></div><div></div><div></div><div></div><div></div><div></div><div></div><div></div><div></div>&lt;</div>					

### Figure A1-1: Drill Logs




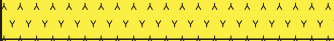
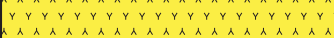








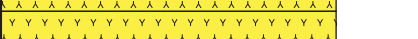








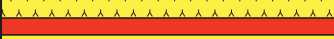


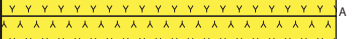



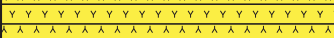


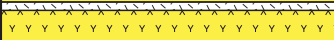
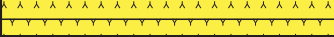









Prospect: Hood 10							Drillhole: H-10-05									
Location: 420661 E 732744S N																
Photo	Alteration						Depth (m)	Lithology							Date Logged: July 24, 2011	
	Hematite	Epidote	Carbonate	Quartz	Sericite	Chlorite		Sulphide	Argillite	Tuff	Lapilli	Tuff Breccia	Flow	Intrusion	Sulphide	Notes
								3.7 m O.V.								
3319															Dark grey dacite with strong mottled to wormy patterned quartz alteration that weakly follows foliation	
3320							10								Very minor Fe-carbonate veins	
															Dark grey fine grained dyke with wide brown aphanitic chill margins; the center of the dyke is carbonate altered	
3321							20								Minor white quartz veins a.a. but quartz alteration is more pervasive	
															Very sharp contact	
															Finely banded dacite with orange Fe-carbonate stain	
3322															Gradual contact into chl + qtz altered dacite	
3323							30								Fine grained veins and blebs of pyrite	
															Brecciation	
															Sharp contact with massive sulfide: fine grained pyrite surrounding chl + qtz altered clasts of dacite	
															27m - 28.7m : Fine grained massive py>> sph with minor py cubes, cpy blebs, chl-altered clasts, fine po increasing with depth	
															28.7m - 31.3m : Fine grained sph > py with increasing po blebs and veins	
															31.3m - 33.4m : Massive fine grained po with buckshot py	
															33.4m - 34.3m : Semi-massive sulfide: chl altered dacite autobreccia with cpy and po fill between the clasts	
															34.3m - 34.7m : Massive fine grained magnetite with Fe-carbonate veins	
							40								Very strong qtz and chl alteration immediately below the sulfides	
															Fine grained, massive to autobrecciated, grey dacite with moderate qtz alteration	
															Common stringer zones of cpy, or po	
															Gradual change to uniform, barren, fine grained massive grey dacite with occasional bands of coarser grained dacite	
3324							50									
															Massive sulfide : fine po around chl altered shards	
															Massive dacite grading into chlorite altered dacite shard in a qtz altered matrix	
															Between 54.6 m to 55.1 m py and po replacement around th eshard	
3325							60								Typical massive dark grey dacite with mottled to wormy white quartz alteration	
3326															Patches of round to flattened quartz amygdules	
															Fine grained green mafic dyke with chlorite spots and fine blebs of po cutting the dacite	
							70								Cpy, py, and po stringers	
															76 m - 76.3 m: Massive sulfide, fine grained po>>py surrounding py cubes grades into	
															76.3 m - 77.1 m: fine grained py>>po with bands of fine grained sph	
															77.1 m - 77.5 m: same as 76 m - 76.3 m	
															77.5 m - 78.3 m: medium grained massive dacite with chl altered fractures and strong qtz alteration	
							80								Very sharp contact with 78.3 m - 78.5 m: fine grained banded py with minor bands of fine grained sph and po	
															78.3 m - 78.5 m: fine grained py >>bands of sph and bands of po	
3327							90								78.5 m - 78.7 m: po with py and chl altered clasts	
															78.7 m - 78.9 m: like 78.3 m to 78.5 m	
															78.9 m - 79.1 m: semi-massive sulfide fine grained to medium grained po and py	
															79.1 m - 80.2 m: po with chlorite and quartz altered clasts	
															80.2 m - 80.4 m: like 78.3 m to 78.5 m	
															80.4 m - 83 m: like 79.1m to 80.2 m	
															A- Banded grey dacite with spotty quartz alteration and common Fe-carbonate veins	
															B- Fine grained green-orange, banded to massive dacite with pervasive quartz alteration and common Fe-carbonate veins	
							100								C - Green-grey dacite with white motting	
															D - Dark grey aphanitic, massive dacite with abundant quartz veins and minor Fe-carbonate veins	
3328															E- Similar to lithology D with chill margins; possible felsic dyke ?	
							110									

Figure A1-1: Drill Logs

Prospect: Hood 10		Drillhole: H-10-05														
Location: 420661 E 7327445 N																
Photo	Alteration						Depth (m)	Lithology						Date Logged: July 24, 2011		
	Hematite	Epoxide	Carbonate	Quartz	Sericite	Chlorite		Sulphide	Argillite	Tuff	Lapilli	Tuff Breccia	Flow	Intrusion	Sulphide	Notes
3329																Dark tan rhyodacite that is aphanitic to the point of appearing cherty. Fractures have a dark black-brown fill Abundant quartz veins with some Fe-carbonate veins

### Figure A1-1: Drill Logs

Prospect: Hood 10		Drillhole: H-10-08														
Location: 420681 E 7327363 N																
Photo	Alteration						Depth (m)	Lithology							Date Logged: July 22, 2011	
	Hematite	Epidote	Carbonate	Quartz	Sericite	Chlorite		Sulphide	Argillite	Tuff	Lapilli	Tuff Breccia	Flow	Intrusion	Sulphide	Notes
								6.4 m Overburden							Common Fe-carbonate veins and quartz veins	
3308															6.4 m - 7.9 m: massive grey-brown dacite with some auto-breccia fracturing with moderate quartz alteration	
3309															Massive cream coloured cherty rhyolite with extensive fracturing and strong chlorite alteration	
															Weak foliation in the dacite	
3310															Sharp contact into finely banded grey-green andesite	
3311															22.8 m to 23.4 m: strong quartz alteration bound by sharp contacts	
															* measurement blocks are inconsistent and uncertain	
3312															Sharp contact into fractured dacite with strong quartz alteration	
															Semi-massive sulfide: py in strong chl altered dacite	
															Varies between massive and banded	
															@ 50.6 m: Fe-carbonate stained fine grained banded dacite	
															53.3 m to 55.9 m: Autobreccia with dark brown filled fractures	
															55.9 m to 56.2 m: green-tan cherty layer with Fe-carbonate and black fill in fractures	
3313															56.2 m to 58.2 m: Massive to autobreccia rhyolite that grades into a massive dark grey dacite with weak spotty qtz alteration from 58.2 m to 63.4 m	
															63.4 m - 64.2 m: cherty rhyolite autobreccia zones with black fill within a qtz altered rhyodacite unit with Fe-carbonate alteration	
															64.2 m - 65.6 m: semi-massive sulfide of pyrite stringers in dacite with strong chlorite alteration	
3314															65.6 m - 66.5 m: sharp contact into grey dacite	
															Massive to 66.1 m where breccia begins and quartz veins with 1cm blebs of chalcopyrite	
															66.5 m - 68.0 m: light to dark grey dacite brecciated in places with Fe-carbonate replacement around some of the breccia clasts	
3315															68.0 m - 69 m: fractured rhyolite with some perlitic arcing fractures near the end of the unit	
															69 m - 69.7 m: missing contact to dacite with strong to moderate chlorite alteration	
															69.7 m - 76.6 m: semi-massive sulfide, pyrite and chalcopyrite with chlorite and quartz altered clasts	
3316															76.6 m - 78.1 m: barren qtz+chl altered dacite with zones of cpy veining	
															78.1 m - 78.7 m: massive sulfide made of chalcopyrite and pyrrhotite replacement around rhyolite	
															78.7 m - 79.6 m: quartz veined rhyolite with cpy blebs and veins	
3317															79.6 m - 81.5 m: fractured to autobrecciated rhyolite that is dark than typical with some slightly cherty/porcelanous zones and Fe-carbonate veins and cpy replacement along fractures	
															81.5 m - 82.6 m: massive green andesitic unit with small white amygdules and some pyrite, quartz and Fe-carb. veins	
3318															82.6 m - 83.3 m: Black dacite with cloudy grey patches	
															83.3 m - 85.4 m: Finely banded grey and black andesite with Fe-carbonate veining and weak chl + qtz alteration	

Figure A1-1: Drill Logs

Prospect: Hood 10		Drillhole: H-10-08								
Location: 420681 E 7327363 N									Date Logged: July 22, 2011	
Photo	Alteration						Lithology			Notes
	Hematite	Epидote	Carbonate	Quartz	Sericite	Chlorite	Argillite	Tuff	Lapilli	
							Depth (m)			
							85.4	Y	Y	85.4 m - 85.85 m: cherty tan green flow? with orange-tan edges (synvolcanic dyke?) with extremely strong carbonate alteration with very fine py and carbonate stringers and veins parallel to foliation
							85.85	Y	Y	85.85 m - 86.2 m: finely laminated dark green and orange dacite with Fe-carbonate veins
							86.2	Y	Y	86.2 m - 86.9 m: carbonate altered cherty rhyolite
							86.9	Y	Y	86.9 m - 87.7 m: like 85.85m to 86.2m with common quartz eyes
							87.7	Y	Y	87.7 m - 88.7 m: carbonate altered dyke
							88.7	Y	Y	88.7 m - 101.8 m: banded dacite with mottled zones grading into banded zones with occasional pyrite veining
							101.8	Y	Y	101.8 m - 103.6 m: fine green mafic dyke with carb veins and rare white carb filled amygdulites
							103.6	Y	Y	103.6 m - 115.2 m: fractured to barely autobreccia dacite with cpy and minor py in veins
							115.2	Y	Y	115.2 m - 121.9 m: medium green andesite with weak banding and thin Fe-carbonate veins
							121.9	Y	Y	
							120	Y	Y	
							130			
							140			
							150			
							160			
							170			
							180			
							190			
							200			
							210			
							220			

Figure A1-1: Drill Logs

Prospect: Hood 10		Drillhole: H-10-10																																																																																																																																																																																																																																																																																																																																																																																																																																																																																																																																																																																																																																																																																																																																																																																																																																																																																																																																																																																																																																																																																																																																																																																																																																																																																																																																																																																		
Location: 420705 E 7327407 N																																																																																																																																																																																																																																																																																																																																																																																																																																																																																																																																																																																																																																																																																																																																																																																																																																																																																																																																																																																																																																																																																																																																																																																																																																																																																																																																																																																				
Photo	Alteration						Depth (m)	Lithology							Date Logged: July 3, 2011																																																																																																																																																																																																																																																																																																																																																																																																																																																																																																																																																																																																																																																																																																																																																																																																																																																																																																																																																																																																																																																																																																																																																																																																																																																																																																																																																																					
	Hematite	Epidote	Carbonate	Quartz	Sericite	Chlorite		Sulphide	Argillite	Tuff	Lapilli	Tuff Breccia	Flow	Intrusion	Sulphide	Notes																																																																																																																																																																																																																																																																																																																																																																																																																																																																																																																																																																																																																																																																																																																																																																																																																																																																																																																																																																																																																																																																																																																																																																																																																																																																																																																																																																				
																																																																																																																																																																																																																																																																																																																																																																																																																																																																																																																																																																																																																																																																																																																																																																																																																																																																																																																																																																																																																																																																																																																																																																																																																																																																																																																																																																																				</

### Figure A1-1: Drill Logs

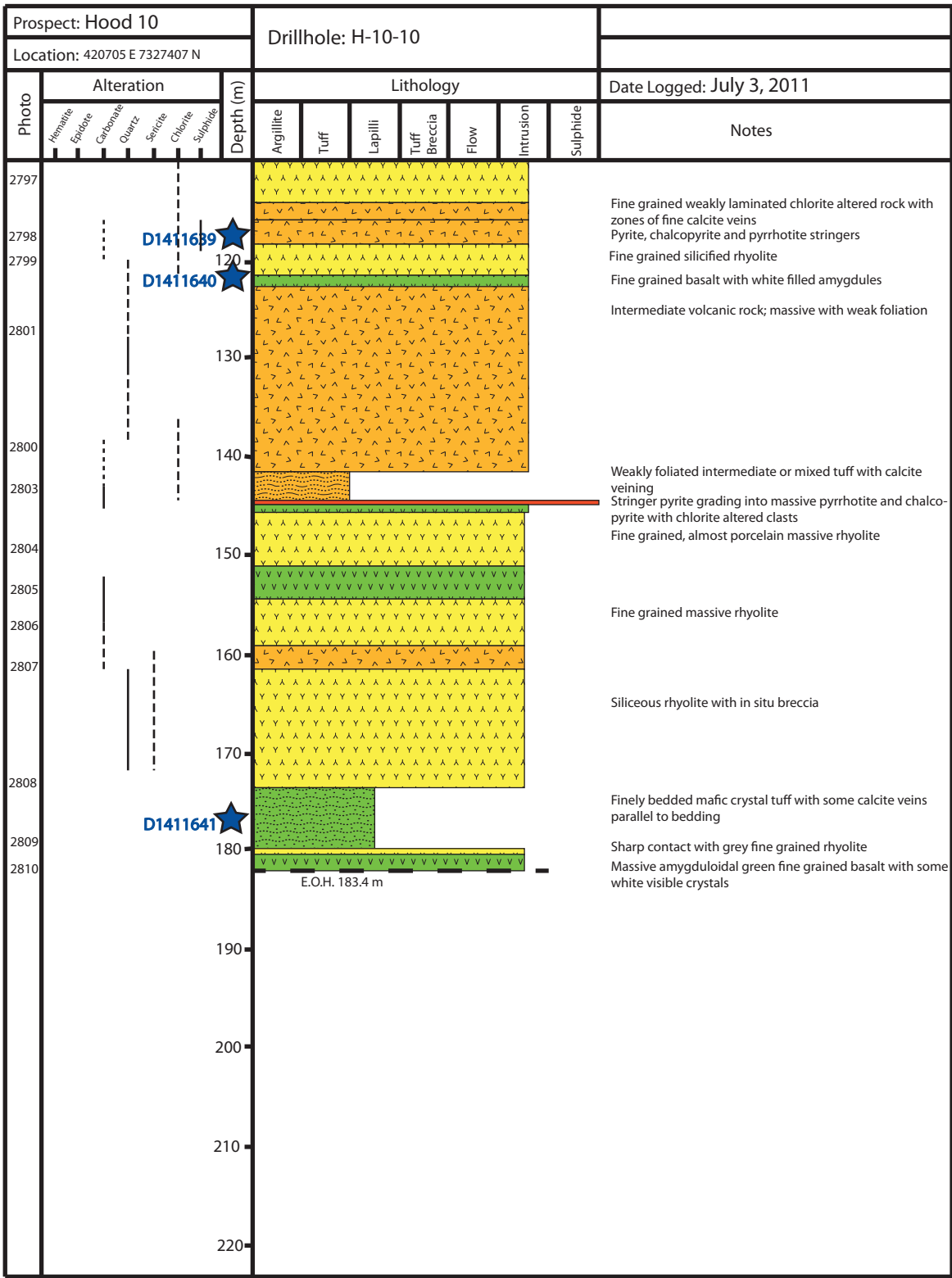




Figure A1-1: Drill Logs

Prospect: Hood 10							Drillhole: H-10-11									
Location: 420704 E 7327407 N																
Photo	Alteration						Depth (m)	Lithology							Date Logged: July 3, 2011	
	Hematite	Epidote	Carbonate	Quartz	Sericite	Chlorite		Sulphide	Argillite	Tuff	Lapilli	Tuff Breccia	Flow	Intrusion	Sulphide	Notes
2811																Massive medium grey intermediate rock with some quartz and dark grey speckles and some minor carbonate veining
2812							10									There is a rapid change in texture from glassy to fine grained
							20									@ 12.9 m there are spherulite @ 17.3 m vuggy, rusted out quartz vein
																Transition to breccia with rounded clasts
							30									Calcite filled vugs Fine grained, magnetic, mafic dyke with small white crystals; sharp contacts with the bottom one offset by calcite and pyrite filled fractures @ 31.3 m there is a 10 cm calcite veining zone
2813																Light green, fine grained, non-magnetic dyke with lots of calcite veining and jagged contact
2814							40									Fine grained green mafic dyke with white carbonate alteration and chill margins
2815																Medium grained, non-magnetic mafic dyke Green, clast-supported breccia flow with jagged fragments
2816							50									Fine grained massive green basalt with white calcite clots
2817																Breccia Andesite breccia
							60									Fine grained light green dyke with white crystals and sharp uneven contacts Clast supported breccia with jagged, felsic fragments
2818							70									
2819																Mafic breccia with very fine clasts, bordering on tuff
2820							80									Massive mafic amygduloidal flow Brecciated transition into rhyolite that coarsens from fine grained to coarse grained
2821																Fine grained, non-magnetic, green-grey dyke
2822							90									Fine grained to coarse grained intermediate volcanic rock with Fe-carbonate veins Fine grained, light green dyke with white pinpoint crystals Mixed, caompacted lapilli tuff
2823																20% sulfide made of pyrite stringers with chalcopyrite
2824																
2825							100									Semi-massive sulfide: pyrrhotite+chalcopyrite+pyrite replacement of the host rock leaving bleached white lapilli clasts
2826																Strong chlorite altered rock grades into chl + qtz altered lapilli tuff
2827																Massive cherty rhyolite with calcite and Fe-carbonate veins and curving fractures
2828							110									

Figure A1-1: Drill Logs

Prospect: Hood 10							Drillhole: H-10-11																																																																																																																																																																																																																																																																																																																																																																																																																																																																																																																																																																																																																																																																																																																																																																																																																																																																																																																																																																																																																																																																																																																																																																																																																																																																																																																																										
Location: 420704 E 7327407 N																																																																																																																																																																																																																																																																																																																																																																																																																																																																																																																																																																																																																																																																																																																																																																																																																																																																																																																																																																																																																																																																																																																																																																																																																																																																																																																																																	
Photo	Alteration						Depth (m)	Lithology							Date Logged: July 3, 2011																																																																																																																																																																																																																																																																																																																																																																																																																																																																																																																																																																																																																																																																																																																																																																																																																																																																																																																																																																																																																																																																																																																																																																																																																																																																																																																																		
	Kfsarinite	Epidote	Carbonate	Quartz	Sulfide	Chlorite		Apatite	Tuff	Lapilli	Tuff Breccia	Flow	Intrusion	Sulphide	Notes																																																																																																																																																																																																																																																																																																																																																																																																																																																																																																																																																																																																																																																																																																																																																																																																																																																																																																																																																																																																																																																																																																																																																																																																																																																																																																																																		
																																																																																																																																																																																																																																																																																																																																																																																																																																																																																																																																																																																																																																																																																																																																																																																																																																																																																																																																																																																																																																																																																																																																																																																																																																																																																																																																																	</

### Figure A1-1: Drill Logs

Prospect: Hood 10		Drillhole: H-10-12													
Location: 420609 E 7327465 N															
Photo	Alteration						Depth (m)	Lithology							Date Logged: July 26, 2011
	Hematite	Epидdite	Carbonate	Quartz	Sericite	Chlorite		Sulphide	Argillite	Tuff	Lapilli	Tuff Breccia	Flow	Intrusion	Sulphide
								3.1 m of Overburden							
							10								Weakly foliated, medium green grey andesite with white varioles (possible spherulites or amygdulles) with quartz and minor Fe-carbonate veins
3352															
							16								White and grey dacitic breccia with small < 1 cm clasts, some of which are armoured
3353															
							20								Massive to banded fine grained dacite with selective qtz alteration grades into a darker layer
							30								Andesite with white crystals and varioles
3354															
							40								Massive to foliated with glassy fractured sections and common narrow Fe-carbonate
							50								Patchy to spotty chlorite alteration with patchy cloudy quartz and sericite alteration
3355															
							55								White varioles grade out and andesite becomes finely laminated with possible selective quartz altered flow banding
3356															
							60								Fe-carbonate veining throughout and patchy Fe-carbonate alteration
							65								Green and beige speckle pattern from the pervasive chl+ qtz alteration
3357															
							70								45.5 m - 46.4 m: massive fine grained gray dacite with fractures
3358															
							75								Chlorite alteration is very strong right before mineralization
							80								Massive to semi-massive sulfide: fine grained pyrrhotite around cubic pyrite and a few blebs of cpy and small to large clasts of chlorite and/or quartz altered andesite
							85								Chlorite alteration is weaker coming out of sulfide
							90								Light grey-green intermediate composition fine grained dyke with 1-2 mm white plagioclase? crystals
							95								Fe-carbonate staining and quartz veining
							100								Andesite as above with slightly weaker chlorite alteration and fewer varioles though still spotty with qtz crystals
							105								Fine grained green mafic dyke with pervasive carbonate alteration and chill margins
							110								Zones of weak banding
							115								
							120								

Figure A1-1: Drill Logs

Prospect: Hood 10							Drillhole: H-10-16									
Location: 420656 E 7327479 N																
Photo	Alteration						Depth (m)	Lithology							Date Logged: July 27, 2011	
	Hematite	Epidote	Carbonate	Quartz	Sericite	Chlorite		Sulphide	Argillite	Tuff	Lapilli	Tuff Breccia	Flow	Intrusion	Sulphide	Notes
								1.2 m of overburden							Porcelainous, fractured rhyolite Cream coloured that darkens to grey  Abundant small Fe-carbonate veins	
							10								Sharp contact with grey and white dacite flow breccia with patches of selective sericite and quartz alteration in addition to black chlorite and quartz alteration along fractures Back into rhyolite Graded contacts with dacite	
3374							20								Aphanitic, brown intermediate composition dyke with narrow chl-filled fractures Fe-carbonate veins in both dyke and dacite Dacite is the typical white and black-green dacite with wormy/mottled white alteration with breccia zones	
3375							30									
3376																
							40								Massive, porcelainous grey dacite with fractures Fe-carbonate veins Dark dacite with fewer fragments than above and common quartz eyes and brown sericite and chlorite alteration Auto-breccia into typical green and white brecciated dacite	
3377							50									
							60								Between 60 - 63 m clasts are quite fine	
							70								70.1 m - 72.4 m: autobreccia with minor pyrite veins	
3378							80								Strongly banded dacite with very fine black chlorite layers interbedded with grey, small white crystal gritty layers Unit gradually coarsens and loses foliation Blue-grey, fine-grained, massive dacite with orange speckles with common calcite filled fractures	
3379							90								The lower part of the unit fines to a porcelainous unit with some chlorite alteration Massive sulfide: fine grained pyrrhotite and sphalerite with pyrite clasts and hematite altered clasts Dacite with fine banding and spherulites	
3383															@ 92.8 m semi-massive sulfide: pyrrhotite stringers and fine grained magnetite replacement on host rock @ 93 m 10cm of dacite with spherulites 93.1 m - 93.8 m: stringer pyrrhotite in silicified massive fractured dacite 93.8 m - 94.7 m: strong chlorite altered dacite with pyrrhotite replacement 94.7 m - 98.4 m: pyrrhotite with hematite altered clasts and sphalerite? and minor pyrite cubes Grey-green dacite with quartz and sericite along foliation with sub-angular to subrounded rare clasts	
3384							100									
3385																
3386							110									

Figure A1-1: Drill Logs

[illegible]

Figure A1-1: Drill Logs

Prospect: Hood 10							Drillhole: H-10-22													
Location: 420732 E 7327478 N																				
Photo	Alteration						Depth (m)	Lithology							Date Logged: July 25, 2011					
	Hematite	Epidote	Carbonate	Quartz	Sericite	Chlorite		Sulphide	Argillite	Tuff	Lapilli	Tuff Breccia	Flow	Intrusion	Sulphide	Notes				
3342								1.0 m of overburden							Dark green-grey massive basalt with pin point white dots with soem quartz veins Olive green aphanitic dyke with pervasive carbonate alteration Dark grey, fine grained dacite with weak foliation and minor pink quartz veins @ 13.8 m fracturing begins					
								10								Dyke similar to one above but slightly lighter in colour Dacite with quartz alteration spots 2-5 mm and black chlorite filled fractures  By 23.3 m rock has become more altered; brown (weak qtz +ser), dark grey (chl?) and cream (qtz) mottling Alteration varies from patchy to banded				
								20												
								3343	D1410411	★	30								29.3 m - 30.5 m: massive brown dacite with brecciated edges 30.5 m - 32.5 m: zone of flow bands with pockets of fine grained beige material with white feldspar crystals Breccia contact back into massive dacite	
								3344			40									
								3345	D1410425	★	50								39.4 m - 40.2 m: massive dacite same as surrounding rock but with visible contacts (syn volcanic??)  After 40.2 m carbonate veins become more abundant	
								3346			60									
								3347	D1410412	★	70								Tan-green dyke with chlorite spots; fine grained and intermediate composition @ 48 m patchy fine hematite  Dacite is dark grey with white quartz alteration mottling and strongly silicified zones  72.5 - 74.1 m matrix supported breccia zone	
											80									
3348			90								75.6 - 81.7 m: cream-banded glassy/ porcelainous rhyolite flow with very fine fracturing with black chl? fill  Massive to flow breccia dacite Porcelainous rhyolite									
			100																	
			110								Light grey-green massive fine grained andesitic with abundant calcite veins and calcite blebs with pyrite cubes  Moderate chloite alteration  Very dark grey fine grained dacite with wormy quartz alteration patterns									

Figure A1-1: Drill Logs

[illegible]

### Figure A1-1: Drill Logs

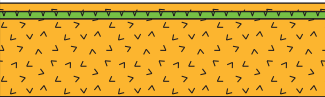













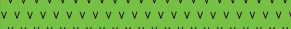
Prospect: Hood 10		Drillhole: H-10-27													
Location: 420775 E 7327528 N															
Photo	Alteration					Depth (m)	Lithology							Date Logged: July 28, 2011	
	Hematite	Epidote	Carbonate	Quartz	Sericite		Chlorite	Sulphide	Argillite	Tuff	Lapilli	Tuff Breccia	Flow	Intrusion	Sulphide
								2.22 m of overburden							
							10								Green-brown, fine grained basalt with weak foliation and fine white crystals and chlorite clots Grey-green andesite with white orange spots
3420															Cream coloured dacite with quartz veins Quartz alteration is weaker than in the andesite
							20								16.7 m - 17.6 m: fine to coarse anhedral pyrite in fractures and disseminated throughout the dacite
3421															@ 25.3 m: large distinct quartz altered rhyodacite clasts begin to appear
							30								Variable banding and fracturing
							40								@ 39 m fine grained chalcopyrite blebs in black and grey spotty dacite
3422							50								Possible dyke (inconclusive contacts); fine grained foliated mafic unit with white crystals and fragments Dacite banding grades into massive and is locally breccia
							60								Light brown-grey spotted andesite with fine plagioclase and quartz crystals and some chl+ser alteration
3423							70								More destructive quartz and sericite alteration
							80								Dark grey cloudy to wispy quartz alteration and abundant quartz veining in dacite
3424															Brown-grey andesite with fine phenocrysts to massive auto-breccia with blotchy quartz alteration; quartz and carbonate veins
3425							90								@ 80.5 m the unit coarsens
							92.61								@ 92.61 m spots of chlorite alteration
							95.69								@ 95.69 m rare round to elliptical white amygdules
							100								Auto-breccia zones
3426															Grey-brown banded to massive dacite
3427							110								Grey-brown banded to massive dacite
-3431															



Figure A1-1: Drill Logs

[illegible]

Figure A1-1: Drill Logs

Prospect:Hood 10		Drillhole: H-10-27																																																																																																																																																																																																																																																																																																																																																																																																																																																																																																																																																																																																																																																																																																																																																																																																																																																																																																																																																																																																																																																																																																																																																																																																																																																																																																																																																	
Location: 420775 E 7327528 N																																																																																																																																																																																																																																																																																																																																																																																																																																																																																																																																																																																																																																																																																																																																																																																																																																																																																																																																																																																																																																																																																																																																																																																																																																																																																																																																																			
Photo	Alteration						Depth (m)	Lithology							Date Logged: July 28, 2011																																																																																																																																																																																																																																																																																																																																																																																																																																																																																																																																																																																																																																																																																																																																																																																																																																																																																																																																																																																																																																																																																																																																																																																																																																																																																																																																				
	Hematite	Epidote	Carbonate	Quartz	Sericite	Chlorite		Sulphide	Argillite	Tuff	Lapilli	Tuff Breccia	Flow	Intrusion	Sulphide	Notes																																																																																																																																																																																																																																																																																																																																																																																																																																																																																																																																																																																																																																																																																																																																																																																																																																																																																																																																																																																																																																																																																																																																																																																																																																																																																																																																			
3438																																																																																																																																																																																																																																																																																																																																																																																																																																																																																																																																																																																																																																																																																																																																																																																																																																																																																																																																																																																																																																																																																																																																																																																																																																																																																																																																																			</

Figure A1-1: Drill Logs

[illegible]

### Figure A1-1: Drill Logs

Prospect: Hood 41							Drillhole: H-41-05								
Location: 422347 E 7324521 N															
Photo	Alteration						Depth (m)	Lithology							Date Logged: July 18, 2011
	Hematite	Epidote	Carbonate	Quartz	Sericite	Chlorite		Sulphide	Argillite	Tuff	Lapilli	Tuff Breccia	Flow	Intrusion	Sulphide
3169															First ~6m is quite chipped
3170															Basalt is stained brown (from storage) with abundant quartz veining and strong chlorite alteration
3171															Vuggy carbonate fracturing
3172															Cut by medium grained diorite dyke
3173															Massive sulfide is very weathered; pyrrhotite and sphalerite hosts pyrite and chalcopyrite stringers
3174															Intruded in diorite with disseminated blebs of sulfide
3175															Where original basalt remains there is very very strong chlorite alteration
3176															Salt and pepper dyke have contacts hidden in the mineralization in places
3177															
3178															Basalt is light to dark green with white and black minerals defining a lenticular foliation with some quartz veining
3179															Green-grey, fine grained, foliated dacite with chlorite and possibly quartz -sericite alteration
3180															Some green and white colour banding but light overall
							E.O.H. 74.39 m								
							There are no blocks for footage so measurements are guessed. Logs indicate that hole is 74.39 m								
							60								
							70								
							80								
							90								
							100								
							110								

Figure A1-1: Drill Logs

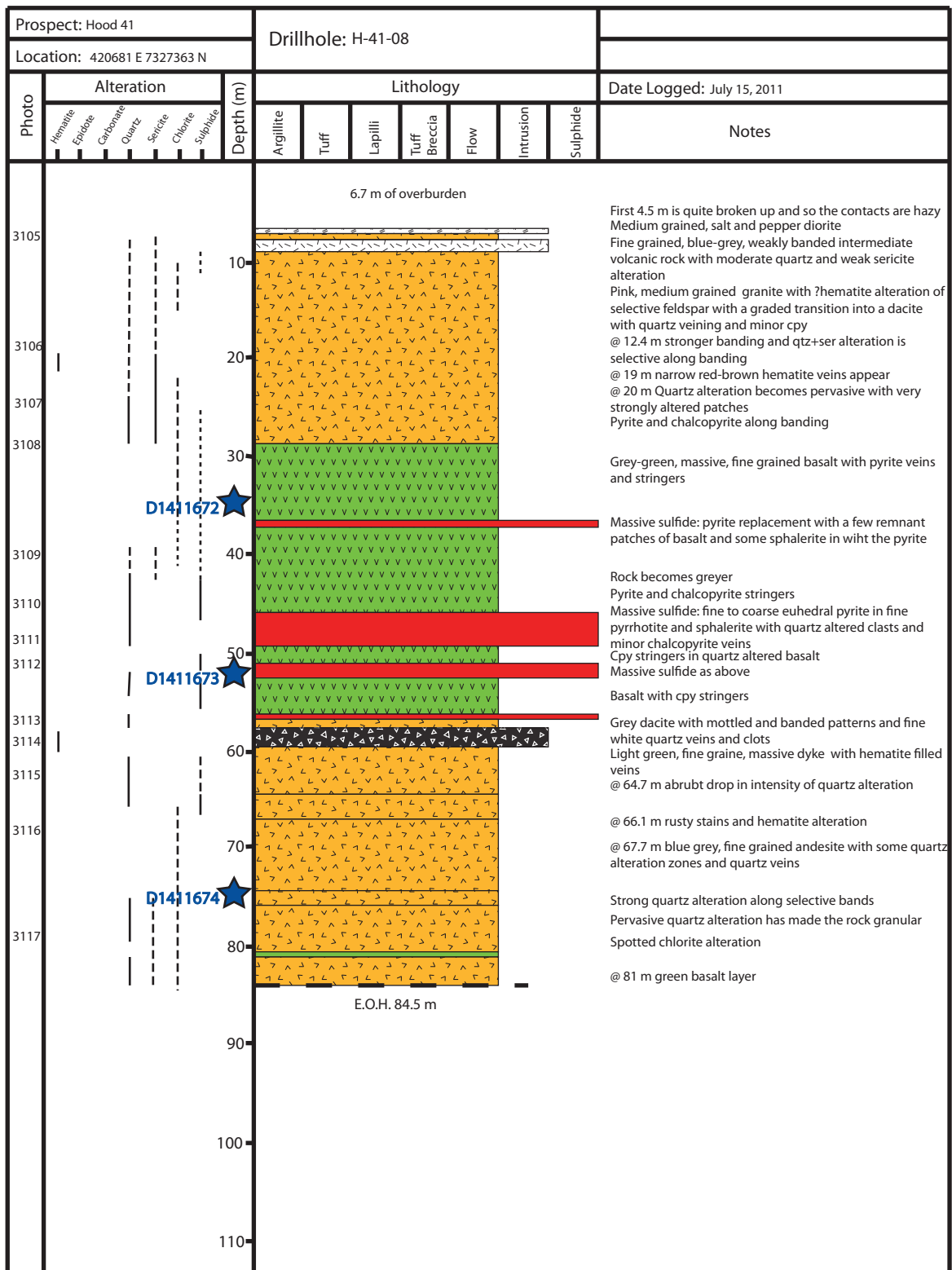


Figure A1-1: Drill Logs

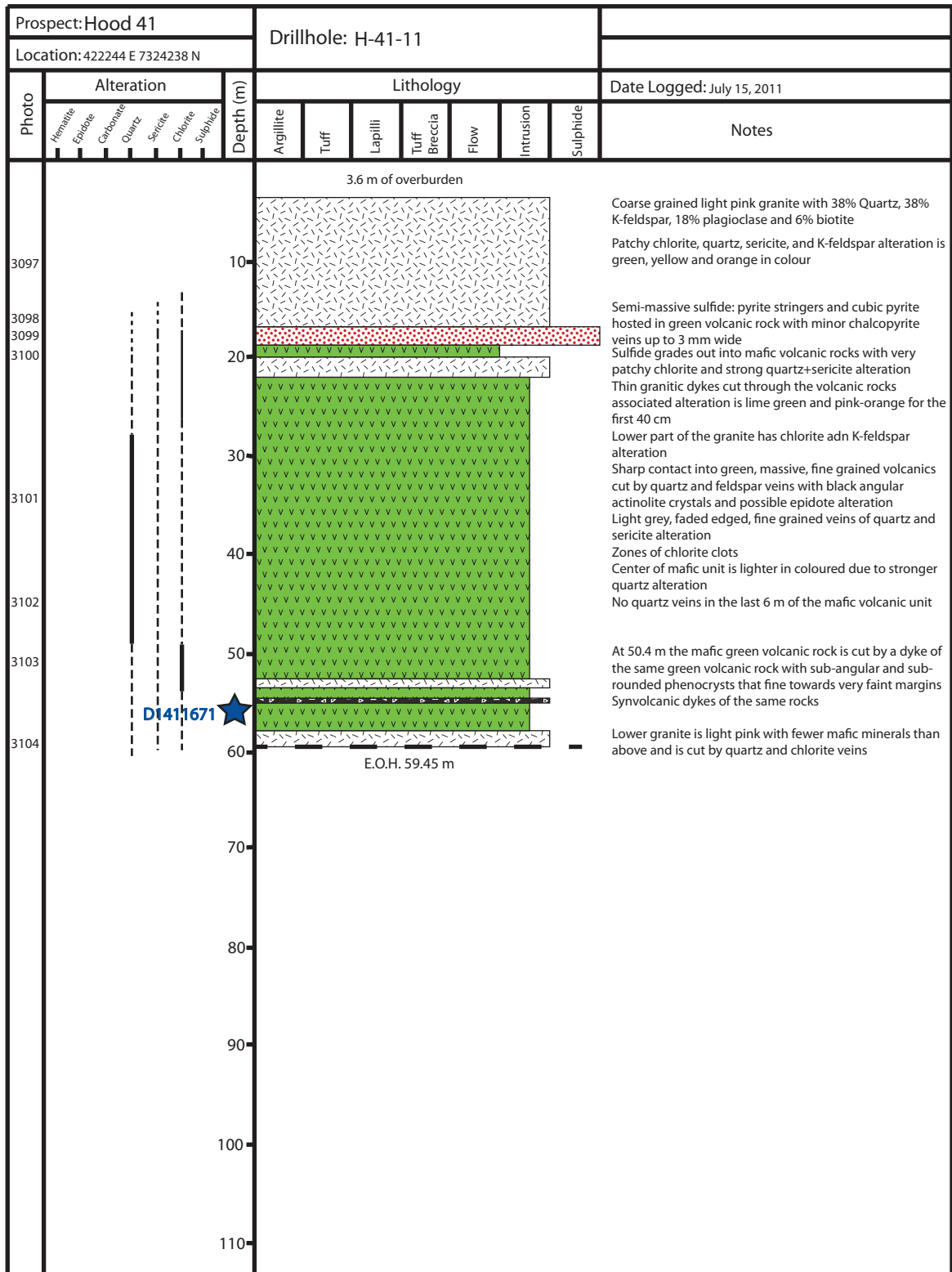


Figure A1-1: Drill Logs

Prospect: Hood 41							Drillhole: H-41-14																																																																																																																																																																																																																																																																																																																																																																																																																																																																																																																																																																																																																																																																																																																																																																																																																																																																																																																																																																																																																																																																																																																																																																																																																																																																																																																																								
Location: 422415 E 7324635 N																																																																																																																																																																																																																																																																																																																																																																																																																																																																																																																																																																																																																																																																																																																																																																																																																																																																																																																																																																																																																																																																																																																																																																																																																																																																																																																																															
Photo	Alteration						Depth (m)	Lithology							Date Logged: July 21, 2011																																																																																																																																																																																																																																																																																																																																																																																																																																																																																																																																																																																																																																																																																																																																																																																																																																																																																																																																																																																																																																																																																																																																																																																																																																																																																																																																
	Hematite	Epiddote	Carbonate	Quartz	Sericite	Chlorite		Sulphide	Argillite	Tuff	Lapilli	Tuff Breccia	Flow	Intrusion	Sulphide	Notes																																																																																																																																																																																																																																																																																																																																																																																																																																																																																																																																																																																																																																																																																																																																																																																																																																																																																																																																																																																																																																																																																																																																																																																																																																																																																																																															
																																																																																																																																																																																																																																																																																																																																																																																																																																																																																																																																																																																																																																																																																																																																																																																																																																																																																																																																																																																																																																																																																																																																																																																																																																																																																																																																															</

### Figure A1-1: Drill Logs

Prospect: Hood 41							Drillhole: H-41-14									
Location: 422415 E 7324635 N																
Photo	Alteration						Depth (m)	Lithology							Date Logged: July 21, 2011	
	Hemimite	Epidote	Carbonate	Quartz	Sericite	Chlorite		Sulphide	Argillite	Tuff	Lapilli	Tuff Breccia	Flow	Intrusion	Sulphide	Notes
3283															Strong chlorite alteration with cpy and py blebs Semi-massive sulfide: fine grained pyrite, chalcopyrite and magnetite disseminated or as stringers	
3284																
3285							120								Grey banded dacite with chlorite and quartz alteration Common cpy and py veins and stringers Abrupt end to mineralization	
3286																
							130								Banded grey dacite	
															White foliated, fine grained granite with chlorite alteration	
															Moderate selective sericite alteration	
3287															Fine grained diorite with quartz, biotite and plagioclase with chlorite alteration and quartz veins	
3288							140									
								E.O.H. 142.14 m								
							150									
							160									
							170									
							180									
							190									
							200									
							210									
							220									



Figure A1-1: Drill Logs

Prospect: Hood 41							Drillhole: H-41-15									
Location: 422310 E 7324496 N																
Photo	Alteration						Depth (m)	Lithology							Date Logged: July 17, 2011	
	Hematite	Epidote	Carbonate	Quartz	Sericite	Chlorite		Sulphide	Argillite	Tuff	Lapilli	Tuff Breccia	Flow	Intrusion	Sulphide	Notes
3128																1.33 m of overburden Aphanitic green massive basalt with light green lines of alteration and weak pervasive chlorite alteration Chlorite clots, qtz and feldspar alteration Variable strength foliation Possible amygdules @ 2.43 m and 9.95 m
3129																Coarse grained, pink granite dykes with qtz+ser+K-spar alteration on the edges 22.03 - 22.49 m chips with strong chlorite alteration Possible epidote and sericite alteration of feldspars
3130																
3131																Large actinolite phenocrysts (or porphyroblasts)
3132																Fine grained mafic dykes with strong chlorite alteration between the two dykes Basalt- same as above with common actinolite
																Cut by very fine carbonate, chlorite, pyrrhotite and pyrite selvages (possible pillow tops but more likely veins)
																Granitic dykes
																"Bedding" only apparent where alteration has highlighted it
																Actinolite is commonly found with coarse quartz crystals
																Less granite dykes but more quartz veining
3133																
3134																Pyrite in quartz and chlorite fractures parallel to foliation Fine grained green mafic dyke with sharp margins but otherwise very similar to the basalt
																Mafic dyke as above, cut by granite dykes

Figure A1-1: Drill Logs

Prospect: Hood 41							Drillhole: H-41-15									
Location: 422310 E 7324496 N																
Photo	Alteration						Depth (m)	Lithology							Date Logged: July 17, 2011	
	Hematite	Epidote	Carbonate	Quartz	Sericite	Chlorite		Sulphide	Argillite	Tuff	Lapilli	Tuff Breccia	Flow	Intrusion	Sulphide	Notes
3135																Pink granite dyke with pink alteration of the rock around it Some of the contacts are missing
																Graded contact This mafic dyke is slightly more olive-brown in colour Quite a lot of small pink granite dykes
																K-spar and quartz alteration and some recrystallization Some small white amygdules in the mafic dykes
																More quartz veins than above
																Chlorite, quartz, sericite and pyrite alteration along fractures and foliation with partial recrystallization and quartz veins
3136																
3137																Semi-massive sulfide: moderately coarse pyrite in bands with quartz and chlorite alteration
3138																Massive sulfide: buckshot pyrite in pyrrhotite and sphalerite with chlorite clasts
3139																Cut by granite Chalcopyrite veining in places and sulfides are remobilized in the dykes
3140																Fine, dark grey, banded dacite with cloudy to wispy quartz, sericite and chlorite alteration
3141																Unit is more massive
3142																Basalt similar to those before sulfides
3143																Lots of granite dyke Few hematite and carbonate veins Chlorite clots and strings Quartz veins
																E.O.H. 198 m

Figure A1-1: Drill Logs

Prospect: Hood 41		Drillhole: H-41-17																																																																																																																																																																																																																																																																																																																																																																																																																																																																																																																																																																																																																																																																																																																																																																																																																																																																																																																																																																																																																																																																																																																																																																																																																																																																																																																																																																																																																															
Location: 422279 E 7324571 N																																																																																																																																																																																																																																																																																																																																																																																																																																																																																																																																																																																																																																																																																																																																																																																																																																																																																																																																																																																																																																																																																																																																																																																																																																																																																																																																																																																																																																	
Photo	Alteration						Depth (m)	Lithology							Date Logged: July 19, 2011																																																																																																																																																																																																																																																																																																																																																																																																																																																																																																																																																																																																																																																																																																																																																																																																																																																																																																																																																																																																																																																																																																																																																																																																																																																																																																																																																																																																																		
	Hematite	Epидote	Carbonate	Quartz	Sericite	Chlorite		Sulphide	Argillite	Tuff	Lapilli	Tuff Breccia	Flow	Intrusion	Sulphide	Notes																																																																																																																																																																																																																																																																																																																																																																																																																																																																																																																																																																																																																																																																																																																																																																																																																																																																																																																																																																																																																																																																																																																																																																																																																																																																																																																																																																																																																	

Figure A1-1: Drill Logs

Prospect: Hood 41		Drillhole: H-41-17																
Location: 422279 E 7324571 N																		
Photo	Alteration						Depth (m)	Lithology							Date Logged: July 19, 2011			
	Hematite	Epidote	Carbonate	Quartz	Sericite	Chlorite		Sulphide	Argillite	Tuff	Lapilli	Tuff Breccia	Flow	Intrusion	Sulphide	Notes		
3194																		

Figure A1-1: Drill Logs

Prospect: Hood 41		Drillhole: H-41-17																
Location: 422279 E 7324571 N																		
Photo	Alteration						Depth (m)	Lithology							Date Logged: July 19, 2011			
	Hematite	Epидdrite	Carbonate	Quartz	Sericite	Chlorite		Sulphide	Argillite	Tuff	Lapilli	Tuff Breccia	Flow	Intrusion	Sulphide	Notes		
3207																Weakly banded dacite with abundant quartz veining		
3208																		
3209																Massive dark green basalt with patchy quartz and sericite alteration		
								E.O.H. 236.38 m										
								240										
								250										
								260										
								270										
								280										
								290										
								300										
								310										
								320										
								330										

### Figure A1-1: Drill Logs

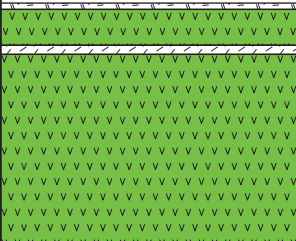

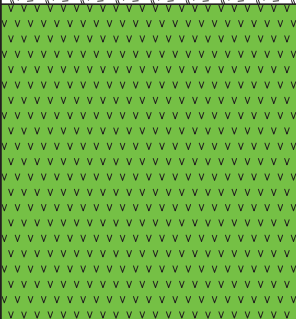

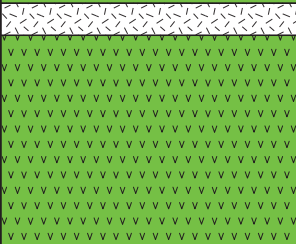






Prospect: Hood 41							Drillhole: H-41-18									
Location: 422335 E 7324628 N																
Photo	Alteration						Depth (m)	Lithology							Date Logged: July 20, 2011	
	Hematite	Epidote	Calcionite	Quartz	Sericite	Chlorite		Sulphide	Argillite	Tuff	Lapilli	Tuff Breccia	Flow	Intrusion	Sulphide	Notes
								3.25 m of overburden								
							10								Medium grained foliated diorite dyke Dark green, fine grained, massive basalt with moderate chlorite alteration Pink granite intrusion	
3212															Zones of actinolite and quartz	
							20									
3213															Pink and green, medium grained granodiorite dyke	
							30								Pink and green, medium grained granodiorite dyke	
3214															White amygdule groups about 1.5 m apart, possible flow tops	
							40									
							50								Abundant pink fine granite dykes	
3215															Stronger quartz alteration for 2 m after the dyke	
							60									
							70								Bands of fine pyrite	
							80								Massive sulfide: pyrrhotite and sphalerite with fine pyrite and associated quartz veins	
3216																
							90								Very minor hematite veins	
							100								Minor calcite veins	
							110								Pink medium grained granite with chlorite alteration along fractures	

Figure A1-1: Drill Logs

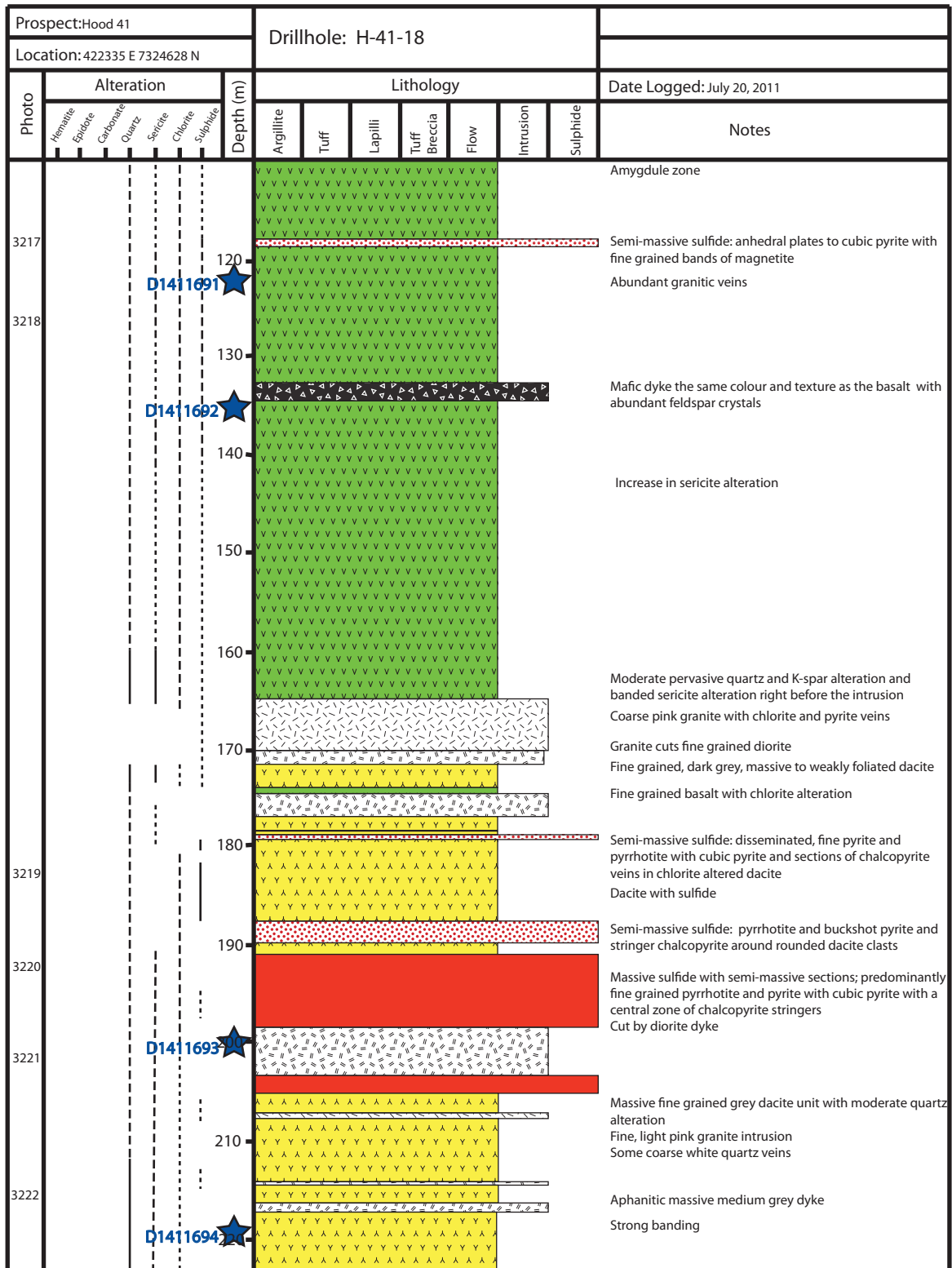


Figure A1-1: Drill Logs

[illegible]



Figure A1-1: Drill Logs

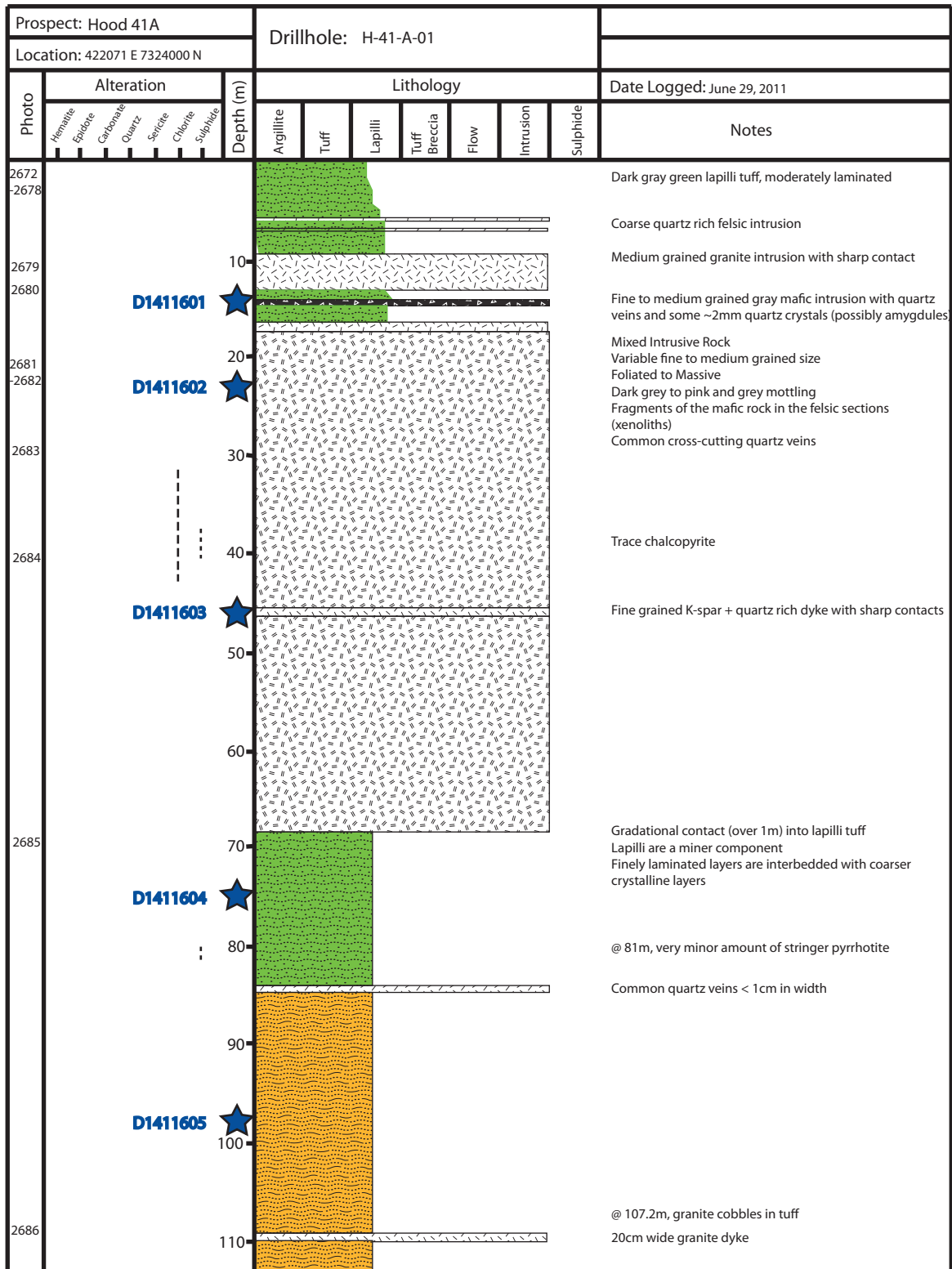


Figure A1-1: Drill Logs

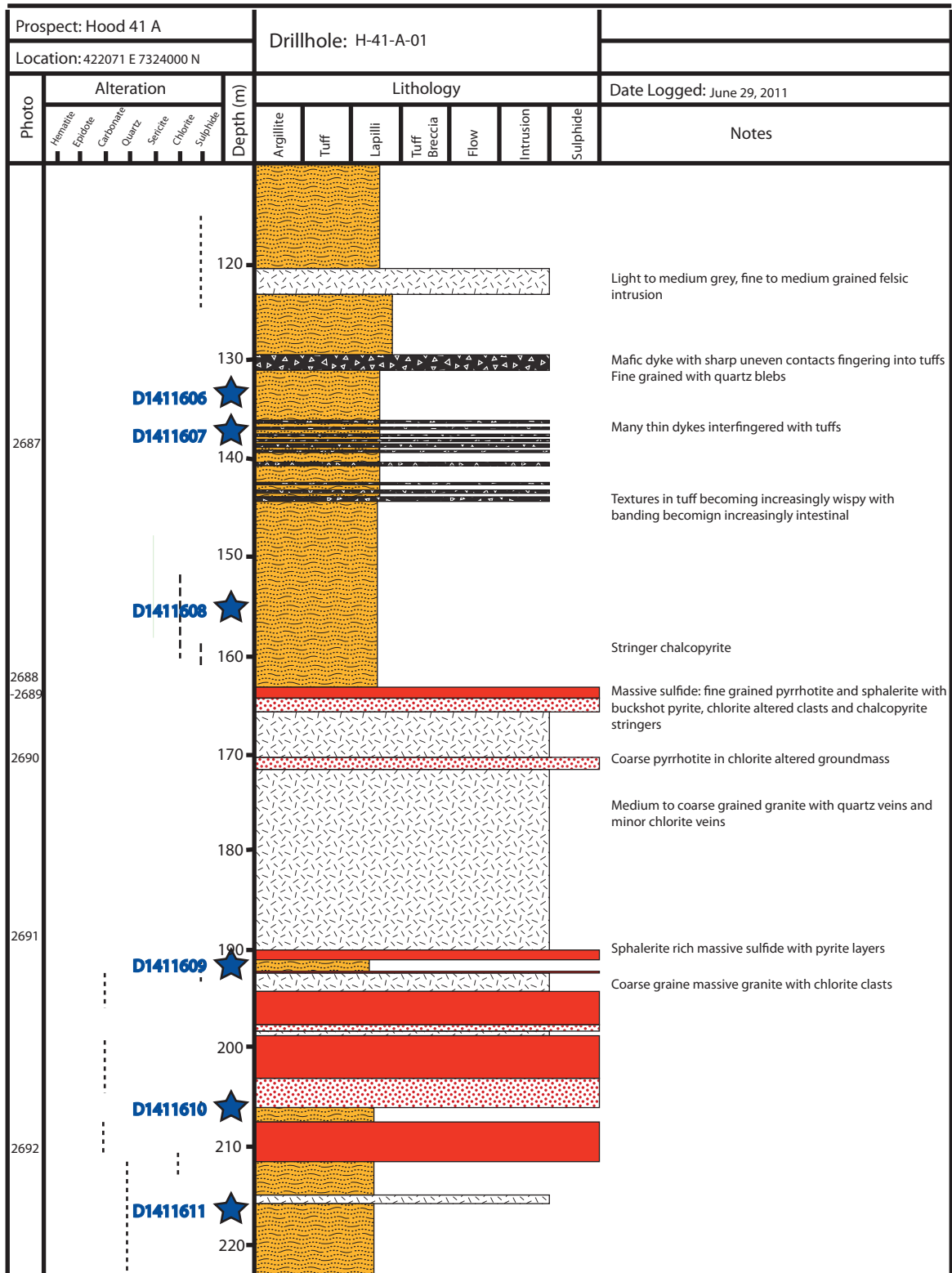


Figure A1-1: Drill Logs

[illegible]

Figure A1-1: Drill Logs

Prospect: Hood 41 A								Drillhole: H-41A-02									
Location: 422071 E 7324000 N																	
Photo	Alteration						Depth (m)	Lithology							Date Logged: June 30, 2011		
	Hematite	Epidote	Carbonate	Quartz	Sericite	Chlorite		Sulphide	Argillite	Tuff	Lapilli	Tuff Breccia	Flow	Intrusion	Sulphide	Notes	
2696																Fine grained, green mafic dyke	
																Fine grained, green tuff with fine banding, white lapilli and light quartz rich layers	
								10								Medium grained, grey-green and white diorite with quartz veins	
2697																Fine grained, dark grey, mafic dyke	
								20									
																Mafic tuff with some weak banding and a few lapilli	
																Medium grained granite intrusion with sharp contacts	
2698								30								Mixed intrusive: medium to coarse grained mixed gabbro to diorite rock with selective chlorite+sericite alteration and common cross-cutting quartz veins	
								40									
																Gradual transition into short section of lapilli tuff that has been "cooked" by granite intrusion	
								50								Mixed lapilli tuff	
																Mixed intrusive unit as above	
								60								Weakly banded lapilli tuff	
																Medium grained granite with weakly foliated tuff sections Sericite alteration	
								70								Finely banded mixed tuff; lapilli decrease downhole and some lapilli are strong out	
																Medium grained, green and pink intermediate unit	
2899								80								Finely laminated lapilli tuff with quartz crystals	
																Medium grained diorite	
								90									
																Mixed lapilli tuff	
								100									
								110									

Figure A1-1: Drill Logs

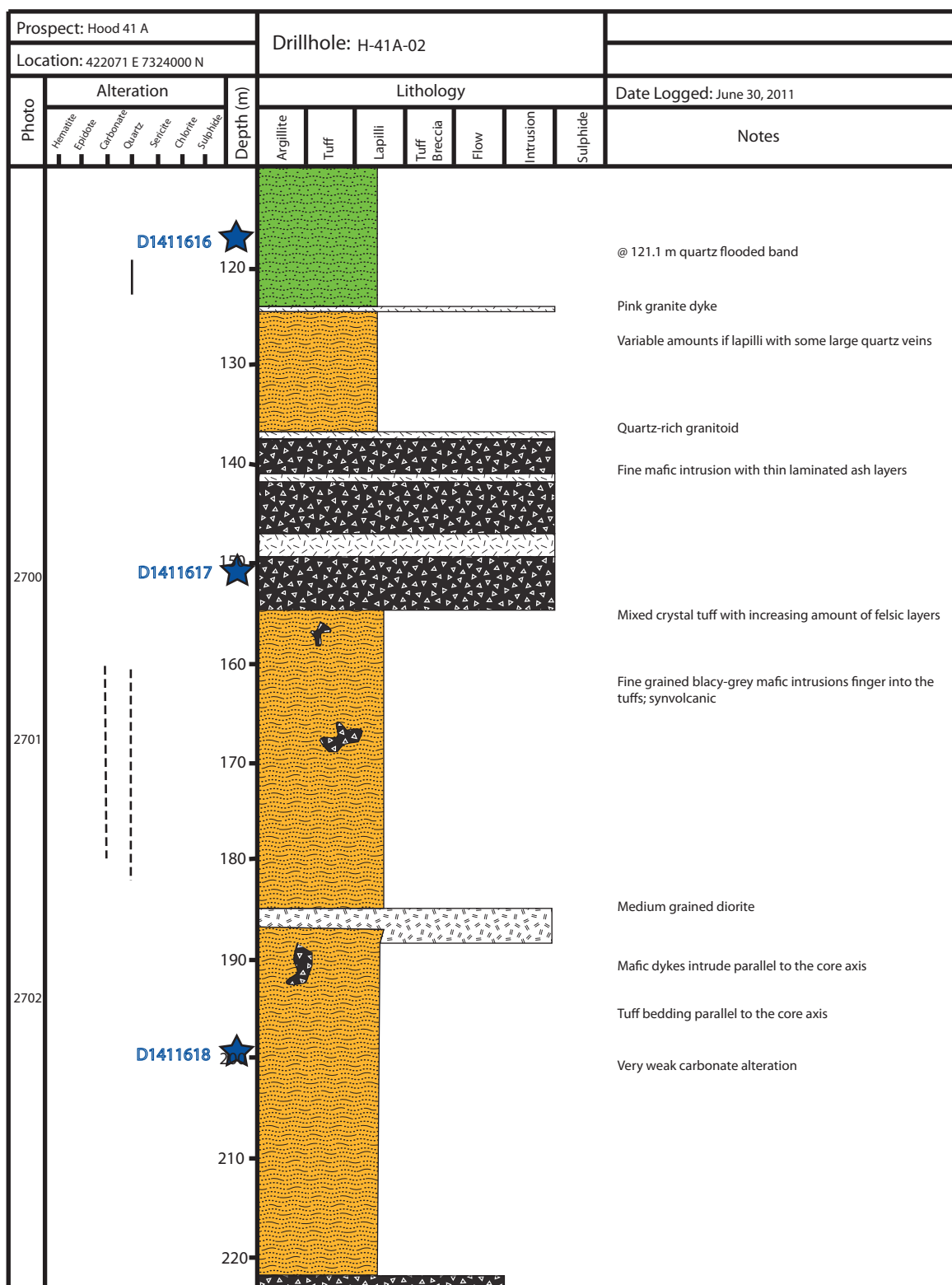
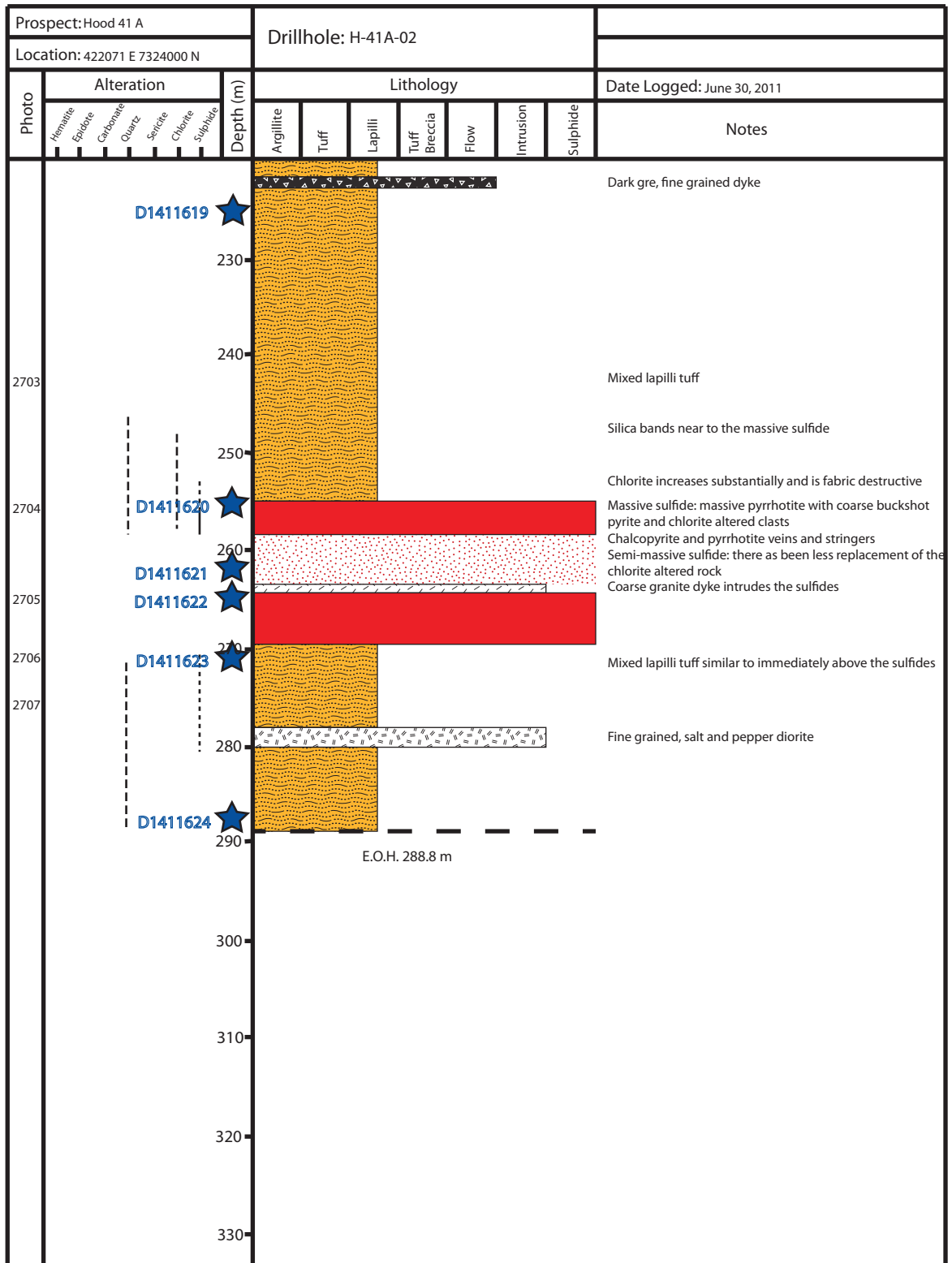


Figure A1-1: Drill Logs



### Figure A1-1: Drill Logs

Prospect: Hood 41A		Drillhole: H-41A-09														
Location: 421889 E 7324076 N																
Photo	Alteration						Depth (m)	Lithology							Date Logged: July 7, 2011	
	Hematite	Epидdite	Carbonate	Quartz	Sericite	Chlorite		Sulphide	Argillite	Tuff	Lapilli	Tuff Breccia	Flow	Intrusion	Sulphide	Notes
																Strained, altered coarse grey-pink granite
																Mafic tuff without lapilli but rather granular with white carbonate clots and veins Lapilli increase downhole
2930																Fine grained andesite with rare flow banding Grey coarse grained granite
																Foliated granite
2931																Andesite with flow banding in green and cream coloured bands
2932																Contact with chill margins sinuously bends into finely banded tuff
2933																Fine grained pink granite dyke Basalt has cobweb alteration that results in pseudoclasts
2934																Foliated andesite (possibly altered dacite) with extensive sericite alteration with coarse quartz crystals Very well banded flow
2935																Silicified flow Flows of varying composition with fine banding More mafic units have carbonate clots and veins Small granite dykes cut the volcanic rocks
2936																Variable quartz and sericite alteration
2937																Laminated felsic flow Finely laminated basalt with quartz crystals and some carbonate alteration Dark grey, finely laminated intermediate flow with minor calcite clots and veins
2938																Fine to medium grained, massive, white granite with a central zone of pink granite with chlorite alteration along fractures Banded mafic flow? White granite with cpy clots and strings along fractures
2939																Fine grained lapilli tuff with chlorite alteration Grainy felsic tuff with pin prick white crystals Pyrite and chalcocopyrite parallel to foliation
2940																Weakly foliated rhyolite with quartz and feldspar crystals Becomes more massive away from the upper contact
2945																
2946																
2947																

### Figure A1-1: Drill Logs

Prospect: Hood 41A							Drillhole: H-41A-09										
Location: 421889 E 7324076 N														Date Logged: July 7, 2011			
Photo	Alteration						Depth (m)	Lithology							Notes		
	Hematite	Epidote	Carbonate	Quartz	Sericite	Chlorite		Sulphide	Argillite	Tuff	Lapilli	Tuff Breccia	Flow	Intrusion		Sulphide	
2948																	
2949																	
2950																	
2951																	
2952																	
2953																	
2954																	
2955																	
2956																	



Figure A1-1: Drill Logs

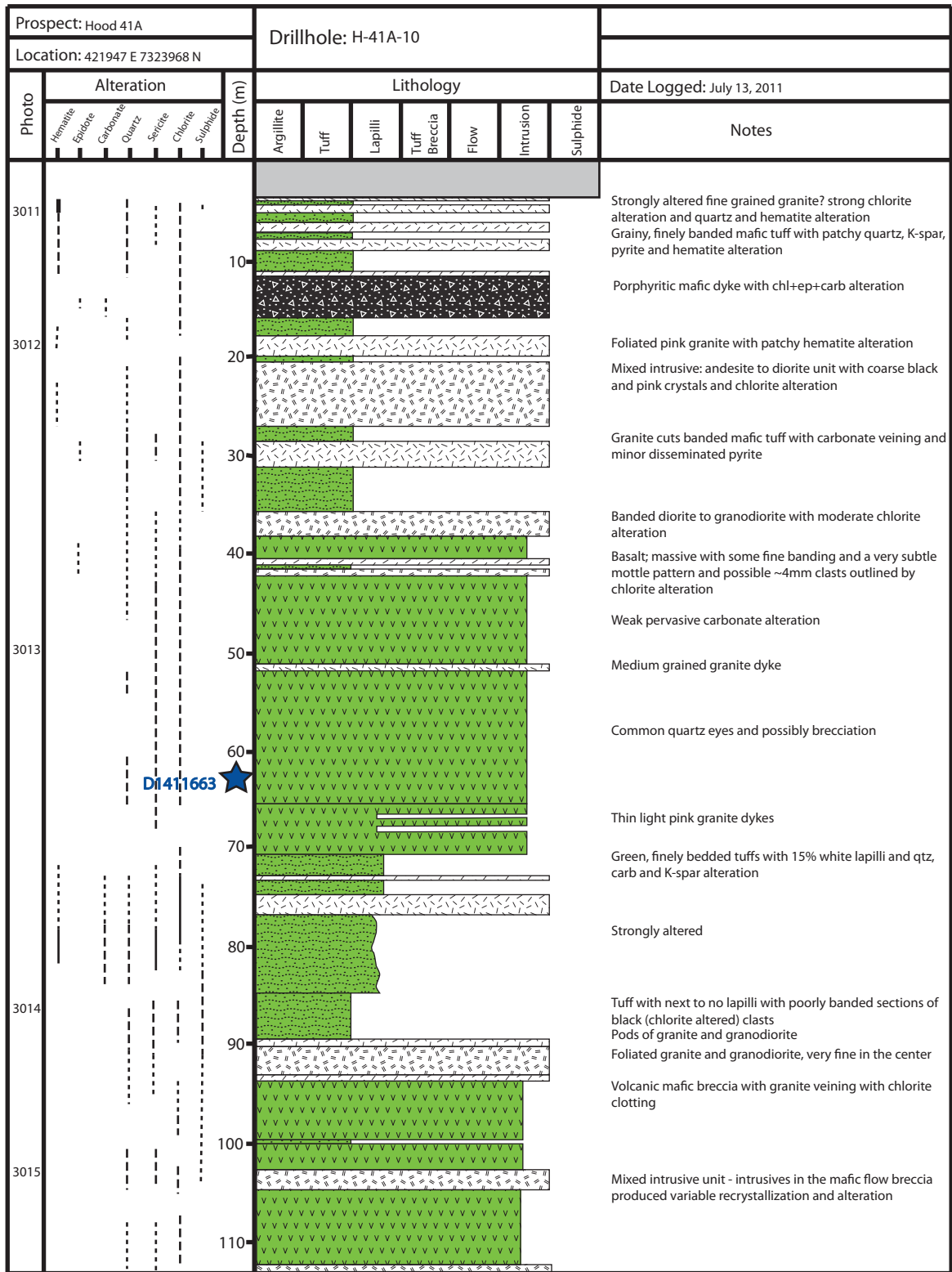


Figure A1-1: Drill Logs

Prospect: Hood 41A							Drillhole: H-41A-10									
Location: 421947 E 7323968 N																
Photo	Alteration						Depth (m)	Lithology							Date Logged: July 13, 2011	
	Hematite	Epidote	Carbonate	Quartz	Sericite	Chlorite		Sulphide	Argillite	Tuff	Lapilli	Tuff Breccia	Flow	Intrusion	Sulphide	Notes
3016																Mixed intrusive unit
																Flow breccia with black clasts
3017																Felsic banded flows interbedded with ?mafic lapilli tuffs Flow units have fine to thick bands with sinuous curving and band selective qtz+ser and chl alteration
																Mafic lapilli tuff Felsic tuff is grey with siliceous quartz and sericite alteration Mixed tuffs have alternating grey and green layers with qtz+ser alteration in the felsic bands and carb alteration in the mafic bands
3018																Light pink, coarse grained granite
																Dark grey flow
3019																Tuff with very few lapilli becoming increasingly felsic
3020																Grey felsic lapilli tuff with patchy strong chlorite, quartz and sericite alteration and some recrystallized zones
3021																Pink granite
																Quartz eyes in the tuff
3022																Narrow felsic flow layers within the tuff
																Green where chlorite alteration is strong
3023																Banded flow with selective quartz alteration Very strong quartz and sericite alteration in foliated rhyolite with a brecciated upper contact Massive grey dacite
																Light grey-green tuff with carbonate veins and blebs

### Figure A1-1: Drill Logs

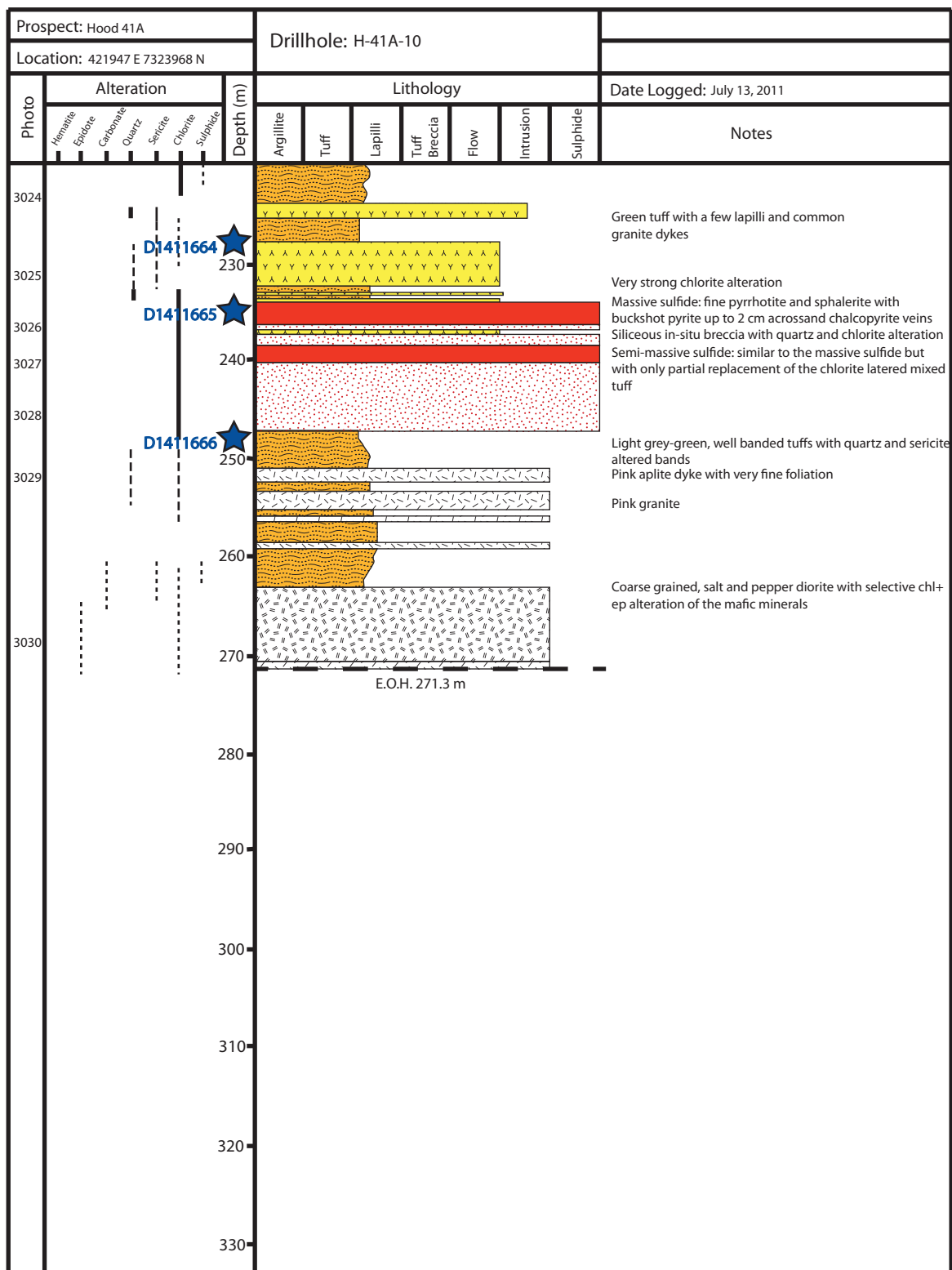


Figure A1-1: Drill Logs

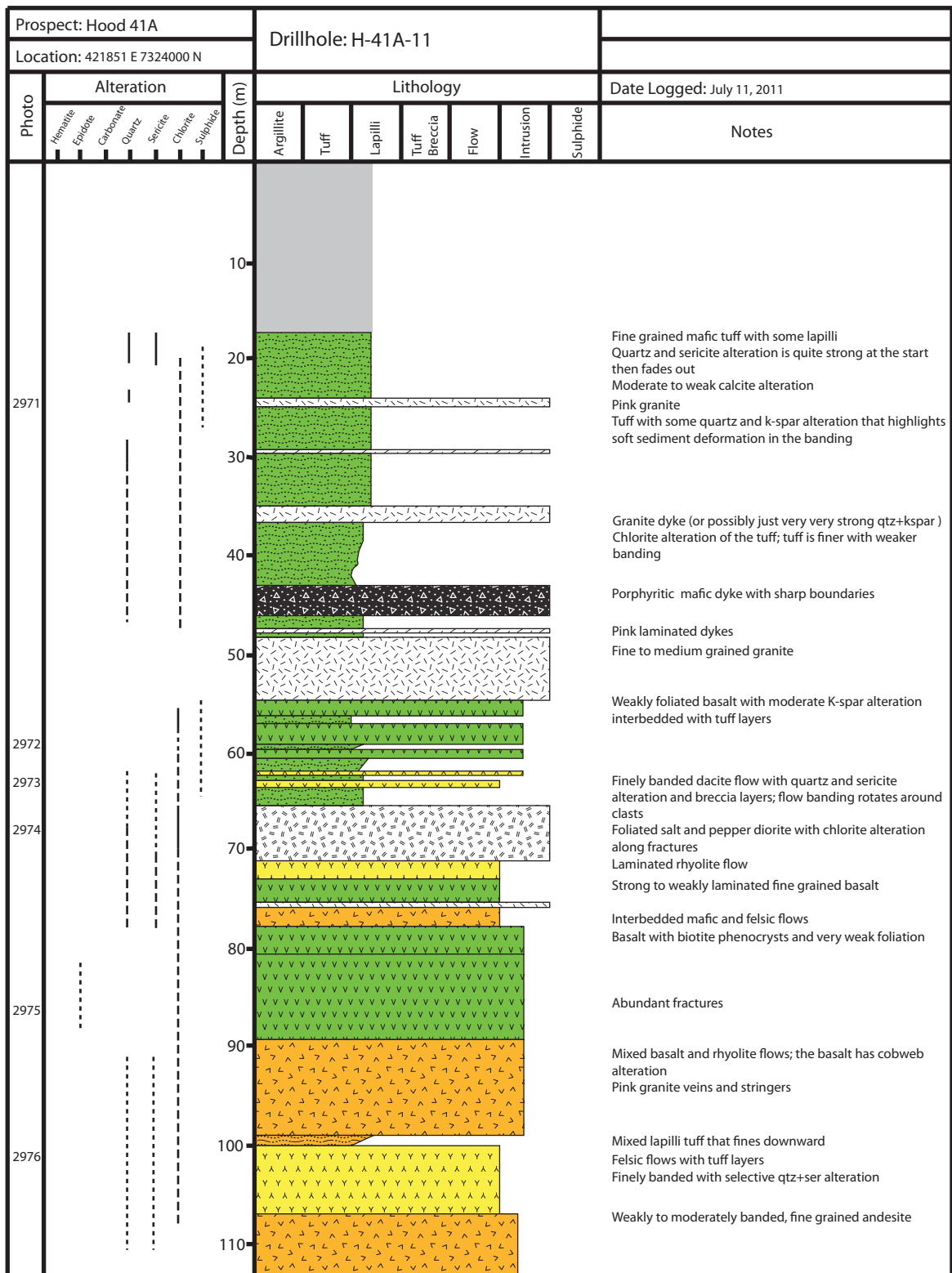


Figure A1-1: Drill Logs

Prospect: Hood 41A							Drillhole: H-41A-11									
Location: 421851 E 7324000 N																
Photo	Alteration						Depth (m)	Lithology							Date Logged: July 11, 2011	
	Hematite	Epaldore	Carbonate	Quartz	Sericite	Chlorite		Sulphide	Argillite	Tuff	Lapilli	Tuff Breccia	Flow	Intrusion	Sulphide	Notes
2977																Zones of strong K-spar+Qtz alteration Pyrrhotite and chalcopyrite stringers
																Medium grained pink granite with calcite veins
							120									Felsic lapilli tuff with coarse lapilli up to 3mm in diameter Qtz+ser+chl alteration of the tuff Chalcopyrite and pyrrhotite stringers (10% sulfides)
2978																Fine grained, finely banded tuff with chlorite clots
							130									Green-grey dacite flow with strong, selective alteration Shears displace some of the banding
							140									Quartz veins Layers of mafic tuffs Patchy flow banding
2979							150									Mafic lapilli tuff Felsic lapilli tuff with selective quartz and sericite alteration
							160									General decrease the amount of lapilli Some minor flow layers
							170									Quartz, carbonate and K-feldspar veins and blebs
																Dacite flow with moderate banding
																Felsic tuff
							190									Banded dacite flow and an increase in quartz alteration
							200									Fine, grey tuff Some flow banding Geochron sample Possible in situ breccia
2981																Tuff with buckshot pyrite and chalcopyrite veins and some pyrrhotite and chalcopyrite replacement Dark grey tuff is less altered than above sulfide
2982																Weakly banded rhyolite with minor flow layers and in situ breccia Blue-grey, coarse, foliated diorite
							220									

### Figure A1-1: Drill Logs

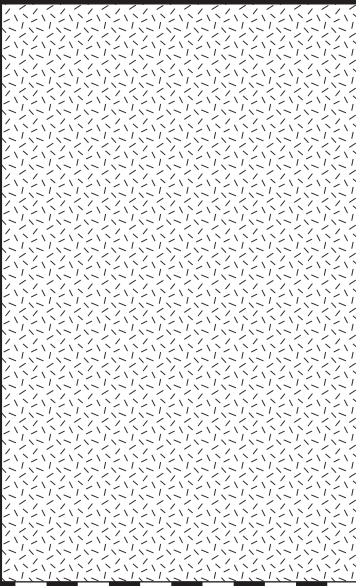
Prospect: Hood 41A		Drillhole: H-41A-11														
Location: 421851 E 7324000 N																
Photo	Alteration						Depth (m)	Lithology							Date Logged: July 11, 2011	
	Hemimatte	Epidote	Carbonate	Quartz	Sericite	Chlorite		Sulphide	Argillite	Tuff	Lapilli	Tuff Breccia	Flow	Intrusion	Sulphide	Notes
							230								Pink granite	
							240									
							250									
							260									
							270									
							270	E.O.H. 268.1 m								
							280									
							290									
							300									
							310									
							320									
							330									

Figure A1-1: Drill Logs

Prospect: Hood 41A		Drillhole: H-41A-15														
Location: 422014 E 7323918 N																
Photo	Alteration						Depth (m)	Lithology					Date Logged: July 6, 2011			
	Hematite	Epидote	Carbonate	Quartz	Sericite	Chlorite		Sulphide	Argillite	Tuff	Lapilli	Tuff Breccia	Flow	Intrusion	Sulphide	Notes
2869																Medium to coarse grained, dark grey and diorite with abundant biotite and amphibole Weak carbonate alteration Massive, fine grained granite dyke with hornblende
																Back into coarse diorite with some variation in crystal size; Hematite staining of calcite veins  @19m 20 cm coarse quartz vein.
2870																Mafic flow breccia with mixed clast size and degree of rounding with wispy parallel alteration. Some thin calcite veins with hematite alteration Granitic blebs and injections - top of the intrusion has sharp contact, bottom has veins that extend into flow dykeltes of granite cut flow and recrystallized it
																Hematite altered coarse grained granite  Alteration in flow becoming less laminated
2871																
2872																Flow with quartz-felspar recrystallized patches with blebs of the porphyritic dyke Porphyritic mafic dyke- sharp brown chill margins Fine grey with pyroxene phenocrysts up to 3mm Some phenocrysts are partially replaces by pyrite No cross cutting calcite veins
2873																Dykes cut parallel to core so they edge in and out of the hematite and granite altered mafic flow
2874																Increase in fine calcite veins  @67.7m coarse well preserved breccia clasts
2875																Fine to coarse grained granite dyke; strong hematite stain
2876																Breccia flow-quite recrystallized  Inaccessible core
2877																Weakly laminated tuff  Finely bedded mixed tuff-green to dark green lightening to olive green-lapilli decrease with depth Coarse diorite with calcite veins
2878																Coarse grained hematite stained granite  Black mafic breccia  Diorite or mixed intrusive
2879																

Figure A1-1: Drill Logs

Prospect: Hood 41A		Drillhole: H-41A-15														
Location: 422014 E 7323918 N																
Photo	Alteration						Depth (m)	Lithology							Date Logged: July 6, 2011	
	Hematite	Epidote	Carbonate	Quartz	Sericite	Chlorite		Sulphide	Argillite	Tuff	Lapilli	Tuff Breccia	Flow	Intrusion	Sulphide	Notes
2880							120									Pink granite
2881							130									Mixed intrusive-mafic with chlorite altered pseudoclasts Variable grain size
2882							140									Coarse granite
							150									Coarse grained diorite with calcite veining and PO
2883							160									Finely banded light green lapilli tuff; some sinuous banding Lots of calcite viens and clots
							170									Coarse grained pink granite with wispy alteration
2884							180									Strongly banded with bands of moderate thickness; silica replaced tuff
							190									Medium to fine grained granite
2885							200									Finely banded tuff; lots of chlorite atleration and quartz and calcite alteration lenses
2886							210									Grey granite
2887							220									Finely laminated tuff
							230									Dark green fine grained tuff with fine laminations and small white pinprick sized crystals
							240									Pink coarse grained massive granite Quite fractured with chlorite fill
							250									Very fine grained mafic tuff with a few rare lapilli; some very well laminated layers and frequently cut by granite



### Figure A1-1: Drill Logs

Prospect: Hood 41A							Drillhole: H-41A-15									
Location: 422014 E 7323918 N																
Photo	Alteration						Depth (m)	Lithology							Date Logged: July 6, 2011	
	Hematite	Epidote	Carbonate	Quartz	Sericite	Chlorite		Sulphide	Argillite	Tuff	Lapilli	Tuff Breccia	Flow	Intrusion	Sulphide	Notes
																</

Figure A1-1: Drill Logs

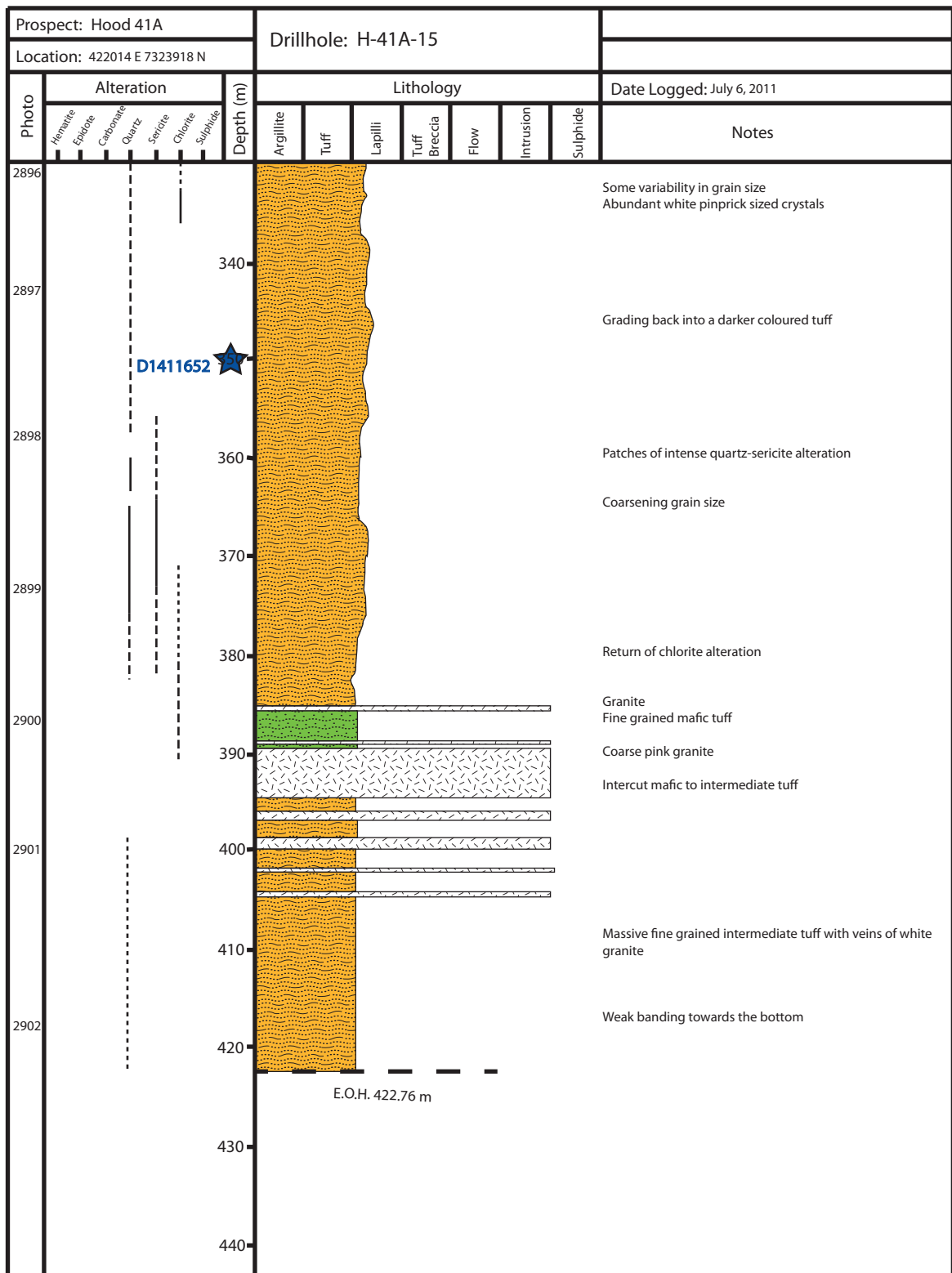


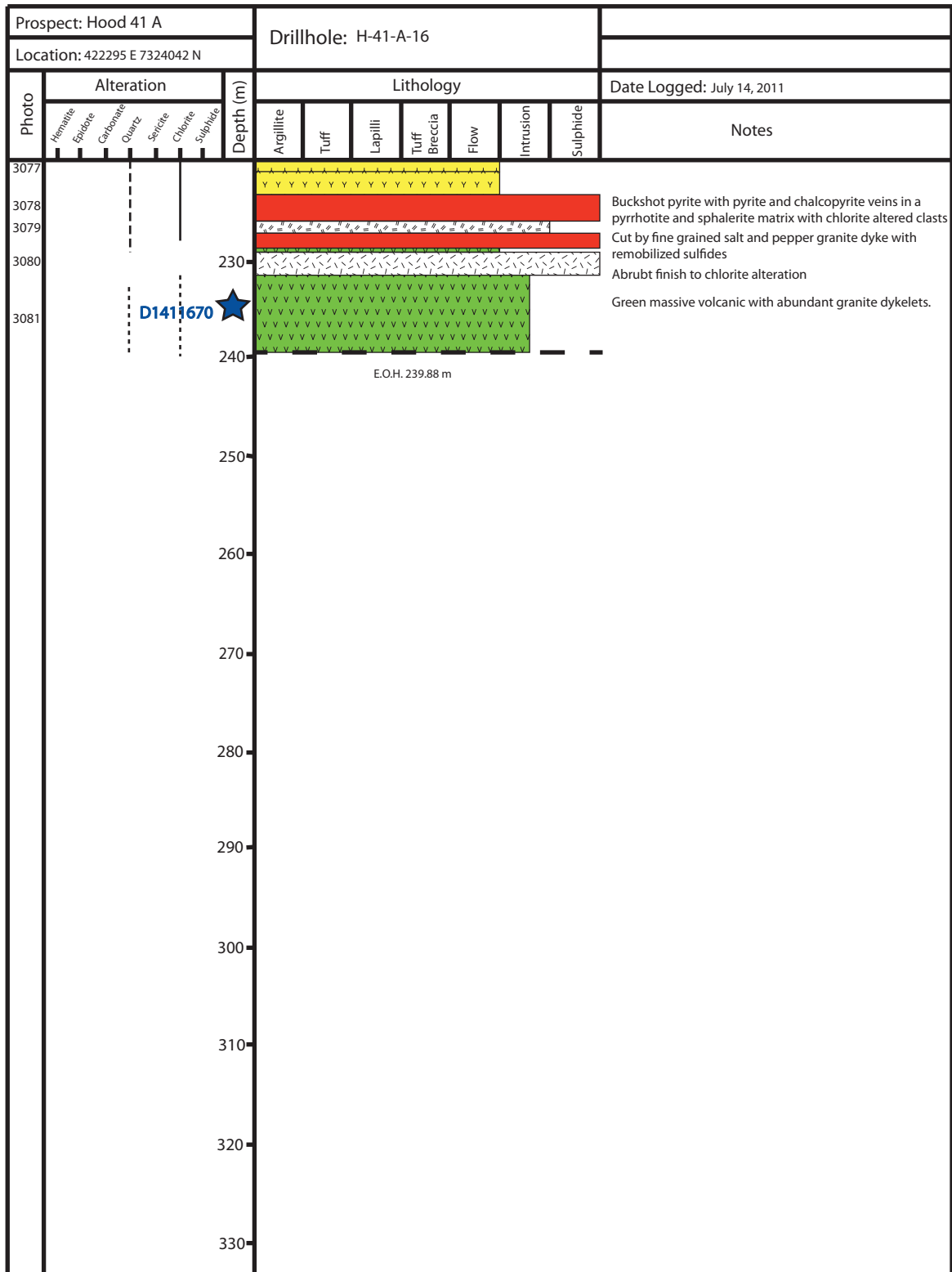
Figure A1-1: Drill Logs

Prospect: Hood 41 A		Drillhole: H-41-A-16													
Location: 422295 E 7324042 N															
Photo	Alteration						Depth (m)	Lithology							Date Logged: July 14, 2011
	Hematite	Epидote	Carbonate	Quartz	Sericite	Chlorite		Sulphide	Argillite	Tuff	Lapilli	Tuff Breccia	Flow	Intrusion	Sulphide
3052															Coarse grained blue-pink grey massive diorite with minor fracturing Cut by very coarse granite with large micas
3053															Light grey green finely banded intermediate composition tuff with common rounded white lapilli in the center of the unit
3054															Poorly foliated, mottle dark grey foliate with some clasts, cut by similar well banded layers with quartz eyes
3055															Pervasive quartz and sericite alteration Medium grained massive plagioclase and quartz granite with chlorite altered fractures
3056															Weakly banded rhyolite with patchy quartz and sericite alteration grading into a well banded flow Banding fades and visible plagioclase and quartz crystals occur with chlorite altered fractures
3057															Very fine, green, banded tuff with sections of fine banding gradually transitioning into a coarser grey tuff with the occasional rounded chlorite altered clasts with small white lapilli
3058															Rhyolite with variable, strong to weak banding and patchy very strong quartz and sericite alteration
3059															Strong flow banding with quartz and sericite replacement Banding grades into flow breccia
3060															Green, mafic, banded tuff. Very fine grained layers and very few lapilli Minor quartz alteration and clots and veining of calcite
3061															Selective quartz and sericite replacement along banding
3062															Coarse grained white rhyolite with possible flow banding changing to massive with alteration along fractures creating pseudobreccia pattern Breccia layers
3063															Spotty hematite; chlorite alteration along fractures with very strong pervasive quartz replacement
3064															Breccia zone with rhyolite clasts and brown glass fragments
3065															Sections of chlorite alteration along veins and fractures with selective patches quartz alteration
-3967															Gradual transition into mafic flow

Figure A1-1: Drill Logs

Prospect: Hood 41 A								Drillhole: H-41-A-16									
Location: 422295 E 7324042 N																	
Photo	Alteration						Depth (m)	Lithology							Date Logged: July 14, 2011		
	Hematite	Epидote	Carbonate	Quartz	Sericite	Chlorite		Sulphide	Argillite	Tuff	Lapilli	Tuff Breccia	Flow	Intrusion	Sulphide	Notes	
3068																Dark green, finely laminated unit with banding running parallel to the core axis Very dark layers of glass shards? Small white pinprick sized crystals Minor carbonate veining and blebs Strong chlorite alteration and chlorite clots	
3069																Granitic dykes with moderate quartz, K-feldspar and sericite alteration around them	
																Colour becomes increasingly grey Fine grained pink granite with chlorite filled fractures Increasingly abundant fine white quartz layers in flows	
3070																	
3071																	
3072																	
3073																	
3074																	
																Pink coarse grained granite Abundant granitic dykes that alter the volcanics around it	
3075																Selective K-spar, quartz, sericite altered rhyolite flow with poorly defined bands Chlorite alteration along fractures	
3076																	

Figure A1-1: Drill Logs



**Appendix 2:**  
**Lithogeochemistry, mass change, fractionation curves, principal components,**  
**and principal component scores**

Table A2-1: Geochemical data for the rocks of the Hood deposits

Samples	Det. Limit	D1425001	D1425002	D1425003	D1425004	D1425005	D1425006	D1425007	D1425008	D1425009	D1425010	D1425011
Deposit		H-461	H-461	H-461	H-461	H-461	H-461	H-461	H-461	H-461	H-461	H-461
Drillhole #		H461-010	H461-010	H461-010	H461-010	H461-010	H461-010	H461-010	H461-010	H461-010	H461-010	H461-010
From (m)		154.88	160.07	172.1	221.7	241.4	248.59	277.65	288.7	221.6	360	360
To (m)		155	160.23	172.26	221.86	241.6	248.74	277.8	288.87	221.74	360.18	360.18
Easting		-	-	-	-	-	-	-	-	-	-	-
Northing		-	-	-	-	-	-	-	-	-	-	-
Rock Type		Mafic	Felsic	Felsic	Felsic	Felsic	Felsic	Inter	Mafic	Felsic	Felsic	Felsic
Sub-type		I	Tuff Group	B	B	B	B	1	I	A	A	A
SiO <sub>2</sub> <sup>#</sup>	0.01	44.5	45.6	76.6	79.2	79	76.5	52.7	46.7	74.4	76.1	76.4
Al <sub>2</sub> O <sub>3</sub> <sup>#</sup>	0.01	9.52	12.9	11.95	10.15	11.05	11.85	16.15	10.05	13.1	12.05	11
Fe <sub>2</sub> O <sub>3</sub> <sup>#</sup>	0.01	11.2	9.68	2.79	0.63	2.61	1.37	12.15	11.6	1.86	1.5	1.77
CaO <sup>#</sup>	0.01	7.91	7.78	0.22	1.13	0.32	0.94	0.86	10.35	0.13	1.28	2.28
MgO <sup>#</sup>	0.01	12.5	7.81	2.59	1.16	2.25	1.91	7.67	11.85	2.49	1.52	1.79
Na <sub>2</sub> O <sup>#</sup>	0.01	0.01	0.31	0.27	2.41	0.16	1.1	2.95	1.45	0.35	1.29	1.44
K <sub>2</sub> O <sup>#</sup>	0.01	0.19	1.82	3.08	2.14	2.98	3.09	0.87	0.17	3.72	3.14	2.67
Cr <sub>2</sub> O <sub>3</sub> <sup>#</sup>	0.01	0.2	0.04	<0.01	<0.01	<0.01	<0.01	0.01	0.22	<0.01	<0.01	<0.01
TiO <sub>2</sub> <sup>#</sup>	0.01	0.94	0.61	0.14	0.12	0.12	0.14	1.24	0.98	0.16	0.15	0.14
MnO <sup>#</sup>	0.01	0.21	0.17	0.01	0.01	0.01	0.01	0.08	0.18	0.01	0.02	0.04
P <sub>2</sub> O <sub>5</sub> <sup>#</sup>	0.01	0.07	0.05	0.01	0.01	<0.01	0.01	0.34	0.08	0.02	0.02	<0.01
SrO <sup>#</sup>	0.01	0.01	<0.01	<0.01	0.01	<0.01	<0.01	<0.01	0.02	<0.01	<0.01	<0.01
BaO <sup>#</sup>	0.01	<0.01	0.05	0.13	0.08	0.17	0.14	0.01	0.01	0.06	0.08	0.07
C <sup>@</sup>	0.01	2.52	2.56	0.09	0.46	0.08	0.22	0.18	0.87	0.03	0.31	0.61
S <sup>@</sup>	0.01	0.16	0.1	<0.01	<0.01	<0.01	<0.01	<0.01	0.11	<0.01	0.02	0.02
Ba <sup>*</sup>	0.5	10.9	430	1200	686	1515	1290	119.5	61	528	744	623
Ce <sup>*</sup>	0.5	19.2	8	100.5	93.6	106.5	101	43.6	14.2	113.5	108	87
Cr <sup>*</sup>	10	1440	270	30	20	20	20	110	1600	20	20	20
Cs <sup>*</sup>	0.01	0.78	0.86	1.31	1.04	1.18	1.46	0.47	0.85	1.97	1.46	1.23
Dy <sup>*</sup>	0.05	3.08	2.42	7.95	7.06	6.82	6.94	5.58	2.78	9.75	8.99	8.31

Table A2-1: Geochemical data for the rocks of the Hood deposits

Samples	Det. Limit	D1425001	D1425002	D1425003	D1425004	D1425005	D1425006	D1425007	D1425008	D1425009	D1425010	D1425011
Er*	0.03	1.6	1.56	5.06	4.45	4.06	4.31	3.53	1.61	5.92	5.88	5.24
Eu*	0.03	1.12	0.29	0.64	0.88	0.72	0.78	1.08	0.95	1.14	1.07	0.95
Ga*	0.1	14.4	14.7	21	11.6	19.4	17.3	23	14.1	22.7	19.3	16.5
Gd*	0.05	3.79	2.08	8.01	6.98	7.49	7.01	5.44	2.99	9.99	9.02	8.45
Hf*	0.2	1.5	9.2	6.7	5.5	6	6.6	5	1.6	9	8.4	7.6
Ho*	0.01	0.59	0.52	1.63	1.47	1.35	1.38	1.17	0.56	1.98	1.88	1.74
La*	0.5	8.6	4.1	50.4	47	53.5	50.3	18.9	6.1	56	53.4	42.6
Lu*	0.01	0.21	0.25	0.77	0.66	0.61	0.67	0.47	0.21	0.9	0.86	0.77
Nb*	0.2	4.6	1.8	17.9	14.6	16.8	18.7	12.6	4.6	23.6	22.1	19.9
Nd*	0.1	11.9	4.6	41.3	37.8	43.2	41.1	23.3	8.9	49.8	47	38.6
Pr*	0.03	2.81	1.06	11.8	11	12.5	11.9	5.77	2.09	13.75	12.85	10.65
Rb*	0.2	3.8	54.9	85.4	70.2	82.3	93.2	32.4	7.5	130.5	104	87.4
Sm*	0.03	3.2	1.44	8.34	7.53	8.33	8.01	5.19	2.52	10.6	9.52	8.39
Sn*	1	1	2	6	2	7	5	3	1	4	2	2
Sr*	0.1	58.4	49.2	12.9	54.9	9.6	21.1	34.8	172.5	7.8	18.3	21
Ta*	0.1	0.3	0.1	1.7	1.4	1.6	1.7	0.9	0.3	1.9	1.8	1.6
Tb*	0.01	0.55	0.37	1.28	1.15	1.18	1.11	0.88	0.46	1.59	1.48	1.35
Th*	0.05	0.57	0.84	21	17.55	19.25	21	3.57	0.57	19.3	17.85	16
Tl*	0.5	<0.5	<0.5	<0.5	<0.5	<0.5	<0.5	<0.5	<0.5	<0.5	<0.5	<0.5
Tm*	0.01	0.25	0.26	0.79	0.68	0.64	0.67	0.52	0.25	0.92	0.88	0.8
U*	0.05	0.44	0.41	5.38	4.54	4.68	5.99	0.78	0.12	5	4.98	4.27
V*	5	252	225	<5	6	<5	<5	178	268	<5	<5	<5
W*	1	1	2	2	1	1	1	1	<1	1	1	1
Y*	0.5	15.6	14.6	47.8	43.3	35.1	36.8	32.6	14.8	55.4	53.8	48.4
Yb*	0.03	1.38	1.61	5.13	4.36	4.15	4.31	3.18	1.42	5.81	5.65	5.03
Zr*	20	50	380	210	170	180	210	220	60	300	280	260



Table A2-1: Geochemical data for the rocks of the Hood deposits

Samples	Det. Limit	D1425001	D1425002	D1425003	D1425004	D1425005	D1425006	D1425007	D1425008	D1425009	D1425010	D1425011
As <sup>^</sup>	0.1	2.5	43.9	0.4	0.2	0.1	0.1	4.8	0.3	0.1	0.2	0.6
Bi <sup>^</sup>	0.01	0.08	0.41	0.02	0.02	0.09	0.01	0.02	0.05	0.02	0.03	0.04
Hg <sup>^</sup>	0.005	<0.005	<0.005	<0.005	<0.005	<0.005	<0.005	<0.005	<0.005	<0.005	<0.005	<0.005
Sb <sup>^</sup>	0.05	0.44	0.25	0.22	0.14	0.09	0.09	<0.05	0.22	0.12	0.09	0.11
Se <sup>^</sup>	0.2	0.7	0.5	0.6	0.5	0.6	0.7	0.6	0.8	1	0.9	0.9
Te <sup>^</sup>	0.01	0.02	0.02	<0.01	<0.01	0.01	<0.01	0.01	0.03	<0.01	<0.01	<0.01
Ag <sup>+</sup>	0.5	<0.5	<0.5	<0.5	<0.5	<0.5	<0.5	<0.5	<0.5	<0.5	<0.5	<0.5
Cd <sup>+</sup>	0.5	<0.5	<0.5	<0.5	<0.5	<0.5	<0.5	<0.5	0.5	<0.5	<0.5	<0.5
Co <sup>+</sup>	1	55	40	4	1	3	1	24	59	2	2	2
Cu <sup>+</sup>	1	128	116	1	<1	<1	<1	<1	138	<1	<1	1
Mo <sup>+</sup>	1	1	1	3	2	1	2	1	1	2	1	2
Ni <sup>+</sup>	1	283	84	<1	1	<1	<1	76	316	<1	<1	<1
Pb <sup>+</sup>	2	28	49	3	2	9	4	<2	19	<2	<2	<2
Zn <sup>+</sup>	2	108	73	13	2	15	12	155	97	40	20	23
Sc <sup>+</sup>	1	30	32	3	3	3	4	18	33	6	5	5
LOI (ppm)	0.01	13.9	13.05	2.93	2.89	2.73	3.01	5.4	6.75	2.87	3.2	4.13
Total (ppm)	0.01	101.16	99.87	100.72	99.94	101.4	100.07	100.43	100.41	99.17	100.35	101.73
La <sup>CN</sup>		36.29	17.30	212.66	198.31	225.74	212.24	79.75	25.74	236.29	225.32	179.75
Yb <sup>CN</sup>		8.12	9.47	30.18	25.65	24.41	25.35	18.71	8.35	34.18	33.24	29.59
La/Yb <sup>CN</sup>		4.47	1.83	7.05	7.73	9.25	8.37	4.26	3.08	6.91	6.78	6.07
La/Sm		2.69	2.85	6.04	6.24	6.42	6.28	3.64	2.42	5.28	5.61	5.08
Zr/Yb		36.23	236.02	40.94	38.99	43.37	48.72	69.18	42.25	51.64	49.56	51.69
Zr/Hf		33.33	41.30	31.34	30.91	30.00	31.82	44.00	37.50	33.33	33.33	34.21
Zr/(TiO <sub>2</sub> *10000)		0.01	0.06	0.15	0.14	0.15	0.15	0.02	0.01	0.19	0.19	0.19
Nb/Yb		3.33	1.12	3.49	3.35	4.05	4.34	3.96	3.24	4.06	3.91	3.96
Nb/Ta		15.33	18.00	10.53	10.43	10.50	11.00	14.00	15.33	12.42	12.28	12.44
LOI; Loss on ignition CN; chondrite normalized - ; not analyzed												

Table A2-1 (continued): Geochemical data for the rocks of the Hood deposits

Samples	Det. Limit	D1425012	D1425013	D1425014	D1425015	D1425016	D1425017	D1425018	D1425019	D1425020	D1425021	D1425022
Deposit		H-461	H-461	H-461	H-461	H-461	H-461	H-461	H-461	H-461	H-461	H-461
Drillhole #		H461-010	H461-010	H461-010	H461-010	H461-010	H461-010	H461-010	H461-010	H461-010	H461-010	H461-010
From (m)		394.09	424.8	443.9	473.67	474.52	517.06	549.35	583.5	616.44	622.7	626.6
To (m)		394.25	424.94	444.07	473.83	474.68	517.23	549.55	583.65	616.6	622.87	626.75
Easting		-	-	-	-	-	-	-	-	-	-	-
Northing		-	-	-	-	-	-	-	-	-	-	-
Rock Type		Felsic	Felsic	Mafic	Mafic	Int.	Int.	Int.	Int.	Int.	Felsic	Int.
Sub-type		A	A	III	III	1	1	1	1	1	A	1
SiO <sub>2</sub> <sup>#</sup>	0.01	78.5	80.1	45.9	44.2	54.4	58.5	56.3	57.4	57.1	78.1	56.7
Al <sub>2</sub> O <sub>3</sub> <sup>#</sup>	0.01	10.3	9.43	14.45	13.9	14.9	14.9	14.55	14.1	14.5	11.9	15.15
Fe <sub>2</sub> O <sub>3</sub> <sup>#</sup>	0.01	2.1	3.18	14.8	14.55	9.48	10.95	11.45	9.27	8.56	1.85	9.73
CaO <sup>#</sup>	0.01	1.47	0.74	8.56	7.95	1.92	0.72	1.14	4.43	4.83	0.87	1.9
MgO <sup>#</sup>	0.01	1.42	2.34	5.17	5.52	8.91	6.76	6.3	3.77	4.26	1.2	6.09
Na <sub>2</sub> O <sup>#</sup>	0.01	1.89	0.39	2.83	2.22	2.72	0.5	1.08	3.74	2.79	3.61	2.79
K <sub>2</sub> O <sup>#</sup>	0.01	2.08	2.3	1.05	1.73	1.18	2.41	1.84	1.01	1.72	1.95	1.22
Cr <sub>2</sub> O <sub>3</sub> <sup>#</sup>	0.01	<0.01	<0.01	0.01	0.01	<0.01	<0.01	<0.01	<0.01	<0.01	<0.01	<0.01
TiO <sub>2</sub> <sup>#</sup>	0.01	0.14	0.11	3.17	3.07	1.33	1.33	1.29	1.19	1.32	0.15	1.35
MnO <sup>#</sup>	0.01	0.02	0.03	0.19	0.14	0.1	0.09	0.11	0.13	0.1	0.02	0.1
P <sub>2</sub> O <sub>5</sub> <sup>#</sup>	0.01	0.01	<0.01	0.33	0.33	0.26	0.27	0.26	0.23	0.27	0.01	0.29
SrO <sup>#</sup>	0.01	<0.01	<0.01	0.07	0.04	<0.01	<0.01	<0.01	0.01	0.01	0.01	<0.01
BaO <sup>#</sup>	0.01	0.1	0.07	0.04	0.08	0.03	0.07	0.07	0.03	0.04	0.06	0.02
C <sup>@</sup>	0.01	0.33	0.23	0.41	1.06	0.15	0.1	0.19	0.76	0.76	0.17	0.13
S <sup>@</sup>	0.01	<0.01	<0.01	0.18	0.23	<0.01	<0.01	<0.01	0.01	0.03	<0.01	<0.01
Ba <sup>*</sup>	0.5	902	624	391	708	244	619	636	241	410	548	227
Ce <sup>*</sup>	0.5	92	66.8	66	62.3	51.3	54.8	53.3	49.6	54.7	105	62.2
Cr <sup>*</sup>	10	20	20	60	60	20	20	20	20	20	20	20
Cs <sup>*</sup>	0.01	0.95	0.91	4.99	3.96	2.68	1.36	0.92	0.45	0.72	0.8	0.65
Dy <sup>*</sup>	0.05	7	7.39	6.26	6.16	5.07	5	4.79	5.5	5.23	8.47	6.04

Table A2-1 (continued): Geochemical data for the rocks of the Hood deposits

Samples	Det. Limit	D1425012	D1425013	D1425014	D1425015	D1425016	D1425017	D1425018	D1425019	D1425020	D1425021	D1425022
Er*	0.03	4.46	4.67	3.03	2.98	3.02	2.94	2.82	3.17	3.02	5.27	3.76
Eu*	0.03	0.86	0.56	2.74	2.7	1.11	1.05	1.55	1.96	1.81	0.98	1.28
Ga*	0.1	15.8	16.5	26.4	25.2	24.4	23.6	22.5	20.6	21.1	18.8	21.2
Gd*	0.05	7.54	6.74	8.05	7.68	5.61	5.48	5.54	5.88	5.77	9.22	6.28
Hf*	0.2	7.3	6.3	6	5.6	5.4	5.2	5.3	5.3	5.3	8.5	5.4
Ho*	0.01	1.46	1.54	1.14	1.14	1.03	0.99	0.98	1.11	1.03	1.74	1.26
La*	0.5	44.9	32.2	29.8	27.9	24.4	26.1	25.7	23.9	26.5	50.8	30.1
Lu*	0.01	0.72	0.67	0.32	0.31	0.44	0.44	0.41	0.46	0.41	0.81	0.5
Nb*	0.2	19.6	17	28.1	27.2	10.8	10.6	10.8	11.3	9.9	21	11
Nd*	0.1	39.9	29.6	36.3	34.7	24.6	26.1	25.1	24.3	26.6	46.4	29.6
Pr*	0.03	11.1	8.18	8.95	8.5	6.47	6.89	6.67	6.28	6.9	12.85	7.73
Rb*	0.2	59.8	68.4	45.3	64.8	52.6	75.6	58.4	30.8	55.1	62.9	40.4
Sm*	0.03	8.05	6.52	8.42	8.11	5.59	5.67	5.53	5.72	5.75	9.76	6.53
Sn*	1	3	5	2	2	2	3	3	4	5	2	2
Sr*	0.1	36.3	13.5	602	337	40.2	12.9	25.1	86.7	76.5	50	40.9
Ta*	0.1	1.5	1.3	2	1.9	0.9	0.9	0.9	0.8	0.9	1.6	0.9
Tb*	0.01	1.15	1.15	1.14	1.12	0.84	0.83	0.81	0.92	0.89	1.42	0.98
Th*	0.05	14.9	13.4	3.64	3.33	7.78	7.71	7.73	8.26	7.61	16.75	7.88
Tl*	0.5	<0.5	<0.5	<0.5	<0.5	<0.5	<0.5	<0.5	<0.5	<0.5	<0.5	<0.5
Tm*	0.01	0.71	0.71	0.41	0.41	0.47	0.46	0.44	0.48	0.45	0.81	0.55
U*	0.05	3.92	3.49	0.71	0.69	1.89	1.92	1.95	1.93	1.85	4.32	1.91
V*	5	<5	<5	368	362	228	233	215	195	212	<5	225
W*	1	1	1	1	1	2	2	4	2	4	2	2
Y*	0.5	39.7	42.4	30	29.2	28.1	27.4	26.5	31.6	29.2	47.5	35.5
Yb*	0.03	4.53	4.4	2.26	2.27	2.8	2.9	2.74	2.99	2.8	5.2	3.28
Zr*	20	260	210	230	220	210	200	210	200	200	300	210

Table A2-1 (continued): Geochemical data for the rocks of the Hood deposits

Samples	Det. Limit	D1425012	D1425013	D1425014	D1425015	D1425016	D1425017	D1425018	D1425019	D1425020	D1425021	D1425022
As <sup>^</sup>	0.1	<0.1	<0.1	3.9	6.8	<0.1	<0.1	0.8	0.1	<0.1	0.2	<0.1
Bi <sup>^</sup>	0.01	0.04	0.02	0.02	0.11	0.01	0.04	0.03	0.03	0.13	0.02	0.05
Hg <sup>^</sup>	0.005	<0.005	<0.005	<0.005	<0.005	<0.005	<0.005	<0.005	<0.005	<0.005	<0.005	<0.005
Sb <sup>^</sup>	0.05	0.1	0.11	0.96	0.8	0.18	0.15	0.15	0.16	0.1	0.14	0.07
Se <sup>^</sup>	0.2	0.5	0.6	1.5	1.9	1	0.6	0.6	0.7	0.7	1	0.8
Te <sup>^</sup>	0.01	0.01	<0.01	<0.01	0.01	<0.01	<0.01	0.01	0.01	0.01	<0.01	0.01
Ag <sup>+</sup>	0.5	<0.5	<0.5	<0.5	<0.5	<0.5	<0.5	<0.5	<0.5	<0.5	<0.5	<0.5
Cd <sup>+</sup>	0.5	<0.5	<0.5	<0.5	<0.5	<0.5	<0.5	<0.5	<0.5	<0.5	<0.5	<0.5
Co <sup>+</sup>	1	2	3	43	41	19	19	24	21	16	3	19
Cu <sup>+</sup>	1	<1	1	47	52	<1	<1	<1	6	201	1	<1
Mo <sup>+</sup>	1	2	2	1	1	2	1	2	2	2	4	3
Ni <sup>+</sup>	1	<1	<1	25	26	8	6	7	7	9	1	8
Pb <sup>+</sup>	2	26	2	18	8	<2	<2	2	<2	7	4	3
Zn <sup>+</sup>	2	29	42	121	93	87	46	68	108	61	12	92
Sc <sup>+</sup>	1	5	4	24	24	17	19	18	16	17	5	18
LOI (ppm)	0.01	2.92	2.95	4.65	7.63	5.42	4.97	5.14	5.63	5.95	2.03	4.68
Total (ppm)	0.01	100.95	101.64	101.22	101.37	100.65	101.47	99.53	100.94	101.45	101.76	100.02
La <sup>CN</sup>		189.45	135.86	125.74	117.72	102.95	110.13	108.44	100.84	111.81	214.35	127.00
Yb <sup>CN</sup>		26.65	25.88	13.29	13.35	16.47	17.06	16.12	17.59	16.47	30.59	19.29
La/Yb <sup>CN</sup>		7.11	5.25	9.46	8.82	6.25	6.46	6.73	5.73	6.79	7.01	6.58
La/Sm		5.58	4.94	3.54	3.44	4.36	4.60	4.65	4.18	4.61	5.20	4.61
Zr/Yb		57.40	47.73	101.77	96.92	75.00	68.97	76.64	66.89	71.43	57.69	64.02
Zr/Hf		35.62	33.33	38.33	39.29	38.89	38.46	39.62	37.74	37.74	35.29	38.89
Zr/(TiO <sub>2</sub> *10000)		0.19	0.19	0.01	0.01	0.02	0.02	0.02	0.02	0.02	0.20	0.02
Nb/Yb		4.33	3.86	12.43	11.98	3.86	3.66	3.94	3.78	3.54	4.04	3.35
Nb/Ta		13.07	13.08	14.05	14.32	12.00	11.78	12.00	14.13	11.00	13.13	12.22
# wt%;lithium borate fusion												
@wt%; combustion furnace												
*ppm; lithium borate fusion												
+ppm; four-acid digestion												
^ppm; aqua regia digestion												
< ; below detection limit												
LOI; Loss on ignition												
CN; chondrite normalized												
- ; not analyzed												

Table A2-1 (continued): Geochemical data for the rocks of the Hood deposits

Samples	Det. Limit	D1425023	D1425024	D1425025	D1425026	D1425027	D1425028	D1425029	D1425030	D1425031	D1425032	D1425033
Deposit		H-10	H-10	H-10	H-10	H-10	H-10	H-10	H-10	H-10	H-10	H-10
Drillhole #		H10-34A	H10-34A	H10-34A	H10-34A	H10-34A	H10-34A	H10-34A	H10-34A	H10-34A	H10-34A	H10-34A
From (m)		8.25	46.7	73.74	101	130.2	185.6	194.44	194.44	199.1	239.45	287.85
To (m)		8.4	46.85	73.9	101.16	130.38	185.75	194.64	194.64	199.26	239.6	288
Easting		-	-	-	-	-	-	-	-	-	-	-
Northing		-	-	-	-	-	-	-	-	-	-	-
Rock Type		Int.	Felsic	Felsic	Int.	Int.	Int.	Int.	Int.	Mafic	Int.	Int.
Sub-type		1	A	A	1	1	1	1	1	I	1	1
SiO <sub>2</sub> <sup>#</sup>	0.01	58.2	77	73.9	55.2	58.4	53.9	57.2	56.7	45	56.8	63.4
Al <sub>2</sub> O <sub>3</sub> <sup>#</sup>	0.01	15	12	11.6	14	14.45	14.95	15.05	14.6	13	14.95	15.1
Fe <sub>2</sub> O <sub>3</sub> <sup>#</sup>	0.01	7.71	1.63	2.56	6.96	8.1	8.56	7.47	7.21	12.75	11.1	6.62
CaO <sup>#</sup>	0.01	4.39	0.52	2.17	5.52	4.91	1.34	0.88	0.9	7.39	0.96	1.73
MgO <sup>#</sup>	0.01	4.72	1.22	1.08	6.42	4.65	10.7	9.61	9.33	8.51	8.17	2.68
Na <sub>2</sub> O <sup>#</sup>	0.01	5.68	4.97	5.52	4.34	5.11	2.9	0.45	0.61	1.79	0.03	5.71
K <sub>2</sub> O <sup>#</sup>	0.01	1.12	0.92	0.38	1.04	0.77	0.32	2.26	2.09	0.31	2.17	0.7
Cr <sub>2</sub> O <sub>3</sub> <sup>#</sup>	0.01	0.02	<0.01	0.01	0.02	0.03	0.01	0.01	0.01	0.04	0.01	<0.01
TiO <sub>2</sub> <sup>#</sup>	0.01	1.37	0.16	0.15	1.24	1.29	1.14	1.05	1.06	1.91	1.15	0.83
MnO <sup>#</sup>	0.01	0.1	0.02	0.03	0.1	0.09	0.1	0.08	0.07	0.13	0.12	0.07
P <sub>2</sub> O <sub>5</sub> <sup>#</sup>	0.01	0.36	0.01	0.02	0.31	0.34	0.28	0.26	0.26	0.29	0.29	0.18
SrO <sup>#</sup>	0.01	0.02	0.01	0.01	0.02	0.02	0.01	<0.01	<0.01	0.01	<0.01	0.02
BaO <sup>#</sup>	0.01	0.05	0.04	0.02	0.07	0.03	0.02	0.07	0.07	0.01	0.09	0.04
C <sup>@</sup>	0.01	0.07	0.09	0.36	0.7	0.32	0.06	0.02	0.01	1.5	0.01	0.22
S <sup>@</sup>	0.01	<0.01	<0.01	<0.01	<0.01	<0.01	0.07	0.02	0.04	0.7	<0.01	0.02
Ba <sup>*</sup>	0.5	430	357	158	630	268	163	694	652	89.1	794	367
Ce <sup>*</sup>	0.5	69.4	122	108	77.8	67	50.7	71.9	67.6	25.1	55.8	68.6
Cr <sup>*</sup>	10	180	40	50	170	210	100	100	90	280	90	40
Cs <sup>*</sup>	0.01	0.3	0.34	0.11	0.39	0.26	0.17	0.83	0.78	0.18	0.79	0.26
Dy <sup>*</sup>	0.05	6.41	8.61	7.18	6.46	6.33	5.22	5.63	5.63	5.19	5.5	5.8

Table A2-1 (continued): Geochemical data for the rocks of the Hood deposits

Samples	Det. Limit	D1425023	D1425024	D1425025	D1425026	D1425027	D1425028	D1425029	D1425030	D1425031	D1425032	D1425033
Er*	0.03	3.78	5.41	4.59	3.71	3.81	3.07	3.05	3.19	2.97	3.26	3.52
Eu*	0.03	1.76	1.25	1.31	2.15	1.74	1.94	2.05	2.19	1.67	1.14	1.51
Ga*	0.1	20	16.8	16.8	20.7	22	21.1	20.5	19.5	18.2	21.9	22.5
Gd*	0.05	7.3	9.09	8.08	7.32	6.49	5.65	6.85	6.79	5.34	6.02	6.26
Hf*	0.2	6.4	8.6	8.2	5.5	5.8	5	4.7	4.8	3.2	4.8	5.7
Ho*	0.01	1.29	1.75	1.49	1.25	1.26	1.04	1.1	1.11	1.04	1.11	1.19
La*	0.5	32	61.2	55.1	37.9	32.7	23.4	34.3	32.3	9.9	26.1	35.1
Lu*	0.01	0.56	0.81	0.78	0.51	0.54	0.44	0.42	0.43	0.42	0.43	0.48
Nb*	0.2	14.7	21	20.9	13	13.5	11.4	10.4	10.9	11.1	11.4	11.4
Nd*	0.1	34.3	52	46.2	36	31.4	25.7	34.5	33.1	17.4	28.7	30
Pr*	0.03	8.92	14.6	12.9	9.66	8.19	6.54	9.04	8.57	3.8	7.29	8.26
Rb*	0.2	27.3	29.5	9.6	24.5	17.9	6.3	67.5	61.8	8.1	63	17.3
Sm*	0.03	7.41	10.3	9.23	7.38	6.68	5.71	7.29	7.21	4.68	6.29	6.36
Sn*	1	3	5	2	7	6	2	3	3	11	3	3
Sr*	0.1	154.5	64	103	168	203	77.8	13.6	16.4	79.4	5.6	161
Ta*	0.1	1.1	1.7	1.7	0.9	1	0.8	0.8	0.8	0.7	0.8	1
Tb*	0.01	1.08	1.42	1.2	1.08	1.03	0.88	0.99	1	0.84	0.92	0.96
Th*	0.05	5.78	16.7	16.05	5.22	5.6	3.7	3.55	3.65	0.76	3.75	11.5
Tl*	0.5	<0.5	<0.5	<0.5	<0.5	<0.5	<0.5	0.5	0.5	<0.5	<0.5	<0.5
Tm*	0.01	0.55	0.81	0.73	0.54	0.56	0.45	0.45	0.46	0.46	0.48	0.53
U*	0.05	1.47	4.15	3.96	1.39	1.34	0.9	0.85	0.85	0.18	0.89	2.75
V*	5	180	<5	<5	170	174	176	172	167	270	179	115
W*	1	2	1	<1	2	1	2	4	3	3	3	1
Y*	0.5	36.2	49.5	42.5	34.2	35.7	29.2	30.4	31.5	27.8	30.6	33.3
Yb*	0.03	3.47	5.26	4.88	3.25	3.51	2.82	2.77	2.84	2.72	2.83	3.16
Zr*	20	270	300	290	230	240	210	190	190	130	200	230

Table A2-1 (continued): Geochemical data for the rocks of the Hood deposits

Samples	Det. Limit	D1425023	D1425024	D1425025	D1425026	D1425027	D1425028	D1425029	D1425030	D1425031	D1425032	D1425033
As <sup>^</sup>	0.1	3.8	0.8	0.2	0.1	0.4	15.8	27.8	29.1	7.9	<0.1	0.5
Bi <sup>^</sup>	0.01	0.02	0.02	0.01	0.02	0.02	0.12	0.04	0.05	0.35	0.14	0.08
Hg <sup>^</sup>	0.005	<0.005	<0.005	<0.005	<0.005	<0.005	<0.005	<0.005	<0.005	0.006	<0.005	<0.005
Sb <sup>^</sup>	0.05	0.23	0.09	0.17	0.19	0.21	0.21	0.16	0.2	0.26	0.06	0.09
Se <sup>^</sup>	0.2	0.8	1.2	1	1	0.7	0.9	0.8	1	1.5	0.7	0.7
Te <sup>^</sup>	0.01	0.01	<0.01	<0.01	<0.01	<0.01	0.01	0.01	0.01	0.02	<0.01	0.02
Ag <sup>+</sup>	0.5	<0.5	<0.5	<0.5	<0.5	<0.5	<0.5	<0.5	<0.5	<0.5	<0.5	<0.5
Cd <sup>+</sup>	0.5	<0.5	<0.5	<0.5	<0.5	<0.5	<0.5	<0.5	<0.5	<0.5	<0.5	<0.5
Co <sup>+</sup>	1	20	3	5	16	19	24	32	30	47	27	11
Cu <sup>+</sup>	1	2	<1	<1	<1	7	37	298	455	109	5	9
Mo <sup>+</sup>	1	2	1	2	<1	1	<1	1	1	2	2	2
Ni <sup>+</sup>	1	75	<1	<1	72	77	64	75	73	187	76	12
Pb <sup>+</sup>	2	4	5	<2	3	2	<2	<2	<2	20	<2	<2
Zn <sup>+</sup>	2	55	14	19	60	46	123	118	114	167	144	39
Sc <sup>+</sup>	1	17	5	5	16	17	18	18	16	28	20	13
LOI (ppm)	0.01	1.95	1.37	2.33	5.16	1.59	4.85	5.47	5.28	8.69	5.18	2.95
Total (ppm)	0.01	100.69	99.87	99.78	100.4	99.78	99.08	99.86	98.19	99.83	101.02	100.03
La <sup>CN</sup>		135.02	258.23	232.49	159.92	137.97	98.73	144.73	136.29	41.77	110.13	148.10
Yb <sup>CN</sup>		20.41	30.94	28.71	19.12	20.65	16.59	16.29	16.71	16.00	16.65	18.59
La/Yb <sup>CN</sup>		6.61	8.35	8.10	8.36	6.68	5.95	8.88	8.16	2.61	6.62	7.97
La/Sm		4.32	5.94	5.97	5.14	4.90	4.10	4.71	4.48	2.12	4.15	5.52
Zr/Yb		77.81	57.03	59.43	70.77	68.38	74.47	68.59	66.90	47.79	70.67	72.78
Zr/Hf		42.19	34.88	35.37	41.82	41.38	42.00	40.43	39.58	40.63	41.67	40.35
Zr/(TiO <sub>2</sub> *10000)		0.02	0.19	0.19	0.02	0.02	0.02	0.02	0.02	0.01	0.02	0.03
Nb/Yb		4.24	3.99	4.28	4.00	3.85	4.04	3.75	3.84	4.08	4.03	3.61
Nb/Ta		13.36	12.35	12.29	14.44	13.50	14.25	13.00	13.63	15.86	14.25	11.40
# wt%;lithium borate fusion												
@wt%; combustion furnace												
*ppm; lithium borate fusion												
+ppm; four-acid digestion												
^ppm; aqua regia digestion												
< ; below detection limit												
LOI; Loss on ignition												
CN; chondrite normalized												
- ; not analyzed												

Table A2-1 (continued): Geochemical data for the rocks of the Hood deposits

Samples	Det. Limit	D1425034	D1425035	D1425036	D1425037	D1425038	D1425039	D1425040	D1425041	D1425042	D1425043	D1425044
Deposit		H-10	H-10	H-10	H-10	H-10	H-10	H-10	H-10	H-10	H-10	H-10
Drillhole #		H10-34A	H10-34A	H10-34A	H10-34A	H10-34A	H10-34A	H10-34A	H10-34A	H10-34A	H10-34A	H10-34A
From (m)		317.55	344.6	363	387.3	399.07	422.55	451.65	485.4	518.67	540.75	566.5
To (m)		317.75	344.78	363.18	387.45	399.25	422.7	451.82	485.57	519.82	540.92	566.66
Easting		-	-	-	-	-	-	-	-	-	-	-
Northing		-	-	-	-	-	-	-	-	-	-	-
Rock Type		Felsic	Felsic	Mafic	Felsic	Int.	Mafic	Felsic	Int.	Int.	Int.	Int.
Sub-type		A	A	II	A	1	II	A	1	1	1	1
SiO <sub>2</sub> <sup>#</sup>	0.01	79.8	59.8	46.3	88.9	71.3	49.8	69.4	57.1	62.8	57.7	49.6
Al <sub>2</sub> O <sub>3</sub> <sup>#</sup>	0.01	9.51	14.2	11.95	5.09	10.5	12.2	15.85	15.1	11.7	16.1	12.4
Fe <sub>2</sub> O <sub>3</sub> <sup>#</sup>	0.01	2.15	7.59	11.85	2.4	6.01	15.3	2.15	8.46	10.05	5.94	7.62
CaO <sup>#</sup>	0.01	0.07	0.15	9.4	0.06	3.51	6.05	0.06	0.8	0.66	0.62	8.72
MgO <sup>#</sup>	0.01	2.55	9.17	8.34	2.07	2.81	7.39	2.67	8.48	8.59	7.26	7.62
Na <sub>2</sub> O <sup>#</sup>	0.01	0.33	<0.01	1.24	0.41	3.61	1.3	0.08	0.02	0.39	0.11	2.89
K <sub>2</sub> O <sup>#</sup>	0.01	2.54	2.24	0.07	0.88	0.27	0.51	4.82	2.45	0.54	3.53	0.32
Cr <sub>2</sub> O <sub>3</sub> <sup>#</sup>	0.01	<0.01	<0.01	0.12	<0.01	0.06	0.07	<0.01	0.01	0.01	0.01	0.04
TiO <sub>2</sub> <sup>#</sup>	0.01	0.12	0.18	1.21	0.07	0.66	2.16	0.21	1.47	0.91	1.6	0.82
MnO <sup>#</sup>	0.01	0.02	0.07	0.15	0.02	0.08	0.17	0.02	0.09	0.09	0.06	0.14
P <sub>2</sub> O <sub>5</sub> <sup>#</sup>	0.01	0.01	0.01	0.25	0.01	0.07	0.22	0.02	0.4	0.23	0.46	1.01
SrO <sup>#</sup>	0.01	<0.01	<0.01	0.01	<0.01	0.03	0.02	<0.01	<0.01	<0.01	<0.01	0.06
BaO <sup>#</sup>	0.01	0.08	0.05	<0.01	0.03	0.02	0.01	0.18	0.07	0.02	0.1	0.03
C <sup>@</sup>	0.01	0.01	0.04	1.79	0.05	0.23	0.54	0.01	0.01	0.02	0.02	1.49
S <sup>@</sup>	0.01	<0.01	<0.01	0.19	<0.01	0.1	0.15	<0.01	<0.01	<0.01	<0.01	0.01
Ba <sup>*</sup>	0.5	746	433	17.2	247	160	91.3	1460	566	144.5	897	218
Ce <sup>*</sup>	0.5	61.4	136	32.2	19.3	61.2	28.8	92.1	59.2	35.9	68.9	347
Cr <sup>*</sup>	10	20	10	840	30	420	490	20	50	60	60	260
Cs <sup>*</sup>	0.01	0.67	1.07	0.12	0.29	0.22	2.34	1.12	0.9	0.28	1.18	1.01
Dy <sup>*</sup>	0.05	6.54	8.53	3.9	1.94	7.76	5.93	9.62	6.5	3.41	7.41	4.99



Table A2-1 (continued): Geochemical data for the rocks of the Hood deposits

Samples	Det. Limit	D1425034	D1425035	D1425036	D1425037	D1425038	D1425039	D1425040	D1425041	D1425042	D1425043	D1425044
Er*	0.03	4.22	6.08	2.25	1.54	4.74	3.29	6.3	3.6	1.97	4.4	2.01
Eu*	0.03	0.48	1.29	1.28	0.16	1.4	1.77	0.6	1.03	0.58	1.2	4.97
Ga*	0.1	15.5	26.4	16.4	7.7	16.3	19.7	28.9	26.1	19.5	33.3	20.7
Gd*	0.05	6.27	9.1	4.27	1.64	7.82	6.36	8.91	7.36	3.83	7.63	11.5
Hf*	0.2	6.9	11	3.4	3.8	6.4	4.2	12	6.5	4	7.6	6.7
Ho*	0.01	1.35	1.86	0.81	0.47	1.61	1.2	2.08	1.3	0.72	1.54	0.85
La*	0.5	28.7	66.2	14.1	9.3	28.2	12	44.2	26.5	16.6	32.1	184.5
Lu*	0.01	0.64	1.39	0.35	0.3	0.69	0.45	1.04	0.49	0.33	0.66	0.25
Nb*	0.2	18.9	27.7	7.9	7.5	20.6	8.1	28.8	14.6	9.6	16.9	12
Nd*	0.1	28.2	61	18.3	8.6	31.8	20	42.3	31.9	18.3	35.1	146.5
Pr*	0.03	7.67	16.25	4.35	2.3	7.85	4.25	11.15	7.77	4.55	8.92	41.2
Rb*	0.2	68.4	67.2	1.4	24.5	6	28.4	128	72.2	15.6	107	15.4
Sm*	0.03	6.35	11.7	4.17	1.7	7.44	5.66	8.95	7.24	3.88	7.63	21.8
Sn*	1	3	2	1	1	2	2	7	4	2	4	2
Sr*	0.1	10.5	4.8	77.3	10.7	222	165.5	9.6	10.1	13	12.9	459
Ta*	0.1	1.5	2.1	0.5	0.7	1.5	0.6	2.3	1	0.6	1.1	0.8
Tb*	0.01	1.06	1.41	0.66	0.29	1.26	1	1.5	1.13	0.59	1.21	1.14
Th*	0.05	14.1	22.1	1.71	9.18	11.9	4.28	24.7	5.25	3.37	5.8	57.3
Tl*	0.5	<0.5	<0.5	<0.5	<0.5	<0.5	<0.5	0.5	<0.5	<0.5	0.5	<0.5
Tm*	0.01	0.64	1.1	0.34	0.26	0.69	0.48	0.97	0.5	0.3	0.65	0.28
U*	0.05	3.68	6.62	0.45	2.56	3.39	1.83	7.53	1.4	0.97	1.59	14
V*	5	6	<5	176	5	68	228	<5	199	127	211	163
W*	1	2	1	1	1	1	2	3	7	2	12	2
Y*	0.5	34.2	45.6	23.4	13.9	47.7	34.5	57.4	36.9	20.2	45.3	25
Yb*	0.03	4.05	8.24	2.21	1.82	4.66	3.06	6.61	3.27	2.08	4.23	1.69
Zr*	20	220	360	140	130	180	150	410	270	170	310	270

Table A2-1 (continued): Geochemical data for the rocks of the Hood deposits

Samples	Det. Limit	D1425034	D1425035	D1425036	D1425037	D1425038	D1425039	D1425040	D1425041	D1425042	D1425043	D1425044
As <sup>Λ</sup>	0.1	0.1	<0.1	21.1	<0.1	0.8	2.1	0.3	<0.1	0.5	0.1	1.2
Bi <sup>Λ</sup>	0.01	0.02	0.02	0.46	0.16	0.15	0.59	0.02	0.12	0.8	0.02	0.05
Hg <sup>Λ</sup>	0.005	<0.005	0.005	<0.005	<0.005	<0.005	0.005	<0.005	<0.005	<0.005	<0.005	0.005
Sb <sup>Λ</sup>	0.05	0.06	0.11	0.06	0.05	0.23	0.26	0.09	0.08	0.06	0.07	0.19
Se <sup>Λ</sup>	0.2	0.9	1	1.1	0.3	1.2	1.1	1.1	0.7	0.6	0.7	0.8
Te <sup>Λ</sup>	0.01	<0.01	0.01	0.01	0.01	0.01	0.02	<0.01	<0.01	0.25	<0.01	0.01
Ag <sup>+</sup>	0.5	<0.5	<0.5	<0.5	<0.5	<0.5	<0.5	<0.5	<0.5	<0.5	<0.5	<0.5
Cd <sup>+</sup>	0.5	<0.5	<0.5	<0.5	<0.5	<0.5	<0.5	<0.5	<0.5	<0.5	<0.5	<0.5
Co <sup>+</sup>	1	4	9	54	5	17	52	3	18	20	11	31
Cu <sup>+</sup>	1	1	2	63	33	33	37	<1	1	4	1	18
Mo <sup>+</sup>	1	2	3	1	5	1	1	6	3	6	1	2
Ni <sup>+</sup>	1	1	<1	332	3	112	197	<1	64	46	60	204
Pb <sup>+</sup>	2	<2	<2	6	<2	3	5	<2	<2	<2	<2	9
Zn <sup>+</sup>	2	23	93	99	21	49	109	12	58	55	36	60
Sc <sup>+</sup>	1	4	5	22	3	8	24	7	20	14	25	15
LOI (ppm)	0.01	2.3	5.53	10.6	1.55	2.28	5.85	3.27	5.46	5.09	5.01	9.78
Total (ppm)	0.01	99.48	98.99	101.49	101.49	101.21	101.05	98.73	99.91	101.08	98.5	101.05
La <sup>CN</sup>		121.10	279.32	59.49	39.24	118.99	50.63	186.50	111.81	70.04	135.44	778.48
Yb <sup>CN</sup>		23.82	48.47	13.00	10.71	27.41	18.00	38.88	19.24	12.24	24.88	9.94
La/Yb <sup>CN</sup>		5.08	5.76	4.58	3.67	4.34	2.81	4.80	5.81	5.72	5.44	78.31
La/Sm		4.52	5.66	3.38	5.47	3.79	2.12	4.94	3.66	4.28	4.21	8.46
Zr/Yb		54.32	43.69	63.35	71.43	38.63	49.02	62.03	82.57	81.73	73.29	159.76
Zr/Hf		31.88	32.73	41.18	34.21	28.13	35.71	34.17	41.54	42.50	40.79	40.30
Zr/(TiO <sub>2</sub> *10000)		0.18	0.20	0.01	0.19	0.03	0.01	0.20	0.02	0.02	0.02	0.03
Nb/Yb		4.67	3.36	3.57	4.12	4.42	2.65	4.36	4.46	4.62	4.00	7.10
Nb/Ta		12.60	13.19	15.80	10.71	13.73	13.50	12.52	14.60	16.00	15.36	15.00
# wt%;lithium borate fusion @wt%; combustion furnace *ppm; lithium borate fusion +ppm; four-acid digestion ^ppm; aqua regia digestion < ; below detection limit LOI; Loss on ignition CN; chondrite normalized - ; not analyzed												

Table A2-1 (continued): Geochemical data for the rocks of the Hood deposits

Samples	Det. Limit	D1425045	D1425046	D1425047	D1425048	D1425049	D1425050	D1425051	D1425052	D1425053	D1425054	D1425055
Deposit		H-10	H-10	H-10	H-10	H-462	H-462	H-462	H-462	H-462	H-462	H-462
Drillhole #		H10-34A	H10-34A	H10-34A	H10-34A	H462-015	H462-015	H462-015	H462-015	H462-015	H462-015	H462-015
From (m)		574.75	589.6	602.53	631	10.1	10.1	15.7	43.83	74.7	89.85	114.7
To (m)		575.9	589.76	602.75	631.17	10.32	10.32	15.87	44	74.86	90.03	114.85
Easting		-	-	-	-	-	-	-	-	-	-	-
Northing		-	-	-	-	-	-	-	-	-	-	-
Rock Type		Int.	Felsic	Int.	Felsic	Felsic	Felsic	Felsic	Int.	Felsic	Felsic	Mafic
Sub-type		1	A		A	C	C	B	1	B	B	II
SiO <sub>2</sub> <sup>#</sup>	0.01	56.4	85.3	54.9	74.4	73.4	73	77.8	51.5	74	75.8	51.5
Al <sub>2</sub> O <sub>3</sub> <sup>#</sup>	0.01	15.3	5.73	14.75	12.35	12.3	12.4	12.6	13.4	12.8	12.05	13.75
Fe <sub>2</sub> O <sub>3</sub> <sup>#</sup>	0.01	5.56	1.78	5.92	2.84	4.21	4.06	1.84	10.45	3.46	2.47	14.6
CaO <sup>#</sup>	0.01	0.76	0.04	0.4	0.03	0.12	0.11	0.17	2.62	0.07	0.18	2.16
MgO <sup>#</sup>	0.01	10.4	3.34	13.45	3.32	3.38	3.31	1.39	9.76	2.9	2.74	5.57
Na <sub>2</sub> O <sup>#</sup>	0.01	0.19	0.05	<0.01	0.03	0.03	0.03	0.04	<0.01	0.02	1.39	3.03
K <sub>2</sub> O <sup>#</sup>	0.01	3.86	1.1	1.44	3.23	2.88	2.93	3.85	1.34	3.48	2.7	0.15
Cr <sub>2</sub> O <sub>3</sub> <sup>#</sup>	0.01	0.01	<0.01	<0.01	<0.01	<0.01	<0.01	<0.01	0.04	<0.01	<0.01	<0.01
TiO <sub>2</sub> <sup>#</sup>	0.01	1.27	0.08	1.14	0.16	0.25	0.25	0.15	1.09	0.16	0.14	2.12
MnO <sup>#</sup>	0.01	0.05	0.02	0.05	0.02	0.03	0.02	0.02	0.09	0.02	0.02	0.13
P <sub>2</sub> O <sub>5</sub> <sup>#</sup>	0.01	0.34	0.01	0.3	0.02	0.05	0.06	0.02	0.19	0.01	<0.01	0.41
SrO <sup>#</sup>	0.01	<0.01	<0.01	<0.01	<0.01	<0.01	<0.01	<0.01	<0.01	<0.01	<0.01	0.01
BaO <sup>#</sup>	0.01	0.1	0.03	0.04	0.07	0.05	0.06	0.06	0.02	0.09	0.06	0.01
C <sup>@</sup>	0.01	0.02	0.01	0.03	0.01	0.03	0.04	0.08	1.05	0.03	0.07	0.7
S <sup>@</sup>	0.01	<0.01	<0.01	<0.01	<0.01	<0.01	<0.01	<0.01	<0.01	<0.01	<0.01	0.12
Ba <sup>*</sup>	0.5	855	275	339	608	455	475	454	177.5	735	487	45.7
Ce <sup>*</sup>	0.5	49.7	31.8	17.9	102.5	93.6	95.2	113.5	37.5	121	106.5	69.9
Cr <sup>*</sup>	10	80	30	20	20	20	20	20	280	20	20	50
Cs <sup>*</sup>	0.01	6.14	0.59	0.76	1.18	0.87	0.92	1.13	0.52	1.11	0.95	0.09
Dy <sup>*</sup>	0.05	6.9	2.27	3.46	8.83	6.03	6.24	7.33	5.61	8.31	7.06	8.5

Table A2-1 (continued): Geochemical data for the rocks of the Hood deposits

Samples	Det. Limit	D1425045	D1425046	D1425047	D1425048	D1425049	D1425050	D1425051	D1425052	D1425053	D1425054	D1425055
Er*	0.03	3.85	1.58	2.43	5.61	3.49	3.63	4.37	3.15	5.8	4.2	4.7
Eu*	0.03	1.06	0.23	0.35	0.56	1.19	1.19	1.06	1.2	1.04	0.94	2.45
Ga*	0.1	32.4	6.5	17	21	19.5	19.9	19.2	18.9	22.3	17.9	23
Gd*	0.05	7.46	2.48	3.06	8.83	6.74	6.84	8.03	5.35	8.38	7.95	10.05
Hf*	0.2	5.7	4.1	7.5	9.3	7.2	7.2	7.3	4	7.9	6.9	6.6
Ho*	0.01	1.38	0.52	0.76	1.86	1.25	1.25	1.53	1.16	1.87	1.46	1.75
La*	0.5	21.6	15.6	8.1	51.1	47.8	49.3	57.6	17.6	62.2	54.7	34.4
Lu*	0.01	0.55	0.3	0.5	0.92	0.58	0.58	0.67	0.43	1.07	0.63	0.69
Nb*	0.2	12.5	7.1	15.2	21.7	14.6	15.1	18.5	8.5	20	16.9	16.8
Nd*	0.1	27.9	14.2	9.2	46.4	39	40.1	47.2	19.5	49.9	43.8	37.6
Pr*	0.03	6.59	3.79	2.26	12.25	10.85	11.05	13.25	4.86	14.15	12.3	9.09
Rb*	0.2	153.5	31.9	42.8	91.9	81.8	83.4	106.5	41.5	94.6	75.5	1.6
Sm*	0.03	6.87	2.68	2.34	9.58	7.64	7.79	9.24	4.69	9.51	8.57	8.75
Sn*	1	2	<1	5	3	4	4	6	2	10	4	1
Sr*	0.1	26.3	5.9	6.2	7.7	3.7	3.7	4	6	4.1	14.7	72.3
Ta*	0.1	0.9	0.8	1.2	1.7	1.3	1.3	1.7	0.6	1.8	1.6	1
Tb*	0.01	1.17	0.38	0.54	1.43	1.05	1.07	1.24	0.94	1.33	1.2	1.48
Th*	0.05	4.79	9.44	12.1	19.15	18.45	18.9	24	3.33	24.4	22.6	4.4
Tl*	0.5	1.2	<0.5	<0.5	0.5	<0.5	<0.5	<0.5	<0.5	<0.5	<0.5	<0.5
Tm*	0.01	0.56	0.26	0.41	0.89	0.53	0.55	0.67	0.44	0.92	0.63	0.68
U*	0.05	1.47	2.41	3	5.51	4.72	4.89	9.18	1.07	6.71	6.24	1.01
V*	5	190	14	75	<5	11	11	<5	191	<5	5	315
W*	1	6	1	21	2	3	3	2	5	2	1	3
Y*	0.5	41.7	14.3	24.7	50.5	37.6	38.6	40.1	31.9	56.2	40.6	49.5
Yb*	0.03	3.54	1.89	2.9	5.93	3.58	3.7	4.49	2.86	6.5	4.18	4.47
Zr*	20	230	140	300	300	260	260	230	160	240	200	260

Table A2-1 (continued): Geochemical data for the rocks of the Hood deposits

Samples	Det. Limit	D1425045	D1425046	D1425047	D1425048	D1425049	D1425050	D1425051	D1425052	D1425053	D1425054	D1425055
As <sup>^</sup>	0.1	0.1	<0.1	<0.1	0.3	0.5	0.5	1.1	25.3	0.7	0.4	11.4
Bi <sup>^</sup>	0.01	0.06	0.01	0.03	0.05	0.04	0.05	0.24	0.2	0.69	0.91	0.07
Hg <sup>^</sup>	0.005	<0.005	<0.005	<0.005	<0.005	<0.005	<0.005	<0.005	<0.005	<0.005	<0.005	<0.005
Sb <sup>^</sup>	0.05	0.15	0.06	0.07	0.09	0.06	0.05	0.09	0.07	0.11	0.09	0.08
Se <sup>^</sup>	0.2	0.9	0.3	0.4	0.9	0.6	0.5	0.8	0.4	0.8	0.9	0.8
Te <sup>^</sup>	0.01	0.01	<0.01	<0.01	0.01	0.03	0.03	0.01	0.01	0.03	0.02	0.01
Ag <sup>+</sup>	0.5	<0.5	<0.5	<0.5	<0.5	<0.5	<0.5	<0.5	<0.5	<0.5	<0.5	<0.5
Cd <sup>+</sup>	0.5	<0.5	<0.5	<0.5	<0.5	<0.5	<0.5	<0.5	<0.5	<0.5	<0.5	<0.5
Co <sup>+</sup>	1	12	3	13	3	4	5	2	32	3	2	37
Cu <sup>+</sup>	1	2	2	3	<1	1	2	20	61	3	<1	62
Mo <sup>+</sup>	1	2	2	1	4	1	1	1	<1	31	5	1
Ni <sup>+</sup>	1	87	7	2	<1	1	1	<1	130	<1	<1	29
Pb <sup>+</sup>	2	<2	<2	<2	<2	<2	<2	4	<2	<2	<2	4
Zn <sup>+</sup>	2	44	13	68	21	73	74	27	213	52	48	224
Sc <sup>+</sup>	1	24	3	11	6	5	5	3	23	5	4	29
LOI (ppm)	0.01	5.11	2.29	6.83	3.07	3.18	3.33	2.58	9.01	3.01	2.97	6.24
Total (ppm)	0.01	99.35	99.77	99.22	99.54	99.88	99.56	100.52	99.51	100.02	100.52	99.68
La <sup>CN</sup>		91.14	65.82	34.18	215.61	201.69	208.02	243.04	74.26	262.45	230.80	145.15
Yb <sup>CN</sup>		20.82	11.12	17.06	34.88	21.06	21.76	26.41	16.82	38.24	24.59	26.29
La/Yb <sup>CN</sup>		4.38	5.92	2.00	6.18	9.58	9.56	9.20	4.41	6.86	9.39	5.52
La/Sm		3.14	5.82	3.46	5.33	6.26	6.33	6.23	3.75	6.54	6.38	3.93
Zr/Yb		64.97	74.07	103.45	50.59	72.63	70.27	51.22	55.94	36.92	47.85	58.17
Zr/Hf		40.35	34.15	40.00	32.26	36.11	36.11	31.51	40.00	30.38	28.99	39.39
Zr/(TiO <sub>2</sub> *10000)		0.02	0.18	0.03	0.19	0.10	0.10	0.15	0.01	0.15	0.14	0.01
Nb/Yb		3.53	3.76	5.24	3.66	4.08	4.08	4.12	2.97	3.08	4.04	3.76
Nb/Ta		13.89	8.88	12.67	12.76	11.23	11.62	10.88	14.17	11.11	10.56	16.80
# wt%;lithium borate fusion @wt%; combustion furnace *ppm; lithium borate fusion												
+ppm; four-acid digestion ^ppm; aqua regia digestion < ; below detection limit												
LOI; Loss on ignition CN; chondrite normalized - ; not analyzed												

Table A2-1 (continued): Geochemical data for the rocks of the Hood deposits

Samples	Det. Limit	D1425056	D1425057	D1425058	D1425059	D1425060	D1425061	D1425062	D1425063	D1425064	D1425065	D1425066
Deposit		H-462	H-462	H-462	H-462	H-462	H-462	H-462	H-462	H-462	H-462	H-462
Drillhole #		H462-015	H462-015	H462-015	H462-015	H462-015	H462-015	H462-015	H462-015	H462-015	H462-015	H462-015
From (m)		132.6	155.6	165.8	170.65	204.8	227.7	231	260.7	269.3	285.4	301.4
To (m)		132.77	155.77	165.96	170.81	204.95	227.85	231.16	260.86	269.47	285.56	301.55
Easting		-	-	-	-	-	-	-	-	-	-	-
Northing		-	-	-	-	-	-	-	-	-	-	-
Rock Type		Felsic	Int.	Int.	Int.	Int.	Int.	Int.	Int.	Mafic	Int.	Int.
Sub-type		A	1	1	1	1	1	1	1	III	1	1
SiO <sub>2</sub> <sup>#</sup>	0.01	73.6	64.5	63.2	49.9	60.6	53	55.8	56.4	43.9	55.9	64.4
Al <sub>2</sub> O <sub>3</sub> <sup>#</sup>	0.01	13.5	14.65	14.75	13.9	15.05	14.05	15.3	14.65	13.8	14.55	13.35
Fe <sub>2</sub> O <sub>3</sub> <sup>#</sup>	0.01	3.2	6.55	5.82	12.15	4.61	10.45	10.45	9.53	13.9	9.88	7.76
CaO <sup>#</sup>	0.01	0.18	0.92	2.07	5.77	1.59	1.11	1.24	2.98	6.94	2.2	1.82
MgO <sup>#</sup>	0.01	2.61	3.58	3.97	5.9	5.51	9	5.43	4.22	6.84	4.36	2.33
Na <sub>2</sub> O <sup>#</sup>	0.01	0.14	3.9	1.18	3.2	2.5	1.8	3.1	3.12	0.4	2.19	2.96
K <sub>2</sub> O <sup>#</sup>	0.01	4.27	2.17	3.34	0.4	2.76	1.43	1.94	2.27	4.44	2.23	1.7
Cr <sub>2</sub> O <sub>3</sub> <sup>#</sup>	0.01	<0.01	<0.01	<0.01	0.04	<0.01	0.01	<0.01	<0.01	0.04	<0.01	<0.01
TiO <sub>2</sub> <sup>#</sup>	0.01	0.18	0.79	0.78	1.39	0.85	1.2	1.67	1.39	1.87	1.41	1.03
MnO <sup>#</sup>	0.01	0.05	0.06	0.08	0.16	0.05	0.09	0.1	0.09	0.2	0.1	0.06
P <sub>2</sub> O <sub>5</sub> <sup>#</sup>	0.01	0.01	0.16	0.17	0.2	0.15	0.29	0.48	0.45	0.51	0.42	0.27
SrO <sup>#</sup>	0.01	<0.01	0.01	<0.01	0.01	<0.01	0.01	0.01	0.01	0.02	0.01	0.01
BaO <sup>#</sup>	0.01	0.06	0.04	0.03	0.01	0.04	0.07	0.06	0.06	0.19	0.06	0.02
C <sup>@</sup>	0.01	0.07	0.31	0.44	1.26	0.62	0.34	0.22	0.59	1.3	0.73	0.36
S <sup>@</sup>	0.01	0.02	0.05	<0.01	0.03	0.01	1.12	0.03	0.02	0.03	0.02	0.06
Ba <sup>*</sup>	0.5	520	367	274	120.5	314	492	503	536	1575	546	202
Ce <sup>*</sup>	0.5	131	55.4	61	32.9	58.8	52.6	70.5	61.6	58.5	77.6	97.5
Cr <sup>*</sup>	10	20	30	30	270	40	90	20	20	310	20	20
Cs <sup>*</sup>	0.01	1.75	0.68	1.41	0.16	1.26	0.41	0.59	0.7	1.37	1.11	0.86
Dy <sup>*</sup>	0.05	10.05	4.35	4.68	5.7	4.52	4.81	6.96	8.02	5.31	7.68	9.22

Table A2-1 (continued): Geochemical data for the rocks of the Hood deposits

Samples	Det. Limit	D1425056	D1425057	D1425058	D1425059	D1425060	D1425061	D1425062	D1425063	D1425064	D1425065	D1425066
Er*	0.03	5.86	2.63	2.65	3.38	2.59	2.8	4.07	4.6	2.85	4.38	5.44
Eu*	0.03	1.91	1.29	1.46	1.56	1.43	1.85	2.44	2.58	2.25	2.48	2.38
Ga*	0.1	24.2	20.3	20.9	18.3	20.4	19.7	23.5	21.6	17.7	22.1	20.8
Gd*	0.05	11.1	4.66	5.32	5.94	5.25	5.76	7.99	9	6.73	8.83	10.1
Hf*	0.2	11.9	5.7	5.8	4.7	5.3	5.6	6.5	6.9	4.3	7.1	10
Ho*	0.01	2.07	0.91	0.95	1.19	0.92	0.98	1.46	1.65	1.05	1.56	1.9
La*	0.5	64.6	28.8	31.5	15.1	31.4	27	32.7	29	28.5	37.2	47.4
Lu*	0.01	0.85	0.41	0.41	0.49	0.39	0.44	0.62	0.65	0.4	0.64	0.81
Nb*	0.2	24.9	10	10.3	8.8	9.1	10.5	21	18.3	25	19.8	24.1
Nd*	0.1	57.1	23.8	26.4	19.5	25.1	25.7	37.3	32.5	30.6	39.7	46.8
Pr*	0.03	15.5	6.44	7.08	4.49	6.76	6.46	9.19	7.93	7.5	9.85	12.05
Rb*	0.2	142	57.9	103	7.4	70	29.7	41.1	48.1	78.3	61.9	43.9
Sm*	0.03	11.1	4.83	5.34	4.99	5.13	5.37	7.99	7.92	6.49	8.45	10
Sn*	1	6	2	2	1	1	2	2	2	1	2	3
Sr*	0.1	5.6	57.6	25.8	106	23.7	39.9	87	81.3	119	59.4	48.9
Ta*	0.1	2.2	0.9	0.9	0.6	0.8	0.8	1.4	1.3	1.5	1.4	1.7
Tb*	0.01	1.69	0.74	0.81	0.94	0.77	0.82	1.18	1.38	0.93	1.3	1.57
Th*	0.05	26.6	9.83	10.7	3.88	8.19	5.34	6.18	6.56	4.04	7.57	10.2
Tl*	0.5	0.6	<0.5	<0.5	<0.5	<0.5	0.7	0.6	<0.5	0.5	<0.5	<0.5
Tm*	0.01	0.85	0.39	0.39	0.5	0.38	0.39	0.59	0.66	0.4	0.63	0.8
U*	0.05	6.82	2.84	3.13	1.13	3.87	1.3	1.89	1.93	0.59	2.08	2.97
V*	5	6	117	111	232	144	194	105	86	243	89	47
W*	1	1	1	1	1	1	1	1	1	1	1	3
Y*	0.5	60.6	27.4	27	31.9	25.6	27.6	38.2	48	29.1	43	52.6
Yb*	0.03	5.64	2.67	2.69	3.17	2.47	2.74	4	4.32	2.62	4.3	5.32
Zr*	20	380	220	230	180	210	230	260	270	160	280	390

Table A2-1 (continued): Geochemical data for the rocks of the Hood deposits

Samples	Det. Limit	D1425056	D1425057	D1425058	D1425059	D1425060	D1425061	D1425062	D1425063	D1425064	D1425065	D1425066
As <sup>^</sup>	0.1	0.8	1.8	1.3	<0.1	23	21.2	1.4	0.5	0.7	<0.1	1.3
Br <sup>^</sup>	0.01	0.08	0.05	0.05	0.28	0.02	0.08	0.05	0.03	0.01	0.01	0.06
Hg <sup>^</sup>	0.005	<0.005	<0.005	<0.005	<0.005	<0.005	<0.005	<0.005	0.005	<0.005	<0.005	<0.005
Sb <sup>^</sup>	0.05	0.19	0.1	0.14	0.05	0.12	0.24	0.1	0.12	0.47	0.15	0.12
Se <sup>^</sup>	0.2	1.3	0.5	0.5	0.6	0.4	0.7	0.8	1	0.8	0.7	0.7
Te <sup>^</sup>	0.01	<0.01	<0.01	<0.01	<0.01	<0.01	<0.01	<0.01	<0.01	<0.01	<0.01	<0.01
Ag <sup>+</sup>	0.5	<0.5	<0.5	<0.5	<0.5	<0.5	<0.5	<0.5	<0.5	<0.5	<0.5	<0.5
Cd <sup>+</sup>	0.5	<0.5	<0.5	<0.5	<0.5	<0.5	<0.5	<0.5	<0.5	<0.5	<0.5	<0.5
Co <sup>+</sup>	1	1	13	13	39	23	35	23	21	48	20	14
Cu <sup>+</sup>	1	2	3	12	66	15	55	8	41	54	89	2
Mo <sup>+</sup>	1	6	1	2	1	2	1	1	3	1	2	3
Ni <sup>+</sup>	1	<1	10	7	118	16	76	3	3	113	3	1
Pb <sup>+</sup>	2	5	<2	<2	2	<2	2	<2	<2	15	<2	<2
Zn <sup>+</sup>	2	52	105	87	215	39	193	107	82	163	86	65
Sc <sup>+</sup>	1	3	12	11	26	12	18	17	16	36	16	13
LOI (ppm)	0.01	3.15	3.67	5.13	8.28	5.53	6.02	4.75	5.22	8.74	6.05	3.72
Total (ppm)	0.01	100.95	101	100.52	101.31	99.24	98.53	100.33	100.39	101.79	99.36	99.43
La <sup>CN</sup>		272.57	121.52	132.91	63.71	132.49	113.92	137.97	122.36	120.25	156.96	200.00
Yb <sup>CN</sup>		33.18	15.71	15.82	18.65	14.53	16.12	23.53	25.41	15.41	25.29	31.29
La/Yb <sup>CN</sup>		8.22	7.74	8.40	3.42	9.12	7.07	5.86	4.82	7.80	6.21	6.39
La/Sm		5.82	5.96	5.90	3.03	6.12	5.03	4.09	3.66	4.39	4.40	4.74
Zr/Yb		67.38	82.40	85.50	56.78	85.02	83.94	65.00	62.50	61.07	65.12	73.31
Zr/Hf		31.93	38.60	39.66	38.30	39.62	41.07	40.00	39.13	37.21	39.44	39.00
Zr/(TiO <sub>2</sub> *10000)		0.21	0.03	0.03	0.01	0.02	0.02	0.02	0.02	0.01	0.02	0.04
Nb/Yb		4.41	3.75	3.83	2.78	3.68	3.83	5.25	4.24	9.54	4.60	4.53
Nb/Ta		11.32	11.11	11.44	14.67	11.38	13.13	15.00	14.08	16.67	14.14	14.18
# wt%;lithium borate fusion @wt%; combustion furnace *ppm; lithium borate fusion +ppm; four-acid digestion ^ppm; aqua regia digestion < ; below detection limit LOI; Loss on ignition CN; chondrite normalized - ; not analyzed												



Table A2-1 (continued): Geochemical data for the rocks of the Hood deposits

Samples	Det. Limit	D1425067	D1425068	R137251	R137252	R137253	R137254	R137255	R137256	R137257	R137258	R137259
Deposit		H-41-A	H-10	H-46	H-46	H-46	H-46	H-46	H-46	H-46	H-46	H-46
Drillhole #		H41A-009	H10-08	H46-012	H46-012	H46-012	H46-012	H46-012	H46-012	H46-012	H46-012	H46-012
From (m)		178.4	95.4	8.23	34.8	61.45	86.75	101	113	136.15	144.4	188
To (m)		182.7	100.5	8.38	35	61.56	86.88	101.15	113.17	136.33	144.55	188.17
Easting		-	-	-	-	-	-	-	-	-	-	-
Northing		-	-	-	-	-	-	-	-	-	-	-
Rock Type		Felsic	Felsic	Felsic	Felsic	Felsic	Felsic	Felsic	Felsic	Felsic	Int.	Felsic
Sub-type		C	A	B	B	B	B	B	B	B	5	B
SiO <sub>2</sub> <sup>#</sup>	0.01	73.1	73	76.5	78.1	80.9	80.3	75.3	47.8	68.3	46	74.5
Al <sub>2</sub> O <sub>3</sub> <sup>#</sup>	0.01	13.15	12.3	11.2	9.91	9.33	8.59	10.8	12.3	13.55	11.1	9.04
Fe <sub>2</sub> O <sub>3</sub> <sup>#</sup>	0.01	2.73	4.26	2.28	3.85	3.04	4.23	3.8	8.62	6.34	8.81	5.33
CaO <sup>#</sup>	0.01	0.87	0.05	0.02	0.01	0.01	0.01	0.01	3.85	0.02	4.97	0.01
MgO <sup>#</sup>	0.01	0.83	2.34	3.63	2.17	2.47	2.31	3.22	13.65	4.88	15.25	5.88
Na <sub>2</sub> O <sup>#</sup>	0.01	4	0.05	0.08	0.07	0.06	0.05	0.07	0.01	0.07	<0.01	0.03
K <sub>2</sub> O <sup>#</sup>	0.01	2.84	3.2	2.52	2.29	2.01	1.68	2.26	1.14	2.38	0.01	0.96
Cr <sub>2</sub> O <sub>3</sub> <sup>#</sup>	0.01	<0.01	<0.01	<0.01	<0.01	<0.01	<0.01	<0.01	0.11	<0.01	0.12	<0.01
TiO <sub>2</sub> <sup>#</sup>	0.01	0.24	0.15	0.14	0.11	0.09	0.1	0.12	0.82	0.15	0.6	0.09
MnO <sup>#</sup>	0.01	0.04	0.02	0.02	0.03	0.02	0.03	0.03	0.15	0.04	0.13	0.04
P <sub>2</sub> O <sub>5</sub> <sup>#</sup>	0.01	0.03	0.01	0.02	0.02	<0.01	0.02	<0.01	0.29	0.02	0.22	0.01
SrO <sup>#</sup>	0.01	0.01	<0.01	<0.01	<0.01	<0.01	<0.01	<0.01	<0.01	<0.01	<0.01	<0.01
BaO <sup>#</sup>	0.01	0.08	0.07	0.03	0.05	0.05	0.04	0.04	<0.01	0.04	<0.01	0.02
C <sup>@</sup>	0.01	0.19	0.02	0.01	0.01	0.01	0.01	0.01	1.52	0.01	2.05	0.01
S <sup>@</sup>	0.01	<0.01	0.11	0.19	0.65	<0.01	0.13	<0.01	0.11	<0.01	0.02	0.06
Ba <sup>*</sup>	0.5	712	616	234	427	407	305	362	17.9	360	1.8	134
Ce <sup>*</sup>	0.5	128.5	154.5	93.2	89.9	81.3	85.1	92.3	91.4	105.5	67.8	65.5
Cr <sup>*</sup>	10	30	20	20	20	20	20	20	840	20	870	20
Cs <sup>*</sup>	0.01	0.7	1.21	0.47	0.47	0.41	0.39	0.51	0.24	0.54	0.03	0.29
Dy <sup>*</sup>	0.05	3.01	9.22	4.14	3.81	3.65	3.53	4.73	3.63	4.75	2.75	3.19

Table A2-1 (continued): Geochemical data for the rocks of the Hood deposits

Samples	Det. Limit	D1425067	D1425068	R137251	R137252	R137253	R137254	R137255	R137256	R137257	R137258	R137259
Er*	0.03	1.76	5.53	2.55	2.08	2.19	2.01	2.87	1.94	2.95	1.56	1.9
Eu*	0.03	1.2	1.1	0.99	0.98	0.69	0.72	0.79	1.3	0.69	0.6	0.54
Ga*	0.1	18.6	20.8	16.1	16.1	13.8	14.4	16.7	17.2	21	13.9	15
Gd*	0.05	4.33	11.1	4.76	4.58	3.9	4.15	5.43	5.18	5.46	3.44	3.45
Hf*	0.2	6.3	8.5	5.3	4.5	4.6	4.1	5.4	4.9	6.5	3.3	4
Ho*	0.01	0.61	1.96	0.85	0.75	0.72	0.71	0.97	0.74	1	0.57	0.65
La*	0.5	77.2	74.5	51.1	48.6	43.2	46.6	49.6	45.2	56.2	30.8	34.9
Lu*	0.01	0.35	0.84	0.38	0.28	0.31	0.31	0.44	0.3	0.5	0.22	0.29
Nb*	0.2	10.3	20.3	9.8	8.6	8.2	7.8	9.9	7.1	12.4	4.5	8.5
Nd*	0.1	40.5	68.6	33.3	31.7	29.1	30.3	34.6	41.8	39.4	30.2	24.2
Pr*	0.03	12.9	18.7	9.86	9.46	8.66	8.95	9.93	10.85	11.5	8.21	7.09
Rb*	0.2	90.2	88.4	69.5	63.8	52	44.3	62.7	4.9	62	0.2	27.1
Sm*	0.03	5.79	12.9	6.04	5.53	5.04	5.06	6.14	7.09	7.05	4.92	4.31
Sn*	1	2	7	3	4	4	4	4	1	5	1	3
Sr*	0.1	91.2	5.5	7	6.7	6.2	7.8	11.9	27.3	14.7	14.7	4.3
Ta*	0.1	0.9	1.7	0.9	0.8	0.9	0.7	1	0.5	1.3	0.3	0.8
Tb*	0.01	0.57	1.59	0.73	0.71	0.6	0.61	0.82	0.68	0.8	0.47	0.55
Th*	0.05	32.7	18.8	16.75	15.7	17.1	13.8	17.6	6.52	21.9	4.76	13.65
Tl*	0.5	<0.5	0.8	1.3	2.9	0.9	0.9	1.2	<0.5	2.2	<0.5	2
Tm*	0.01	0.29	0.83	0.4	0.29	0.33	0.31	0.43	0.3	0.49	0.25	0.3
U*	0.05	6.77	5.44	4.09	3.82	3.52	3.81	4.25	1.36	5.35	1.05	3.27
V*	5	14	8	6	5	<5	5	6	183	7	153	5
W*	1	1	2	2	4	3	2	2	3	3	5	2
Y*	0.5	18.4	53	23.3	17.5	17.4	18.2	27.4	20.8	26.5	15.4	17.5
Yb*	0.03	2.06	5.48	2.56	1.89	2.07	1.91	2.71	1.91	2.97	1.39	1.89
Zr*	20	220	280	180	150	140	140	170	160	210	120	130

Table A2-1 (continued): Geochemical data for the rocks of the Hood deposits

Samples	Det. Limit	D1425067	D1425068	R137251	R137252	R137253	R137254	R137255	R137256	R137257	R137258	R137259
As <sup>^</sup>	0.1	0.3	18.1	4.4	29.8	3.5	68.4	0.4	1.6	3.4	250	78.3
Br <sup>^</sup>	0.01	0.03	0.24	0.16	2.15	0.1	0.66	0.18	0.19	0.16	1.6	2.42
Hg <sup>^</sup>	0.005	<0.005	<0.005	0.018	0.078	<0.005	0.007	0.005	0.005	<0.005	0.008	0.049
Sb <sup>^</sup>	0.05	<0.05	0.28	0.68	1.26	0.15	0.42	0.25	0.19	0.74	1.1	1.63
Se <sup>^</sup>	0.2	0.5	1.5	0.4	2	0.3	1.2	0.4	0.4	0.5	1	1.4
Te <sup>^</sup>	0.01	<0.01	0.02	<0.01	0.02	<0.01	0.08	<0.01	0.02	0.01	0.03	0.01
Ag <sup>+</sup>	0.5	<0.5	0.6	<0.5	<0.5	<0.5	<0.5	<0.5	<0.5	<0.5	0.5	0.8
Cd <sup>+</sup>	0.5	<0.5	<0.5	<0.5	<0.5	<0.5	<0.5	<0.5	<0.5	<0.5	<0.5	1.6
Co <sup>+</sup>	1	4	17	2	7	4	7	5	35	8	46	8
Cu <sup>+</sup>	1	4	1010	26	1510	36	75	22	5	43	3	242
Mo <sup>+</sup>	1	1	8	2	2	2	2	3	1	2	1	3
Ni <sup>+</sup>	1	<1	<1	<1	<1	<1	<1	<1	294	<1	424	<1
Pb <sup>+</sup>	2	5	24	2	<2	<2	2	<2	<2	<2	77	56
Zn <sup>+</sup>	2	23	68	101	94	35	83	84	289	87	157	623
Sc <sup>+</sup>	1	2	7	3	3	3	3	3	20	4	19	3
LOI (ppm)	0.01	1.86	2.87	2.94	2.57	2.28	2.19	2.8	10.85	3.76	13	3.52
Total (ppm)	0.01	99.78	98.32	99.38	99.18	100.26	99.55	98.45	99.59	99.55	100.21	99.43
La <sup>CN</sup>		325.74	314.35	215.61	205.06	182.28	196.62	209.28	190.72	237.13	129.96	147.26
Yb <sup>CN</sup>		12.12	32.24	15.06	11.12	12.18	11.24	15.94	11.24	17.47	8.18	11.12
La/Yb <sup>CN</sup>		26.88	9.75	14.32	18.44	14.97	17.50	13.13	16.97	13.57	15.89	13.25
La/Sm		13.33	5.78	8.46	8.79	8.57	9.21	8.08	6.38	7.97	6.26	8.10
Zr/Yb		106.80	51.09	70.31	79.37	67.63	73.30	62.73	83.77	70.71	86.33	68.78
Zr/Hf		34.92	32.94	33.96	33.33	30.43	34.15	31.48	32.65	32.31	36.36	32.50
Zr/(TiO <sub>2</sub> *10000)		0.09	0.19	0.13	0.14	0.16	0.14	0.14	0.02	0.14	0.02	0.14
Nb/Yb		5.00	3.70	3.83	4.55	3.96	4.08	3.65	3.72	4.18	3.24	4.50
Nb/Ta		11.44	11.94	10.89	10.75	9.11	11.14	9.90	14.20	9.54	15.00	10.63
# wt%;lithium borate fusion												
@wt%; combustion furnace												
*ppm; lithium borate fusion												
+ppm; four-acid digestion												
^ppm; aqua regia digestion												
< ; below detection limit												
LOI; Loss on ignition												
CN; chondrite normalized												
- ; not analyzed												

Table A2-1 (continued): Geochemical data for the rocks of the Hood deposits

Samples	Det. Limit	R137260	R137261	R137262	R137263	R137264	R137265	R137266	R137267	R137268	R137269	R137270
Deposit		H-46	H-46	H-46	H-46	H-46	H-46	H-46	H-46	H-46	H-46	H-46
Drillhole #		H46-012	H46-012	H46-012	H46-012	H46-012	H46-012	H46-012	H46-012	H46-012	H46-012	H46-012
From (m)		224.86	255.97	292.7	296.5	310.83	323.6	365.75	406.57	429.05	455.98	455.98
To (m)		225.03	256.1	292.87	296.66	311	323.72	365.9	406.74	429.2	456.19	456.19
Easting		-	-	-	-	-	-	-	-	-	-	-
Northing		-	-	-	-	-	-	-	-	-	-	-
Rock Type		Felsic	Felsic	Felsic	Int.	Felsic	Felsic	Felsic	Felsic	Int.	Felsic	Felsic
Sub-type		B	B	B	1	B	B	Tuff Group	Tuff Group	1	B	B
SiO <sub>2</sub> <sup>#</sup>	0.01	74.9	74.5	75	52.5	81.3	73.4	66.9	67.9	64.6	75.7	76
Al <sub>2</sub> O <sub>3</sub> <sup>#</sup>	0.01	12.8	12.5	12.4	15.5	10.85	14.55	14.75	13.95	14.3	12.5	12.4
Fe <sub>2</sub> O <sub>3</sub> <sup>#</sup>	0.01	3.12	3.08	3.29	12.7	1.97	2.18	5.88	5.58	6.6	3.41	3.02
CaO <sup>#</sup>	0.01	0.03	0.02	0.02	0.27	0.33	0.81	0.95	1.36	1.7	0.03	0.03
MgO <sup>#</sup>	0.01	2.87	2.88	2.8	8.38	0.83	1.3	2.28	1.8	2.41	2.18	1.99
Na <sub>2</sub> O <sup>#</sup>	0.01	0.08	0.06	0.05	0.03	1.9	3.19	4.53	4.81	3.05	0.07	0.06
K <sub>2</sub> O <sup>#</sup>	0.01	2.97	3.2	3.23	1.76	2.31	2.72	1.06	0.81	1.77	3.22	3.3
Cr <sub>2</sub> O <sub>3</sub> <sup>#</sup>	0.01	<0.01	<0.01	<0.01	0.02	<0.01	<0.01	<0.01	<0.01	<0.01	<0.01	<0.01
TiO <sub>2</sub> <sup>#</sup>	0.01	0.14	0.15	0.13	1.03	0.13	0.17	0.59	0.52	0.92	0.14	0.15
MnO <sup>#</sup>	0.01	0.02	0.03	0.03	0.14	0.02	0.04	0.09	0.09	0.1	0.04	0.04
P <sub>2</sub> O <sub>5</sub> <sup>#</sup>	0.01	<0.01	<0.01	0.01	0.2	0.01	0.01	0.15	0.12	0.28	<0.01	0.03
SrO <sup>#</sup>	0.01	<0.01	<0.01	<0.01	<0.01	0.01	0.01	0.01	0.01	0.01	<0.01	<0.01
BaO <sup>#</sup>	0.01	0.04	0.04	0.09	0.05	0.14	0.08	0.05	0.04	0.11	0.15	0.15
C <sup>@</sup>	0.01	0.02	<0.01	<0.01	0.01	0.07	0.17	0.17	0.26	0.31	<0.01	0.01
S <sup>@</sup>	0.01	0.09	0.02	<0.01	0.14	0.09	0.03	<0.01	0.01	<0.01	<0.01	<0.01
Ba <sup>*</sup>	0.5	313	308	720	456	1120	699	425	333	956	1215	1245
Ce <sup>*</sup>	0.5	106	104.5	114	39.2	88.3	124	83.1	82.2	76.4	120.5	109.5
Cr <sup>*</sup>	10	20	20	20	120	20	20	30	30	20	20	20
Cs <sup>*</sup>	0.01	0.61	0.85	0.89	0.64	0.72	0.77	0.33	0.25	0.57	0.95	0.94
Dy <sup>*</sup>	0.05	4.94	6.97	4.86	3.76	5.15	7.03	5.66	5.99	5.15	6.32	6.33

Table A2-1 (continued): Geochemical data for the rocks of the Hood deposits

Samples	Det. Limit	R137260	R137261	R137262	R137263	R137264	R137265	R137266	R137267	R137268	R137269	R137270
Er*	0.03	3.08	4.16	2.65	2.13	2.91	4.16	3.44	3.47	3.05	3.73	3.81
Eu*	0.03	1.2	1.19	0.9	0.66	0.9	1.35	1.92	1.92	1.72	1.01	0.95
Ga*	0.1	18.6	19.6	18.8	19.8	13.3	23.4	22.2	20.8	20.2	18.4	18.6
Gd*	0.05	5.83	7.43	6	3.75	5.69	7.86	6.53	6.38	6.03	7.07	6.78
Hf*	0.2	5.9	7	6.2	4.1	5.6	7.3	11.4	10.6	5.8	6.2	6.2
Ho*	0.01	1.05	1.42	0.95	0.75	1.03	1.46	1.19	1.25	1.04	1.29	1.26
La*	0.5	57.2	53.2	60.6	19.3	45.9	65.2	41.7	40.9	39.3	61.6	56.9
Lu*	0.01	0.5	0.64	0.38	0.32	0.43	0.59	0.54	0.55	0.44	0.57	0.57
Nb*	0.2	11.6	16	11.5	7.9	11.3	15.7	14	13.7	11.2	13.6	14.1
Nd*	0.1	39.3	42.1	41.1	18.5	33.9	47.6	36	35.6	32.5	46.4	42.2
Pr*	0.03	11.35	11.85	12.2	4.71	9.78	13.75	9.66	9.62	8.78	13.35	12.15
Rb*	0.2	75.5	90.1	84.2	46.7	61.1	72.9	26.9	19.7	45	73.7	76.4
Sm*	0.03	6.88	8.37	7.55	3.96	6.32	9.2	7.11	7.11	6.57	8.47	7.99
Sn*	1	4	6	5	8	3	5	5	4	6	5	5
Sr*	0.1	7.4	6.3	5.4	5.5	41.7	76.9	71.6	80.5	64.3	7.8	7.4
Ta*	0.1	1.2	1.5	1.2	0.6	1.1	1.5	1.1	1.1	1	1.3	1.4
Tb*	0.01	0.85	1.17	0.91	0.62	0.89	1.2	0.96	1.03	0.89	1.1	1.03
Th*	0.05	20.5	20.5	20.4	3.71	18.85	25	13.15	13.35	12.65	21.7	21.7
Tl*	0.5	3.8	7	2.9	1.5	1.2	1.2	<0.5	<0.5	<0.5	<0.5	<0.5
Tm*	0.01	0.48	0.65	0.41	0.34	0.44	0.63	0.53	0.54	0.45	0.58	0.59
U*	0.05	4.99	5.06	5.13	0.94	4.64	6.24	3.63	3.61	3.23	5.27	5.36
V*	5	7	5	6	203	6	6	36	36	83	6	7
W*	1	1	3	1	5	1	2	2	1	2	1	1
Y*	0.5	28.5	37.7	21.5	19.4	25.6	38.4	29.9	32.1	27.7	34.6	34.9
Yb*	0.03	3.05	4.12	2.51	2	2.77	3.82	3.44	3.44	2.8	3.55	3.69
Zr*	20	190	220	200	160	180	230	480	450	210	200	200

Table A2-1 (continued): Geochemical data for the rocks of the Hood deposits

Samples	Det. Limit	R137260	R137261	R137262	R137263	R137264	R137265	R137266	R137267	R137268	R137269	R137270
As <sup>^</sup>	0.1	9.1	3.1	2.7	62.2	0.6	1.5	5.2	4.4	8.3	1.5	1.9
Bi <sup>^</sup>	0.01	0.72	0.34	0.11	3.07	0.15	0.07	0.34	0.53	0.28	0.32	0.38
Hg <sup>^</sup>	0.005	0.012	0.006	<0.005	0.074	<0.005	<0.005	<0.005	<0.005	0.005	<0.005	<0.005
Sb <sup>^</sup>	0.05	0.41	0.39	0.3	0.42	0.48	0.36	0.2	0.14	0.1	0.1	0.1
Se <sup>^</sup>	0.2	0.8	1	0.5	1.2	0.7	0.9	0.3	0.6	0.5	0.6	0.6
Te <sup>^</sup>	0.01	<0.01	<0.01	<0.01	0.09	0.01	<0.01	<0.01	0.02	0.01	0.1	0.13
Ag <sup>+</sup>	0.5	<0.5	<0.5	<0.5	0.9	<0.5	<0.5	<0.5	<0.5	<0.5	<0.5	<0.5
Cd <sup>+</sup>	0.5	<0.5	<0.5	<0.5	8.1	<0.5	<0.5	<0.5	<0.5	<0.5	<0.5	<0.5
Co <sup>+</sup>	1	4	1	3	35	1	1	9	8	11	5	5
Cu <sup>+</sup>	1	245	39	4	251	21	10	1	17	42	1	1
Mo <sup>+</sup>	1	2	3	2	1	2	2	2	1	1	2	2
Ni <sup>+</sup>	1	<1	<1	<1	68	<1	<1	8	4	3	<1	<1
Pb <sup>+</sup>	2	4	6	3	14	4	<2	3	17	2	<2	2
Zn <sup>+</sup>	2	77	57	58	2040	108	41	97	73	98	58	53
Sc <sup>+</sup>	1	4	4	3	23	3	4	9	8	10	3	4
LOI (ppm)	0.01	2.82	2.9	2.83	5.47	1.61	2.58	2.69	2.76	3.51	2.7	2.55
Total (ppm)	0.01	99.79	99.36	99.88	98.05	101.41	101.04	99.93	99.75	99.36	100.14	99.72
La <sup>CN</sup>		241.35	224.47	255.70	81.43	193.67	275.11	175.95	172.57	165.82	259.92	240.08
Yb <sup>CN</sup>		17.94	24.24	14.76	11.76	16.29	22.47	20.24	20.24	16.47	20.88	21.71
La/Yb <sup>CN</sup>		13.45	9.26	17.32	6.92	11.89	12.24	8.70	8.53	10.07	12.45	11.06
La/Sm		8.31	6.36	8.03	4.87	7.26	7.09	5.86	5.75	5.98	7.27	7.12
Zr/Yb		62.30	53.40	79.68	80.00	64.98	60.21	139.53	130.81	75.00	56.34	54.20
Zr/Hf		32.20	31.43	32.26	39.02	32.14	31.51	42.11	42.45	36.21	32.26	32.26
Zr/(TiO <sub>2</sub> *10000)		0.14	0.15	0.15	0.02	0.14	0.14	0.08	0.09	0.02	0.14	0.13
Nb/Yb		3.80	3.88	4.58	3.95	4.08	4.11	4.07	3.98	4.00	3.83	3.82
Nb/Ta		9.67	10.67	9.58	13.17	10.27	10.47	12.73	12.45	11.20	10.46	10.07
# wt%;lithium borate fusion @wt%; combustion furnace *ppm; lithium borate fusion +ppm; four-acid digestion ^ppm; aqua regia digestion < ; below detection limit LOI; Loss on ignition CN; chondrite normalized - ; not analyzed												

Table A2-1 (continued): Geochemical data for the rocks of the Hood deposits

Samples	Det. Limit	R137271	R137272	R137273	R137274	R137275	R137276	R137277	R137278	R137279	R137280	R137281
Deposit		H-46	H-46	H-46	H-46	H-46	H-46	H-10	H-10	H-10	H-10	H-10
Drillhole #		H46-012	H46-012	H46-012	H46-012	H46-012	H46-012	H10-032	H10-032	H10-032	H10-032	H10-032
From (m)		464.55	497.28	520.75	525.52	350	449	7.8	40.7	63.08	88.6	127.4
To (m)		464.73	497.46	520.91	525.68	353	452	8	40.86	63.22	88.75	127.55
Easting		-	-	-	-	-	-	-	-	-	-	-
Northing		-	-	-	-	-	-	-	-	-	-	-
Rock Type		Int.	Felsic	Felsic	Int.	Felsic	Felsic	Int.	Int.	Felsic	Int.	Int.
Sub-type		1	B	B	1	Tuff Group	B	1	1	A	1	1
SiO <sub>2</sub> <sup>#</sup>	0.01	59.5	76.4	79.3	53	68.7	80.4	58.7	56.3	73.5	53.5	52.7
Al <sub>2</sub> O <sub>3</sub> <sup>#</sup>	0.01	14.45	12.3	10.2	15.35	13.6	10.35	15.05	15.15	14	15.25	14.8
Fe <sub>2</sub> O <sub>3</sub> <sup>#</sup>	0.01	10.05	3.55	3.34	12.2	6.37	2.24	8.57	7.81	1.24	6.42	7.81
CaO <sup>#</sup>	0.01	2.41	0.08	0.04	1.11	0.38	0.16	2.85	5.92	1.47	6.32	8.26
MgO <sup>#</sup>	0.01	3.57	1.41	1.84	7.08	3.33	0.99	5.57	4.16	1.39	4.62	4.95
Na <sub>2</sub> O <sup>#</sup>	0.01	2.44	0.83	0.04	0.03	3.47	3.08	4.41	4.75	4.23	4.63	2.42
K <sub>2</sub> O <sup>#</sup>	0.01	1.39	3.2	2.78	2.09	0.98	1.26	1.01	1	1.95	0.65	1.25
Cr <sub>2</sub> O <sub>3</sub> <sup>#</sup>	0.01	<0.01	<0.01	<0.01	<0.01	<0.01	<0.01	0.01	0.01	<0.01	0.01	0.01
TiO <sub>2</sub> <sup>#</sup>	0.01	1.31	0.14	0.12	1.44	0.57	0.12	1.14	1.2	0.17	1.11	1.06
MnO <sup>#</sup>	0.01	0.12	0.04	0.04	0.12	0.08	0.03	0.08	0.11	0.01	0.07	0.1
P <sub>2</sub> O <sub>5</sub> <sup>#</sup>	0.01	0.42	0.01	0.01	0.47	0.14	0.03	0.29	0.3	0.01	0.28	0.28
SrO <sup>#</sup>	0.01	0.01	<0.01	<0.01	<0.01	0.01	0.01	0.02	0.03	0.01	0.02	0.03
BaO <sup>#</sup>	0.01	0.11	0.22	0.1	0.09	0.03	0.07	0.02	0.02	0.04	0.02	0.03
C <sup>@</sup>	0.01	0.44	0.01	<0.01	0.01	0.05	0.03	0.09	0.47	0.25	0.97	0.98
S <sup>@</sup>	0.01	<0.01	0.01	<0.01	<0.01	<0.01	<0.01	0.16	0.09	0.07	0.02	0.01
Ba <sup>*</sup>	0.5	941	1830	847	743	238	576	198.5	191.5	367	117	288
Ce <sup>*</sup>	0.5	61	105	72.7	64.9	77.4	87.9	53.5	46.3	101	46.7	45.9
Cr <sup>*</sup>	10	20	20	20	20	30	40	100	90	30	90	100
Cs <sup>*</sup>	0.01	0.44	1.15	0.96	0.78	0.3	0.45	2.65	1.51	0.63	0.36	0.47
Dy <sup>*</sup>	0.05	4.85	5.2	4.67	5.43	5.83	5.22	5.54	5.38	8.61	5.24	4.93

Table A2-1 (continued): Geochemical data for the rocks of the Hood deposits

Samples	Det. Limit	R137271	R137272	R137273	R137274	R137275	R137276	R137277	R137278	R137279	R137280	R137281
Er*	0.03	2.75	2.76	2.97	3.09	3.43	2.95	3.08	3.21	5.54	2.96	2.92
Eu*	0.03	1.72	1.27	0.42	1.27	1.59	1.3	1.98	1.72	1.51	2.04	1.65
Ga*	0.1	23.1	14	14.8	24.2	20.6	14.3	18.9	20.2	21.6	17.4	18.7
Gd*	0.05	5.64	5.86	4.64	6.18	6.05	5.52	6	5.78	8.42	5.57	5.49
Hf*	0.2	4.9	6.3	5.3	5.3	10.5	5	5	5.4	10.9	4.5	4.6
Ho*	0.01	0.98	1.02	0.99	1.12	1.2	1.04	1.11	1.13	1.77	1.04	1.01
La*	0.5	29.8	54.7	37.1	31.1	38.5	46.2	24.4	20.6	49.8	21.1	20.7
Lu*	0.01	0.38	0.38	0.47	0.42	0.53	0.46	0.43	0.45	0.92	0.41	0.39
Nb*	0.2	10.3	13.3	11.2	11.5	12.8	10.9	10.9	11.7	24.5	9.9	10.3
Nd*	0.1	28.9	39.9	28	30.6	34.3	34.1	27.5	24.1	44.3	23.8	24
Pr*	0.03	7.43	11.5	8.1	7.87	9.02	9.72	6.82	5.99	12	5.99	5.94
Rb*	0.2	33.5	74.9	64.1	47	25.6	29.9	43.3	31.3	66.3	18.8	37.6
Sm*	0.03	6.18	7.56	5.45	6.69	6.8	6.37	6.29	5.65	9.28	5.58	5.54
Sn*	1	10	8	4	6	4	3	3	11	8	8	5
Sr*	0.1	60.5	16.5	5	8.3	53	49.3	173.5	242	92.4	136.5	242
Ta*	0.1	0.9	1.3	1.1	0.9	1	1.1	0.7	0.9	2	0.7	0.7
Tb*	0.01	0.83	0.93	0.74	0.93	0.97	0.87	0.93	0.9	1.36	0.87	0.82
Th*	0.05	7.97	21.4	17.85	8.53	12.25	17.7	4.18	4.42	21.9	3.78	3.83
Tl*	0.5	<0.5	<0.5	<0.5	<0.5	<0.5	<0.5	<0.5	<0.5	0.5	<0.5	<0.5
Tm*	0.01	0.4	0.41	0.46	0.45	0.52	0.48	0.46	0.47	0.85	0.42	0.43
U*	0.05	2.21	4.96	4.24	2.33	3.25	4.95	1.05	1.12	5.43	1.02	1
V*	5	121	<5	9	132	40	8	174	184	15	162	167
W*	1	1	1	1	4	2	1	1	1	1	2	1
Y*	0.5	25.3	24.2	26.6	29.2	31.3	27.2	29.2	28.3	48.3	26.9	25.6
Yb*	0.03	2.42	2.51	2.94	2.71	3.25	3	2.78	2.93	5.66	2.6	2.52
Zr*	20	190	200	170	200	440	160	200	210	350	180	190



Table A2-1 (continued): Geochemical data for the rocks of the Hood deposits

Samples	Det. Limit	R137271	R137272	R137273	R137274	R137275	R137276	R137277	R137278	R137279	R137280	R137281
As <sup>^</sup>	0.1	10.5	50.6	3.4	15.2	7.1	2.9	2.5	2.1	1.5	<0.1	2.5
Bi <sup>^</sup>	0.01	0.12	0.35	0.31	0.33	0.09	0.3	0.05	0.08	0.24	0.06	0.06
Hg <sup>^</sup>	0.005	<0.005	<0.005	<0.005	<0.005	<0.005	<0.005	<0.005	0.005	<0.005	<0.005	0.005
Sb <sup>^</sup>	0.05	0.09	0.13	0.07	0.06	0.19	0.1	0.22	0.23	0.14	0.1	0.18
Se <sup>^</sup>	0.2	0.5	0.7	0.6	0.3	0.4	0.6	0.9	0.7	1.1	0.7	0.6
Te <sup>^</sup>	0.01	0.02	0.08	0.07	0.07	0.01	0.07	0.02	0.01	0.01	<0.01	0.01
Ag <sup>+</sup>	0.5	<0.5	<0.5	<0.5	<0.5	<0.5	<0.5	<0.5	<0.5	<0.5	<0.5	<0.5
Cd <sup>+</sup>	0.5	<0.5	<0.5	<0.5	<0.5	<0.5	<0.5	<0.5	<0.5	<0.5	<0.5	<0.5
Co <sup>+</sup>	1	15	5	5	24	10	3	29	23	4	17	21
Cu <sup>+</sup>	1	3	2	1	3	<1	7	71	1	69	4	18
Mo <sup>+</sup>	1	1	1	3	2	1	6	1	1	7	1	2
Ni <sup>+</sup>	1	2	<1	<1	1	6	7	69	68	5	70	70
Pb <sup>+</sup>	2	<2	<2	<2	<2	<2	7	3	7	18	8	4
Zn <sup>+</sup>	2	92	36	28	99	87	48	55	47	21	42	61
Sc <sup>+</sup>	1	13	3	3	15	9	3	17	19	5	18	17
LOI (ppm)	0.01	4.81	2.23	2.39	5.13	2.82	1.4	3.22	3.83	2.42	6.14	6.47
Total (ppm)	0.01	100.59	100.41	100.2	98.11	100.48	100.14	100.94	100.59	100.44	99.04	100.17
La <sup>CN</sup>		125.74	230.80	156.54	131.22	162.45	194.94	102.95	86.92	210.13	89.03	87.34
Yb <sup>CN</sup>		14.24	14.76	17.29	15.94	19.12	17.65	16.35	17.24	33.29	15.29	14.82
La/Yb <sup>CN</sup>		8.83	15.63	9.05	8.23	8.50	11.05	6.30	5.04	6.31	5.82	5.89
La/Sm		4.82	7.24	6.81	4.65	5.66	7.25	3.88	3.65	5.37	3.78	3.74
Zr/Yb		78.51	79.68	57.82	73.80	135.38	53.33	71.94	71.67	61.84	69.23	75.40
Zr/Hf		38.78	31.75	32.08	37.74	41.90	32.00	40.00	38.89	32.11	40.00	41.30
Zr/(TiO <sub>2</sub> *10000)		0.01	0.14	0.14	0.01	0.08	0.13	0.02	0.02	0.21	0.02	0.02
Nb/Yb		4.26	5.30	3.81	4.24	3.94	3.63	3.92	3.99	4.33	3.81	4.09
Nb/Ta		11.44	10.23	10.18	12.78	12.80	9.91	15.57	13.00	12.25	14.14	14.71
# wt%;lithium borate fusion												
@wt%; combustion furnace												
*ppm; lithium borate fusion												
+ppm; four-acid digestion												
^ppm; aqua regia digestion												
< ; below detection limit												
LOI; Loss on ignition												
CN; chondrite normalized												
- ; not analyzed												

Table A2-1 (continued): Geochemical data for the rocks of the Hood deposits

Samples	Det. Limit	R137282	R137283	R137284	R137285	R137286	R137287	R137288	R137289	R137290	R137291	R137292
Deposit		H-10	H-10	H-10	H-10	H-10	H-10	H-10	H-10	H-10	H-10	H-10
Drillhole #		H10-032	H10-032	H10-032	H10-032	H10-032	H10-032	H10-032	H10-032	H10-032	H10-032	H10-032
From (m)		150.75	176.5	198.7	239.35	285.5	338	369.05	427.35	427.35	430.3	459.97
To (m)		150.9	176.68	198.88	239.52	285.65	338.15	369.22	427.6	427.6	430.45	460.14
Easting		-	-	-	-	-	-	-	-	-	-	-
Northing		-	-	-	-	-	-	-	-	-	-	-
Rock Type		Int.	Felsic	Int.	Int.	Int.	Felsic	Mafic	Felsic	Felsic	Int.	Int.
Sub-type		1	C	1	1	1	A	I	A	A	3	3
SiO <sub>2</sub> <sup>#</sup>	0.01	49.8	72.5	52.6	51.7	52.3	83.1	44.4	81.9	80.6	49.7	52.2
Al <sub>2</sub> O <sub>3</sub> <sup>#</sup>	0.01	14.65	14.35	14.95	15.25	15.6	6.87	11.6	6.58	7.45	14.8	15.55
Fe <sub>2</sub> O <sub>3</sub> <sup>#</sup>	0.01	13.3	1.83	8.32	11.9	11	1.58	13.8	2.27	2.3	3.02	7.42
CaO <sup>#</sup>	0.01	0.8	0.28	3.16	0.67	0.64	0.3	8.23	0.46	0.57	6.38	4.92
MgO <sup>#</sup>	0.01	10.75	1.8	8.21	9.93	8.62	2.4	8.15	2.84	2.99	6.8	6.59
Na <sub>2</sub> O <sup>#</sup>	0.01	0.02	1.25	3.7	0.05	1.47	1.38	0.8	0.28	0.37	2.74	3.48
K <sub>2</sub> O <sup>#</sup>	0.01	1.03	3.94	0.28	1.63	1.28	1.06	0.14	1.38	1.62	3.22	1.05
Cr <sub>2</sub> O <sub>3</sub> <sup>#</sup>	0.01	0.01	<0.01	0.01	0.01	<0.01	<0.01	0.08	<0.01	<0.01	0.01	0.01
TiO <sub>2</sub> <sup>#</sup>	0.01	1.28	0.27	1.34	1.24	1.45	0.08	2.36	0.08	0.1	1.22	1.29
MnO <sup>#</sup>	0.01	0.16	0.02	0.11	0.13	0.08	0.02	0.23	0.02	0.02	0.1	0.06
P <sub>2</sub> O <sub>5</sub> <sup>#</sup>	0.01	0.34	0.04	0.35	0.31	0.27	<0.01	0.19	0.1	0.12	0.17	0.18
SrO <sup>#</sup>	0.01	<0.01	<0.01	0.01	<0.01	<0.01	<0.01	0.01	<0.01	<0.01	0.01	0.01
BaO <sup>#</sup>	0.01	0.02	0.1	0.01	0.05	0.03	0.02	<0.01	0.03	0.03	0.05	0.02
C <sup>@</sup>	0.01	0.01	0.07	0.43	0.07	0.08	0.13	1.77	0.14	0.19	2.66	1.08
S <sup>@</sup>	0.01	<0.01	<0.01	0.04	<0.01	<0.01	<0.01	0.04	<0.01	<0.01	<0.01	<0.01
Ba <sup>*</sup>	0.5	204	873	92.2	381	270	201	26.4	263	298	448	174.5
Ce <sup>*</sup>	0.5	56.7	160	56.7	52.8	58.1	40.4	22.1	22.6	21.4	71.9	57.9
Cr <sup>*</sup>	10	100	20	120	100	20	40	580	40	20	60	50
Cs <sup>*</sup>	0.01	0.62	1.15	0.34	0.9	0.87	0.66	0.98	0.91	1.01	2.28	0.63
Dy <sup>*</sup>	0.05	5.5	11.55	5.79	5.58	6.3	2.76	6.23	3.48	3.9	13.15	7.1

Table A2-1 (continued): Geochemical data for the rocks of the Hood deposits

Samples	Det. Limit	R137282	R137283	R137284	R137285	R137286	R137287	R137288	R137289	R137290	R137291	R137292
Er*	0.03	3.14	6.52	3.33	3.17	3.48	1.91	3.31	2.05	2.34	7.04	3.82
Eu*	0.03	0.68	1.58	1.88	1.08	0.99	0.24	1.42	0.33	0.35	1.69	1.47
Ga*	0.1	20.7	20.5	19.9	20.9	25	8.7	21.1	12.1	12.7	21.4	22.9
Gd*	0.05	6.05	13.4	6.29	5.98	6.58	3.12	6.78	3.66	3.79	13.85	8.29
Hf*	0.2	5.4	9.9	4.7	5	5.9	4.9	3.7	4.5	5.6	3.7	4.4
Ho*	0.01	1.11	2.31	1.18	1.12	1.31	0.63	1.25	0.73	0.83	2.57	1.42
La*	0.5	25.4	82.4	25.9	23.7	29.6	19.7	7.7	10.5	10	21.9	25.3
Lu*	0.01	0.44	0.95	0.47	0.44	0.54	0.37	0.44	0.38	0.45	0.84	0.53
Nb*	0.2	12.4	22.1	11.8	11.8	16	11.2	6.7	12.1	13.8	8.3	9.2
Nd*	0.1	29.9	70.8	29	28.1	27.2	18.1	18.2	11.6	11.1	44.1	31.1
Pr*	0.03	7.26	18.95	7.23	6.85	6.7	4.73	3.54	2.78	2.69	10.55	7.42
Rb*	0.2	35.4	107.5	7.5	49.5	44.6	34.7	7.4	45.2	51.6	109	37.4
Sm*	0.03	6.61	15.35	6.57	6.52	5.94	3.46	5.3	3.01	2.96	11.6	7.19
Sn*	1	2	7	4	2	3	1	2	2	2	11	9
Sr*	0.1	4.4	29.1	108.5	6.2	25.5	33	114	11.8	13.4	99.1	113.5
Ta*	0.1	0.9	1.9	0.8	0.8	1	0.8	0.4	1	1.2	0.5	0.7
Tb*	0.01	0.94	2.01	0.98	0.95	1.13	0.47	1.11	0.61	0.69	2.29	1.27
Th*	0.05	4.09	21.2	3.53	3.8	9.04	10.65	0.66	10.1	12.35	3.76	4.94
Tl*	0.5	<0.5	<0.5	<0.5	<0.5	<0.5	<0.5	<0.5	<0.5	<0.5	0.5	<0.5
Tm*	0.01	0.47	0.95	0.49	0.46	0.5	0.31	0.46	0.31	0.39	1.01	0.57
U*	0.05	1.07	4.48	0.88	1.04	2.48	2.56	0.27	3.46	4.07	2.48	1.49
V*	5	201	34	206	199	244	7	317	6	7	285	291
W*	1	2	5	1	2	8	1	1	1	1	3	2
Y*	0.5	28.8	65.4	30.4	29.7	35.9	17.9	34.2	19.3	21	63.6	36.4
Yb*	0.03	2.82	5.97	2.89	2.81	3.15	2.11	2.97	2.33	2.57	5.79	3.52
Zr*	20	220	330	190	200	240	180	140	170	200	150	180

Table A2-1 (continued): Geochemical data for the rocks of the Hood deposits

Samples	Det. Limit	R137282	R137283	R137284	R137285	R137286	R137287	R137288	R137289	R137290	R137291	R137292
As <sup>Λ</sup>	0.1	<0.1	<0.1	3.3	6.7	0.1	0.2	2.1	2.5	2.8	11.2	23.7
Br <sup>Λ</sup>	0.01	0.19	0.12	1.47	0.01	0.02	0.03	0.11	0.02	0.02	0.01	0.15
Hg <sup>Λ</sup>	0.005	0.005	<0.005	<0.005	<0.005	<0.005	<0.005	0.007	<0.005	<0.005	<0.005	<0.005
Sb <sup>Λ</sup>	0.05	0.05	0.09	0.19	0.12	0.12	0.13	0.22	0.24	0.23	0.22	0.08
Se <sup>Λ</sup>	0.2	0.5	0.9	1.8	0.5	0.5	0.2	0.8	0.4	0.4	0.7	0.3
Te <sup>Λ</sup>	0.01	<0.01	0.01	0.09	0.01	<0.01	<0.01	0.01	<0.01	0.01	<0.01	0.01
Ag <sup>+</sup>	0.5	<0.5	<0.5	0.6	<0.5	<0.5	<0.5	<0.5	<0.5	<0.5	<0.5	<0.5
Cd <sup>+</sup>	0.5	<0.5	<0.5	<0.5	<0.5	<0.5	<0.5	<0.5	<0.5	<0.5	<0.5	<0.5
Co <sup>+</sup>	1	32	3	25	30	22	4	41	4	5	9	21
Cu <sup>+</sup>	1	4	1	479	2	<1	1	15	<1	<1	<1	<1
Mo <sup>+</sup>	1	1	2	2	<1	1	2	<1	14	11	<1	<1
Ni <sup>+</sup>	1	62	2	70	69	6	4	211	4	4	28	31
Pb <sup>+</sup>	2	<2	<2	13	7	2	8	<2	4	5	<2	16
Zn <sup>+</sup>	2	145	15	83	91	92	21	126	22	22	21	51
Sc <sup>+</sup>	1	18	8	21	19	17	3	24	2	3	24	24
LOI (ppm)	0.01	6.17	2.74	5.76	6.41	5.61	2.16	10.95	2.54	2.83	12.3	7.8
Total (ppm)	0.01	98.33	99.12	98.81	99.28	98.35	98.97	100.94	98.48	99	100.52	100.58
La <sup>CN</sup>		107.17	347.68	109.28	100.00	124.89	83.12	32.49	44.30	42.19	92.41	106.75
Yb <sup>CN</sup>		16.59	35.12	17.00	16.53	18.53	12.41	17.47	13.71	15.12	34.06	20.71
La/Yb <sup>CN</sup>		6.46	9.90	6.43	6.05	6.74	6.70	1.86	3.23	2.79	2.71	5.16
La/Sm		3.84	5.37	3.94	3.63	4.98	5.69	1.45	3.49	3.38	1.89	3.52
Zr/Yb		78.01	55.28	65.74	71.17	76.19	85.31	47.14	72.96	77.82	25.91	51.14
Zr/Hf		40.74	33.33	40.43	40.00	40.68	36.73	37.84	37.78	35.71	40.54	40.91
Zr/(TiO <sub>2</sub> *10000)		0.02	0.12	0.01	0.02	0.02	0.23	0.01	0.21	0.20	0.01	0.01
Nb/Yb		4.40	3.70	4.08	4.20	5.08	5.31	2.26	5.19	5.37	1.43	2.61
Nb/Ta		13.78	11.63	14.75	14.75	16.00	14.00	16.75	12.10	11.50	16.60	13.14
# wt%;lithium borate fusion												
@wt%; combustion furnace												
*ppm; lithium borate fusion												
+ppm; four-acid digestion												
^ppm; aqua regia digestion												
< ; below detection limit												
LOI; Loss on ignition												
CN; chondrite normalized												
- ; not analyzed												

Table A2-1 (continued): Geochemical data for the rocks of the Hood deposits

Samples	Det. Limit	R137293	R137294	R137295	R137296	R137297	R137298	R137299	R137300	D1411601	D1411602	D1411603	D1411604
Deposit		H-10	H-10	H-461	H-461	H-461	H-461	H-461	H-461	H-41-A	H-41-A	H-41-A	H-41-A
Drillhole #		H10-032	H10-032	H461-010	H461-010	H461-010	H461-010	H461-010	H461-010	H-41-A-01	H-41-A-01	H-41-A-01	H-41-A-01
From (m)		503.7	516.1	16.75	46.16	82.55	114.85	120.63	140.6	14.1	22.9	45.9	75.1
To (m)		503.85	516.26	16.9	46.32	82.69	115	120.82	140.76	14.3	23	46.2	75.2
Easting		-	-	-	-	-	-	-	-	-	-	-	-
Northing		-	-	-	-	-	-	-	-	-	-	-	-
Rock Type		Int.	Felsic	Felsic	Felsic	Felsic	Felsic	Int.	Int.	Mafic	Mafic	Felsic	Mafic
Sub-type		3	A	A	A	A	A	1	3	IV	I	Rim Granite	II
SiO <sub>2</sub> <sup>#</sup>	0.01	55.6	79.1	77.7	78.1	78.4	75.5	45.6	49.5	52.9	54.1	79.1	54.3
Al <sub>2</sub> O <sub>3</sub> <sup>#</sup>	0.01	14.55	10.95	11.95	10.55	11.1	11.25	18.1	16.75	13.65	14.8	12.35	14.85
Fe <sub>2</sub> O <sub>3</sub> <sup>#</sup>	0.01	12.15	1.24	1.18	1.4	1.98	1.98	7.41	9.85	11	12.9	0.68	11.95
CaO <sup>#</sup>	0.01	2.29	0.35	0.39	0.53	0.27	0.62	2.26	3.87	7.12	7.62	0.59	3.54
MgO <sup>#</sup>	0.01	4.37	0.61	0.82	1.28	1.59	2.57	12.05	6.26	3.25	3.16	0.18	5.49
Na <sub>2</sub> O <sup>#</sup>	0.01	2.27	5.41	5.5	3	4	1.04	1.46	3.24	2.56	2.73	4.73	2.17
K <sub>2</sub> O <sup>#</sup>	0.01	1.47	0.53	0.75	1.62	0.99	2.62	2.15	1.21	0.64	0.66	2.86	1.26
Cr <sub>2</sub> O <sub>3</sub> <sup>#</sup>	0.01	<0.01	<0.01	<0.01	<0.01	<0.01	<0.01	0.01	0.01	0.01	<0.01	<0.01	0.03
TiO <sub>2</sub> <sup>#</sup>	0.01	1.65	0.13	0.17	0.17	0.14	0.14	1.4	1.2	1.76	1.86	0.05	1.69
MnO <sup>#</sup>	0.01	0.17	0.01	0.02	0.02	0.02	0.02	0.07	0.11	0.14	0.2	0.01	0.13
P <sub>2</sub> O <sub>5</sub> <sup>#</sup>	0.01	0.43	<0.01	<0.01	<0.01	<0.01	<0.01	0.37	0.31	0.1	0.41	<0.01	0.18
SrO <sup>#</sup>	0.01	0.01	0.01	0.01	<0.01	0.01	<0.01	0.01	0.01	0.02	0.02	0.01	0.01
BaO <sup>#</sup>	0.01	0.03	0.02	0.01	0.02	0.02	0.05	0.05	0.04	0.02	0.02	0.06	0.03
C <sup>@</sup>	0.01	0.41	0.07	0.1	0.22	0.09	0.29	0.82	0.94	0.77	0.1	0.04	0.15
S <sup>@</sup>	0.01	<0.01	<0.01	<0.01	<0.01	<0.01	<0.01	<0.01	<0.01	0.13	0.12	0.02	0.07
Ba <sup>*</sup>	0.5	277	137.5	121	215	128.5	435	446	325	169.5	196.5	537	269
Ce <sup>*</sup>	0.5	80.6	149.5	282	209	416	133.5	66.9	52	21.1	47.3	27.9	26.6
Cr <sup>*</sup>	10	30	20	30	20	30	20	100	110	60	<10	10	240
Cs <sup>*</sup>	0.01	0.93	0.32	0.38	0.79	0.52	1.48	1.66	0.7	0.36	0.43	0.49	0.45
Dy <sup>*</sup>	0.05	7.03	12.75	15.3	8.86	13.5	12.55	8.17	5.98	2.77	5.96	4.01	4.22

Table A2-1 (continued): Geochemical data for the rocks of the Hood deposits

Samples	Det. Limit	R137293	R137294	R137295	R137296	R137297	R137298	R137299	R137300	D1411601	D1411602	D1411603	D1411604
Er*	0.03	4.36	7.14	9.39	5.24	6.82	7.52	4.25	3.31	1.34	3.4	2.83	3.04
Eu*	0.03	2.88	2.15	3.41	2.16	3.06	1.52	1.67	2.51	1.23	2.06	0.4	1.28
Ga*	0.1	25.4	20.6	24.1	24.6	21.5	24	30.1	23.1	20.4	22	14.4	21.5
Gd*	0.05	9.31	14.2	20.7	11.85	20.3	13.75	9.79	7.35	3.49	6.98	3.25	3.87
Hf*	0.2	6.8	9.9	12.3	10.6	10.2	10.4	5.7	5	2.6	5.6	3.5	3.6
Ho*	0.01	1.48	2.57	3.31	1.84	2.48	2.61	1.64	1.21	0.53	1.2	0.88	0.95
La*	0.5	37	74.6	149	108.5	241	65.5	33.5	24.8	9.8	20.3	14.2	12.4
Lu*	0.01	0.61	1.15	1.33	0.95	1.03	1.15	0.64	0.48	0.16	0.54	0.54	0.53
Nb*	0.2	18.7	37.5	36.5	36.7	42.8	35.3	15.4	12.8	4.8	13.9	11.1	9.6
Nd*	0.1	39.9	66.5	123.5	74.6	145.5	57.7	31.4	26.5	12.8	28.1	10.7	14.4
Pr*	0.03	9.87	17.25	33.9	21.9	45.2	15.7	7.88	6.59	2.75	6.28	2.92	3.31
Rb*	0.2	53.1	19.3	25.2	60.5	35	90.9	78.6	39.3	26.1	24.5	64.3	44.1
Sm*	0.03	8.67	13.1	23.3	13.4	23.9	12.1	7.19	5.85	3.32	6.69	2.76	3.46
Sn*	1	3	3	6	12	9	4	7	3	1	2	1	8
Sr*	0.1	79.9	89.6	66.3	29.1	44.3	17	35	74.7	166.5	155	47.9	98.3
Ta*	0.1	1.1	2.4	2.5	2.3	2.5	2.4	0.9	0.8	0.3	1	2.1	0.7
Tb*	0.01	1.37	2.15	2.81	1.74	2.64	2.25	1.47	1.12	0.5	1.02	0.6	0.63
Th*	0.05	5.09	20.3	19.8	18.55	21.7	19.25	4.08	3.69	1.45	1.37	22.3	3.21
Tl*	0.5	<0.5	<0.5	<0.5	<0.5	<0.5	<0.5	<0.5	<0.5	<0.5	<0.5	<0.5	<0.5
Tm*	0.01	0.63	1.14	1.41	0.83	1.02	1.14	0.62	0.48	0.19	0.52	0.48	0.52
U*	0.05	1.24	4.63	3.98	4.24	4.71	5.27	1.49	0.91	0.3	0.6	14.45	1.35
V*	5	255	<5	<5	6	6	<5	228	195	176	285	<5	230
W*	1	1	1	2	3	2	2	5	1	2	2	1	4
Y*	0.5	42.5	74.4	91	47.5	63.8	76.2	44.2	31.5	14.1	33	25.7	25.9
Yb*	0.03	4.02	7.31	8.7	5.46	6.5	7.46	4.02	3.03	1.1	3.22	3.26	3.38
Zr*	20	330	330	420	370	330	340	260	240	89	226	69	131

Table A2-1 (continued): Geochemical data for the rocks of the Hood deposits

Samples	Det. Limit	R137293	R137294	R137295	R137296	R137297	R137298	R137299	R137300	D1411601	D1411602	D1411603	D1411604
As <sup>^</sup>	0.1	0.4	0.3	0.1	0.3	0.4	0.2	<0.1	<0.1	18.3	0.2	2.8	4.9
Bi <sup>^</sup>	0.01	0.05	0.02	0.06	0.56	0.16	0.14	0.01	0.02	0.19	0.06	0.04	0.2
Hg <sup>^</sup>	0.005	0.007	<0.005	<0.005	<0.005	<0.005	<0.005	0.005	0.005	0.007	<0.005	<0.005	0.005
Sb <sup>^</sup>	0.05	0.15	0.1	0.14	0.11	0.11	0.21	0.08	0.06	0.09	0.11	0.08	0.16
Se <sup>^</sup>	0.2	1.1	1.2	1.1	0.8	1.3	1.3	0.6	0.4	0.4	0.6	0.5	0.3
Te <sup>^</sup>	0.01	0.01	<0.01	<0.01	0.01	0.01	0.04	<0.01	<0.01	0.01	0.01	<0.01	0.02
Ag <sup>+</sup>	0.5	<0.5	<0.5	<0.5	<0.5	<0.5	<0.5	<0.5	<0.5	<0.5	<0.5	<0.5	<0.5
Cd <sup>+</sup>	0.5	<0.5	<0.5	<0.5	<0.5	<0.5	<0.5	<0.5	<0.5	<0.5	<0.5	<0.5	<0.5
Co <sup>+</sup>	1	30	1	1	1	2	2	12	28	35	27	3	33
Cu <sup>+</sup>	1	<1	1	8	2	<1	<1	<1	<1	60	71	22	11
Mo <sup>+</sup>	1	<1	1	<1	<1	<1	2	<1	<1	<1	1	1	<1
Ni <sup>+</sup>	1	33	<1	<1	<1	1	<1	67	84	55	5	<1	62
Pb <sup>+</sup>	2	<2	5	4	7	<2	5	<2	<2	12	10	7	26
Zn <sup>+</sup>	2	51	17	17	24	31	49	45	55	182	137	7	163
Sc <sup>+</sup>	1	21	2	3	2	3	2	19	18	-	-	-	-
LOI (ppm)	0.01	5.07	1.03	1.36	2.17	1.85	3.39	9.27	7.5	5.96	2.8	0.9	4.94
Total (ppm)	0.01	100.06	99.39	99.86	98.86	100.37	99.18	100.21	99.86	99.1	101.5	101.5	100.5
La <sup>CN</sup>		156.12	314.77	628.69	457.81	1016.88	276.37	141.35	104.64	41.35	85.65	59.92	52.32
Yb <sup>CN</sup>		23.65	43.00	51.18	32.12	38.24	43.88	23.65	17.82	6.47	18.94	19.18	19.88
La/Yb <sup>CN</sup>		6.60	7.32	12.28	14.25	26.60	6.30	5.98	5.87	6.39	4.52	3.12	2.63
La/Sm		4.27	5.69	6.39	8.10	10.08	5.41	4.66	4.24	2.95	3.03	5.14	3.58
Zr/Yb		82.09	45.14	48.28	67.77	50.77	45.58	64.68	79.21	80.91	70.19	21.17	38.76
Zr/Hf		48.53	33.33	34.15	34.91	32.35	32.69	45.61	48.00	34.23	40.36	19.71	36.39
Zr/(TiO <sub>2</sub> *10000)		0.02	0.25	0.25	0.22	0.24	0.24	0.02	0.02	0.01	0.01	0.14	0.01
Nb/Yb		4.65	5.13	4.20	6.72	6.58	4.73	3.83	4.22	4.36	4.32	3.40	2.84
Nb/Ta		17.00	15.63	14.60	15.96	17.12	14.71	17.11	16.00	16.00	13.90	5.29	13.71
# wt%; lithium borate fusion @wt%; combustion furnace *ppm; lithium borate fusion													# wt%; lithium @wt%; combustion furnace *ppm; lithium
+ppm; four-acid digestion ^ppm; aqua regia digestion < ; below detection limit													LOI; Loss on ignition CN; chondrite normalized - ; not analyzed

Table A2-1 (continued): Geochemical data for the rocks of the Hood deposits

Samples	Det. Limit	D1411605	D1411606	D1411607	D1411608	D1411609	D1411610	D1411611	D1411612	D1411613	D1411614
Deposit		H-41-A	H-41-A	H-41-A	H-41-A	H-41-A	H-41-A	H-41-A	H-41-A	H-41-A	H-41-A
Drillhole #		H-41-A-01	H-41-A-01	H-41-A-01	H-41-A-01	H-41-A-01	H-41-A-01	H-41-A-01	H-41-A-02	H-41-A-02	H-41-A-02
From (m)		98.6	133.6	137.3	156	191.1	206.76	216.95	8.2	16.29	43.3
To (m)		98.8	133.8	137.4	156.1	191.2	206.93	217.1	8.35	16.46	43.48
Easting		-	-	-	-	-	-	-	-	-	-
Northing		-	-	-	-	-	-	-	-	-	-
Rock Type		Int.	Int.	Mafic	Int.	Mafic	Felsic	Mafic	Mafic	Mafic	Mafic
Sub-type		1	1	II	2	II	A	II	II	IV	II
SiO <sub>2</sub> <sup>#</sup>	0.01	54.1	64.9	51.4	50.7	49.1	21.3	51.1	50.2	52.3	51.7
Al <sub>2</sub> O <sub>3</sub> <sup>#</sup>	0.01	15.9	10.15	15.2	15.6	13.7	14.75	15.2	14.7	13.85	16.2
Fe <sub>2</sub> O <sub>3</sub> <sup>#</sup>	0.01	12.3	9.64	12.4	11.45	14	27	14.35	12.75	11.45	12.45
CaO <sup>#</sup>	0.01	4.18	0.37	8.47	4.22	7.16	0.16	3.72	4.94	6.6	7.35
MgO <sup>#</sup>	0.01	5.85	7.65	5.32	7.39	8.93	16.9	4.79	4.99	3.34	3.56
Na <sub>2</sub> O <sup>#</sup>	0.01	1.15	0.03	0.29	1.62	0.97	0.05	2.8	2.59	3.09	2.68
K <sub>2</sub> O <sup>#</sup>	0.01	0.88	0.47	0.31	1.02	0.67	0.04	0.37	1.28	0.97	1.02
Cr <sub>2</sub> O <sub>3</sub> <sup>#</sup>	0.01	<0.01	<0.01	0.01	0.03	0.1	<0.01	<0.01	<0.01	0.01	<0.01
TiO <sub>2</sub> <sup>#</sup>	0.01	1.3	0.5	1.5	1.28	1.33	0.2	1.35	1.83	1.75	1.9
MnO <sup>#</sup>	0.01	0.13	0.08	0.13	0.1	0.38	0.2	0.13	0.18	0.14	0.2
P <sub>2</sub> O <sub>5</sub> <sup>#</sup>	0.01	0.34	0.06	0.31	0.27	0.3	0.03	0.19	0.4	0.12	0.46
SrO <sup>#</sup>	0.01	0.02	<0.01	0.04	0.02	0.02	<0.01	0.02	0.01	0.01	0.03
BaO <sup>#</sup>	0.01	0.02	0.01	0.01	0.03	0.02	<0.01	0.01	0.03	0.03	0.04
C <sup>@</sup>	0.01	0.04	0.01	0.28	0.23	0.02	<0.01	0.01	0.65	1.02	0.12
S <sup>@</sup>	0.01	0.03	0.01	0.33	0.56	0.06	8.98	1.78	0.13	0.08	0.06
Ba <sup>*</sup>	0.5	142	114.5	46.1	261	222	1.8	106.5	284	283	344
Ce <sup>*</sup>	0.5	71.8	40.3	44.1	43.2	32.9	159	53.7	56.3	20.7	49.3
Cr <sup>*</sup>	10	10	10	100	200	700	10	10	10	60	10
Cs <sup>*</sup>	0.01	0.97	0.31	0.43	0.76	0.58	0.05	0.19	0.4	0.41	0.86
Dy <sup>*</sup>	0.05	5.33	4.08	5.12	4.81	3.67	12.25	3.67	5.95	2.67	5.56



Table A2-1 (continued): Geochemical data for the rocks of the Hood deposits

Samples	Det. Limit	D1411605	D1411606	D1411607	D1411608	D1411609	D1411610	D1411611	D1411612	D1411613	D1411614
Er*	0.03	3.12	2.6	2.95	2.88	2.11	7.45	2.12	3.5	1.3	3.15
Eu*	0.03	2.22	0.39	1.96	1.77	1.37	0.57	2.05	2.02	1.14	1.98
Ga*	0.1	23.4	16.6	20.8	22.4	16.6	17.6	23.4	22.9	20.6	23.5
Gd*	0.05	6.5	4.14	5.62	5.41	4.23	13.1	4.54	6.68	3.24	6.5
Hf*	0.2	7.7	6	4.8	4.4	3	11.7	3.6	5.7	2.5	5.8
Ho*	0.01	1.08	0.87	1.02	1	0.75	2.51	0.73	1.19	0.49	1.13
La*	0.5	34.3	19	18.9	19.3	14.6	72.3	27	25.3	9.8	21.8
Lu*	0.01	0.51	0.41	0.47	0.44	0.33	1.25	0.36	0.56	0.17	0.49
Nb*	0.2	12.6	12.5	10.6	9.7	7.4	27.1	10.1	14.9	4.6	14.8
Nd*	0.1	34.5	19.1	24	23.2	18.5	74	25	30.4	12.3	27.8
Pr*	0.03	8.56	4.71	5.62	5.49	4.2	19.1	6.26	7.06	2.7	6.36
Rb*	0.2	46	18.2	14.9	42.3	32.4	0.5	9.4	41.1	35.3	44.1
Sm*	0.03	7.07	4.3	5.41	5.24	4.22	15.25	5.2	6.84	3.22	6.45
Sn*	1	2	1	3	8	7	8	2	4	1	4
Sr*	0.1	125.5	2.9	275	126.5	130.5	1.2	145.5	85.8	103	203
Ta*	0.1	0.8	1	0.7	0.7	0.5	1.8	0.8	1	0.3	1
Tb*	0.01	0.92	0.66	0.83	0.82	0.62	2.07	0.64	0.99	0.48	0.95
Th*	0.05	6	9.35	2.21	1.63	2.14	30.6	2.2	4.6	1.26	2.86
Tl*	0.5	<0.5	<0.5	<0.5	0.7	1	<0.5	<0.5	<0.5	<0.5	<0.5
Tm*	0.01	0.47	0.4	0.45	0.45	0.33	1.2	0.32	0.54	0.18	0.48
U*	0.05	1.15	2.43	0.64	0.92	0.47	6.55	0.52	1.17	0.27	0.9
V*	5	196	8	279	217	222	<5	242	270	172	291
W*	1	2	2	3	4	2	3	2	4	2	2
Y*	0.5	30.5	24.8	28.1	28.1	20.6	61.7	20.9	34.2	13.9	30.8
Yb*	0.03	3.06	2.54	2.84	2.79	2.02	7.76	2.08	3.43	1.09	2.95
Zr*	20	325	243	194	184	121	381	134	228	88	234

Table A2-1 (continued): Geochemical data for the rocks of the Hood deposits

Samples	Det. Limit	D1411605	D1411606	D1411607	D1411608	D1411609	D1411610	D1411611	D1411612	D1411613	D1411614
As <sup>A</sup>	0.1	3.9	0.4	19.3	10.8	148	32	0.7	10.3	17.2	1.7
Bi <sup>A</sup>	0.01	0.24	0.02	0.24	5.86	6.2	54.1	0.47	1.22	0.17	0.27
Hg <sup>A</sup>	0.005	0.008	0.007	<0.005	0.012	0.027	0.568	0.026	0.011	<0.005	<0.005
Sb <sup>A</sup>	0.05	0.11	<0.05	0.15	0.12	1.06	0.51	0.64	0.08	<0.05	0.06
Se <sup>A</sup>	0.2	0.4	0.3	0.6	1.5	4.4	24.1	1.1	0.7	0.4	0.4
Te <sup>A</sup>	0.01	0.02	0.01	0.06	0.33	0.02	0.12	0.03	0.01	0.01	<0.01
Ag <sup>+</sup>	0.5	<0.5	<0.5	<0.5	0.5	2.4	10.5	<0.5	<0.5	<0.5	<0.5
Cd <sup>+</sup>	0.5	<0.5	<0.5	<0.5	<0.5	<0.5	16	3.7	<0.5	<0.5	<0.5
Co <sup>+</sup>	1	25	28	41	32	41	27	45	32	30	26
Cu <sup>+</sup>	1	56	2	255	744	170	500	296	136	59	15
Mo <sup>+</sup>	1	<1	2	1	1	<1	<1	<1	<1	<1	<1
Ni <sup>+</sup>	1	26	<1	52	90	204	<1	24	9	57	10
Pb <sup>+</sup>	2	14	8	25	35	362	1580	14	22	2	10
Zn <sup>+</sup>	2	122	83	70	122	268	10000	1185	304	151	159
Sc <sup>+</sup>	1	-	-	-	-	-	-	-	-	-	-
LOI (ppm)	0.01	4.46	5.19	5.36	5.57	3.67	11.45	4.39	5.79	6.13	2.58
Total (ppm)	0.01	100.5	99.1	101	99.3	100.5	92.1	98.4	99.7	99.8	100
La <sup>CN</sup>		144.73	80.17	79.75	81.43	61.60	305.06	113.92	106.75	41.35	91.98
Yb <sup>CN</sup>		18.00	14.94	16.71	16.41	11.88	45.65	12.24	20.18	6.41	17.35
La/Yb <sup>CN</sup>		8.04	5.37	4.77	4.96	5.18	6.68	9.31	5.29	6.45	5.30
La/Sm		4.85	4.42	3.49	3.68	3.46	4.74	5.19	3.70	3.04	3.38
Zr/Yb		106.21	95.67	68.31	65.95	59.90	49.10	64.42	66.47	80.73	79.32
Zr/Hf		42.21	40.50	40.42	41.82	40.33	32.56	37.22	40.00	35.20	40.34
Zr/(TiO <sub>2</sub> *10000)		0.03	0.05	0.01	0.01	0.01	0.19	0.01	0.01	0.01	0.01
Nb/Yb		4.12	4.92	3.73	3.48	3.66	3.49	4.86	4.34	4.22	5.02
Nb/Ta		15.75	12.50	15.14	13.86	14.80	15.06	12.63	14.90	15.33	14.80
μm borate fusion		+ppm; four-acid digestion									
μm borate fusion		+ppm; aqua regia digestion									
μm borate fusion		< ; below detection limit									
		LOI; Loss on ignition									
		CN; chondrite normalized									
		- ; not analyzed									

Table A2-1 (continued): Geochemical data for the rocks of the Hood deposits

Samples	Det. Limit	D1411615	D1411616	D1411617	D1411618	D1411619	D1411621	D1411623	D1411624	D1411625	D1411626	D1411627
Deposit		H-41-A	H-41-A	H-41-A	H-41-A	H-41-A	H-41-A	H-41-A	H-41-A	H-10	H-10	H-10
Drillhole #		H-41-A-02	H-41-A-02	H-41-A-02	H-41-A-02	H-41-A-02	H-41-A-02	H-41-A-02	H-41-A-02	H-10-01	H-10-01	H-10-01
From (m)		87.5	117.03	150.64	199.8	254.9	262.01	271.84	288.46	6.6	16.7	38.9
To (m)		87.62	117.15	150.78	199.91	254.99	262.1	271.99	288.57	6.7	16.8	39
Easting		-	-	-	-	-	-	-	-	-	-	-
Northing		-	-	-	-	-	-	-	-	-	-	-
Rock Type		Mafic	Mafic	Felsic	Int.	Int.	Felsic	Felsic	Int.	Int.	Mafic	Felsic
Sub-type		II	II	Tuff Group	3	2	A	Tuff Group	3	3	II	B
SiO <sub>2</sub> #	0.01	50.6	39.4	61	49.5	50.8	29.6	65.1	48.2	53.4	53	75.2
Al <sub>2</sub> O <sub>3</sub> #	0.01	15.5	16.85	12.65	12.6	14.75	13.1	13.4	16.8	13.7	13.95	11.8
Fe <sub>2</sub> O <sub>3</sub> #	0.01	9.61	11.45	10.45	12.85	9.3	23.8	5.58	12.7	13.6	8.01	1.76
CaO #	0.01	8.68	1.72	0.14	2.28	6.73	1.43	0.72	6.93	1.73	5.91	0.53
MgO #	0.01	4.33	17.5	6.83	8.65	5	16.6	5.76	7.03	5.65	5.62	1.14
Na <sub>2</sub> O #	0.01	2.59	0.02	0.04	0.02	3.1	0.03	0.06	1.7	3.59	4.13	5.26
K <sub>2</sub> O #	0.01	0.85	0.15	1.41	0.69	0.45	0.08	2.44	0.22	0.59	0.49	0.56
Cr <sub>2</sub> O <sub>3</sub> #	0.01	0.01	0.03	<0.01	<0.01	<0.01	<0.01	0.01	<0.01	<0.01	0.01	<0.01
TiO <sub>2</sub> #	0.01	1.16	1.72	0.53	1.68	1.27	0.22	0.4	1.74	1.12	1.42	0.15
MnO #	0.01	0.13	0.13	0.1	0.15	0.11	0.15	0.07	0.14	0.09	0.09	0.01
P <sub>2</sub> O <sub>5</sub> #	0.01	0.25	0.59	0.03	0.76	0.27	0.11	0.08	0.28	0.31	0.27	0.01
SrO #	0.01	0.02	<0.01	<0.01	<0.01	0.02	<0.01	<0.01	0.03	0.01	0.03	0.01
BaO #	0.01	0.02	<0.01	0.04	0.02	<0.01	<0.01	0.07	0.01	0.02	0.02	0.02
C <sup>@</sup>	0.01	0.94	0.03	0.01	0.02	1.06	0.02	0.15	0.04	0.32	1.19	0.13
S <sup>@</sup>	0.01	0.07	0.03	0.02	0.01	0.01	6.08	0.03	0.83	0.02	0.02	0.02
Ba*	0.5	181	27.4	345	185.5	34.1	5.7	478	55.5	159	138	162.5
Ce*	0.5	44.6	63.9	140	67.2	45.9	31.2	61.3	95.7	156.5	101.5	103
Cr*	10	60	260	<10	<10	20	<10	40	20	30	110	10
Cs*	0.01	0.4	0.18	0.65	0.42	0.21	0.65	0.78	0.2	4.16	2.58	0.34
Dy*	0.05	5.04	4.01	8.13	7.65	4.91	3	3.32	8.81	13.6	5.76	7.94

Table A2-1 (continued): Geochemical data for the rocks of the Hood deposits

Samples	Det. Limit	D1411615	D1411616	D1411617	D1411618	D1411619	D1411621	D1411623	D1411624	D1411625	D1411626	D1411627
Er*	0.03	2.91	2.07	4.75	4.31	2.82	1.67	2.07	5.15	8	3.04	5.11
Eu*	0.03	1.43	1.32	0.93	0.82	1.6	0.33	0.63	3.73	5.56	2.42	0.94
Ga*	0.1	19	20.3	20.4	20.8	19.6	27.6	20.3	31.9	52.1	19	17.8
Gd*	0.05	5.56	5.65	10	9.39	5.68	3.9	4.43	9.4	16.2	7.27	7.82
Hf*	0.2	3.3	4.3	7.6	8.7	5.4	9.5	10.2	7.2	12.7	3.7	7.6
Ho*	0.01	1.03	0.75	1.66	1.54	0.98	0.58	0.7	1.85	2.76	1.1	1.67
La*	0.5	19.4	26.4	72.3	31.8	20.6	13.7	29.5	46	77.8	47.6	51
Lu*	0.01	0.43	0.31	0.79	0.64	0.42	0.32	0.45	0.85	1.3	0.43	0.88
Nb*	0.2	9	11.8	19.8	17.4	10.3	13.9	8.9	25.7	36.5	9.8	18.3
Nd*	0.1	24.4	31.8	59.3	38.3	24.3	16.2	27.5	45.5	74.1	43.6	42.2
Pr*	0.03	5.71	7.74	15.7	8.57	5.74	3.88	7.02	11	18.45	11.55	11.5
Rb*	0.2	32	7.6	50	27.6	15.5	7.6	69.7	6.8	47.5	26.9	18.6
Sm*	0.03	5.75	6.46	11.55	9.12	5.6	4.04	5.26	9.86	16.15	8.54	8.34
Sn*	1	3	2	1	1	2	38	2	3	4	16	2
Sr*	0.1	187	4.9	4.2	5	130	2.4	7.7	236	315	210	95
Ta*	0.1	0.7	0.7	1.4	1	0.7	1	0.5	1.7	2.5	0.6	1.7
Tb*	0.01	0.84	0.73	1.4	1.33	0.84	0.55	0.6	1.41	2.38	1.05	1.28
Th*	0.05	4.39	4.27	14.7	2.77	2.06	20.7	9.94	4.03	12.9	2.38	23.8
Tl*	0.5	<0.5	<0.5	<0.5	<0.5	<0.5	0.5	0.6	<0.5	0.6	<0.5	<0.5
Tm*	0.01	0.43	0.29	0.76	0.63	0.43	0.27	0.35	0.79	1.21	0.44	0.82
U*	0.05	0.88	0.75	2.59	0.79	0.66	1.58	1.9	0.8	2.71	0.81	5.1
V*	5	204	278	7	55	210	17	43	295	518	257	5
W*	1	4	3	3	3	4	2	2	4	6	4	1
Y*	0.5	28.8	20.5	49.1	46.5	26.7	15	19	51.5	78.2	30.1	48.2
Yb*	0.03	2.72	1.9	4.75	3.92	2.68	1.87	2.39	5.21	7.84	2.76	5.51
Zr*	20	120	182	300	358	218	317	358	307	526	155	235

Table A2-1 (continued): Geochemical data for the rocks of the Hood deposits

Samples	Det. Limit	D1411615	D1411616	D1411617	D1411618	D1411619	D1411621	D1411623	D1411624	D1411625	D1411626	D1411627
As <sup>^</sup>	0.1	5.3	0.2	0.6	2.7	1.1	20.5	0.3	3.5	0.2	<0.1	1.2
Bi <sup>^</sup>	0.01	0.21	0.05	0.04	0.05	0.23	38.6	0.17	1.26	0.1	0.08	0.33
Hg <sup>^</sup>	0.005	<0.005	<0.005	<0.005	<0.005	<0.005	0.217	<0.005	<0.005	<0.005	<0.005	<0.005
Sb <sup>^</sup>	0.05	0.15	<0.05	<0.05	<0.05	<0.05	0.13	<0.05	0.28	0.16	0.12	0.23
Se <sup>^</sup>	0.2	0.3	0.3	0.4	0.4	0.3	37.9	0.3	2.4	0.4	0.3	0.3
Te <sup>^</sup>	0.01	0.01	<0.01	0.01	<0.01	0.02	0.31	0.01	0.21	0.01	0.01	0.01
Ag <sup>+</sup>	0.5	<0.5	<0.5	<0.5	<0.5	<0.5	17.2	<0.5	1	<0.5	<0.5	<0.5
Cd <sup>+</sup>	0.5	<0.5	<0.5	<0.5	<0.5	<0.5	23.9	<0.5	<0.5	<0.5	<0.5	<0.5
Co <sup>+</sup>	1	27	38	26	41	28	85	13	51	23	19	4
Cu <sup>+</sup>	1	38	<1	<1	<1	3	10000	78	444	16	6	13
Mo <sup>+</sup>	1	<1	<1	<1	<1	<1	<1	<1	<1	<1	1	<1
Ni <sup>+</sup>	1	48	78	1	4	33	<1	17	37	7	38	<1
Pb <sup>+</sup>	2	6	6	<2	<2	2	699	3	23	9	5	11
Zn <sup>+</sup>	2	115	184	130	186	108	9340	120	106	59	65	32
Sc <sup>+</sup>	1	-	-	-	-	-	-	-	-	-	-	-
LOI (ppm)	0.01	6.19	9.32	4.86	5.09	5.88	10.4	4.61	4.65	4.11	7.13	1.39
Total (ppm)	0.01	99.9	98.9	98.1	94.3	97.7	95.5	98.3	100.5	97.9	100	97.8
La <sup>CN</sup>		81.86	111.39	305.06	134.18	86.92	57.81	124.47	194.09	328.27	200.84	215.19
Yb <sup>CN</sup>		16.00	11.18	27.94	23.06	15.76	11.00	14.06	30.65	46.12	16.24	32.41
La/Yb <sup>CN</sup>		5.12	9.97	10.92	5.82	5.51	5.26	8.85	6.33	7.12	12.37	6.64
La/Sm		3.37	4.09	6.26	3.49	3.68	3.39	5.61	4.67	4.82	5.57	6.12
Zr/Yb		44.12	95.79	63.16	91.33	81.34	169.52	149.79	58.93	67.09	56.16	42.65
Zr/Hf		36.36	42.33	39.47	41.15	40.37	33.37	35.10	42.64	41.42	41.89	30.92
Zr/(TiO <sub>2</sub> *10000)		0.01	0.01	0.06	0.02	0.02	0.14	0.09	0.02	0.05	0.01	0.16
Nb/Yb		3.31	6.21	4.17	4.44	3.84	7.43	3.72	4.93	4.66	3.55	3.32
Nb/Ta		12.86	16.86	14.14	17.40	14.71	13.90	17.80	15.12	14.60	16.33	10.76
# wt%;lithium borate fusion												
@wt%; combustion furnace												
*ppm; lithium borate fusion												
+ppm; four-acid digestion												
^ppm; aqua regia digestion												
< ; below detection limit												
LOI; Loss on ignition												
CN; chondrite normalized												
- ; not analyzed												

Table A2-1 (continued): Geochemical data for the rocks of the Hood deposits

Samples	Det. Limit	D1411628	D1411629	D1411630	D1411631	D1411632	D1411633	D1411634	D1411636	D1411637	D1411638	D1411639
Deposit		H-10	H-10	H-10	H-10	H-10	H-10	H-10	H-10	H-10	H-10	H-10
Drillhole #		H-10-01	H-10-01	H-10-02	H-10-02	H-10-02	H-10-02	H-10-02	H-10-10	H-10-10	H-10-10	H-10-10
From (m)		53.4	62.3	29.1	67.4	98.1	113.8	122.2	9.8	32.4	35.6	113.7
To (m)		53.53	62.4	29.2	67.5	98.2	113.95	122.3	10	32.54	35.75	113.8
Easting		-	-	-	-	-	-	-	-	-	-	-
Northing		-	-	-	-	-	-	-	-	-	-	-
Rock Type		Int.	Felsic	Int.	Felsic	Mafic	Mafic	Felsic	Int.	Mafic	Mafic	Felsic
Sub-type		1	A	1	B	II	II	A	1	I	III	A
SiO <sub>2</sub> <sup>#</sup>	0.01	56.6	69.5	58.1	76.4	51.4	49.2	68.1	50.7	44.4	40.9	75
Al <sub>2</sub> O <sub>3</sub> <sup>#</sup>	0.01	13.15	9.98	15.15	11.1	15.2	12.6	12.6	15.15	13.15	14.6	10.95
Fe <sub>2</sub> O <sub>3</sub> <sup>#</sup>	0.01	12.55	7.67	5.79	1.38	11.2	12	6.1	8.28	12.8	18	2.53
CaO <sup>#</sup>	0.01	0.43	0.21	0.66	0.53	1.42	5.83	0.2	3.68	9.58	7.45	0.32
MgO <sup>#</sup>	0.01	7.13	5.93	7.75	1.08	8.27	6.99	3.99	9.29	6.51	6.27	3.82
Na <sub>2</sub> O <sup>#</sup>	0.01	0.05	0.87	4.54	4.57	2.46	2.14	1.23	3.71	2.57	2.12	1.11
K <sub>2</sub> O <sup>#</sup>	0.01	1.28	0.64	0.63	0.83	0.54	0.04	1.93	2.42	0.42	2.14	2.4
Cr <sub>2</sub> O <sub>3</sub> <sup>#</sup>	0.01	0.01	<0.01	0.01	<0.01	0.01	0.06	<0.01	0.01	0.03	0.02	<0.01
TiO <sub>2</sub> <sup>#</sup>	0.01	1.27	0.14	1.22	0.15	1.27	1.84	0.15	1.06	1.94	3.08	0.16
MnO <sup>#</sup>	0.01	0.06	0.06	0.04	0.02	0.1	0.15	0.04	0.1	0.19	0.18	0.02
P <sub>2</sub> O <sub>5</sub> <sup>#</sup>	0.01	0.32	0.01	0.35	<0.01	0.36	0.26	<0.01	0.35	0.17	0.36	0.07
SrO <sup>#</sup>	0.01	<0.01	<0.01	0.01	0.01	0.01	0.01	<0.01	0.01	0.01	0.03	<0.01
BaO <sup>#</sup>	0.01	0.04	0.02	0.01	0.02	0.03	<0.01	0.05	0.03	0.01	0.07	0.07
C <sup>@</sup>	0.01	0.01	0.09	0.04	0.67	0.23	1.24	0.05	0.59	1.72	0.63	0.06
S <sup>@</sup>	0.01	0.02	0.02	0.02	0.08	0.07	0.26	0.08	0.01	0.16	0.05	0.01
Ba <sup>*</sup>	0.5	369	186.5	114	200	232	21.2	492	260	70	585	608
Ce <sup>*</sup>	0.5	38.8	82.5	40.3	85.4	47.5	31.4	121	32.3	13.5	60.2	40.7
Cr <sup>*</sup>	10	50	<10	80	10	100	400	10	70	180	110	10
Cs <sup>*</sup>	0.01	0.89	0.69	2.78	0.47	0.53	0.25	0.98	9.61	2.01	7.2	1.94
Dy <sup>*</sup>	0.05	4.38	5.16	5.41	7.12	4.41	5.25	9.48	4.73	5.33	5.95	6.03

Table A2-1 (continued): Geochemical data for the rocks of the Hood deposits

Samples	Det. Limit	D1411628	D1411629	D1411630	D1411631	D1411632	D1411633	D1411634	D1411636	D1411637	D1411638	D1411639
Er*	0.03	2.71	3.21	3.17	4.83	2.48	3.08	5.32	2.87	3.01	3.12	3.97
Eu*	0.03	0.59	0.55	0.88	0.94	1.46	1.28	1.88	1.42	1.81	2.52	0.86
Ga*	0.1	20	16.4	20.4	14.8	19.5	16.4	18.5	17.8	16.6	21.4	18.2
Gd*	0.05	4.79	5.88	5.72	6.7	5.28	5.69	10.55	4.74	5.34	6.51	5.25
Hf*	0.2	5.1	7.9	5.4	7	4.4	4	8.2	5.1	3.5	5.4	8.2
Ho*	0.01	0.91	1.07	1.09	1.55	0.88	1.07	1.84	0.98	1.06	1.13	1.28
La*	0.5	17.7	38	17	41.8	21.2	12.9	61	11.6	4.3	26.3	19.8
Lu*	0.01	0.45	0.6	0.47	0.79	0.39	0.47	0.83	0.4	0.39	0.38	0.61
Nb*	0.2	12	16.8	12.1	14.9	11	9.7	19.4	11	5.9	24.8	27.5
Nd*	0.1	20.1	36	22.1	35.7	25.2	20	52.7	21.1	13.5	32	18.9
Pr*	0.03	4.76	9.52	5.19	9.62	5.98	4.3	13.85	4.87	2.46	7.88	4.93
Rb*	0.2	42.2	22.7	33.8	28	18.4	1.2	60.9	105.5	16.3	60.2	71
Sm*	0.03	4.6	6.94	5.33	7.06	5.43	5.11	11.05	5.1	4.71	7.23	4.79
Sn*	1	3	2	3	4	3	3	3	3	1	2	2
Sr*	0.1	6.1	13.9	64.5	84.9	55.3	106.5	24.9	90.5	101	273	24.4
Ta*	0.1	0.8	1.5	0.8	1.6	0.7	0.6	1.6	0.8	0.4	1.8	1.9
Tb*	0.01	0.74	0.86	0.87	1.12	0.75	0.87	1.61	0.74	0.86	1.02	0.94
Th*	0.05	3.6	16.6	4.28	21.7	3.26	2.78	18.3	3.95	0.71	2.91	16
Tl*	0.5	0.8	0.7	<0.5	<0.5	<0.5	<0.5	0.5	0.8	<0.5	0.6	0.6
Tm*	0.01	0.41	0.54	0.46	0.78	0.37	0.46	0.82	0.42	0.42	0.44	0.64
U*	0.05	0.99	3.99	1.07	4.95	0.73	0.76	4.62	1.19	0.12	0.53	7.17
V*	5	192	7	193	7	199	207	<5	144	228	290	<5
W*	1	7	2	9	2	2	2	2	1	1	1	1
Y*	0.5	25.1	28.5	31.1	46.1	24.5	30.4	51.1	25.6	27.1	28.5	33.3
Yb*	0.03	2.7	3.52	2.89	4.93	2.39	2.91	5.17	2.75	2.53	2.71	4.24
Zr*	20	209	264	218	219	178	146	268	186	110	179	244

Table A2-1 (continued): Geochemical data for the rocks of the Hood deposits

Samples	Det. Limit	D1411628	D1411629	D1411630	D1411631	D1411632	D1411633	D1411634	D1411636	D1411637	D1411638	D1411639
As <sup>^</sup>	0.1	36.6	9.1	0.9	1.8	1	1.9	0.9	<0.1	11.2	4.3	0.8
Bi <sup>^</sup>	0.01	0.15	0.15	0.03	0.32	0.2	0.26	0.03	0.04	0.54	0.03	0.05
Hg <sup>^</sup>	0.005	<0.005	<0.005	<0.005	<0.005	<0.005	<0.005	<0.005	<0.005	<0.005	<0.005	<0.005
Sb <sup>^</sup>	0.05	0.21	0.23	0.24	0.34	0.17	0.16	0.2	0.18	0.24	0.56	0.41
Se <sup>^</sup>	0.2	0.2	0.2	0.2	0.3	0.4	0.5	0.4	0.7	1.2	0.7	0.3
Te <sup>^</sup>	0.01	0.01	0.01	0.01	<0.01	0.01	0.02	<0.01	0.01	0.02	<0.01	<0.01
Ag <sup>+</sup>	0.5	<0.5	<0.5	<0.5	<0.5	<0.5	<0.5	<0.5	<0.5	<0.5	<0.5	<0.5
Cd <sup>+</sup>	0.5	<0.5	<0.5	<0.5	<0.5	<0.5	<0.5	<0.5	<0.5	<0.5	<0.5	<0.5
Co <sup>+</sup>	1	36	16	15	3	34	40	7	20	41	56	5
Cu <sup>+</sup>	1	4	12	1	4	75	26	8	<1	178	69	15
Mo <sup>+</sup>	1	<1	2	3	1	<1	<1	1	<1	<1	<1	10
Ni <sup>+</sup>	1	58	3	56	3	135	149	2	62	116	107	14
Pb <sup>+</sup>	2	3	8	<2	9	7	3	4	4	16	7	9
Zn <sup>+</sup>	2	165	142	57	19	349	139	59	69	64	116	50
Sc <sup>+</sup>	1	-	-	-	-	-	-	-	-	-	-	-
LOI (ppm)	0.01	5.55	4.89	4.53	2.08	6.09	8.4	4	6.2	9.29	5.5	2.59
Total (ppm)	0.01	98.4	99.9	98.8	98.2	98.4	99.5	98.4	101	101	100.5	99
La <sup>CN</sup>		74.68	160.34	71.73	176.37	89.45	54.43	257.38	48.95	18.14	110.97	83.54
Yb <sup>CN</sup>		15.88	20.71	17.00	29.00	14.06	17.12	30.41	16.18	14.88	15.94	24.94
La/Yb <sup>CN</sup>		4.70	7.74	4.22	6.08	6.36	3.18	8.46	3.03	1.22	6.96	3.35
La/Sm		3.85	5.48	3.19	5.92	3.90	2.52	5.52	2.27	0.91	3.64	4.13
Zr/Yb		77.41	75.00	75.43	44.42	74.48	50.17	51.84	67.64	43.48	66.05	57.55
Zr/Hf		40.98	33.42	40.37	31.29	40.45	36.50	32.68	36.47	31.43	33.15	29.76
Zr/(TiO <sub>2</sub> *10000)		0.02	0.19	0.02	0.15	0.01	0.01	0.18	0.02	0.01	0.01	0.15
Nb/Yb		4.44	4.77	4.19	3.02	4.60	3.33	3.75	4.00	2.33	9.15	6.49
Nb/Ta		15.00	11.20	15.13	9.31	15.71	16.17	12.13	13.75	14.75	13.78	14.47
# wt%;lithium borate fusion												
@wt%; combustion furnace												
*ppm; lithium borate fusion												
+ppm; four-acid digestion												
^ppm; aqua regia digestion												
< ; below detection limit												
LOI; Loss on ignition												
CN; chondrite normalized												
- ; not analyzed												



Table A2-1 (continued): Geochemical data for the rocks of the Hood deposits

Samples	Det. Limit	D1411640	D1411641	D1411642	D1411643	D1411645	D1411646	D1411647	D1411648	D1411649	D1411650	D1411651
Deposit		H-10	H-10	H-10	H-10	H-10	H-10	H-41-A	H-41-A	H-41-A	H-41-A	H-41-A
Drillhole #		H-10-10	H-10-10	H-10-11	H-10-11	H-10-11	H-10-11	H-41-A-15	H-41-A-15	H-41-A-15	H-41-A-15	H-41-A-15
From (m)		116.7	171.2	24.6	87.5	129	141	48.77	60.77	185.64	233.37	318.32
To (m)		116.8	171.3	24.8	87.65	129.2	141.2	48.92	60.95	185.81	235.54	318.51
Easting		-	-	-	-	-	-	-	-	-	-	-
Northing		-	-	-	-	-	-	-	-	-	-	-
Rock Type		Int.	Felsic	Int.	Felsic	Mafic	Felsic	Mafic	Mafic	Mafic	Felsic	Int.
Sub-type		1	Tuff Group	1	A	I	A	I	I	II	Rim Granite	1
SiO <sub>2</sub> <sup>#</sup>	0.01	51.6	70	51.1	69.9	42.6	58.6	46.6	47.3	47.8	75	53.3
Al <sub>2</sub> O <sub>3</sub> <sup>#</sup>	0.01	11.65	14.05	16.45	11.35	12.05	12.7	9.34	13.85	11.7	13.35	14.75
Fe <sub>2</sub> O <sub>3</sub> <sup>#</sup>	0.01	19.9	2.31	11.2	5.6	12.15	15.85	12.95	15.85	14.1	0.94	10.45
CaO <sup>#</sup>	0.01	0.36	1.26	2.97	0.24	8.43	0.11	8.93	6.98	6.99	0.96	2.11
MgO <sup>#</sup>	0.01	7.14	1.68	7.18	3.8	8.09	8.89	14.05	5.83	9.85	0.54	10.1
Na <sub>2</sub> O <sup>#</sup>	0.01	0.18	3.76	4.29	2.29	1.48	0.04	0.77	3.41	0.73	5.87	0.74
K <sub>2</sub> O <sup>#</sup>	0.01	0.1	2.05	0.6	1.21	0.06	0.23	0.47	0.74	0.74	0.94	0.99
Cr <sub>2</sub> O <sub>3</sub> <sup>#</sup>	0.01	<0.01	<0.01	0.01	0.01	0.06	<0.01	0.24	<0.01	0.1	<0.01	0.01
TiO <sub>2</sub> <sup>#</sup>	0.01	0.74	0.36	1.18	0.16	1.58	0.16	1.24	2.1	1.13	0.06	0.86
MnO <sup>#</sup>	0.01	0.14	0.02	0.14	0.03	0.17	0.1	0.19	0.21	0.2	0.01	0.13
P <sub>2</sub> O <sub>5</sub> <sup>#</sup>	0.01	0.15	0.06	0.29	0.08	0.31	0.03	0.17	0.6	0.21	0.01	0.24
SrO <sup>#</sup>	0.01	<0.01	0.01	0.01	0.01	0.02	<0.01	0.01	0.02	0.01	0.01	<0.01
BaO <sup>#</sup>	0.01	<0.01	0.04	0.02	0.03	<0.01	0.01	0.01	0.02	0.02	0.02	0.02
C <sup>@</sup>	0.01	0.04	0.25	0.39	0.11	1.98	0.05	0.16	0.02	0.17	0.06	0.39
S <sup>@</sup>	0.01	1.93	0.02	0.01	0.03	0.08	0.01	0.15	0.02	0.02	0.01	0.01
Ba <sup>*</sup>	0.5	16.1	356	128	247	13	74.9	91.1	162.5	149	190	184.5
Ce <sup>*</sup>	0.5	53.2	152	69.5	131	31.8	142	16.2	51.6	32.1	52.5	82.3
Cr <sup>*</sup>	10	10	10	70	<10	420	<10	1560	50	670	30	90
Cs <sup>*</sup>	0.01	0.31	1.01	1.89	0.75	0.16	0.39	0.46	0.45	0.42	0.25	0.78
Dy <sup>*</sup>	0.05	3.28	9.87	4.94	8.25	4.52	10.9	2.95	7.18	3.49	3.95	5.84

Table A2-1 (continued): Geochemical data for the rocks of the Hood deposits

Samples	Det. Limit	D1411640	D1411641	D1411642	D1411643	D1411645	D1411646	D1411647	D1411648	D1411649	D1411650	D1411651
Er*	0.03	1.85	6.1	2.95	4.82	2.58	6.53	1.58	4.08	2.17	2.6	3.29
Eu*	0.03	1.39	1.42	1.92	1.48	1.12	2.13	0.9	2.37	1.2	0.44	1.47
Ga*	0.1	18.7	18.6	20.5	21.9	15.7	23.4	13.6	20.5	17.7	13.1	18
Gd*	0.05	4.11	9.56	5.55	9.55	4.86	11.55	2.92	7.26	3.46	3.54	6.41
Hf*	0.2	4.5	8.1	5.3	8.3	3.2	8.9	2	5.8	3.5	4.2	7.2
Ho*	0.01	0.65	2.04	0.98	1.65	0.93	2.2	0.56	1.4	0.74	0.85	1.17
La*	0.5	25.7	73.2	32.6	63.2	12.7	69.7	6.1	20.5	14.4	26.9	39
Lu*	0.01	0.28	0.84	0.42	0.71	0.35	0.9	0.2	0.58	0.36	0.43	0.49
Nb*	0.2	7.4	22.3	11.8	21.4	10.9	26.4	7.7	14.5	9.7	10.8	13.9
Nd*	0.1	24.4	60.8	31.1	55.7	20	59.4	10.6	30.7	15.8	19.4	37.2
Pr*	0.03	6.36	17.45	8.39	15.2	4.52	16.7	2.3	7.16	4.12	5.83	10.05
Rb*	0.2	2.1	61.4	19.7	36	1.2	8.6	19.7	25.6	25.7	24.5	36.7
Sm*	0.03	4.97	11.5	6.34	11.25	4.77	12	2.76	7.3	3.56	4.15	7.41
Sn*	1	1	9	2	2	2	2	1	2	6	1	3
Sr*	0.1	5.4	68.8	106.5	42.3	133.5	3.6	39.5	133.5	97	92.9	25.9
Ta*	0.1	0.7	1.9	0.9	1.7	0.7	1.8	0.6	1	0.7	2.2	1.1
Tb*	0.01	0.59	1.59	0.84	1.45	0.77	1.8	0.48	1.14	0.56	0.6	0.97
Th*	0.05	7.64	22.1	4.21	17.95	1.16	19.05	0.71	1.45	2.17	31.4	13
Tl*	0.5	<0.5	0.6	<0.5	<0.5	<0.5	<0.5	<0.5	<0.5	<0.5	<0.5	<0.5
Tm*	0.01	0.28	0.96	0.44	0.76	0.38	0.99	0.23	0.59	0.33	0.43	0.53
U*	0.05	2	5.69	1.01	5.08	0.19	5.77	0.1	0.41	0.96	12.55	3.11
V*	5	120	24	148	5	208	<5	203	256	177	<5	127
W*	1	1	1	1	<1	1	<1	<1	1	1	<1	2
Y*	0.5	17.2	57.6	27.1	41.5	24.2	66.3	14.6	37.8	20.4	26.3	33
Yb*	0.03	1.91	5.85	2.93	4.8	2.56	6.11	1.43	3.94	2.23	2.89	3.29
Zr*	20	155	243	196	258	118	302	60	226	132	82	235

Table A2-1 (continued): Geochemical data for the rocks of the Hood deposits

Samples	Det. Limit	D1411640	D1411641	D1411642	D1411643	D1411645	D1411646	D1411647	D1411648	D1411649	D1411650	D1411651
As <sup>^</sup>	0.1	18	1.5	<0.1	10	4.6	<0.1	2.4	0.6	<0.1	1	<0.1
Bi <sup>^</sup>	0.01	0.78	3.19	0.03	0.12	0.97	0.07	0.02	0.03	0.05	0.02	0.11
Hg <sup>^</sup>	0.005	<0.005	<0.005	<0.005	<0.005	<0.005	<0.005	<0.005	<0.005	<0.005	<0.005	<0.005
Sb <sup>^</sup>	0.05	0.47	0.18	0.18	0.21	0.35	0.16	0.13	0.05	0.05	0.07	<0.05
Se <sup>^</sup>	0.2	4.8	1.1	0.4	0.3	0.4	0.3	0.7	0.4	0.2	0.2	0.4
Te <sup>^</sup>	0.01	0.08	0.04	0.01	0.02	0.01	0.01	0.01	<0.01	<0.01	<0.01	0.01
Ag <sup>+</sup>	0.5	1	1.1	<0.5	<0.5	<0.5	<0.5	<0.5	<0.5	<0.5	<0.5	<0.5
Cd <sup>+</sup>	0.5	<0.5	<0.5	<0.5	<0.5	<0.5	<0.5	<0.5	<0.5	<0.5	<0.5	<0.5
Co <sup>+</sup>	1	44	4	28	11	44	12	65	40	43	3	26
Cu <sup>+</sup>	1	1425	8	<1	21	54	2	140	4	<1	6	2
Mo <sup>+</sup>	1	1	<1	<1	2	<1	<1	<1	<1	<1	<1	<1
Ni <sup>+</sup>	1	8	6	72	2	204	1	588	36	275	12	43
Pb <sup>+</sup>	2	10	28	6	6	3	4	6	4	5	4	3
Zn <sup>+</sup>	2	213	35	58	54	240	206	117	93	159	5	139
Sc <sup>+</sup>	1	-	-	-	-	-	-	-	-	-	-	-
LOI (ppm)	0.01	6.48	2	4.4	2.9	11.4	4.4	4.4	2	4.98	0.7	6.69
Total (ppm)	0.01	98.4	97.6	99.8	97.6	98.4	101	99.4	98.9	98.6	98.4	100.5
La <sup>CN</sup>		108.44	308.86	137.55	266.67	53.59	294.09	25.74	86.50	60.76	113.50	164.56
Yb <sup>CN</sup>		11.24	34.41	17.24	28.24	15.06	35.94	8.41	23.18	13.12	17.00	19.35
La/Yb <sup>CN</sup>		9.65	8.98	7.98	9.44	3.56	8.18	3.06	3.73	4.63	6.68	8.50
La/Sm		5.17	6.37	5.14	5.62	2.66	5.81	2.21	2.81	4.04	6.48	5.26
Zr/Yb		81.15	41.54	66.89	53.75	46.09	49.43	41.96	57.36	59.19	28.37	71.43
Zr/Hf		34.44	30.00	36.98	31.08	36.88	33.93	30.00	38.97	37.71	19.52	32.64
Zr/(TiO <sub>2</sub> *10000)		0.02	0.07	0.02	0.16	0.01	0.19	0.00	0.01	0.01	0.14	0.03
Nb/Yb		3.87	3.81	4.03	4.46	4.26	4.32	5.38	3.68	4.35	3.74	4.22
Nb/Ta		10.57	11.74	13.11	12.59	15.57	14.67	12.83	14.50	13.86	4.91	12.64
# wt%;lithium borate fusion @wt%; combustion furnace *ppm; lithium borate fusion												
+ppm; four-acid digestion ^ppm; aqua regia digestion < ; below detection limit												
LOI; Loss on ignition CN; chondrite normalized - ; not analyzed												

Table A2-1 (continued): Geochemical data for the rocks of the Hood deposits

Samples	Det. Limit	D1411652	D1411653	D1411656	D1411657	D1411658	D1411659	D1411660	D1411661	D1411662	D1411663	D1411664
Deposit		H-41-A	H-41-A	H-41-A	H-41-A	H-41-A	H-41-A	H-41-A	H-41-A	H-41-A	H-41-A	H-41-A
Drillhole #		H-41-A-15	H-41-A-09	H-41-A-09	H-41-A-09	H-41-A-09	H-41-A-11	H-41-A-11	H-41-A-11	H-41-A-11	H-41-A-10	H-41-A-10
From (m)		350.19	10.8	94.04	114.74	147.91	122.3	132.46	179.51	209.4	63.99	227.34
To (m)		350.37	10.92	94.32	114.92	148.05	122.46	132.67	179.68	209.56	64.15	227.5
Easting		-	-	-	-	-	-	-	-	-	-	-
Northing		-	-	-	-	-	-	-	-	-	-	-
Rock Type		Int.	Mafic	Int.	Int.	Felsic	Felsic	Mafic	Felsic	Mafic	Mafic	Mafic
Sub-type		4	II	1	1	C	Tuff	I	A	II	I	II
SiO <sub>2</sub> <sup>#</sup>	0.01	59.1	48.8	56.7	62.1	75.7	71.4	47.2	70.5	48.8	47.3	52.4
Al <sub>2</sub> O <sub>3</sub> <sup>#</sup>	0.01	16.5	13.05	11.9	14.6	11.95	13.85	12.5	15.2	16	11.5	15.65
Fe <sub>2</sub> O <sub>3</sub> <sup>#</sup>	0.01	6.39	13.85	12.2	6.59	1.39	4.37	15.95	2.4	14.25	13.4	13.25
CaO <sup>#</sup>	0.01	8.47	5.57	0.87	5.33	2.77	3.52	8.65	1.14	6.52	6.65	6.1
MgO <sup>#</sup>	0.01	2.55	6.19	10.2	2.18	0.44	0.57	3.95	1.28	4.04	11.55	4.96
Na <sub>2</sub> O <sup>#</sup>	0.01	1.55	1.74	0.7	2.98	3.8	4.34	0.97	2.72	2.98	1.67	2.38
K <sub>2</sub> O <sup>#</sup>	0.01	1.35	0.38	0.14	1.37	1.52	0.87	0.15	2.83	0.74	1.15	0.25
Cr <sub>2</sub> O <sub>3</sub> <sup>#</sup>	0.01	<0.01	0.03	0.01	<0.01	<0.01	<0.01	<0.01	<0.01	<0.01	0.13	<0.01
TiO <sub>2</sub> <sup>#</sup>	0.01	0.29	1.71	0.58	0.71	0.21	0.54	2.54	0.18	2.05	1.21	1.87
MnO <sup>#</sup>	0.01	0.09	0.16	0.12	0.09	0.03	0.04	0.28	0.03	0.15	0.19	0.14
P <sub>2</sub> O <sub>5</sub> <sup>#</sup>	0.01	0.06	0.41	0.09	0.13	0.03	0.12	1	0.03	0.15	0.35	0.43
SrO <sup>#</sup>	0.01	0.02	0.01	<0.01	0.03	0.01	0.02	0.02	0.01	0.02	0.01	0.03
BaO <sup>#</sup>	0.01	0.07	0.01	<0.01	0.06	0.03	0.06	<0.01	0.12	0.02	0.02	0.01
C <sup>@</sup>	0.01	0.56	0.84	0.28	0.25	0.51	0.07	0.62	0.18	0.93	0.18	0.16
S <sup>@</sup>	0.01	0.01	0.01	0.53	0.03	0.01	0.49	0.52	0.03	0.51	0.03	0.02
Ba <sup>*</sup>	0.5	542	90.3	34.7	488	230	460	25.5	953	194.5	193	59.1
Ce <sup>*</sup>	0.5	19.1	48.3	65.1	51.9	107	178	57.5	141	36.2	24.1	52.9
Cr <sup>*</sup>	10	10	160	90	20	<10	10	10	<10	<10	860	20
Cs <sup>*</sup>	0.01	0.69	0.19	0.26	0.9	1	0.62	0.31	1.43	0.85	0.46	0.17
Dy <sup>*</sup>	0.05	2.19	5.59	4.84	5.65	7.12	7.61	8.67	8.48	4.1	3.74	5.67

Table A2-1 (continued): Geochemical data for the rocks of the Hood deposits

Samples	Det. Limit	D1411652	D1411653	D1411656	D1411657	D1411658	D1411659	D1411660	D1411661	D1411662	D1411663	D1411664
Er*	0.03	1.45	3.39	3.16	3.44	4.39	3.4	4.74	4.87	2.56	2.21	3.26
Eu*	0.03	1.7	1.9	0.81	1.31	1.44	3.11	3.13	1.62	1.68	1.19	2.05
Ga*	0.1	26.1	18.9	15.8	18.1	15.4	19.3	21.8	21.6	22.3	13.9	20.9
Gd*	0.05	2.03	5.83	4.69	5.36	7.28	11.45	9.24	9.81	3.62	3.87	5.95
Hf*	0.2	2.1	6	5.9	4	7.3	12.6	5.8	11.2	4	2.6	6.1
Ho*	0.01	0.47	1.14	1.03	1.16	1.47	1.36	1.73	1.69	0.84	0.77	1.13
La*	0.5	10	21.5	31.4	23.4	51	85.3	22.2	66.4	18.6	9.4	24.2
Lu*	0.01	0.23	0.51	0.5	0.56	0.65	0.5	0.62	0.66	0.4	0.32	0.46
Nb*	0.2	4.4	15.2	13.2	9.8	18.1	16	18.2	33.2	8.2	8.9	15
Nd*	0.1	8.3	26	28.2	25.2	44.2	76.4	36.3	60.6	15.1	14.2	25.5
Pr*	0.03	2.24	6.29	7.71	6.58	12.45	20.9	8.25	16.7	4.09	3.3	6.63
Rb*	0.2	44.5	10.2	4.8	40	56.5	29	4.4	94.2	25.4	36.1	5.8
Sm*	0.03	1.85	5.83	5.65	5.61	8.68	13.9	9.08	11.85	3.4	3.46	5.8
Sn*	1	5	2	12	2	4	2	3	4	3	2	2
Sr*	0.1	184	67.7	17.2	204	64.8	175	180	58	163.5	48.7	220
Ta*	0.1	0.4	1	1.2	0.9	1.4	0.7	1.2	2.6	0.8	0.6	1.1
Tb*	0.01	0.34	0.93	0.75	0.87	1.14	1.49	1.45	1.44	0.63	0.6	0.94
Th*	0.05	4.84	2.45	17.85	6.56	17.3	19.7	0.94	26.4	11.45	0.95	3.3
Tl*	0.5	<0.5	<0.5	<0.5	0.6	<0.5	<0.5	<0.5	<0.5	<0.5	<0.5	<0.5
Tm*	0.01	0.23	0.52	0.5	0.54	0.69	0.47	0.7	0.73	0.42	0.33	0.49
U*	0.05	1.68	0.61	3.82	2.06	3.4	2.52	0.34	5.83	3.33	0.18	1.08
V*	5	129	207	59	103	29	18	186	<5	506	196	179
W*	1	1	2	1	1	1	41	2	2	2	1	2
Y*	0.5	14.2	31.5	27.9	33.9	41.3	34.4	45.9	41.9	22.5	19.9	30.7
Yb*	0.03	1.59	3.3	3.29	3.67	4.45	3.04	4.32	4.74	2.68	2.21	3.05
Zr*	20	71	224	194	130	228	422	219	307	142	94	236

Table A2-1 (continued): Geochemical data for the rocks of the Hood deposits

Samples	Det. Limit	D1411652	D1411653	D1411656	D1411657	D1411658	D1411659	D1411660	D1411661	D1411662	D1411663	D1411664
As <sup>^</sup>	0.1	0.2	<0.1	13.1	8.9	<0.1	6.5	<0.1	0.1	5.8	7.9	0.4
Bi <sup>^</sup>	0.01	0.08	0.09	37.4	0.49	0.04	0.17	0.72	0.11	0.29	0.04	1.03
Hg <sup>^</sup>	0.005	<0.005	<0.005	0.005	<0.005	<0.005	0.033	<0.005	<0.005	<0.005	<0.005	<0.005
Sb <sup>^</sup>	0.05	0.1	<0.05	0.05	0.26	<0.05	0.16	0.27	<0.05	0.46	<0.05	0.18
Se <sup>^</sup>	0.2	0.2	0.4	5.5	0.4	0.4	1.2	1	0.4	0.7	0.3	0.4
Te <sup>^</sup>	0.01	<0.01	0.01	0.99	0.01	<0.01	0.03	0.03	<0.01	0.01	0.01	0.02
Ag <sup>+</sup>	0.5	<0.5	<0.5	13.3	<0.5	<0.5	<0.5	<0.5	<0.5	<0.5	<0.5	<0.5
Cd <sup>+</sup>	0.5	<0.5	<0.5	<0.5	<0.5	<0.5	<0.5	<0.5	<0.5	<0.5	<0.5	<0.5
Co <sup>+</sup>	1	12	34	36	18	1	18	30	3	35	55	22
Cu <sup>+</sup>	1	<1	<1	458	32	3	212	52	16	44	21	8
Mo <sup>+</sup>	1	<1	<1	2	<1	<1	1	<1	2	<1	2	<1
Ni <sup>+</sup>	1	12	102	40	21	2	5	8	<1	12	293	16
Pb <sup>+</sup>	2	13	5	1680	43	2	6	10	5	13	6	21
Zn <sup>+</sup>	2	57	111	148	95	9	24	135	23	107	110	92
Sc <sup>+</sup>	1	-	-	-	-	-	-	-	-	-	-	-
LOI (ppm)	0.01	4.49	7.19	5.69	2.9	2.89	1.8	5.3	2.5	5.69	4.4	3.3
Total (ppm)	0.01	101	99.1	99.2	99.1	101	101.5	98.5	98.9	101.5	99.5	101
La <sup>CN</sup>		42.19	90.72	132.49	98.73	215.19	359.92	93.67	280.17	78.48	39.66	102.11
Yb <sup>CN</sup>		9.35	19.41	19.35	21.59	26.18	17.88	25.41	27.88	15.76	13.00	17.94
La/Yb <sup>CN</sup>		4.51	4.67	6.85	4.57	8.22	20.13	3.69	10.05	4.98	3.05	5.69
La/Sm		5.41	3.69	5.56	4.17	5.88	6.14	2.44	5.60	5.47	2.72	4.17
Zr/Yb		44.65	67.88	58.97	35.42	51.24	138.82	50.69	64.77	52.99	42.53	77.38
Zr/Hf		33.81	37.33	32.88	32.50	31.23	33.49	37.76	27.41	35.50	36.15	38.69
Zr/(TiO <sub>2</sub> *10000)		0.02	0.01	0.03	0.02	0.11	0.08	0.01	0.17	0.01	0.01	0.01
Nb/Yb		2.77	4.61	4.01	2.67	4.07	5.26	4.21	7.00	3.06	4.03	4.92
Nb/Ta		11.00	15.20	11.00	10.89	12.93	22.86	15.17	12.77	10.25	14.83	13.64
# wt%;lithium borate fusion @wt%; combustion furnace *ppm; lithium borate fusion +ppm; four-acid digestion ^ppm; aqua regia digestion < ; below detection limit LOI; Loss on ignition CN; chondrite normalized - ; not analyzed												

Table A2-1 (continued): Geochemical data for the rocks of the Hood deposits

Samples	Det. Limit	D1411666	D1411667	D1411668	D1411669	D1411670	D1411671	D1411672	D1411674	D1411675	D1411676	D1411677
Deposit		H-41-A	H-41-A	H-41-A	H-41-A	H-41-A	H-41	H-41	H-41	H-41	H-41	H-41
Drillhole #		H-41-A-10	H-41-A-16	H-41-A-16	H-41-A-16	H-41-A-16	H-41-11	H-41-08	H-41-08	H-41-15	H-41-15	H-41-15
From (m)		248.8	7.98	90.54	189.2	235.45	56.6	35.28	75.76	17.52	107.11	145.08
To (m)		248.95	8.2	90.77	189.45	235.59	56.87	35.48	75.9	17.69	107.34	145.25
Easting		-	-	-	-	-	-	-	-	-	-	-
Northing		-	-	-	-	-	-	-	-	-	-	-
Rock Type		Mafic	Mafic	Felsic	Mafic	Int.	Mafic	Int.	Felsic	Int.	Mafic	Mafic
Sub-type		III	II	Rim Granite	II	1	I	1	A	2	I	I
SiO <sub>2</sub> <sup>#</sup>	0.01	50.5	51.4	76.4	48.3	57.9	52	45.1	78.7	48.9	46.4	44.8
Al <sub>2</sub> O <sub>3</sub> <sup>#</sup>	0.01	14.95	13.2	13.25	15.6	15.95	17	14.45	9.02	16.3	16.35	14.95
Fe <sub>2</sub> O <sub>3</sub> <sup>#</sup>	0.01	11.55	13.9	0.57	18.85	9.66	11.8	19.6	4.55	11.7	14.15	16.05
CaO <sup>#</sup>	0.01	6.72	4.39	3.03	2	5.6	6.8	0.64	0.04	5.73	8.84	6.6
MgO <sup>#</sup>	0.01	4.3	4.85	0.12	6.91	4.33	5.16	11.8	2.44	8.37	4.6	7.46
Na <sub>2</sub> O <sup>#</sup>	0.01	3.15	1.05	4.49	0.86	2.91	3.51	0.1	0.06	3.17	2.53	0.24
K <sub>2</sub> O <sup>#</sup>	0.01	0.33	1.76	0.64	0.34	0.34	0.17	0.04	1.76	0.85	0.57	0.12
Cr <sub>2</sub> O <sub>3</sub> <sup>#</sup>	0.01	<0.01	<0.01	<0.01	0.04	<0.01	<0.01	0.02	<0.01	0.02	<0.01	0.05
TiO <sub>2</sub> <sup>#</sup>	0.01	1.36	1.56	0.05	1.64	1.16	1.45	1.31	0.11	1.38	2.09	1.73
MnO <sup>#</sup>	0.01	0.16	0.17	0.01	0.15	0.1	0.19	0.28	0.02	0.13	0.17	0.2
P <sub>2</sub> O <sub>5</sub> <sup>#</sup>	0.01	0.22	0.34	0.02	0.28	0.24	0.31	0.32	0.1	0.37	0.43	0.28
SrO <sup>#</sup>	0.01	0.02	0.01	0.03	0.01	0.03	0.03	<0.01	<0.01	0.02	0.04	0.02
BaO <sup>#</sup>	0.01	0.01	0.04	0.03	0.01	0.02	0.02	<0.01	0.08	0.04	0.01	<0.01
C <sup>@</sup>	0.01	0.5	0.46	0.21	0.04	0.13	0.03	0.01	<0.01	0.05	0.15	0.14
S <sup>@</sup>	0.01	0.17	0.11	0.01	0.02	0.02	0.01	0.07	0.01	0.6	0.24	0.17
Ba*	0.5	76.2	338	204	70	125	174.5	9.7	648	316	95.9	29.4
Ce*	0.5	48.2	54.5	42.3	31.5	49.3	48.6	51	79.7	50.5	47.6	34.1
Cr*	10	30	40	<10	240	<10	10	110	<10	100	20	300
Cs*	0.01	0.53	0.49	0.51	0.29	0.2	0.13	0.21	0.56	0.34	0.44	0.19
Dy*	0.05	6.4	6.02	4.24	3.53	4	4.02	5.46	5.89	5.3	6.12	5.48

Table A2-1 (continued): Geochemical data for the rocks of the Hood deposits

Samples	Det. Limit	D1411666	D1411667	D1411668	D1411669	D1411670	D1411671	D1411672	D1411674	D1411675	D1411676	D1411677
Er*	0.03	3.94	3.58	2.55	2.07	2.33	2.3	3.29	3.24	3.27	3.34	3.19
Eu*	0.03	1.8	2	0.43	1.74	1.67	1.92	0.76	0.35	2.58	2.28	1.52
Ga*	0.1	21.2	21.5	13.2	20.4	19.3	21.7	29.7	14.7	19.8	20.9	19.1
Gd*	0.05	6.33	6.18	3.69	3.77	4.36	4.75	5.65	6.3	5.84	6.05	5.3
Hf*	0.2	3.5	5.3	3.7	4.3	5	5.4	5.7	7.8	4.9	5.2	3.8
Ho*	0.01	1.33	1.22	0.87	0.72	0.79	0.8	1.08	1.12	1.12	1.27	1.18
La*	0.5	21.8	24.6	21.2	14.2	23.6	23.3	22.2	34	22.1	21.7	14.9
Lu*	0.01	0.53	0.53	0.44	0.32	0.33	0.36	0.49	0.42	0.45	0.46	0.42
Nb*	0.2	19.2	14.3	12.4	11.8	9.5	12	13.6	11.1	13.2	13.3	10.5
Nd*	0.1	24.7	27.4	15.2	16	21.9	23.3	25.1	35.3	25.5	26	20.3
Pr*	0.03	6.2	6.94	4.64	3.98	5.91	6.01	6.44	9.64	6.44	5.89	4.41
Rb*	0.2	10.3	60.5	22.2	12.3	11.1	3.5	2.4	52.2	20.4	15.5	3.1
Sm*	0.03	5.86	6.15	3.68	3.68	4.56	4.88	5.57	6.98	5.58	6.07	5.04
Sn*	1	3	5	1	2	1	1	11	1	1	2	5
Sr*	0.1	196.5	87.9	243	75.3	285	271	9.3	7.9	142	284	163.5
Ta*	0.1	1.2	1.1	3.1	0.9	0.8	0.9	1	0.7	0.8	0.9	0.7
Tb*	0.01	1.02	1	0.66	0.57	0.66	0.68	0.93	1.01	0.88	0.94	0.86
Th*	0.05	2.49	5.09	28.7	2.16	4.26	1.71	4.14	16.45	1.62	1.14	1.39
Tl*	0.5	<0.5	<0.5	<0.5	<0.5	<0.5	<0.5	<0.5	<0.5	<0.5	<0.5	<0.5
Tm*	0.01	0.57	0.53	0.44	0.33	0.35	0.34	0.49	0.47	0.47	0.45	0.44
U*	0.05	0.69	1.28	11.7	0.67	1.27	0.73	1.71	2.34	0.38	0.62	0.54
V*	5	302	232	<5	209	179	236	162	9	197	250	227
W*	1	1	2	<1	2	1	<1	3	1	1	2	4
Y*	0.5	35.6	33.2	27.3	18.5	21.5	21.9	30.9	31.1	29.7	30.3	28.9
Yb*	0.03	3.82	3.47	2.9	2.15	2.19	2.26	3.3	2.99	3.05	2.94	2.82
Zr*	20	124	198	71	155	176	211	217	228	199	231	161



Table A2-1 (continued): Geochemical data for the rocks of the Hood deposits

Samples	Det. Limit	D1411666	D1411667	D1411668	D1411669	D1411670	D1411671	D1411672	D1411674	D1411675	D1411676	D1411677
As <sup>A</sup>	0.1	1.2	3	0.3	0.6	4.8	6	9.9	0.2	3.6	1.4	8.3
Bi <sup>A</sup>	0.01	0.16	0.16	0.03	0.08	0.08	0.08	1.4	0.89	0.07	0.05	0.31
Hg <sup>A</sup>	0.005	<0.005	<0.005	<0.005	<0.005	<0.005	0.006	<0.005	<0.005	<0.005	0.005	<0.005
Sb <sup>A</sup>	0.05	0.25	0.09	0.09	<0.05	0.18	0.25	0.12	<0.05	0.47	0.2	0.43
Se <sup>A</sup>	0.2	0.5	0.6	0.3	0.2	0.4	0.3	0.3	0.2	0.5	0.9	0.6
Te <sup>A</sup>	0.01	0.01	0.01	<0.01	0.01	<0.01	<0.01	0.01	0.2	<0.01	<0.01	0.01
Ag <sup>+</sup>	0.5	<0.5	<0.5	<0.5	<0.5	<0.5	0.5	0.6	<0.5	<0.5	<0.5	0.5
Cd <sup>+</sup>	0.5	<0.5	<0.5	<0.5	<0.5	<0.5	<0.5	<0.5	<0.5	<0.5	<0.5	<0.5
Co <sup>+</sup>	1	26	32	1	40	21	31	17	13	33	34	45
Cu <sup>+</sup>	1	28	75	1	5	9	29	5	1	60	51	330
Mo <sup>+</sup>	1	<1	1	<1	<1	<1	<1	<1	<1	<1	<1	<1
Ni <sup>+</sup>	1	46	20	<1	87	21	27	81	<1	105	17	141
Pb <sup>+</sup>	2	15	4	13	5	11	20	15	<2	8	7	10
Zn <sup>+</sup>	2	152	186	4	112	95	162	281	32	131	113	165
Sc <sup>+</sup>	1	-	-	-	-	-	-	-	-	-	-	-
LOI (ppm)	0.01	4.69	5.18	1	4.8	3	2.4	6	2.2	2.79	2.9	5.09
Total (ppm)	0.01	98	97.9	99.6	99.8	101	101	99.7	99.1	99.8	99.1	97.6
La <sup>CN</sup>		91.98	103.80	89.45	59.92	99.58	98.31	93.67	143.46	93.25	91.56	62.87
Yb <sup>CN</sup>		22.47	20.41	17.06	12.65	12.88	13.29	19.41	17.59	17.94	17.29	16.59
La/Yb <sup>CN</sup>		4.09	5.09	5.24	4.74	7.73	7.40	4.83	8.16	5.20	5.29	3.79
La/Sm		3.72	4.00	5.76	3.86	5.18	4.77	3.99	4.87	3.96	3.57	2.96
Zr/Yb		32.46	57.06	24.48	72.09	80.37	93.36	65.76	76.25	65.25	78.57	57.09
Zr/Hf		35.43	37.36	19.19	36.05	35.20	39.07	38.07	29.23	40.61	44.42	42.37
Zr/(TiO <sub>2</sub> *10000)		0.01	0.01	0.14	0.01	0.02	0.01	0.02	0.21	0.01	0.01	0.01
Nb/Yb		5.03	4.12	4.28	5.49	4.34	5.31	4.12	3.71	4.33	4.52	3.72
Nb/Ta		16.00	13.00	4.00	13.11	11.88	13.33	13.60	15.86	16.50	14.78	15.00
# wt%;lithium borate fusion												
@wt%; combustion furnace												
*ppm; lithium borate fusion												
+ppm; four-acid digestion												
^ppm; aqua regia digestion												
< ; below detection limit												
LOI; Loss on ignition												
CN; chondrite normalized												
- ; not analyzed												

Table A2-1 (continued): Geochemical data for the rocks of the Hood deposits

Samples	Det. Limit	D1411679	D1411680	D1411682	D1411683	D1411684	D1411687	D1411688	D1411690	D1411691	D1411693	D1411694
Deposit		H-41	H-41	H-41	H-41	H-41	H-41	H-41	H-41	H-41	H-41	H-41
Drillhole #		H-41-15	H-41-15	H-41-05	H-41-17	H-41-17	H-41-17	H-41-17	H-41-18	H-41-18	H-41-18	H-41-18
From (m)		177.02	190.75	50.68	52.72	59.45	219.03	230.94	96.15	122.48	200.05	219.8
To (m)		177.19	190.97	50.8	52.89	59.64	219.29	231.13	96.32	122.67	200.35	219.96
Easting		-	-	-	-	-	-	-	-	-	-	-
Northing		-	-	-	-	-	-	-	-	-	-	-
Rock Type		Felsic	Int.	Felsic	Int.	Int.	Felsic	Felsic	Mafic	Int.	Int.	Felsic
Sub-type		A	2	A	3	1	A	A	I	1	1	A
SiO <sub>2</sub> <sup>#</sup>	0.01	76.6	48.3	77	56.4	64.1	73.9	70.7	48.7	58.2	69.2	71.4
Al <sub>2</sub> O <sub>3</sub> <sup>#</sup>	0.01	8.07	15.25	10.6	16.4	14.45	8.97	12.3	17.9	15.3	12.45	13.1
Fe <sub>2</sub> O <sub>3</sub> <sup>#</sup>	0.01	4.56	14.25	4.79	9.27	6.6	5.58	5.99	12.8	8.82	5.19	4.42
CaO <sup>#</sup>	0.01	0.13	7.87	0.09	4.31	1.58	0.41	0.04	7.66	9.28	2.26	0.05
MgO <sup>#</sup>	0.01	4.43	5.68	3.08	5.61	5.65	4.62	2.87	4.65	3.28	2.62	3.47
Na <sub>2</sub> O <sup>#</sup>	0.01	0.03	2.39	0.1	4.38	2.88	0.04	0.07	3.76	2.11	2.25	0.09
K <sub>2</sub> O <sup>#</sup>	0.01	1.02	0.46	1.84	1.52	0.95	1.12	2.36	0.48	0.57	1.18	2.5
Cr <sub>2</sub> O <sub>3</sub> <sup>#</sup>	0.01	<0.01	0.02	<0.01	0.02	<0.01	<0.01	<0.01	<0.01	0.01	<0.01	<0.01
TiO <sub>2</sub> <sup>#</sup>	0.01	0.1	1.84	0.13	1.22	1.03	0.1	0.15	1.46	0.81	0.64	0.17
MnO <sup>#</sup>	0.01	0.05	0.25	0.08	0.1	0.06	0.07	0.05	0.17	0.12	0.08	0.03
P <sub>2</sub> O <sub>5</sub> <sup>#</sup>	0.01	<0.01	0.44	0.03	0.3	0.16	0.03	0.01	0.33	0.26	0.09	<0.01
SrO <sup>#</sup>	0.01	<0.01	0.03	<0.01	0.01	0.01	<0.01	<0.01	0.04	0.04	0.01	<0.01
BaO <sup>#</sup>	0.01	0.03	0.01	0.05	0.03	0.06	0.04	0.12	0.02	0.01	0.04	0.04
C <sup>@</sup>	0.01	0.01	0.2	0.01	0.07	0.02	0.13	<0.01	0.03	0.01	0.05	0.01
S <sup>@</sup>	0.01	0.01	0.03	0.01	0.02	0.01	0.17	0.02	0.09	0.01	0.11	0.01
Ba <sup>*</sup>	0.5	284	106	431	216	477	315	997	152	71.1	320	342
Ce <sup>*</sup>	0.5	57.6	61	109	110.5	98.8	67.9	116	37.7	65.9	65.6	72.8
Cr <sup>*</sup>	10	10	130	<10	100	10	<10	<10	20	30	20	<10
Cs <sup>*</sup>	0.01	0.43	0.7	0.71	3.9	0.78	0.37	0.69	0.21	0.14	1.34	0.74
Dy <sup>*</sup>	0.05	4.59	7.65	7.64	14.5	7.11	5.14	7.03	4	9.2	4.27	4.36

Table A2-1 (continued): Geochemical data for the rocks of the Hood deposits

Samples	Det. Limit	D1411679	D1411680	D1411682	D1411683	D1411684	D1411687	D1411688	D1411690	D1411691	D1411693	D1411694
Er*	0.03	2.97	4.39	4.22	8.43	4.08	3.09	3.95	2.17	5.28	2.25	2.57
Eu*	0.03	0.29	2.57	0.63	3.18	2.02	0.28	0.44	1.78	1.69	1.35	0.4
Ga*	0.1	11.3	19.9	15.6	22.2	17.4	12.1	19.8	21	22.2	16.1	19.9
Gd*	0.05	3.79	7.81	7.33	14.55	7.32	4.78	7.17	4.42	8.53	4.59	4.64
Hf*	0.2	6	6.3	8.4	5.9	10.6	7.4	9.2	2.3	8	4.7	11.4
Ho*	0.01	1.02	1.63	1.52	3.05	1.48	1.12	1.45	0.86	1.95	0.87	0.92
La*	0.5	28.5	25.6	55.7	42.2	49.9	34.6	58.6	18.1	30.5	33.5	36.6
Lu*	0.01	0.49	0.59	0.61	1.02	0.63	0.47	0.58	0.26	0.63	0.29	0.43
Nb*	0.2	9.9	17.2	13.2	12.8	15	10.2	16.2	6.6	9	14.5	18
Nd*	0.1	24.2	35.5	45.6	66.7	42.9	27.7	48.2	20.2	35.1	27.5	30.5
Pr*	0.03	6.29	7.95	11.85	15.25	11.05	7.27	12.8	4.6	8.08	7.11	8
Rb*	0.2	32.7	16.2	71	70.1	23.7	33.7	81.5	11.7	10.8	43.6	105
Sm*	0.03	4.47	7.99	8.99	15.7	8.52	5.34	8.98	4.51	8.37	5.29	5.9
Sn*	1	1	3	2	7	2	4	2	2	8	4	1
Sr*	0.1	5.2	226	8.6	99.4	83.6	3.6	8.5	301	321	104	7.1
Ta*	0.1	0.8	1.1	1.3	0.9	1.1	0.8	1.1	0.4	0.8	0.9	1.1
Tb*	0.01	0.66	1.23	1.18	2.28	1.1	0.79	1.14	0.68	1.42	0.72	0.69
Th*	0.05	14.85	1.17	17.1	2.42	13.65	14.2	17.55	0.82	10.7	8.69	15.25
Tl*	0.5	<0.5	<0.5	0.9	0.5	<0.5	0.6	0.8	<0.5	<0.5	1.5	0.9
Tm*	0.01	0.45	0.59	0.6	1.15	0.58	0.45	0.57	0.28	0.71	0.29	0.38
U*	0.05	1.76	0.55	4.09	1.56	2.99	2.44	4.67	0.22	2.41	1.54	4.18
V*	5	<5	252	<5	171	121	<5	<5	260	168	90	<5
W*	1	1	2	2	2	3	2	2	2	4	2	2
Y*	0.5	24.7	39.6	36.8	80	34.7	28.1	35.6	19.7	48.4	20.4	22.5
Yb*	0.03	3.15	3.97	4.12	7.42	4.02	3.16	3.85	1.8	4.54	1.87	2.63
Zr*	20	199	277	297	253	425	249	324	103	324	192	409

Table A2-1 (continued): Geochemical data for the rocks of the Hood deposits

Samples	Det. Limit	D1411679	D1411680	D1411682	D1411683	D1411684	D1411687	D1411688	D1411690	D1411691	D1411693	D1411694
As <sup>^</sup>	0.1	0.3	<0.1	0.4	<0.1	<0.1	16.1	5	1	0.5	12.4	<0.1
Bi <sup>^</sup>	0.01	0.5	1.02	0.1	0.03	0.06	0.8	0.17	0.02	0.16	1.14	0.04
Hg <sup>^</sup>	0.005	<0.005	<0.005	<0.005	<0.005	<0.005	<0.005	<0.005	<0.005	<0.005	0.006	<0.005
Sb <sup>^</sup>	0.05	<0.05	0.1	<0.05	<0.05	<0.05	0.31	<0.05	0.05	0.21	0.53	<0.05
Se <sup>^</sup>	0.2	0.2	0.5	0.2	0.5	0.5	0.6	0.2	0.4	0.3	1	0.2
Te <sup>^</sup>	0.01	0.01	0.02	0.01	<0.01	<0.01	0.01	0.02	0.01	<0.01	0.05	<0.01
Ag <sup>+</sup>	0.5	<0.5	0.7	<0.5	<0.5	<0.5	1	<0.5	<0.5	<0.5	0.8	<0.5
Cd <sup>+</sup>	0.5	<0.5	<0.5	<0.5	<0.5	<0.5	<0.5	<0.5	<0.5	<0.5	<0.5	<0.5
Co <sup>+</sup>	1	12	36	7	17	12	9	13	49	14	15	8
Cu <sup>+</sup>	1	6	102	19	6	13	1235	14	21	13	270	5
Mo <sup>+</sup>	1	1	<1	<1	1	1	<1	2	<1	<1	<1	1
Ni <sup>+</sup>	1	<1	41	<1	73	10	<1	<1	64	27	18	<1
Pb <sup>+</sup>	2	5	44	2	4	8	27	5	11	14	593	4
Zn <sup>+</sup>	2	58	111	62	79	81	79	58	214	94	154	47
Sc <sup>+</sup>	1	-	-	-	-	-	-	-	-	-	-	-
LOI (ppm)	0.01	2.89	3.1	2.8	1.8	3	4	3.1	1.9	1.6	2.3	3.29
Total (ppm)	0.01	97.9	99.9	100.5	101.5	100.5	98.9	97.8	99.9	100.5	98.3	98.6
La <sup>CN</sup>		120.25	108.02	235.02	178.06	210.55	145.99	247.26	76.37	128.69	141.35	154.43
Yb <sup>CN</sup>		18.53	23.35	24.24	43.65	23.65	18.59	22.65	10.59	26.71	11.00	15.47
La/Yb <sup>CN</sup>		6.49	4.63	9.70	4.08	8.90	7.85	10.92	7.21	4.82	12.85	9.98
La/Sm		6.38	3.20	6.20	2.69	5.86	6.48	6.53	4.01	3.64	6.33	6.20
Zr/Yb		63.17	69.77	72.09	34.10	105.72	78.80	84.16	57.22	71.37	102.67	155.51
Zr/Hf		33.17	43.97	35.36	42.88	40.09	33.65	35.22	44.78	40.50	40.85	35.88
Zr/(TiO <sub>2</sub> *10000)		0.20	0.02	0.23	0.02	0.04	0.25	0.22	0.01	0.04	0.03	0.24
Nb/Yb		3.14	4.33	3.20	1.73	3.73	3.23	4.21	3.67	1.98	7.75	6.84
Nb/Ta		12.38	15.64	10.15	14.22	13.64	12.75	14.73	16.50	11.25	16.11	16.36
# wt%;lithium borate fusion												
@wt%; combustion furnace												
*ppm; lithium borate fusion												
+ppm; four-acid digestion												
^ppm; aqua regia digestion												
< ; below detection limit												
LOI; Loss on ignition												
CN; chondrite normalized												
- ; not analyzed												

Table A2-1 (continued): Geochemical data for the rocks of the Hood deposits

Samples	Det. Limit	D1411695	D1411696	D1411697	D1411698	D1411700	D1410401	D1410402	D1410403	D1410405	D1410406	D1410408
Deposit		H-41	H-41	H-41	H-41	H-41	H-41-A	H-10	H-10	H-10	H-10	H-10
Drillhole #		H-41-04	H-41-04	H-41-14	H-41-14	H-41-14	H-41-A-11	H-10-08	H-10-08	H-10-08	H-10-05	H-10-05
From (m)		22.5	86.6	15.37	73.97	137.96	197	11.29	54.5	96.14	14.8	54.04
To (m)		22.68	86.86	15.56	74.13	138.13	203.1	11.4	54.71	96.36	15.01	54.2
Easting		-	-	-	-	-	-	-	-	-	-	-
Northing		-	-	-	-	-	-	-	-	-	-	-
Rock Type		Int.	Felsic	Int.	Int.	Felsic	Int.	Felsic	Int.	Felsic	Felsic	Int.
Sub-type		1	A	2	1	A	2	C	1	A	Anomalous	1
SiO <sub>2</sub> <sup>#</sup>	0.01	40.3	60.2	42.7	49.2	71.8	47.7	71.1	52.1	73	73.9	74.8
Al <sub>2</sub> O <sub>3</sub> <sup>#</sup>	0.01	19.95	18.05	14.65	16.9	12.2	16.55	12.3	15.7	13.7	10.7	7.07
Fe <sub>2</sub> O <sub>3</sub> <sup>#</sup>	0.01	12.8	7.49	19.2	11	5.74	7.75	2.19	9.03	3.46	2.15	8.25
CaO <sup>#</sup>	0.01	1.83	0.04	9.14	5.85	0.06	8.14	1.92	2.62	0.3	0.21	0.23
MgO <sup>#</sup>	0.01	12.1	5.45	5.92	8.53	3.93	6.58	2.17	4.97	1.68	7.36	3.97
Na <sub>2</sub> O <sup>#</sup>	0.01	0.88	0.06	2.27	2.3	0.03	1.63	3.97	3.03	0.13	0.07	0.12
K <sub>2</sub> O <sup>#</sup>	0.01	3.97	3.28	0.74	1.26	2.44	1.31	0.57	1.64	3.68	1.96	0.35
Cr <sub>2</sub> O <sub>3</sub> <sup>#</sup>	0.01	0.02	<0.01	0.02	0.02	<0.01	0.01	<0.01	0.01	<0.01	<0.01	<0.01
TiO <sub>2</sub> <sup>#</sup>	0.01	1.56	0.23	1.59	1.27	0.13	1.34	0.23	1.01	0.19	0.09	0.57
MnO <sup>#</sup>	0.01	0.18	0.05	0.19	0.18	0.08	0.09	0.03	0.08	0.01	0.02	0.06
P <sub>2</sub> O <sub>5</sub> <sup>#</sup>	0.01	0.45	<0.01	0.42	0.36	<0.01	0.31	0.04	0.21	0.07	0.04	0.17
SrO <sup>#</sup>	0.01	0.01	<0.01	0.03	0.02	<0.01	0.02	0.01	0.01	<0.01	<0.01	<0.01
BaO <sup>#</sup>	0.01	0.23	0.05	0.01	0.03	0.07	0.01	0.02	0.05	0.08	0.04	0.01
C <sup>@</sup>	0.01	<0.01	<0.01	0.17	<0.01	<0.01	0.96	0.73	1.05	0.05	0.02	0.03
S <sup>@</sup>	0.01	0.06	0.02	0.61	0.04	0.05	0.01	0.02	0.19	0.4	0.01	0.03
Ba <sup>*</sup>	0.5	1615	385	114	280	532	137	134.5	420	790	372	102.5
Ce <sup>*</sup>	0.5	52	131.5	78.3	52.5	77.7	38.3	136	42.8	155.5	7.7	40.2
Cr <sup>*</sup>	10	160	<10	130	130	<10	60	20	90	<10	<10	10
Cs <sup>*</sup>	0.01	3.26	0.92	0.43	1.36	1	1.92	0.29	0.93	1.74	1.29	0.31
Dy <sup>*</sup>	0.05	6.89	9.87	8.28	5.72	6.34	5.53	7.34	3.93	10.1	2.05	3.05

Table A2-1 (continued): Geochemical data for the rocks of the Hood deposits

Samples	Det. Limit	D1411695	D1411696	D1411697	D1411698	D1411700	D1410401	D1410402	D1410403	D1410405	D1410406	D1410408
Er*	0.03	3.6	5.44	4.49	3.21	4.08	3.38	4.48	2.42	6.11	2.03	1.79
Eu*	0.03	1.52	1.42	2.64	1.85	0.29	2.09	1.34	1.5	0.87	0.16	1
Ga*	0.1	24.1	29.3	17.7	19.9	19.2	23.2	16.6	19.9	23.3	16.6	12.5
Gd*	0.05	7.43	10.6	8.78	5.61	5.67	5.09	6.66	3.68	9	1.06	3.07
Hf*	0.2	5.1	15.1	5.8	4.3	8.7	4.7	7.1	4.5	10.7	8.5	3.5
Ho*	0.01	1.37	2.01	1.71	1.18	1.41	1.18	1.6	0.88	2.18	0.57	0.66
La*	0.5	22.3	70.4	36.4	24	37.7	18	72.5	21.1	76.9	3.9	20.1
Lu*	0.01	0.44	0.73	0.55	0.44	0.7	0.5	0.65	0.35	0.88	0.45	0.26
Nb*	0.2	12.5	21.1	12.7	10.9	21.8	12.8	15.6	9.3	25.7	12.2	8.2
Nd*	0.1	28.6	54.8	40.4	26.9	34.2	21	50.1	20	66.4	3.3	18.4
Pr*	0.03	6.54	14.1	9.45	6.33	8.79	4.72	14.05	5	17.55	0.86	4.54
Rb*	0.2	120.5	125	30.9	49.1	107.5	62.6	19.2	64.1	133.5	67.7	13.3
Sm*	0.03	6.81	11.1	8.6	5.91	6.74	4.99	8.49	4.27	12.7	0.77	3.85
Sn*	1	2	1	4	1	3	7	3	6	7	1	2
Sr*	0.1	43.7	4.6	268	135	4.4	176.5	103	76.3	12.4	5	5.6
Ta*	0.1	0.8	1.5	0.7	0.7	1.6	0.8	1.5	0.6	2	1.2	0.6
Tb*	0.01	1.13	1.64	1.34	0.91	0.95	0.83	1.09	0.62	1.52	0.25	0.49
Th*	0.05	4.35	23.7	1.36	3.81	16.9	1.13	22.4	3.9	22.9	15.25	4.58
Tl*	0.5	3.5	1.1	<0.5	1.1	0.5	<0.5	<0.5	0.5	0.8	0.9	0.5
Tm*	0.01	0.47	0.73	0.6	0.44	0.62	0.47	0.67	0.33	0.89	0.35	0.26
U*	0.05	1.04	4.4	0.39	0.74	5.63	0.88	4.73	0.95	6.08	3.13	1.17
V*	5	246	<5	213	212	<5	214	36	196	6	6	46
W*	1	16	2	5	2	2	5	4	4	3	1	10
Y*	0.5	35.5	47.8	41.7	31.1	33.9	33.4	43	23.2	57.5	18.3	19.6
Yb*	0.03	3.09	4.83	3.77	2.93	4.53	3.24	4.4	2.25	6.03	2.63	1.78
Zr*	20	218	555	267	188	294	229	242	208	402	319	162

Table A2-1 (continued): Geochemical data for the rocks of the Hood deposits

Samples	Det. Limit	D1411695	D1411696	D1411697	D1411698	D1411700	D1410401	D1410402	D1410403	D1410405	D1410406	D1410408
As <sup>^</sup>	0.1	1.6	<0.1	4	1.4	0.6	14.3	0.3	43.9	15.1	0.2	8.8
Bi <sup>^</sup>	0.01	0.04	0.38	0.12	0.06	0.2	0.05	0.15	0.22	0.33	0.03	0.44
Hg <sup>^</sup>	0.005	0.014	<0.005	<0.005	<0.005	<0.005	<0.005	<0.005	<0.005	<0.005	<0.005	0.005
Sb <sup>^</sup>	0.05	0.13	<0.05	0.07	0.16	0.08	0.08	0.3	0.28	0.2	0.5	0.26
Se <sup>^</sup>	0.2	0.8	0.2	1.5	0.5	0.3	0.3	0.3	0.3	1.8	<0.2	0.3
Te <sup>^</sup>	0.01	<0.01	0.02	0.01	<0.01	0.02	<0.01	0.03	0.02	0.04	<0.01	0.01
Ag <sup>+</sup>	0.5	<0.5	<0.5	<0.5	<0.5	<0.5	<0.5	<0.5	<0.5	<0.5	<0.5	<0.5
Cd <sup>+</sup>	0.5	<0.5	<0.5	<0.5	<0.5	<0.5	<0.5	<0.5	<0.5	<0.5	<0.5	<0.5
Co <sup>+</sup>	1	38	12	47	33	9	28	6	23	8	3	9
Cu <sup>+</sup>	1	5	10	885	17	21	5	4	24	215	5	111
Mo <sup>+</sup>	1	<1	3	<1	<1	3	<1	36	<1	2	<1	<1
Ni <sup>+</sup>	1	98	<1	95	72	<1	64	13	57	<1	<1	<1
Pb <sup>+</sup>	2	11	4	16	20	5	3	4	6	21	<2	29
Zn <sup>+</sup>	2	271	66	130	197	84	111	56	114	41	61	208
Sc <sup>+</sup>	1	-	-	-	-	-	-	-	-	-	-	-
LOI (ppm)	0.01	5.59	4.9	2.3	3.29	3.7	7.23	3.6	7.09	2.8	4.4	2.9
Total (ppm)	0.01	99.9	99.8	99.2	100	100	98.7	98.2	97.6	99.1	101	98.5
La <sup>CN</sup>		94.09	297.05	153.59	101.27	159.07	75.95	305.91	89.03	324.47	16.46	84.81
Yb <sup>CN</sup>		18.18	28.41	22.18	17.24	26.65	19.06	25.88	13.24	35.47	15.47	10.47
La/Yb <sup>CN</sup>		5.18	10.46	6.93	5.88	5.97	3.98	11.82	6.73	9.15	1.06	8.10
La/Sm		3.27	6.34	4.23	4.06	5.59	3.61	8.54	4.94	6.06	5.06	5.22
Zr/Yb		70.55	114.91	70.82	64.16	64.90	70.68	55.00	92.44	66.67	121.29	91.01
Zr/Hf		42.75	36.75	46.03	43.72	33.79	48.72	34.08	46.22	37.57	37.53	46.29
Zr/(TiO <sub>2</sub> *10000)		0.01	0.24	0.02	0.01	0.23	0.02	0.11	0.02	0.21	0.35	0.03
Nb/Yb		4.05	4.37	3.37	3.72	4.81	3.95	3.55	4.13	4.26	4.64	4.61
Nb/Ta		15.63	14.07	18.14	15.57	13.63	16.00	10.40	15.50	12.85	10.17	13.67
# wt%;lithium borate fusion												
@wt%; combustion furnace												
*ppm; lithium borate fusion												
+ppm; four-acid digestion												
^ppm; aqua regia digestion												
< ; below detection limit												
LOI; Loss on ignition												
CN; chondrite normalized												
- ; not analyzed												

Table A2-1 (continued): Geochemical data for the rocks of the Hood deposits

Samples	Det. Limit	D1410410	D1410411	D1410412	D1410413	D1410415	D1410416	D1410417	D1410418	D1410419	D1410420	D1410422
Deposit		H-10	H-10	H-10	H-10	H-10	H-10	H-10	H-10	H-10	H-10	H-10
Drillhole #		H-10-05	H-10-22	H-10-22	H-10-22	H-10-22	H-10-12	H-10-12	H-10-12	H-10-12	H-10-16	H-10-16
From (m)		106.28	30.81	87.21	121.38	187.76	9.25	13.59	46.93	64.27	2.1	105.9
To (m)		106.54	31.04	87.37	121.59	187.99	9.48	13.85	47.24	64.54	2.4	106.18
Easting		-	-	-	-	-	-	-	-	-	-	-
Northing		-	-	-	-	-	-	-	-	-	-	-
Rock Type		Felsic	Int.	Felsic	Felsic	Int.	Int.	Felsic	Int.	Int.	Felsic	Int.
Sub-type		A	4	A	A	1	1	Anomalous	1	1	A	1
SiO <sub>2</sub> <sup>#</sup>	0.01	63.3	55.9	79.1	74.8	47.8	52.1	72.7	48.4	52.6	75.6	53.8
Al <sub>2</sub> O <sub>3</sub> <sup>#</sup>	0.01	14.25	15.4	12.7	8.12	16.85	14.8	8.54	16.25	17.65	12.75	14.5
Fe <sub>2</sub> O <sub>3</sub> <sup>#</sup>	0.01	7.68	2.41	0.94	4.28	12.4	15.8	7.76	15.85	11.65	1.35	12.4
CaO <sup>#</sup>	0.01	0.1	0.43	0.26	0.03	0.52	0.44	0.1	0.46	0.42	0.35	0.36
MgO <sup>#</sup>	0.01	5.45	16.55	1.01	6.72	10.35	7.85	4.49	8.61	6.2	1.38	8.69
Na <sub>2</sub> O <sup>#</sup>	0.01	0.11	0.09	5.12	0.05	1.36	0.03	0.04	0.86	0.07	5.27	0.05
K <sub>2</sub> O <sup>#</sup>	0.01	2.47	1.32	0.92	0.69	0.74	0.8	0.7	0.75	2.9	0.66	1.13
Cr <sub>2</sub> O <sub>3</sub> <sup>#</sup>	0.01	<0.01	0.01	<0.01	<0.01	0.01	0.01	<0.01	0.01	0.01	<0.01	0.01
TiO <sub>2</sub> <sup>#</sup>	0.01	0.16	1.19	0.19	0.1	1.34	1.24	0.22	1.27	1.26	0.17	1.02
MnO <sup>#</sup>	0.01	0.04	0.04	0.01	0.04	0.09	0.12	0.05	0.08	0.07	0.01	0.09
P <sub>2</sub> O <sub>5</sub> <sup>#</sup>	0.01	<0.01	0.3	0.01	0.01	0.39	0.32	0.02	0.3	0.33	<0.01	0.25
SrO <sup>#</sup>	0.01	<0.01	<0.01	0.01	<0.01	<0.01	<0.01	<0.01	<0.01	<0.01	0.01	<0.01
BaO <sup>#</sup>	0.01	0.07	0.03	0.03	0.02	0.02	0.02	0.02	0.02	0.07	0.01	0.03
C <sup>@</sup>	0.01	0.03	<0.01	0.02	0.01	<0.01	0.02	0.03	0.05	0.01	0.07	<0.01
S <sup>@</sup>	0.01	0.02	0.02	0.01	0.01	0.02	0.04	0.01	0.02	0.04	0.01	0.01
Ba <sup>*</sup>	0.5	601	256	262	136.5	163	166.5	144	155.5	607	130.5	260
Ce <sup>*</sup>	0.5	120.5	10	45	71.2	47.9	76	88	60.6	67.4	132.5	53.9
Cr <sup>*</sup>	10	<10	70	10	<10	110	60	<10	60	80	10	70
Cs <sup>*</sup>	0.01	1.47	1.06	0.43	0.65	0.84	0.57	0.39	0.58	1.54	0.34	0.99
Dy <sup>*</sup>	0.05	9.2	10.95	5.17	5	5.99	6.45	6.71	6.31	6.76	9.73	5.83



Table A2-1 (continued): Geochemical data for the rocks of the Hood deposits

Samples	Det. Limit	D1410410	D1410411	D1410412	D1410413	D1410415	D1410416	D1410417	D1410418	D1410419	D1410420	D1410422
Er*	0.03	4.87	8.23	3.68	3.16	3.52	3.56	3.99	3.51	3.68	6.09	3.24
Eu*	0.03	1.7	0.41	0.79	0.63	1.18	1.69	0.92	2.26	1.71	1.11	1.39
Ga*	0.1	24.5	35.7	17.3	12.3	21.4	25.3	15.6	24.8	22.2	18.8	20.2
Gd*	0.05	9.38	6.32	4	4.65	5.77	6.75	6.56	6.03	6.99	8.51	5.25
Hf*	0.2	10.4	5.8	8.3	6.4	5.1	5.5	8.4	5.8	6	9.6	4.7
Ho*	0.01	1.86	2.74	1.18	1.08	1.27	1.33	1.43	1.31	1.41	2.08	1.23
La*	0.5	64.4	4.4	22.5	35.1	22.8	38	44.9	28.8	32.6	67.2	26.3
Lu*	0.01	0.68	1.09	0.62	0.5	0.46	0.47	0.58	0.46	0.51	0.91	0.41
Nb*	0.2	23.3	14	20	15.2	13.1	14.1	16.2	13.5	13	23.9	11.1
Nd*	0.1	51.2	6.2	18.6	30.1	24.4	36.5	38.4	29.7	32.8	52.2	26.6
Pr*	0.03	13.3	1.26	4.88	7.82	5.7	8.87	9.84	7.16	7.96	14.3	6.37
Rb*	0.2	80.7	44.7	27.6	22.2	24.4	28.6	23.6	26.9	94.1	20.3	42.1
Sm*	0.03	10.6	2.55	4.07	5.73	5.62	7.77	7.8	6.58	7.23	10.2	5.79
Sn*	1	5	1	3	2	5	4	3	11	5	2	6
Sr*	0.1	6.7	6.1	100.5	3.1	24.9	5.8	3.3	19.7	9.8	83.6	7
Ta*	0.1	2	0.9	1.8	1.2	0.8	0.9	1.3	0.9	0.9	2.1	0.7
Tb*	0.01	1.54	1.43	0.74	0.76	0.93	1.01	1.06	0.98	1.08	1.5	0.87
Th*	0.05	22.4	10.25	25.4	12.4	3.47	4.36	12.65	4.79	4.78	28.8	3.68
Tl*	0.5	1.1	<0.5	<0.5	<0.5	0.6	0.6	0.6	0.9	1.6	<0.5	3.1
Tm*	0.01	0.67	1.12	0.55	0.48	0.47	0.48	0.56	0.47	0.51	0.89	0.43
U*	0.05	5.45	1.55	5.94	3.23	0.91	1.12	3.41	1.23	1.13	6.39	0.95
V*	5	<5	240	9	7	210	204	5	199	198	5	173
W*	1	2	6	3	2	9	6	3	11	5	2	4
Y*	0.5	49.4	105.5	35.9	28.8	34.4	38.6	38.7	34.6	36.9	54.7	34.3
Yb*	0.03	4.64	7.45	3.93	3.33	3.17	3.07	3.9	3.22	3.35	6.03	2.85
Zr*	20	370	277	301	225	237	272	377	269	263	324	224

Table A2-1 (continued): Geochemical data for the rocks of the Hood deposits

Samples	Det. Limit	D1410410	D1410411	D1410412	D1410413	D1410415	D1410416	D1410417	D1410418	D1410419	D1410420	D1410422
As <sup>^</sup>	0.1	0.5	<0.1	<0.1	4.1	42.7	2.6	3.8	5	23	1.1	21.9
Bi <sup>^</sup>	0.01	0.1	0.02	0.04	0.2	0.18	0.31	0.07	0.1	0.11	0.13	0.07
Hg <sup>^</sup>	0.005	<0.005	<0.005	<0.005	<0.005	<0.005	<0.005	<0.005	<0.005	<0.005	<0.005	<0.005
Sb <sup>^</sup>	0.05	0.19	0.13	0.2	0.27	0.11	0.34	0.35	0.15	0.23	0.36	0.53
Se <sup>^</sup>	0.2	0.2	<0.2	<0.2	<0.2	0.2	0.2	<0.2	0.2	<0.2	0.2	<0.2
Te <sup>^</sup>	0.01	0.01	<0.01	<0.01	<0.01	0.01	0.05	<0.01	<0.01	0.01	0.01	<0.01
Ag <sup>+</sup>	0.5	<0.5	<0.5	<0.5	<0.5	<0.5	<0.5	<0.5	<0.5	<0.5	<0.5	<0.5
Cd <sup>+</sup>	0.5	<0.5	<0.5	<0.5	<0.5	<0.5	<0.5	<0.5	<0.5	<0.5	<0.5	<0.5
Co <sup>+</sup>	1	4	4	2	17	29	22	12	12	30	3	16
Cu <sup>+</sup>	1	36	<1	1	15	1	10	7	1	1	3	3
Mo <sup>+</sup>	1	1	<1	7	1	4	32	<1	1	<1	<1	<1
Ni <sup>+</sup>	1	<1	49	1	5	94	58	<1	51	56	1	69
Pb <sup>+</sup>	2	<2	<2	2	14	4	<2	3	9	<2	3	4
Zn <sup>+</sup>	2	105	59	8	114	217	209	108	235	68	18	201
Sc <sup>+</sup>	1	-	-	-	-	-	-	-	-	-	-	-
LOI (ppm)	0.01	4.3	7.6	1	3.9	5.89	5.59	3.4	5.69	5.4	1	5.4
Total (ppm)	0.01	97.9	101.5	101.5	98.8	97.8	99.1	98	98.6	98.6	98.6	97.7
La <sup>CN</sup>		271.73	18.57	94.94	148.10	96.20	160.34	189.45	121.52	137.55	283.54	110.97
Yb <sup>CN</sup>		27.29	43.82	23.12	19.59	18.65	18.06	22.94	18.94	19.71	35.47	16.76
La/Yb <sup>CN</sup>		9.96	0.42	4.11	7.56	5.16	8.88	8.26	6.42	6.98	7.99	6.62
La/Sm		6.08	1.73	5.53	6.13	4.06	4.89	5.76	4.38	4.51	6.59	4.54
Zr/Yb		79.74	37.18	76.59	67.57	74.76	88.60	96.67	83.54	78.51	53.73	78.60
Zr/Hf		35.58	47.76	36.27	35.16	46.47	49.45	44.88	46.38	43.83	33.75	47.66
Zr/(TiO <sub>2</sub> *10000)		0.23	0.02	0.16	0.23	0.02	0.02	0.17	0.02	0.02	0.19	0.02
Nb/Yb		5.02	1.88	5.09	4.56	4.13	4.59	4.15	4.19	3.88	3.96	3.89
Nb/Ta		11.65	15.56	11.11	12.67	16.38	15.67	12.46	15.00	14.44	11.38	15.86
# wt%;lithium borate fusion @wt%; combustion furnace *ppm; lithium borate fusion +ppm; four-acid digestion ^ppm; aqua regia digestion < ; below detection limit LOI; Loss on ignition CN; chondrite normalized - ; not analyzed												

Table A2-1 (continued): Geochemical data for the rocks of the Hood deposits

Samples	Det. Limit	D1410423	D1410424	D1410425	D1410426	D1410427	D1410428	D1410429	D1410430	R143430
Deposit		H-10	H-10	H-10	H-10	H-10	H-10	H-10	H-10	-
Drillhole #		H-10-16	H-10-02	H-10-22	H-10-27	H-10-27	H-10-27	H-10-27	H-10-27	-
From (m)		156.55	106.3	78.03	27.1	110.59	163.49	186.26	232.65	-
To (m)		156.78	112.6	82.18	27.29	110.81	163.68	186.46	232.87	-
Easting		-	-	-	-	-	-	-	-	419868
Northing		-	-	-	-	-	-	-	-	7325866
Rock Type		Int.	Felsic	Felsic	Felsic	Mafic	Felsic	Int.	Felsic	Felsic
Sub-type		1	A	B	A	II	A	3	A	Rim Granite
SiO <sub>2</sub> <sup>#</sup>	0.01	59.8	81.4	78.2	76.5	49.7	46.1	60.9	76.4	76.5
Al <sub>2</sub> O <sub>3</sub> <sup>#</sup>	0.01	10.8	7.68	12.35	10.6	12.35	11.35	16.8	9.62	11.35
Fe <sub>2</sub> O <sub>3</sub> <sup>#</sup>	0.01	11.5	2.1	0.63	2.44	13.45	3.47	6.38	4.26	2.02
CaO <sup>#</sup>	0.01	0.58	0.22	0.68	0.09	5.45	0.83	0.64	0.04	0.37
MgO <sup>#</sup>	0.01	7.97	1.96	0.57	2.9	6.91	25.7	5.35	2.91	0.42
Na <sub>2</sub> O <sup>#</sup>	0.01	0.02	1.17	5.21	0.1	1.7	0.06	3.56	0.05	3.85
K <sub>2</sub> O <sup>#</sup>	0.01	0.19	1.13	0.76	2.35	0.07	6.95	1.5	1.82	3.84
Cr <sub>2</sub> O <sub>3</sub> <sup>#</sup>	0.01	<0.01	<0.01	<0.01	<0.01	0.06	<0.01	<0.01	<0.01	<0.01
TiO <sub>2</sub> <sup>#</sup>	0.01	1.31	0.1	0.16	0.14	1.96	0.16	1.5	0.12	0.14
MnO <sup>#</sup>	0.01	0.09	0.02	0.01	0.02	0.16	0.03	0.03	0.03	0.02
P <sub>2</sub> O <sub>5</sub> <sup>#</sup>	0.01	0.43	0.01	0.02	0.02	0.21	0.01	0.34	0.01	<0.01
SrO <sup>#</sup>	0.01	<0.01	<0.01	0.01	<0.01	0.01	<0.01	0.01	<0.01	<0.02
BaO <sup>#</sup>	0.01	0.01	0.05	0.02	0.09	<0.01	0.03	0.03	0.06	0.11
C <sup>@</sup>	0.01	0.01	0.04	0.12	0.03	1.09	0.12	0.03	<0.01	0.07
S <sup>@</sup>	0.01	0.01	0.01	0.02	0.01	0.34	0.01	0.01	0.01	0.01
Ba <sup>*</sup>	0.5	50.6	408	198.5	752	24.7	270	303	544	958
Ce <sup>*</sup>	0.5	37.1	58.7	130.5	100.5	29.5	3.5	105.5	89.4	161
Cr <sup>*</sup>	10	<10	<10	10	10	380	<10	10	<10	20
Cs <sup>*</sup>	0.01	0.24	0.66	0.36	0.77	0.26	18.95	0.97	1.06	0.39
Dy <sup>*</sup>	0.05	6.79	5.11	8.78	7.3	5.36	1.36	9.12	5.18	13.1

Table A2-1 (continued): Geochemical data for the rocks of the Hood deposits

Samples	Det. Limit	D1410423	D1410424	D1410425	D1410426	D1410427	D1410428	D1410429	D1410430	R143430
Er*	0.03	4.16	3.34	4.98	4.36	2.97	1.07	5.25	3.42	8.16
Eu*	0.03	0.77	0.5	1.66	0.91	1.69	0.34	1.75	0.41	1.84
Ga*	0.1	16.8	11.9	19.5	17.6	17.4	55.8	32.8	15.7	20.5
Gd*	0.05	6.31	4.98	9.33	7.83	5.8	1.07	9.94	5.59	14.55
Hf*	0.2	7.1	5.7	7.6	7.9	4	7.9	7.9	6.6	9.6
Ho*	0.01	1.41	1.11	1.73	1.48	1.04	0.32	1.86	1.11	2.79
La*	0.5	17.3	29.7	71.3	51.2	13.3	0.5	46	43.3	86
Lu*	0.01	0.65	0.6	0.78	0.71	0.44	0.21	0.8	0.62	1.25
Nb*	0.2	17.8	14	17.3	18.4	7.8	15.7	18.6	13.8	37.4
Nd*	0.1	21.3	26.2	53.7	44.7	19.5	1.7	51.5	35.9	75.4
Pr*	0.03	4.93	7.01	14.75	11.95	4.18	0.4	13.7	10.3	20.8
Rb*	0.2	7	41.2	23.3	73.4	1.9	321	57	65.7	104.5
Sm*	0.03	5.55	5.5	10.85	9.28	5.37	0.56	11.9	7.29	14.5
Sn*	1	1	4	21	3	2	<1	16	4	3
Sr*	0.1	8.7	28.4	91.5	6.7	82.6	7.6	56.8	4	45.9
Ta*	0.1	1.1	1.1	1.6	1.4	0.7	1.5	1.3	1.3	2.8
Tb*	0.01	1.07	0.82	1.47	1.24	0.91	0.19	1.57	0.86	2.16
Th*	0.05	5.26	12.55	23.6	14.45	4.9	76.9	10.65	19.6	23.7
Tl*	0.5	<0.5	<0.5	<0.5	<0.5	<0.5	4.9	1.4	2.7	0.25
Tm*	0.01	0.66	0.57	0.8	0.69	0.44	0.18	0.8	0.54	1.25
U*	0.05	1.57	3.38	5.42	3.65	1.95	3.14	3.51	4.73	2.36
V*	5	87	<5	<5	<5	214	56	223	<5	12
W*	1	9	2	2	2	2	<1	9	2	0.5
Y*	0.5	40	30.1	48.4	40.9	28	9.8	51.6	31.8	82
Yb*	0.03	3.83	3.36	4.63	4.05	2.54	1.24	4.87	3.67	8.3
Zr*	20	289	188	236	275	140	283	320	222	260

Table A2-1 (continued): Geochemical data for the rocks of the Hood deposits

Samples	Det. Limit	D1410423	D1410424	D1410425	D1410426	D1410427	D1410428	D1410429	D1410430	R143430
As <sup>^</sup>	0.1	21	0.2	1.1	0.1	3	0.3	9.4	7	0.2
Bi <sup>^</sup>	0.01	0.22	0.2	1.13	0.08	0.47	0.02	0.29	0.03	0.02
Hg <sup>^</sup>	0.005	<0.005	<0.005	<0.005	<0.005	<0.005	<0.005	<0.005	<0.005	<0.005
Sb <sup>^</sup>	0.05	0.69	0.17	0.38	0.06	0.2	1.74	0.32	0.26	<0.05
Se <sup>^</sup>	0.2	0.2	<0.2	0.3	0.2	0.6	0.2	0.2	0.2	0.9
Te <sup>^</sup>	0.01	0.01	0.01	0.02	<0.01	0.01	<0.01	0.02	<0.01	<0.01
Ag <sup>+</sup>	0.5	<0.5	<0.5	<0.5	<0.5	<0.5	<0.5	<0.5	<0.5	<0.5
Cd <sup>+</sup>	0.5	<0.5	<0.5	<0.5	<0.5	<0.5	<0.5	<0.5	<0.5	<0.5
Co <sup>+</sup>	1	25	3	1	3	45	6	9	8	1
Cu <sup>+</sup>	1	7	26	4	5	73	7	6	3	1
Mo <sup>+</sup>	1	2	2	2	<1	<1	<1	<1	1	<1
Ni <sup>+</sup>	1	8	1	3	<1	167	21	11	<1	<1
Pb <sup>+</sup>	2	<2	7	26	3	<2	17	4	2	5
Zn <sup>+</sup>	2	118	31	5	34	104	141	98	76	13
Sc <sup>+</sup>	1	-	-	-	-	-	-	-	-	2
LOI (ppm)	0.01	4.8	2.2	1.2	2.6	7.5	4.1	3.9	2.6	1.16
Total (ppm)	0.01	97.5	98	99.8	97.9	99.5	98.8	101	97.9	99.79
La <sup>CN</sup>		73.00	125.32	300.84	216.03	56.12	2.11	194.09	182.70	362.87
Yb <sup>CN</sup>		22.53	19.76	27.24	23.82	14.94	7.29	28.65	21.59	48.82
La/Yb <sup>CN</sup>		3.24	6.34	11.05	9.07	3.76	0.29	6.78	8.46	7.43
La/Sm		3.12	5.40	6.57	5.52	2.48	0.89	3.87	5.94	5.93
Zr/Yb		75.46	55.95	50.97	67.90	55.12	228.23	65.71	60.49	31.33
Zr/Hf		40.70	32.98	31.05	34.81	35.00	35.82	40.51	33.64	27.08
Zr/(TiO <sub>2</sub> *10000)		0.02	0.19	0.15	0.20	0.01	0.18	0.02	0.19	0.19
Nb/Yb		4.65	4.17	3.74	4.54	3.07	12.66	3.82	3.76	4.51
Nb/Ta		16.18	12.73	10.81	13.14	11.14	10.47	14.31	10.62	13.36
# wt%; lithium borate fusion										LOI; Loss on
@wt%; combustion furnace										CN; chondrite
*ppm; lithium borate fusion										- ; not analyzed
+ppm; four-acid digestion										
^ppm; aqua regia digestion										
< ; below detection limit										

Table A2-2: Major element mass change based on the MacLean (1990) multiple precursor method, SWIR mineralogy, and alteration indexes.

Samples	D1425001	D1425002	D1425003	D1425004	D1425005	D1425006	D1425007	D1425008	D1425009	D1425010	D1425011	D1425012	D1425013	D1425014	D1425015
Rock Type	Mafic	Felsic	Felsic	Felsic	Felsic	Felsic	Inter	Mafic	Felsic	Felsic	Felsic	Felsic	Felsic	Mafic	Mafic
Sub-type	I	Tuff Group	B	B	B	B	1	I	A	A	A	A	A	III	III
SWIR Min 1	FeMgChlorite	FeMgChlorite	FeMgChlorite	Muscovite	Muscovite	Muscovite	FeMgChlorite	FeMgChlorite	Muscovite	Illitic Muscovite	Illitic Muscovite	Muscovite	FeMgChlorite	FeMgChlorite	FeMgChlorite
SWIR MIN 2	-	Muscovite	Muscovite	-	FeMgChlorite	FeMgChlorite	Phengite	Hornblende	FeMgChlorite	FeMgChlorite	FeMgChlorite	FeMgChlorite	Muscovite	-	-
$\Delta\text{Al}_2\text{O}_3^\#$	-0.82	-0.80	2.21	2.22	2.22	2.20	-0.19	-0.83	2.24	2.25	2.24	2.24	2.23	-0.08	-0.12
$\Delta\text{TiO}_2^\#$	-0.19	-0.98	0.01	0.01	0.00	0.02	-0.27	-0.21	-0.06	-0.06	-0.06	-0.05	-0.09	1.98	1.98
$\Delta\text{CaO}^\#$	8.98	5.47	-0.71	0.68	-0.56	0.23	-2.65	12.05	-1.11	0.37	1.88	0.89	-0.12	5.75	5.41
$\Delta\text{MgO}^\#$	12.82	1.92	2.11	0.53	1.90	1.27	0.91	10.73	1.39	0.43	0.94	0.55	2.19	-0.71	-0.18
$\Delta\text{SiO}_2^\#$	22.69	4.93	24.32	45.64	35.64	24.96	-3.10	22.35	14.78	24.43	34.25	44.63	58.16	-5.16	-4.82
$\Delta\text{Fe}_2\text{O}_3^\#$	8.03	1.46	0.67	-2.03	0.66	-1.08	2.31	7.67	-1.67	-1.91	-1.45	-0.82	1.12	6.66	6.95
$\Delta\text{Na}_2\text{O}^\#$	-4.59	-4.22	-3.09	0.23	-3.18	-2.04	-1.31	-2.39	-2.64	-1.42	-1.03	-0.22	-2.37	-1.02	-1.61
$\Delta\text{K}_2\text{O}^\#$	-1.10	0.78	1.83	1.16	2.04	1.86	-0.48	-1.15	2.61	2.25	2.00	1.39	2.06	-0.18	0.62
Total major element mass change (wt%)	45.82	8.56	27.36	48.45	38.71	27.42	-4.78	48.21	15.54	26.33	38.77	48.59	63.17	7.24	8.22
$\Delta\text{Cu}^\oplus$	194.03	125.12	-7.53	-8.39	-8.30	-7.99	-14.27	198.48	-11.16	-11.04	-10.52	-11.24	-10.58	35.34	42.94
$\Delta\text{Zn}^\oplus$	122.10	33.82	-29.34	-44.90	-26.32	-29.40	85.38	96.14	-16.67	-37.53	-32.27	-21.59	2.23	64.88	39.53
$\Delta\text{Pb}^\oplus$	43.99	57.20	-1.07	-1.99	7.45	0.30	-1.70	27.76	-4.48	-4.37	-4.29	32.84	-2.49	16.37	6.10
$\Delta\text{Cs}^\oplus$	-1.02	-1.24	1.26	1.18	1.23	1.44	-1.31	-0.99	2.13	1.68	1.55	1.26	1.33	3.67	2.70
$\Delta\text{Rb}^\oplus$	-40.39	19.49	48.21	46.40	53.72	58.24	-9.16	-35.16	106.07	85.40	76.12	43.80	66.96	9.29	32.47
$\Delta\text{Ba}^\oplus$	-317.42	180.21	981.36	487.92	1543.24	1106.44	-227.67	-241.14	124.61	450.19	377.42	851.15	529.34	74.17	443.53
$\Delta\text{Nb}^\oplus$	-3.08	-8.44	8.82	7.83	9.12	10.09	0.37	-3.45	12.83	13.34	12.92	14.34	12.79	18.15	18.42
$\Delta\text{Zr}^\oplus$	-73.38	299.44	5.92	-10.91	-15.95	10.51	12.48	-61.36	53.39	59.19	63.13	87.04	39.80	40.38	41.97
$\Delta\text{La}^\oplus$	-1.95	-11.20	-6.44	0.61	3.47	-6.42	-3.94	-6.41	2.34	4.50	-3.26	4.40	-9.28	8.68	8.29
$\Delta\text{Sm}^\oplus$	0.58	-2.93	2.64	3.24	3.45	2.34	-0.66	-0.72	3.85	3.57	3.13	3.41	2.01	3.20	3.28
$\Delta\text{Yb}^\oplus$	-1.77	-2.15	-1.27	-1.38	-1.26	-1.22	-1.88	-1.79	-1.61	-1.54	-1.62	-1.63	-1.77	-0.69	-0.68
Al	61.57	54.35	92.05	48.25	91.59	71.02	69.15	50.46	92.83	64.45	54.52	51.02	80.42	35.32	41.62
CCPI	99.16	89.14	61.63	28.23	60.75	43.91	83.84	93.54	51.66	40.54	46.41	47.00	67.24	83.73	83.56

# wt%

Al; Alteration Index =  $100 * (\text{K}_2\text{O} + \text{MgO}) / (\text{K}_2\text{O} + \text{MgO} + \text{CaO} + \text{Na}_2\text{O})$

CCPI =  $100 * (\text{Fe}_2\text{O}_3 + \text{MgO}) / (\text{Fe}_2\text{O}_3 + \text{MgO} + \text{K}_2\text{O} + \text{Na}_2\text{O})$

Least Altered samples

Table A2-2 (continued): Major element mass change based on the MacLean (1990) multiple precursor method, SWIR mineralogy, and alteration indexes.

Samples	D1425016	D1425017	D1425018	D1425019	D1425020	D1425021	D1425022	D1425023	D1425024	D1425025	D1425026	D1425027	D1425028	D1425029	D1425030
Rock Type	Int.	Int.	Int.	Int.	Int.	Felsic	Int.	Int.	Felsic	Felsic	Int.	Int.	Int.	Int.	Int.
Sub-type	1	1	1	1	1	A	1	1	A	A	1	1	1	1	1
SWIR Min 1	FeMgChlorite	FeMgChlorite	FeMgChlorite	FeMgChlorite	FeMgChlorite	Phengite	FeMgChlorite	FeMgChlorite	FeMgChlorite	FeMgChlorite	FeMgChlorite	FeMgChlorite	FeMgChlorite	FeMgChlorite	-
SWIR MIN 2	-	Phengite	Phengite	Phengite	-	-	Phengite	Hornblende	Muscovite	-	Hornblende	Hornblende	-	-	-
$\Delta\text{Al}_2\text{O}_3^\#$	0.79	0.77	0.81	0.96	0.79	2.22	0.78	0.37	2.21	2.21	0.33	0.38	-0.09	-0.14	-0.09
$\Delta\text{TlO}_{2\#}$	0.34	0.33	0.34	0.34	0.37	-0.08	0.33	0.19	-0.08	-0.09	0.13	0.16	-0.24	-0.36	-0.29
$\Delta\text{CaO}^\#$	-0.80	-2.05	-1.56	2.18	2.35	-0.22	-0.86	1.43	-0.70	1.49	2.97	2.16	-2.02	-2.53	-2.45
$\Delta\text{MgO}^\#$	4.50	2.25	2.00	-0.28	-0.17	-0.09	1.47	-0.59	-0.10	-0.25	1.55	-0.47	4.79	3.53	3.62
$\Delta\text{SiO}_2^\#$	-3.59	0.73	-0.41	1.65	0.77	28.79	-2.14	2.73	26.68	26.05	3.97	5.17	1.56	4.85	5.80
$\Delta\text{Fe}_2\text{O}_3^\#$	1.99	3.49	4.36	2.62	1.30	-1.70	2.08	-0.55	-2.06	-0.79	-0.87	0.18	-0.33	-1.57	-1.54
$\Delta\text{Na}_2\text{O}^\#$	-0.64	-2.94	-2.29	0.75	-0.48	1.64	-0.61	2.12	3.35	4.30	1.03	1.73	-1.06	-3.63	-3.41
$\Delta\text{K}_2\text{O}^\#$	0.00	1.27	0.72	-0.12	0.60	0.85	0.02	-0.10	-0.46	-1.12	-0.11	-0.43	-0.97	1.01	0.91
Total major element mass change (wt%)	2.58	3.86	3.98	8.10	5.53	31.41	1.06	5.60	28.85	31.79	9.01	8.89	1.63	1.17	2.56
$\Delta\text{Cu}^\oplus$	-15.02	-15.02	-15.02	-9.04	197.90	-11.03	-15.03	-13.25	-11.80	-11.85	-14.72	-7.84	23.35	290.92	466.26
$\Delta\text{Zn}^\oplus$	15.24	-27.00	-2.95	41.67	-9.96	-50.98	18.90	-13.69	-49.27	-42.42	-3.66	-21.23	62.85	57.47	56.25
$\Delta\text{Pb}^\oplus$	-3.31	-3.29	-2.27	-3.53	3.08	-0.62	-1.28	0.46	0.59	-4.46	-0.28	-1.53	-1.80	-1.73	-1.79
$\Delta\text{Cs}^\oplus$	1.81	0.43	0.03	-0.34	-0.19	0.89	-0.30	-0.98	0.30	0.02	-0.89	-1.01	-1.50	-0.86	-0.84
$\Delta\text{Rb}^\oplus$	21.75	45.45	29.33	1.86	25.94	37.46	8.42	-7.26	-5.10	-29.70	-8.64	-16.17	-32.74	29.61	26.18
$\Delta\text{Ba}^\oplus$	-110.15	277.82	309.94	-104.85	72.86	224.62	-131.41	90.17	-21.41	-266.31	342.94	-66.02	-175.00	369.29	345.97
$\Delta\text{Nb}^\oplus$	-2.15	-2.33	-1.92	-1.25	-2.81	12.20	-2.12	2.47	11.96	12.74	1.75	1.75	-0.07	-1.10	-0.33
$\Delta\text{Zr}^\oplus$	-42.64	-52.19	-38.93	-51.29	-47.72	83.81	-45.88	42.88	79.60	79.11	21.22	20.99	12.57	-6.58	-3.99
$\Delta\text{La}^\oplus$	-7.67	-5.74	-6.00	-9.01	-4.83	4.15	-2.22	4.87	17.31	12.20	14.17	6.79	1.17	12.63	11.07
$\Delta\text{Sm}^\oplus$	-1.32	-1.21	-1.28	-1.10	-1.00	3.97	-0.45	1.13	4.54	3.58	1.70	0.63	0.13	1.77	1.84
$\Delta\text{Yb}^\oplus$	-2.50	-2.49	-2.50	-2.67	-2.48	-1.83	-2.51	-2.02	-1.73	-1.66	-2.13	-2.09	-1.99	-1.96	-1.97
Al	68.50	88.26	78.57	36.91	43.97	41.28	60.92	36.71	28.05	15.96	43.07	35.10	72.21	89.92	88.32
CCPI	82.50	85.89	85.87	73.30	73.98	35.42	79.78	64.64	32.61	38.16	71.32	68.44	85.68	86.31	85.97

# wt%

Al; Alteration Index =  $100 * (\text{K}_2\text{O} + \text{MgO}) / (\text{K}_2\text{O} + \text{MgO} + \text{CaO} + \text{Na}_2\text{O})$

CCPI =  $100 * (\text{Fe}_2\text{O}_3 + \text{MgO}) / (\text{Fe}_2\text{O}_3 + \text{MgO} + \text{K}_2\text{O} + \text{Na}_2\text{O})$

Least Altered samples

Table A2-2 (continued): Major element mass change based on the MacLean (1990) multiple precursor method, SWIR mineralogy, and alteration indexes.

Samples	D1425031	D1425032	D1425033	D1425034	D1425035	D1425036	D1425037	D1425038	D1425039	D1425040	D1425041	D1425042	D1425043	D1425044	D1425045
Rock Type	Mafic	Int.	Int.	Felsic	Felsic	Mafic	Felsic	Int.	Mafic	Felsic	Int.	Int.	Int.	Int.	Int.
Sub-type	I	1	1	A	A	II	A	1	II	A	1	1	1	1	1
SWIR Min 1	FeMgChlorite	FeMgChlorite	FeMgChlorite	Muscovite	FeMgChlorite	FeMgChlorite	FeMgChlorite	FeMgChlorite	FeMgChlorite	Muscovite	FeMgChlorite	FeMgChlorite	FeMgChlorite	FeMgChlorite	MgChlorite
SWIR MIN 2	-	Phengite	-	FeMgChlorite	Muscovite	-	Muscovite	-	-	-	-	Muscovite	Muscovite	-	Phengite
$\Delta\text{Al}_2\text{O}_3^\#$	-0.83	-0.08	1.39	2.25	2.26	-0.49	2.19	2.00	0.26	2.26	0.25	0.05	0.29	-9.25	0.13
$\Delta\text{TiO}_2^\#$	0.55	-0.22	0.08	-0.05	-0.02	-0.01	0.05	0.52	1.46	-0.01	0.23	-0.16	0.28	-2.04	-0.04
$\Delta\text{CaO}^\#$	4.91	-2.41	-0.55	-1.14	-1.01	8.50	-0.77	3.42	4.49	-1.12	-2.35	-2.44	-2.55	7.89	-2.48
$\Delta\text{MgO}^\#$	2.63	2.20	-0.86	2.60	8.46	3.86	5.03	1.82	3.70	1.19	3.00	5.32	1.37	-3.90	4.62
$\Delta\text{SiO}_2^\#$	3.97	4.48	0.53	56.09	-8.17	8.22	192.35	35.03	6.59	-5.63	2.02	27.83	-1.30	26.25	1.32
$\Delta\text{Fe}_2\text{O}_3^\#$	4.99	2.31	0.04	-0.36	4.60	5.60	4.44	3.64	10.70	-1.47	-0.02	4.29	-2.91	10.39	-3.23
$\Delta\text{Na}_2\text{O}^\#$	-2.48	-4.02	2.71	-2.53	-3.13	-2.75	-2.29	2.38	-2.16	-3.06	-3.79	-3.44	-3.67	-15.84	-3.70
$\Delta\text{K}_2\text{O}^\#$	-1.04	0.94	-0.53	2.34	0.59	-1.26	0.47	-1.02	-0.61	2.82	1.24	-0.57	2.12	-10.71	2.62
Total major element mass change (wt%)	12.71	3.20	2.81	59.21	3.57	21.67	201.45	47.81	24.43	-5.04	0.59	30.88	-6.36	2.80	-0.75
$\Delta\text{Cu}^\oplus$	115.77	-9.71	-6.32	-10.06	-8.82	67.09	90.38	33.93	31.57	-10.47	-14.18	-9.73	-14.28	85.27	-13.08
$\Delta\text{Zn}^\oplus$	145.42	84.37	-39.03	-25.89	41.03	69.51	20.29	-4.26	68.94	-47.18	-9.49	6.43	-34.76	533.14	-22.88
$\Delta\text{Pb}^\oplus$	22.30	-1.82	-4.22	-4.03	-4.41	5.64	-1.73	-1.49	2.86	-4.51	-2.42	-1.77	-2.56	40.72	-2.23
$\Delta\text{Cs}^\oplus$	-2.08	-0.85	-0.25	0.91	0.94	-1.85	0.39	0.17	1.58	0.86	-0.47	-1.19	-0.22	-13.38	4.71
$\Delta\text{Rb}^\oplus$	-36.99	25.92	-13.11	63.39	22.44	-41.23	9.84	-26.07	-0.29	73.32	37.48	-17.39	66.55	-442.15	117.57
$\Delta\text{Ba}^\oplus$	-229.07	476.42	-12.14	704.78	-41.18	-316.04	181.28	-200.44	-234.07	898.04	228.85	-155.01	509.11	-1290.07	515.10
$\Delta\text{Nb}^\oplus$	2.66	-0.09	-2.59	15.68	15.23	-0.94	8.60	15.20	-2.21	13.20	2.48	0.57	3.68	33.19	0.37
$\Delta\text{Zr}^\oplus$	0.46	1.43	-57.30	57.73	98.48	3.20	134.56	-47.83	-37.90	106.55	48.92	10.47	67.44	1490.30	12.55
$\Delta\text{La}^\oplus$	-4.08	3.83	-5.34	-17.11	5.87	-0.85	-44.04	-11.79	-11.61	-22.75	0.40	-2.59	3.63	101.50	-3.62
$\Delta\text{Sm}^\oplus$	0.95	0.71	-1.44	1.70	4.17	0.24	-2.78	2.30	0.84	0.22	1.09	-0.87	0.94	45.35	0.80
$\Delta\text{Yb}^\oplus$	-1.42	-2.00	-2.77	-1.41	-1.48	-1.87	-1.25	-1.81	-2.32	-1.52	-2.05	-2.13	-2.04	13.68	-2.08
Al	49.00	91.26	31.24	92.71	98.66	44.15	86.26	30.20	51.80	98.17	93.02	89.69	93.66	40.61	93.75
CCPI	91.01	89.75	59.20	62.09	88.19	93.91	77.60	69.45	92.61	49.59	87.27	95.25	78.38	82.60	79.76

# wt%

Al; Alteration Index =  $100 \times (\text{K}_2\text{O} + \text{MgO}) / (\text{K}_2\text{O} + \text{MgO} + \text{CaO} + \text{Na}_2\text{O})$

CCPI =  $100 \times (\text{Fe}_2\text{O}_3 + \text{MgO}) / (\text{Fe}_2\text{O}_3 + \text{MgO} + \text{K}_2\text{O} + \text{Na}_2\text{O})$

Least Altered samples



Table A2-2 (continued): Major element mass change based on the MacLean (1990) multiple precursor method, SWIR mineralogy, and alteration indexes.

Samples	D1425046	D1425047	D1425048	D1425049	D1425050	D1425051	D1425052	D1425053	D1425054	D1425055	D1425056	D1425057	D1425058	D1425059	D1425060
Rock Type	Felsic	Int.	Felsic	Felsic	Felsic	Felsic	Int.	Felsic	Felsic	Mafic	Felsic	Int.	Int.	Int.	Int.
Sub-type	A		A	C	C	B	1	B	B	II	A	1	1	1	1
SWIR Min 1	MgChlorite	MgChlorite	MgChlorite	FelMgChlorite	FelMgChlorite	FelMgChlorite	Muscovite	Muscovite	Muscovite	FelMgChlorite	Phengite	FelMgChlorite	FelMgChlorite	FelMgChlorite	MgChlorite
SWIR MIN 2	Muscovite	Muscovite	Muscovite	Muscovite	Muscovite	Muscovite	-	FelMgChlorite	FelMgChlorite	-	FelMgChlorite	Phengite	Phengite	-	Phengite
$\Delta\text{Al}_2\text{O}_3^\#$	2.25	1.51	2.26	2.25	2.25	2.11	-0.09	2.11	2.14	0.16	2.05	1.18	1.30	0.02	0.85
$\Delta\text{TiO}_2^\#$	0.02	0.48	-0.02	0.07	0.08	0.03	-0.16	0.04	0.02	1.07	0.05	-0.03	0.01	0.17	-0.14
$\Delta\text{CaO}^\#$	-0.98	-1.79	-1.14	-1.09	-1.07	-0.67	-0.38	-0.79	-0.67	-0.81	-0.63	-1.52	-0.22	3.08	-1.11
$\Delta\text{MgO}^\#$	7.60	10.65	2.71	2.73	2.64	0.55	4.99	2.31	2.32	0.43	1.81	-0.23	0.39	0.48	1.04
$\Delta\text{SiO}_2^\#$	153.97	-7.72	19.51	18.99	17.59	20.31	5.21	14.33	22.14	2.08	9.23	5.21	2.46	0.60	1.76
$\Delta\text{Fe}_2\text{O}_3^\#$	1.49	-0.27	-0.06	1.48	1.33	-0.21	2.87	1.68	0.60	7.58	1.37	-0.23	-0.79	4.48	-2.98
$\Delta\text{Na}_2\text{O}^\#$	-3.12	-3.03	-3.09	-3.04	-3.06	-3.67	-4.05	-3.70	-1.90	-0.48	-3.71	0.88	-1.91	-0.42	-0.85
$\Delta\text{K}_2\text{O}^\#$	0.99	0.24	2.18	1.82	1.82	2.32	0.24	1.81	1.13	-1.10	2.37	1.05	2.25	-0.84	1.60
Total major element mass change (wt%)	162.22	0.08	22.33	23.21	21.59	20.76	8.64	17.79	25.77	8.93	12.53	6.32	3.49	7.57	0.16
$\Delta\text{Cu}^\oplus$	-4.72	-12.25	-10.41	-10.26	-8.82	17.16	55.42	-3.38	-6.71	54.45	-3.82	-12.43	-3.02	58.31	-0.22
$\Delta\text{Zn}^\oplus$	-18.79	-8.19	-33.23	28.65	30.41	-1.84	181.18	27.46	23.74	183.78	29.74	32.48	12.25	173.02	-35.34
$\Delta\text{Pb}^\oplus$	-2.59	-4.36	-4.26	-4.36	-4.32	0.53	-1.69	-3.11	-3.17	1.21	1.63	-3.89	-4.08	-0.81	-3.42
$\Delta\text{Cs}^\oplus$	1.28	0.36	1.25	0.90	0.94	0.73	-1.07	0.69	0.62	-1.36	1.22	0.05	0.90	-1.40	0.38
$\Delta\text{Rb}^\oplus$	30.48	13.76	64.02	54.34	54.37	58.45	8.60	42.21	27.22	-35.24	85.14	29.76	76.55	-30.02	39.32
$\Delta\text{Ba}^\oplus$	207.04	-39.28	245.69	68.93	84.30	-31.92	-138.88	292.83	41.50	-296.25	-9.67	9.18	-96.14	-211.29	-42.99
$\Delta\text{Nb}^\oplus$	4.58	1.47	12.27	3.49	4.00	8.89	-2.06	10.32	7.77	6.57	14.87	-3.40	-3.35	-2.26	-4.10
$\Delta\text{Zr}^\oplus$	94.92	15.57	81.72	28.79	28.43	41.85	-20.20	49.68	11.17	70.82	205.27	-50.23	-47.87	-11.86	-48.40
$\Delta\text{La}^\oplus$	-26.23	-34.56	-1.96	-4.36	-3.68	-4.94	-2.75	-0.60	-4.67	12.94	-3.38	-7.78	-7.02	-7.39	-1.53
$\Delta\text{Sm}^\oplus$	-1.11	-5.62	3.43	1.01	1.15	3.59	-0.37	3.74	3.16	3.66	5.16	-2.57	-2.24	-0.40	-1.93
$\Delta\text{Yb}^\oplus$	-1.48	-2.60	-1.64	-2.19	-2.17	-1.09	-2.13	-1.00	-1.18	-1.88	-0.51	-2.73	-2.81	-2.23	-2.65
Al	98.01	97.35	99.09	97.66	97.81	96.15	80.87	98.61	77.60	52.43	95.56	54.40	69.22	41.26	66.91
CCPI	81.66	93.06	65.39	72.29	71.35	45.37	93.76	64.50	56.02	86.38	56.85	62.53	68.41	83.37	65.80

# wt%

Al; Alteration Index =  $100 \times (\text{K}_2\text{O} + \text{MgO}) / (\text{K}_2\text{O} + \text{MgO} + \text{CaO} + \text{Na}_2\text{O})$

CCPI =  $100 \times (\text{Fe}_2\text{O}_3 + \text{MgO}) / (\text{Fe}_2\text{O}_3 + \text{MgO} + \text{K}_2\text{O} + \text{Na}_2\text{O})$

Least Altered samples

Table A2-2 (continued): Major element mass change based on the MacLean (1990) multiple precursor method, SWIR mineralogy, and alteration indexes.

Samples	D1425061	D1425062	D1425063	D1425064	D1425065	D1425066	D1425067	D1425068	R137251	R137252	R137253	R137254	R137255	R137256	R137257
Rock Type	Int.	Int.	Int.	Mafic	Int.	Int.	Felsic	Felsic	Felsic	Felsic	Felsic	Felsic	Felsic	Int.	Felsic
Sub-type	1	1	1	III	1	1	C	A	B	B	B	B	B	5	B
SWIR Min 1	FeMgChlorite	FeMgChlorite	FeMgChlorite	FeMgChlorite	FeMgChlorite	FeChlorite	-	-	-	FeMgChlorite	FeMgChlorite	FeMgChlorite	FeMgChlorite	FeMgChlorite	FeMgChlorite
SWIR MIN 2	-	Phengite	Phengite	-	Phengite	Muscovite	-	-	-	Muscovite	Muscovite	Muscovite	Muscovite	-	Muscovite
$\Delta\text{Al}_2\text{O}_3^\#$	0.36	0.43	0.57	0.06	0.78	1.39	1.18	2.25	2.25	2.26	2.17	2.25	2.25	0.81	2.25
$\Delta\text{TiO}_2^\#$	0.09	0.49	0.33	0.74	0.45	0.43	0.00	-0.04	-0.05	-0.04	-0.01	-0.02	-0.03	0.00	-0.03
$\Delta\text{CaO}^\#$	-1.88	-1.79	0.19	4.46	-0.46	-0.21	0.35	-1.14	-1.21	-1.13	-0.91	-1.11	-1.09	2.05	-1.09
$\Delta\text{MgO}^\#$	4.40	0.13	-0.66	1.66	-0.11	-0.90	-0.69	1.48	3.47	1.99	2.88	2.78	3.25	12.42	4.18
$\Delta\text{SiO}_2^\#$	1.18	-1.26	0.96	-6.02	-0.62	10.10	11.92	18.29	32.18	47.61	58.45	69.83	33.49	-0.13	4.13
$\Delta\text{Fe}_2\text{O}_3^\#$	2.97	2.15	1.86	6.60	2.64	2.25	2.24	1.64	-0.65	2.47	2.31	4.13	2.06	3.03	3.79
$\Delta\text{Na}_2\text{O}^\#$	-1.76	-0.56	-0.31	-3.50	-1.13	0.31	-0.84	-3.04	-2.96	-3.06	-3.47	-3.11	-3.13	-3.42	-3.13
$\Delta\text{K}_2\text{O}^\#$	0.32	0.71	1.15	3.68	1.14	0.72	-0.23	2.18	1.69	1.67	1.07	1.10	1.28	0.20	0.78
Total major element mass change (wt%)	5.68	0.30	4.08	7.71	2.70	14.08	13.94	21.62	34.71	51.76	62.48	75.85	38.08	14.96	10.87
$\Delta\text{Cu}^\oplus$	45.07	-7.29	27.69	45.36	78.65	-13.17	7.00	1241.21	23.87	2312.15	50.79	122.61	20.81	-9.29	38.00
$\Delta\text{Zn}^\oplus$	141.78	36.89	13.80	115.94	16.40	-3.92	53.49	23.94	75.46	87.37	16.83	91.37	64.04	286.90	42.54
$\Delta\text{Pb}^\oplus$	-1.43	-2.75	-2.93	13.66	-3.27	-4.09	5.12	24.22	-2.88	-3.88	-2.98	-1.81	-3.89	-3.12	-4.21
$\Delta\text{Cs}^\oplus$	-0.85	-0.65	-0.40	-0.01	0.21	0.48	-1.24	1.31	0.47	0.49	0.15	0.44	0.45	-0.64	0.35
$\Delta\text{Rb}^\oplus$	-2.85	6.53	16.66	49.73	32.87	19.81	-15.94	61.21	47.76	47.06	19.53	26.40	35.07	-26.36	17.03
$\Delta\text{Ba}^\oplus$	188.49	153.68	207.42	1415.37	215.69	-153.35	89.30	263.06	-175.84	145.28	100.07	25.20	-9.81	-340.57	-112.99
$\Delta\text{Nb}^\oplus$	-1.09	8.42	6.29	15.84	7.65	13.54	1.83	10.60	-1.28	-1.22	-0.35	-0.56	-0.38	-4.46	-0.43
$\Delta\text{Zr}^\oplus$	18.83	23.62	37.30	-35.91	36.98	157.25	172.27	56.24	-48.91	-54.28	-20.72	-34.02	-39.74	-60.67	-45.06
$\Delta\text{La}^\oplus$	1.80	4.25	0.24	7.21	6.55	13.42	0.78	27.94	6.09	8.78	-2.17	16.09	2.76	23.42	-3.65
$\Delta\text{Sm}^\oplus$	-0.57	1.48	1.55	1.24	1.86	3.59	1.87	7.57	-0.24	0.16	0.44	0.67	0.40	1.75	-0.36
$\Delta\text{Yb}^\oplus$	-2.26	-1.78	-1.92	-1.25	-1.95	-1.83	-0.35	-1.66	-2.58	-2.47	-1.82	-2.43	-2.23	-2.82	-2.19
Al	78.19	62.94	51.55	60.58	60.02	45.74	42.97	98.23	98.40	98.24	98.46	98.52	98.56	79.30	98.78
CCPI	85.76	75.91	71.84	81.08	76.31	68.41	34.23	67.01	69.45	71.84	72.69	79.08	75.08	95.09	82.08

# wt%

Al; Alteration Index =  $100 * (\text{K}_2\text{O} + \text{MgO}) / (\text{K}_2\text{O} + \text{MgO} + \text{CaO} + \text{Na}_2\text{O})$

CCPI =  $100 * (\text{Fe}_2\text{O}_3 + \text{MgO}) / (\text{Fe}_2\text{O}_3 + \text{MgO} + \text{K}_2\text{O} + \text{Na}_2\text{O})$

Least Altered samples

Table A2-2 (continued): Major element mass change based on the MacLean (1990) multiple precursor method, SWIR mineralogy, and alteration indexes.

Samples	R137258	R137259	R137260	R137261	R137262	R137263	R137264	R137265	R137266	R137267	R137268	R137269	R137270	R137271	R137272
Rock Type	Int.	Felsic	Felsic	Felsic	Felsic	Int.	Felsic	Felsic	Felsic	Felsic	Int.	Felsic	Felsic	Int.	Felsic
Sub-type	5	B	B	B	B	1	B	B	Tuff Group	Tuff Group	1	B	B	1	B
SWIR Min 1	FeMgChlorite	FeMgChlorite	FeMgChlorite	FeMgChlorite	FeMgChlorite	FeMgChlorite	Muscovite	-	FeMgChlorite	FeChlorite	-	FeMgChlorite	Muscovite	-	Phengite
SWIR MIN 2	-	Muscovite	Muscovite	Muscovite	Muscovite	Muscovite	-	-	Muscovite	Muscovite	-	Muscovite	MgChlorite	-	FeMgChlorite
$\Delta\text{Al}_2\text{O}_3^\#$	0.51	2.25	2.25	2.25	2.25	-0.12	2.22	2.23	1.64	1.76	1.63	2.22	2.21	0.87	2.22
$\Delta\text{TiO}_2^\#$	-0.33	-0.08	-0.04	-0.01	-0.03	-0.40	0.01	0.00	-0.02	0.00	0.35	0.00	0.02	0.40	0.00
$\Delta\text{CaO}^\#$	3.91	-1.21	-1.09	-1.07	-1.06	-3.16	-0.54	-0.17	-1.09	-0.48	-0.27	-0.97	-0.96	-0.16	-0.90
$\Delta\text{MgO}^\#$	15.97	8.47	2.09	2.22	2.16	2.04	-0.04	0.15	-0.70	-0.86	-0.51	1.45	1.25	-0.76	0.55
$\Delta\text{SiO}_2^\#$	5.88	53.60	16.57	18.01	19.33	-1.62	40.89	3.70	3.69	7.84	3.51	19.02	20.08	3.02	21.37
$\Delta\text{Fe}_2\text{O}_3^\#$	3.98	5.29	0.32	0.49	0.79	3.43	-0.18	-0.73	0.00	0.29	0.93	1.20	0.80	3.04	1.45
$\Delta\text{Na}_2\text{O}^\#$	-3.62	-3.03	-3.10	-3.17	-3.19	-4.05	-0.73	-0.03	1.74	2.35	0.29	-3.31	-3.34	-0.79	-2.37
$\Delta\text{K}_2\text{O}^\#$	-1.22	-0.14	1.66	1.97	2.04	0.45	1.18	0.81	-0.18	-0.42	0.62	1.86	1.97	0.26	1.90
Total major element mass change (wt%)	25.08	65.14	18.67	20.70	22.28	-3.43	42.81	5.96	5.07	10.48	6.55	21.48	22.03	5.88	24.21
$\Delta\text{Cu}^\oplus$	-11.23	396.97	281.22	37.42	-5.15	235.20	20.42	1.20	-14.15	3.71	29.86	-7.84	-7.67	-12.37	-6.54
$\Delta\text{Zn}^\oplus$	146.18	989.95	35.49	15.65	17.76	1968.31	104.20	-5.75	21.98	1.72	26.21	23.22	18.64	22.59	-2.59
$\Delta\text{Pb}^\oplus$	103.03	88.92	-0.61	2.05	-1.57	11.17	0.65	-3.98	-2.44	13.01	-3.40	-3.75	-2.46	-3.41	-3.72
$\Delta\text{Cs}^\oplus$	-1.14	0.31	0.48	0.75	0.81	-1.06	0.62	0.44	0.00	0.00	0.26	0.77	0.75	-0.43	1.03
$\Delta\text{Rb}^\oplus$	-34.05	-1.84	37.95	55.88	49.24	7.00	26.35	18.02	-3.19	-10.15	17.16	30.46	33.66	3.50	33.17
$\Delta\text{Ba}^\oplus$	-352.43	-271.18	-142.27	-147.22	360.97	111.34	1028.63	192.72	41.41	-42.98	626.03	937.20	982.79	637.65	1721.51
$\Delta\text{Nb}^\oplus$	-6.62	-0.26	-0.60	5.18	-0.18	-3.92	1.81	2.33	0.05	0.42	-2.48	2.52	3.31	-2.46	2.43
$\Delta\text{Zr}^\oplus$	-76.53	-73.40	-56.77	-10.12	-31.88	-42.97	-12.10	-26.83	197.26	188.86	-76.27	-21.27	-17.19	-61.97	-16.74
$\Delta\text{La}^\oplus$	13.18	-5.03	1.65	-2.66	6.82	-3.47	-5.70	-1.37	-1.93	-2.45	-2.91	4.95	-0.59	-2.16	-2.47
$\Delta\text{Sm}^\oplus$	0.14	-1.18	-0.12	1.96	1.04	-1.78	0.83	1.55	-0.82	-0.52	-1.15	2.28	1.80	-0.63	1.33
$\Delta\text{Yb}^\oplus$	-2.83	-2.44	-2.25	-1.79	-2.14	-2.19	-1.92	-1.93	-2.76	-2.74	-2.83	-1.89	-1.73	-2.53	-1.85
Al	75.41	99.42	98.15	98.70	98.85	97.13	58.47	50.12	37.87	29.73	46.81	98.18	98.33	50.56	83.51
CCPI	99.94	91.89	66.26	64.64	64.99	92.17	39.94	37.06	59.35	56.77	65.15	62.95	59.86	78.05	55.17

# wt%

Al; Alteration Index =  $100 * (\text{K}_2\text{O} + \text{MgO}) / (\text{K}_2\text{O} + \text{MgO} + \text{CaO} + \text{Na}_2\text{O})$

CCPI =  $100 * (\text{Fe}_2\text{O}_3 + \text{MgO}) / (\text{Fe}_2\text{O}_3 + \text{MgO} + \text{K}_2\text{O} + \text{Na}_2\text{O})$

Least Altered samples

Table A2-2 (continued): Major element mass change based on the MacLean (1990) multiple precursor method, SWIR mineralogy, and alteration indexes.

Samples	R137273	R137274	R137275	R137276	R137277	R137278	R137279	R137280	R137281	R137282	R137283	R137284	R137285	R137286	R137287
Rock Type	Felsic	Int.	Felsic	Felsic	Int.	Int.	Felsic	Int.	Int.	Int.	Felsic	Int.	Int.	Int.	Felsic
Sub-type	B	1	Tuff Group	B	1	1	A	1	1	1	C	1	1	1	A
SWIR Min 1	Muscovite	FeMgChlorite	-	-	FeMgChlorite	FeMgChlorite	Phengite	FeMgChlorite	FeMgChlorite	FeMgChlorite	Muscovite	FeMgChlorite	FeMgChlorite	FeMgChlorite	MgChlorite
SWIR MIN 2	FeMgChlorite	Muscovite	-	-	-	Epidote	Ankerite	-	-	-	-	-	Muscovite	FeTourmaline	Phengite
$\Delta\text{Al}_2\text{O}_3^\#$	2.21	0.88	1.66	2.23	0.01	0.06	2.26	-0.09	-0.05	0.02	2.24	-0.14	-0.09	0.94	2.26
$\Delta\text{TiO}_2^\#$	0.01	0.45	0.02	0.00	-0.20	-0.13	-0.03	-0.29	-0.29	-0.02	0.04	-0.05	-0.16	0.46	-0.04
$\Delta\text{CaO}^\#$	-0.94	-1.60	-1.64	-0.79	-0.41	2.73	0.43	2.99	5.24	-2.49	-0.96	-0.17	-2.72	-2.04	-0.52
$\Delta\text{MgO}^\#$	1.55	2.56	0.72	0.24	-0.36	-1.75	0.14	-1.58	-1.03	5.26	0.41	2.15	3.80	4.08	3.93
$\Delta\text{SiO}_2^\#$	45.12	-7.29	11.47	45.20	5.42	2.26	7.62	0.06	0.62	-2.34	5.18	0.49	-1.80	-9.28	112.10
$\Delta\text{Fe}_2\text{O}_3^\#$	2.08	4.59	1.11	0.26	-0.23	-0.99	-2.17	-2.67	-0.97	5.00	-1.88	-0.64	2.88	3.32	-0.06
$\Delta\text{Na}_2\text{O}^\#$	-3.36	-3.36	0.94	1.18	0.54	0.89	1.46	0.63	-1.51	-3.96	-1.72	-0.27	-4.00	-1.90	-0.06
$\Delta\text{K}_2\text{O}^\#$	2.07	0.87	-0.18	-0.17	-0.25	-0.26	0.30	-0.64	0.01	-0.20	2.46	-1.02	0.35	0.04	0.54
Total major element mass change (wt%)	48.75	-2.90	14.10	48.14	4.52	2.81	10.00	-1.60	2.01	1.27	5.78	0.36	-1.73	-4.36	118.15
$\Delta\text{Cu}^\oplus$	-7.40	-12.56	-14.60	0.95	57.84	-14.00	64.26	-10.81	3.88	-10.76	-10.65	479.90	-12.84	-15.09	-8.81
$\Delta\text{Zn}^\oplus$	-4.64	23.76	19.26	21.40	-9.23	-18.41	-35.51	-21.67	-1.10	87.06	-47.11	22.12	27.87	14.70	-12.57
$\Delta\text{Pb}^\oplus$	-3.43	-3.49	-4.45	5.24	0.05	4.02	14.14	5.26	1.27	-1.98	-4.58	10.67	4.24	-2.62	12.26
$\Delta\text{Cs}^\oplus$	1.03	-0.11	0.00	0.31	1.13	-0.01	0.47	-1.31	-1.15	-0.93	1.06	-1.36	-0.76	0.02	1.26
$\Delta\text{Rb}^\oplus$	35.53	15.00	-2.37	-13.81	6.12	-5.97	22.10	-20.20	0.34	-0.94	68.19	-31.88	10.92	12.17	27.59
$\Delta\text{Ba}^\oplus$	718.49	379.91	-133.36	310.35	-141.44	-150.76	-107.99	-224.90	-43.55	-130.17	437.13	-247.49	42.29	-100.94	-58.81
$\Delta\text{Nb}^\oplus$	2.71	-1.92	-0.09	1.91	-0.85	-0.19	12.19	-1.82	-1.17	1.03	8.84	0.42	0.09	2.23	10.33
$\Delta\text{Zr}^\oplus$	-9.00	-64.46	193.72	-33.30	-6.30	-0.70	93.94	-22.16	-8.80	20.04	55.19	-5.33	-2.23	-31.87	110.80
$\Delta\text{La}^\oplus$	-15.07	-2.86	-2.17	-1.42	0.91	-3.64	-11.20	-1.65	-1.82	2.60	24.61	4.18	0.94	-5.67	-21.32
$\Delta\text{Sm}^\oplus$	0.13	-0.52	-0.56	1.27	0.51	-0.26	1.73	-0.12	-0.05	1.02	7.83	1.08	0.82	-1.46	-0.72
$\Delta\text{Yb}^\oplus$	-1.80	-2.59	-2.78	-1.90	-2.18	-2.01	-1.55	-2.11	-2.11	-1.95	-1.80	-1.96	-2.01	-2.55	-1.97
Al	98.30	88.94	52.82	40.98	47.54	32.60	36.95	32.49	36.73	93.49	78.95	55.31	94.14	82.43	67.32
CCPI	64.75	90.09	68.55	42.67	72.29	67.55	29.85	67.65	77.66	95.82	41.16	80.59	92.85	87.71	61.99

# wt%

Al; Alteration Index =  $100 * (\text{K}_2\text{O} + \text{MgO}) / (\text{K}_2\text{O} + \text{MgO} + \text{CaO} + \text{Na}_2\text{O})$

CCPI =  $100 * (\text{Fe}_2\text{O}_3 + \text{MgO}) / (\text{Fe}_2\text{O}_3 + \text{MgO} + \text{K}_2\text{O} + \text{Na}_2\text{O})$

Least Altered samples

Table A2-2 (continued): Major element mass change based on the MacLean (1990) multiple precursor method, SWIR mineralogy, and alteration indexes.

Samples	R137288	R137289	R137290	R137291	R137292	R137293	R137294	R137295	R137296	R137297	R137298	R137299	R137300	D1411601	D1411602
Rock Type	Mafic	Felsic	Felsic	Int.	Int.	Int.	Felsic	Felsic	Felsic	Felsic	Felsic	Int.	Int.	Mafic	Mafic
Sub-type	I	A	A	3	3	3	A	A	A	A	A	1	3	IV	I
SWIR Min 1	FeMgChlorite	FeMgChlorite	FeMgChlorite	Phengite	FeMgChlorite	FeMgChlorite	FeMgChlorite	Muscovite	FeMgChlorite	Muscovite	Muscovite	FeMgChlorite	FeMgChlorite	FeMgChlorite	FeMgChlorite
SWIR MIN 2	-	Muscovite	Muscovite	Ankerite	Phengite	Phengite	Phengite	Phengite	Muscovite	Muscovite	FeMgChlorite	Muscovite	Muscovite	-	-
$\Delta\text{Al}_2\text{O}_3^\#$	-0.83	2.25	2.25	-0.07	0.15	0.26	2.15	2.25	2.21	2.06	2.23	-0.18	-0.19	-0.63	-0.69
$\Delta\text{TiO}_2^\#$	1.42	-0.04	0.02	-0.13	-0.03	0.48	0.03	0.03	0.08	0.04	0.01	-0.26	-0.35	0.35	0.28
$\Delta\text{CaO}^\#$	7.09	-0.13	0.09	3.27	1.64	-0.74	-0.43	-0.58	-0.22	-0.48	-0.19	-1.53	0.10	4.31	4.17
$\Delta\text{MgO}^\#$	3.36	5.17	4.85	0.87	0.70	-1.02	-0.29	-0.22	0.66	1.05	2.26	3.88	-0.66	-3.49	-3.96
$\Delta\text{SiO}_2^\#$	9.67	117.57	91.94	-2.40	-3.86	2.59	36.38	26.18	39.43	33.72	29.10	-14.69	-7.84	9.15	6.10
$\Delta\text{Fe}_2\text{O}_3^\#$	8.21	1.64	1.50	-5.99	-1.45	4.23	-0.86	-1.71	-0.86	0.43	-0.35	-2.97	-0.23	2.54	3.48
$\Delta\text{Na}_2\text{O}^\#$	-3.55	-2.46	-2.51	-1.18	-0.43	-1.40	3.90	3.74	0.90	1.64	-1.95	-2.87	-1.15	-1.56	-1.65
$\Delta\text{K}_2\text{O}^\#$	-1.22	1.41	1.36	2.06	-0.23	0.30	-1.50	-0.99	0.25	-1.05	1.52	0.52	-0.20	-0.65	-0.70
Total major element mass change (wt%)	24.16	125.40	99.48	-3.58	-3.51	4.71	39.37	28.70	42.44	37.42	32.64	-18.08	-10.52	10.02	7.04
$\Delta\text{Cu}^\oplus$	6.10	-10.02	-8.91	-14.36	-14.61	-14.68	-6.23	0.26	-5.91	-5.60	-8.66	-14.34	-14.28	53.77	60.07
$\Delta\text{Zn}^\oplus$	114.84	-9.03	-7.71	-42.59	-16.85	-14.76	-14.96	-31.08	-11.20	12.31	17.17	-24.66	-12.08	149.82	87.67
$\Delta\text{Pb}^\oplus$	-0.15	3.74	5.01	-1.83	12.61	-2.39	2.42	-0.12	5.21	-2.70	1.72	-1.84	-1.73	11.74	8.69
$\Delta\text{Cs}^\oplus$	-0.99	1.91	1.77	0.72	-0.85	-0.40	-0.10	0.19	0.73	0.00	1.65	-0.33	-1.11	-1.72	-1.73
$\Delta\text{Rb}^\oplus$	-36.83	56.05	50.62	74.66	0.01	20.07	-39.81	-22.72	26.66	-25.63	65.17	27.06	-3.94	-14.98	-19.53
$\Delta\text{Ba}^\oplus$	-299.82	107.56	83.12	123.62	-174.25	-55.80	-377.13	-371.82	-237.04	-415.28	51.51	38.34	-42.26	-144.82	-130.99
$\Delta\text{Nb}^\oplus$	-1.60	13.49	13.94	-3.23	-3.14	7.38	38.44	32.25	38.97	45.36	33.65	1.44	0.13	-5.46	3.72
$\Delta\text{Zr}^\oplus$	32.92	103.71	132.99	-49.40	-41.81	122.49	213.11	259.34	272.39	226.14	191.63	22.86	23.57	-66.99	72.13
$\Delta\text{La}^\oplus$	-5.54	-40.29	-47.53	-0.39	-0.47	12.48	30.47	121.99	85.87	254.16	19.24	6.41	0.88	-6.59	4.04
$\Delta\text{Sm}^\oplus$	2.46	-1.44	-2.16	6.29	0.99	2.88	10.48	21.49	11.35	25.33	8.28	0.49	-0.22	-1.16	2.15
$\Delta\text{Yb}^\oplus$	-1.71	-1.44	-1.14	-2.31	-2.30	-1.91	0.09	-0.41	-0.11	0.40	-0.26	-1.99	-2.00	-2.07	-1.32
Al	47.86	85.08	83.06	52.35	47.63	56.15	16.52	21.05	45.10	37.66	75.77	79.24	51.23	28.67	26.96
CCPI	95.89	75.48	72.66	62.23	75.57	81.54	23.75	24.24	36.71	41.71	55.42	84.35	78.36	81.66	82.57

# wt%

Al; Alteration Index =  $100 * (\text{K}_2\text{O} + \text{MgO}) / (\text{K}_2\text{O} + \text{MgO} + \text{CaO} + \text{Na}_2\text{O})$

CCPI =  $100 * (\text{Fe}_2\text{O}_3 + \text{MgO}) / (\text{Fe}_2\text{O}_3 + \text{MgO} + \text{K}_2\text{O} + \text{Na}_2\text{O})$

Least Altered samples

Table A2-2 (continued): Major element mass change based on the MacLean (1990) multiple precursor method, SWIR mineralogy, and alteration indexes.

Samples	D1411603	D1411604	D1411605	D1411606	D1411607	D1411608	D1411609	D1411610	D1411611	D1411612	D1411613	D1411614	D1411615	D1411616	D1411617
Rock Type	Felsic	Mafic	Int.	Int.	Mafic	Int.	Mafic	Felsic	Mafic	Mafic	Mafic	Mafic	Mafic	Mafic	Felsic
Sub-type	Rim Granite	II	1	1	II	2	II	A	II	II	IV	II	II	II	Tuff Group
SWIR Min 1	FeMgChlorite	FeMgChlorite	FeMgChlorite	FeMgChlorite	FeMgChlorite	FeMgChlorite	FeMgChlorite	-	FeMgChlorite	FeMgChlorite	FeMgChlorite	FeMgChlorite	FeMgChlorite	MgChlorite	FeMgChlorite
SWIR MIN 2	Muscovite	-	Muscovite	-	-	-	-	-	-	-	-	-	-	-	-
$\Delta\text{Al}_2\text{O}_3^\#$	2.18	-0.21	0.35	1.70	-0.48	-0.64	-0.44	1.93	-0.48	0.13	-0.69	-0.36	0.03	-0.07	2.04
$\Delta\text{TiO}_2^\#$	-0.10	0.29	0.03	0.15	-0.05	-0.37	-0.06	0.05	-0.20	0.60	0.29	0.29	-0.21	0.17	0.22
$\Delta\text{CaO}^\#$	-0.22	0.20	0.95	-1.47	4.96	0.42	4.45	-0.61	0.13	1.94	3.57	3.43	5.32	-1.81	-1.49
$\Delta\text{MgO}^\#$	-0.94	-0.75	0.18	8.60	-1.50	0.14	3.23	16.23	-2.04	-0.63	-3.54	-3.31	-1.73	9.81	6.07
$\Delta\text{SiO}_2^\#$	24.07	3.09	-4.46	31.77	0.55	-0.47	3.41	-51.63	0.26	-2.86	8.01	-3.15	-4.52	-18.13	4.57
$\Delta\text{Fe}_2\text{O}_3^\#$	-1.89	3.09	3.42	8.58	2.90	1.42	6.14	25.84	4.88	4.54	2.78	2.33	0.58	1.35	7.64
$\Delta\text{Na}_2\text{O}^\#$	2.31	-1.89	-2.63	-2.91	-4.05	-2.86	-3.22	-4.07	-1.50	-1.17	-1.06	-1.70	-1.39	-4.03	-2.84
$\Delta\text{K}_2\text{O}^\#$	1.36	0.00	-0.40	-0.58	-1.04	-0.37	-0.59	-2.58	-0.98	0.07	-0.30	-0.36	-0.44	-1.16	0.27
Total major element mass change (wt%)	26.77	3.83	-2.56	45.82	1.28	-2.73	12.92	-14.86	0.05	2.62	9.05	-2.84	-2.35	-13.88	16.49
$\Delta\text{Cu}^\oplus$	18.87	-3.29	39.03	-12.08	244.86	723.13	177.29	509.82	286.55	127.65	51.77	-0.24	22.85	-14.42	-13.42
$\Delta\text{Zn}^\oplus$	-33.69	106.94	48.39	46.65	12.52	64.71	242.99	10268.79	1146.16	251.83	113.22	91.20	48.61	104.12	82.28
$\Delta\text{Pb}^\oplus$	3.91	24.41	9.97	6.47	23.28	32.84	406.08	1622.04	12.10	19.85	0.49	7.18	2.92	2.63	-4.67
$\Delta\text{Cs}^\oplus$	0.13	-1.30	-0.37	0.15	-1.56	-1.38	-1.31	-0.90	-1.81	-1.06	-1.72	-1.07	-1.17	-1.49	0.64
$\Delta\text{Rb}^\oplus$	15.69	5.55	9.10	-3.92	-27.80	-2.70	-5.98	-81.97	-33.42	5.91	-5.78	0.31	-6.25	-32.09	25.01
$\Delta\text{Ba}^\oplus$	104.05	-61.94	-213.56	-231.38	-291.51	-78.07	-88.46	-617.91	-230.07	-49.01	-20.28	-11.71	-165.10	-318.54	-20.64
$\Delta\text{Nb}^\oplus$	-0.14	-1.66	-0.38	4.32	-0.39	-1.27	-2.90	15.24	-0.90	3.40	-5.65	2.73	-3.10	-1.07	9.11
$\Delta\text{Zr}^\oplus$	-168.63	-60.44	82.15	63.34	18.77	15.04	-44.86	193.00	-42.05	19.96	-65.28	36.50	-93.18	-38.96	52.73
$\Delta\text{La}^\oplus$	-54.40	-8.93	5.53	-17.55	0.04	1.50	-3.12	-4.23	8.30	1.15	-6.17	0.44	-4.99	0.97	33.69
$\Delta\text{Sm}^\oplus$	-4.46	-1.99	0.41	-1.78	0.33	0.28	-0.48	8.77	0.12	1.06	-1.23	0.79	-0.24	0.12	5.40
$\Delta\text{Yb}^\oplus$	-0.76	-2.00	-2.36	-2.41	-1.81	-1.71	-1.99	-0.87	-1.71	-1.93	-2.02	-1.66	-2.21	-2.19	-2.30
Al	36.36	54.17	55.80	95.31	39.12	59.02	54.15	98.78	44.18	45.43	30.79	31.35	31.49	91.03	97.86
CCPI	10.18	83.56	89.94	97.19	96.72	87.71	93.33	99.80	85.79	82.09	78.46	81.23	80.21	99.42	92.26

# wt%

Al; Alteration Index =  $100 * (\text{K}_2\text{O} + \text{MgO}) / (\text{K}_2\text{O} + \text{MgO} + \text{CaO} + \text{Na}_2\text{O})$

CCPI =  $100 * (\text{Fe}_2\text{O}_3 + \text{MgO}) / (\text{Fe}_2\text{O}_3 + \text{MgO} + \text{K}_2\text{O} + \text{Na}_2\text{O})$

Least Altered samples

Table A2-2 (continued): Major element mass change based on the MacLean (1990) multiple precursor method, SWIR mineralogy, and alteration indexes.

Samples	D1411618	D1411619	D1411621	D1411623	D1411624	D1411625	D1411626	D1411627	D1411628	D1411629	D1411630	D1411631	D1411632	D1411633	D1411634
Rock Type	Int.	Int.	Felsic	Felsic	Int.	Int.	Mafic	Felsic	Int.	Felsic	Int.	Felsic	Mafic	Mafic	Felsic
Sub-type	3	2	A	Tuff Group	3	3	II	B	1	A	1	B	II	II	A
SWIR Min 1	FeMgChlorite	FeMgChlorite	FeMgChlorite	FeMgChlorite	FeMgChlorite	FeMgChlorite	FeMgChlorite	FeMgChlorite	FeMgChlorite	FeMgChlorite	FeMgChlorite	FeMgChlorite	FeMgChlorite	FeMgChlorite	FeMgChlorite
SWIR MIN 2	-	-	-	Muscovite	-	-	-	Phengite	Muscovite	Muscovite	Phengite	Phengite	-	-	Muscovite
$\Delta\text{Al}_2\text{O}_3^\#$	-0.20	-0.50	2.26	1.34	-0.12	1.73	-0.38	2.00	0.00	2.24	0.03	2.06	-0.22	-0.19	2.24
$\Delta\text{TiO}_2^\#$	0.60	-0.25	0.05	-0.32	0.17	0.66	0.04	0.04	0.11	0.03	-0.12	0.05	-0.18	0.80	-0.08
$\Delta\text{CaO}^\#$	-0.68	3.38	0.51	-1.52	2.95	-0.06	2.95	-0.13	-2.84	-0.75	-2.65	-0.12	-2.04	3.68	-1.04
$\Delta\text{MgO}^\#$	4.17	-1.71	17.96	2.93	0.15	3.43	-0.52	0.33	2.27	7.79	1.85	0.35	1.94	2.14	3.29
$\Delta\text{SiO}_2^\#$	7.20	1.65	-38.07	11.00	-9.63	-6.81	6.39	23.17	11.75	33.18	4.30	30.99	-1.12	6.82	10.75
$\Delta\text{Fe}_2\text{O}_3^\#$	6.43	0.00	24.23	-0.38	2.46	9.32	-0.70	0.16	5.69	8.52	-3.09	-0.39	2.03	5.39	3.48
$\Delta\text{Na}_2\text{O}^\#$	-4.11	-1.11	-3.13	-3.05	-2.52	1.07	0.30	2.79	-3.93	-1.95	0.66	2.42	-1.65	-1.51	-1.54
$\Delta\text{K}_2\text{O}^\#$	-0.47	-0.89	-1.75	1.56	-1.10	-0.64	-0.80	-1.79	0.21	-0.98	-0.64	-1.27	-0.77	-1.26	0.64
Total major element mass change (wt%)	12.96	0.58	2.06	11.55	-7.64	8.71	7.28	26.57	13.26	48.08	0.33	34.09	-2.00	15.86	17.73
$\Delta\text{Cu}^\oplus$	-14.13	-11.22	11626.81	73.94	393.22	2.88	-7.87	11.31	-10.26	8.45	-13.97	-0.81	61.48	17.12	-2.24
$\Delta\text{Zn}^\oplus$	165.20	54.84	10812.00	59.06	33.63	-12.60	11.89	16.62	128.22	164.41	-7.79	-4.12	292.11	107.55	7.18
$\Delta\text{Pb}^\oplus$	-1.43	0.00	808.04	-1.74	18.35	4.42	3.22	10.40	0.52	7.01	-2.04	8.25	4.50	1.02	-0.84
$\Delta\text{Cs}^\oplus$	-1.24	-1.80	0.53	0.35	-1.51	4.36	0.94	-0.40	-0.55	0.75	1.26	-0.07	-1.24	-1.45	1.03
$\Delta\text{Rb}^\oplus$	-6.36	-26.93	-42.04	49.20	-33.25	21.54	-12.18	-54.13	11.13	-20.55	-3.70	-35.21	-21.68	-38.69	28.71
$\Delta\text{Ba}^\oplus$	-114.52	-302.40	-504.14	164.76	-291.91	-229.05	-186.65	-396.71	88.33	-242.71	-229.15	-317.42	-105.88	-315.93	109.36
$\Delta\text{Nb}^\oplus$	9.66	-0.34	1.71	-3.92	11.82	26.25	-0.49	10.62	2.08	11.38	0.27	7.18	-0.46	0.22	8.81
$\Delta\text{Zr}^\oplus$	241.18	51.48	83.42	121.26	79.67	283.82	-13.44	90.17	34.83	127.73	9.58	74.22	-15.41	-18.84	26.84
$\Delta\text{La}^\oplus$	17.01	2.63	-49.93	-6.56	19.56	40.18	32.59	-11.59	-3.19	-10.13	-6.97	-18.47	-0.23	-6.19	11.59
$\Delta\text{Sm}^\oplus$	5.56	0.73	-3.65	-1.82	3.33	9.77	4.13	3.58	-0.52	2.39	-0.53	2.28	-0.07	0.64	4.87
$\Delta\text{Yb}^\oplus$	-1.51	-1.77	-2.54	-3.19	-1.23	-1.14	-1.93	-0.68	-1.94	-1.30	-2.09	-0.83	-2.01	-2.01	-1.91
Al	80.24	35.67	91.95	91.31	45.65	53.98	37.83	22.70	94.60	85.88	61.71	27.25	69.42	46.87	80.54
CCPI	96.80	80.11	99.73	81.94	91.13	82.16	74.68	33.26	93.67	90.01	72.37	31.30	86.65	89.70	76.15

# wt%

Al; Alteration Index =  $100 * (\text{K}_2\text{O} + \text{MgO}) / (\text{K}_2\text{O} + \text{MgO} + \text{CaO} + \text{Na}_2\text{O})$

CCPI =  $100 * (\text{Fe}_2\text{O}_3 + \text{MgO}) / (\text{Fe}_2\text{O}_3 + \text{MgO} + \text{K}_2\text{O} + \text{Na}_2\text{O})$

Least Altered samples

Table A2-2 (continued): Major element mass change based on the MacLean (1990) multiple precursor method, SWIR mineralogy, and alteration indexes.

Samples	D1411636	D1411637	D1411638	D1411639	D1411640	D1411641	D1411642	D1411643	D1411645	D1411646	D1411647	D1411648	D1411649	D1411650	D1411651
Rock Type	Int.	Mafic	Mafic	Felsic	Int.	Felsic	Int.	Felsic	Mafic	Felsic	Mafic	Mafic	Mafic	Felsic	Int.
Sub-type	1	I	III	A	1	Tuff Group	1	A	I	A	I	I	II	Rim Granite	1
SWIR Min 1	FeMgChlorite	FeMgChlorite	FeMgChlorite	Muscovite	FeMgChlorite	FeMgChlorite	FeMgChlorite	FeMgChlorite	FeMgChlorite	FeMgChlorite	MgChlorite	FeMgChlorite	FeMgChlorite	Muscovite	FeMgChlorite
SWIR MIN 2	-	-	-	-	-	Phengite	-	-	-	-	-	-	-	Ankerite	-
$\Delta\text{Al}_2\text{O}_3^\#$	-0.05	-0.84	-0.27	2.24	1.14	2.26	-0.06	2.26	-0.67	2.25	-0.75	-0.64	-0.32	1.47	1.63
$\Delta\text{TiO}_2^\#$	-0.32	0.56	1.77	-0.03	0.10	0.18	-0.30	0.01	0.37	-0.05	0.36	0.70	-0.02	-0.15	0.25
$\Delta\text{CaO}^\#$	0.38	7.38	4.36	-0.83	-2.04	0.21	-0.60	-0.83	7.04	-1.10	10.95	4.03	5.67	0.41	0.10
$\Delta\text{MgO}^\#$	3.29	0.13	0.07	3.79	5.37	0.46	0.53	3.75	3.14	9.21	15.89	-0.67	6.36	-0.81	7.40
$\Delta\text{SiO}_2^\#$	-2.74	2.77	-9.72	32.73	5.89	3.48	-6.33	21.37	4.15	-1.66	27.15	2.08	10.45	12.22	-10.31
$\Delta\text{Fe}_2\text{O}_3^\#$	-0.67	4.85	9.62	-0.36	19.10	-0.99	1.38	4.06	5.62	15.30	11.36	7.76	9.12	-0.15	4.71
$\Delta\text{Na}_2\text{O}^\#$	-0.24	-1.61	-1.95	-1.49	-2.99	0.92	-0.01	-0.09	-2.60	-3.02	-3.28	-0.66	-3.27	1.69	-2.22
$\Delta\text{K}_2\text{O}^\#$	1.17	-0.92	0.94	1.64	-1.09	0.39	-0.73	-0.22	-1.31	-1.47	-0.62	-0.55	-0.35	-2.12	-0.25
Total major element mass change (wt%)	0.82	12.32	4.82	37.70	25.47	6.91	-6.13	30.30	15.74	19.45	61.05	12.05	27.63	12.57	1.30
$\Delta\text{Cu}^\oplus$	-14.40	195.48	58.35	9.05	1865.51	-2.13	-14.42	17.48	55.16	-9.10	217.78	-9.71	-13.93	6.75	-13.14
$\Delta\text{Zn}^\oplus$	5.49	22.31	61.04	5.83	203.67	-19.91	-10.16	15.14	252.25	185.57	139.31	47.60	149.01	16.24	65.65
$\Delta\text{Pb}^\oplus$	1.16	17.36	4.89	6.88	8.31	24.94	2.74	2.64	2.07	-0.79	8.31	2.62	4.18	2.87	-2.42
$\Delta\text{Cs}^\oplus$	8.16	0.05	5.79	2.55	-0.28	0.87	0.12	0.78	-1.96	0.29	-1.47	-1.63	-1.31	-1.36	0.45
$\Delta\text{Rb}^\oplus$	68.68	-27.65	22.78	53.53	-28.34	16.10	-20.49	-2.60	-43.42	-36.79	-13.23	-16.03	-7.48	-78.65	7.08
$\Delta\text{Ba}^\oplus$	-79.13	-252.60	278.04	359.19	-353.26	-123.06	-223.66	-179.28	-319.73	-405.46	-184.85	-155.34	-143.45	-476.19	-207.51
$\Delta\text{Nb}^\oplus$	-0.72	-3.57	14.70	23.65	-4.08	9.72	-0.82	14.28	3.16	17.10	2.07	5.30	1.36	1.27	-0.03
$\Delta\text{Zr}^\oplus$	-17.92	-23.52	-3.10	42.99	-74.61	-22.61	-22.37	61.20	-13.61	69.09	-59.93	84.90	-14.66	-30.88	-56.91
$\Delta\text{La}^\oplus$	-11.66	-10.63	6.62	-34.96	-3.57	13.76	7.29	18.98	-1.02	20.08	-6.44	5.25	-1.67	-54.53	-4.40
$\Delta\text{Sm}^\oplus$	-0.65	0.96	2.15	-1.83	-1.03	4.11	0.13	6.76	1.26	5.95	-0.16	3.23	-0.71	-0.87	-0.49
$\Delta\text{Yb}^\oplus$	-2.03	-1.77	-0.78	-1.19	-2.73	-1.65	-1.99	-1.42	-1.48	-1.64	-1.32	-1.28	-1.72	0.62	-2.75
Al	61.31	36.32	46.77	81.31	93.06	42.63	51.73	66.45	45.13	98.38	59.95	38.74	57.84	17.81	79.56
CCPI	74.14	86.59	85.07	64.40	98.98	40.71	78.99	72.87	92.93	98.92	95.61	83.93	94.22	17.85	92.24

# wt%

Al; Alteration Index =  $100 * (\text{K}_2\text{O} + \text{MgO}) / (\text{K}_2\text{O} + \text{MgO} + \text{CaO} + \text{Na}_2\text{O})$

CCPI =  $100 * (\text{Fe}_2\text{O}_3 + \text{MgO}) / (\text{Fe}_2\text{O}_3 + \text{MgO} + \text{K}_2\text{O} + \text{Na}_2\text{O})$

Least Altered samples



Table A2-2 (continued): Major element mass change based on the MacLean (1990) multiple precursor method, SWIR mineralogy, and alteration indexes.

Samples	D1411652	D1411653	D1411656	D1411657	D1411658	D1411659	D1411660	D1411661	D1411662	D1411663	D1411664	D1411666	D1411667	D1411668	D1411669
Rock Type	Int.	Mafic	Int.	Int.	Felsic	Felsic	Mafic	Felsic	Mafic	Mafic	Mafic	Mafic	Mafic	Felsic	Mafic
Sub-type	4	II	1	1	C	Tuff	I	A	II	I	II	III	II	Rim Granite	II
SWIR Min 1	FeMgChlorite	FeMgChlorite	Aspectral	FeMgChlorite	Phengite	FeMgChlorite	FeMgChlorite	Muscovite	FeMgChlorite	FeMgChlorite	FeMgChlorite	FeMgChlorite	FeMgChlorite	Muscovite	FeChlorite
SWIR MIN 2	Muscovite	-	-	-	-	Muscovite	-	FeMgChlorite	-	Hornblende	-	-	-	Ankerite	-
$\Delta\text{Al}_2\text{O}_3^\#$	0.07	-0.31	2.25	0.57	2.24	2.23	-0.76	2.22	1.28	-0.73	-0.23	-0.40	0.37	1.80	-0.50
$\Delta\text{TiO}_2^\#$	-1.08	0.52	0.51	-0.38	0.01	0.33	1.45	0.01	1.16	-0.05	0.37	-0.14	0.61	-0.11	0.04
$\Delta\text{CaO}^\#$	4.63	3.04	-0.12	2.68	2.25	2.56	6.87	0.14	3.86	5.13	2.53	3.34	2.04	2.73	-1.69
$\Delta\text{MgO}^\#$	-3.60	0.69	11.61	-2.79	-0.99	-0.97	-2.49	0.08	0.09	8.20	-1.59	-2.33	0.22	-1.08	-0.11
$\Delta\text{SiO}_2^\#$	0.15	5.05	0.64	7.14	24.98	7.17	8.40	-2.57	-16.35	13.43	-1.55	-0.03	2.94	14.02	-3.69
$\Delta\text{Fe}_2\text{O}_3^\#$	-2.96	6.91	11.90	-1.20	-2.15	0.80	9.65	-0.55	6.79	7.97	3.71	2.34	7.76	-1.04	8.93
$\Delta\text{Na}_2\text{O}^\#$	-2.49	-2.16	-2.18	-0.44	1.83	1.78	-3.36	-0.67	-0.29	-2.29	-1.81	-1.03	-2.50	0.76	-3.51
$\Delta\text{K}_2\text{O}^\#$	-0.02	-0.88	-1.57	0.21	0.25	-0.71	-1.21	0.77	-0.52	0.15	-1.07	-1.00	0.81	-2.06	-1.02
Total major element mass change (wt%)	-5.30	12.85	23.03	5.79	28.40	13.19	18.55	-0.56	-3.97	31.81	0.36	0.77	12.26	15.01	-1.57
$\Delta\text{Cu}^\oplus$	-14.56	-14.01	575.69	18.33	-8.14	221.52	50.32	6.98	26.73	14.19	-6.81	14.44	72.30	-2.02	-9.40
$\Delta\text{Zn}^\oplus$	-13.05	70.34	127.85	27.77	-53.02	-39.25	112.66	-24.32	24.49	93.08	28.50	97.22	147.02	-5.40	52.71
$\Delta\text{Pb}^\oplus$	9.04	3.48	2148.28	41.39	-3.14	0.89	10.75	0.04	7.39	6.39	18.13	13.21	1.02	11.96	2.86
$\Delta\text{Cs}^\oplus$	-0.89	-1.63	0.16	-0.18	1.13	0.54	-1.85	1.04	0.23	-1.59	-1.62	-1.38	-0.72	-0.57	-1.73
$\Delta\text{Rb}^\oplus$	3.81	-29.26	-40.97	8.31	27.30	-11.87	-40.43	35.00	-6.40	2.99	-34.78	-31.48	35.36	-64.48	-31.04
$\Delta\text{Ba}^\oplus$	161.00	-233.40	-450.95	158.57	-192.00	25.87	-304.10	411.78	-193.76	-76.40	-283.09	-260.56	42.96	-409.17	-268.74
$\Delta\text{Nb}^\oplus$	-8.01	6.53	2.30	-2.62	8.42	2.90	11.85	19.21	-6.17	1.24	3.19	8.53	4.06	2.05	0.57
$\Delta\text{Zr}^\oplus$	-148.56	75.62	-44.99	-109.77	-6.95	165.10	111.89	42.75	-150.02	-34.76	37.53	-55.90	-3.43	-95.05	-23.05
$\Delta\text{La}^\oplus$	-15.33	4.68	-23.39	-5.62	2.97	32.58	10.96	-3.59	-21.65	-4.15	2.25	2.56	0.70	-56.52	-4.85
$\Delta\text{Sm}^\oplus$	-4.29	1.47	-1.22	-0.86	2.57	6.78	6.51	3.83	-4.51	-0.12	0.16	0.76	0.70	-2.31	-1.48
$\Delta\text{Yb}^\oplus$	-2.56	-1.46	-2.26	-2.34	-2.06	-3.10	-0.82	-0.86	-2.96	-1.52	-1.63	-1.35	-1.87	1.08	-1.61
Al	28.02	47.33	86.82	29.93	22.98	15.48	29.88	51.57	33.47	60.42	38.06	31.93	54.85	9.18	71.71
CCPI	75.51	90.43	96.39	66.84	25.59	48.67	94.67	39.87	83.10	89.85	87.38	82.00	86.97	11.86	95.55

# wt%

Al; Alteration Index =  $100 \times (\text{K}_2\text{O} + \text{MgO}) / (\text{K}_2\text{O} + \text{MgO} + \text{CaO} + \text{Na}_2\text{O})$

CCPI =  $100 \times (\text{Fe}_2\text{O}_3 + \text{MgO}) / (\text{Fe}_2\text{O}_3 + \text{MgO} + \text{K}_2\text{O} + \text{Na}_2\text{O})$

Least Altered samples

Table A2-2 (continued): Major element mass change based on the MacLean (1990) multiple precursor method, SWIR mineralogy, and alteration indexes.

Samples	D1411670	D1411671	D1411672	D1411674	D1411675	D1411676	D1411677	D1411679	D1411680	D1411682	D1411683	D1411684	D1411687	D1411688	D1411690
Rock Type	Int.	Mafic	Int.	Felsic	Int.	Mafic	Mafic	Mafic	Int.	Felsic	Int.	Int.	Felsic	Felsic	Mafic
Sub-type	1	I	1	A	2	I	I	I	2	A	3	1	A	A	I
SWIR Min 1	FeMgChlorite	FeMgChlorite	FeMgChlorite	FeMgChlorite	FeMgChlorite	FeMgChlorite	FeMgChlorite	FeMgChlorite	FeMgChlorite	FeMgChlorite	FeMgChlorite	FeMgChlorite	FeMgChlorite	FeMgChlorite	FeMgChlorite
SWIR MIN 2	-	-	-	Muscovite	Hornblende	Epidote	-	Muscovite	-	Muscovite	Phlogopite	-	Muscovite	Muscovite	Phlogopite
$\Delta\text{Al}_2\text{O}_3^\#$	-0.03	-0.65	0.04	2.17	-0.66	-0.78	-0.68	2.16	-0.75	2.25	-0.47	1.74	2.26	2.23	-0.88
$\Delta\text{TiO}_2^\#$	-0.26	-0.33	0.04	0.03	-0.34	0.28	0.13	0.03	0.18	-0.01	-0.42	0.51	-0.04	-0.08	-0.48
$\Delta\text{CaO}^\#$	2.06	2.42	-2.63	-0.87	1.66	4.51	3.04	-0.68	4.15	-0.99	0.41	-0.32	-0.45	-1.27	2.71
$\Delta\text{MgO}^\#$	-1.95	-2.51	6.58	2.96	0.72	-3.06	0.46	7.20	-1.61	3.11	-1.61	3.12	6.50	1.97	-3.56
$\Delta\text{SiO}_2^\#$	1.49	-3.33	-6.80	59.31	-4.21	-5.96	-4.10	70.92	-1.05	38.03	1.38	1.40	53.07	16.18	-7.16
$\Delta\text{Fe}_2\text{O}_3^\#$	0.28	0.78	11.96	5.00	1.14	3.27	6.61	5.97	4.37	3.53	-0.96	1.11	6.03	3.43	0.81
$\Delta\text{Na}_2\text{O}^\#$	-1.19	-1.29	-3.85	-3.45	-1.48	-2.19	-4.26	-3.53	-2.13	-3.06	-0.21	0.11	-3.10	-2.92	-1.41
$\Delta\text{K}_2\text{O}^\#$	-0.96	-1.23	-1.24	0.78	-0.58	-0.86	-1.26	-0.29	-0.93	0.76	0.08	-0.29	0.05	1.26	-1.00
Total major element mass change (wt%)	-0.56	-6.15	4.10	65.92	-3.73	-4.80	-0.07	81.78	2.23	43.62	-1.80	7.37	64.31	20.81	-10.97
$\Delta\text{Cu}^\oplus$	-6.22	12.22	-9.66	-6.32	42.76	34.27	327.18	3.51	89.41	16.92	-8.75	-1.22	2088.21	5.23	4.32
$\Delta\text{Zn}^\oplus$	26.81	91.37	234.07	13.03	68.37	52.89	115.17	69.65	58.11	33.65	15.66	7.34	76.97	6.49	132.51
$\Delta\text{Pb}^\oplus$	7.69	16.38	12.94	-2.96	5.78	5.04	8.59	4.85	42.98	-2.47	1.61	2.83	40.47	0.48	8.11
$\Delta\text{Cs}^\oplus$	-1.42	-2.03	-1.34	0.44	-1.83	-1.84	-1.98	0.28	-1.52	0.76	1.69	0.54	0.40	0.71	-2.16
$\Delta\text{Rb}^\oplus$	-27.87	-41.60	-35.45	23.36	-25.48	-31.46	-41.90	-4.09	-29.38	49.53	23.19	-6.51	6.25	57.14	-37.09
$\Delta\text{Ba}^\oplus$	-223.43	-177.88	-335.16	531.33	-36.80	-244.75	-305.88	-29.82	-228.21	102.39	-134.94	98.83	24.01	755.50	-203.32
$\Delta\text{Nb}^\oplus$	-2.77	0.06	2.44	4.97	1.67	1.95	0.06	4.97	6.76	4.59	0.88	1.31	2.88	5.38	-4.75
$\Delta\text{Zr}^\oplus$	-38.60	25.67	18.35	133.95	22.87	61.03	2.42	127.39	121.41	145.40	59.35	145.88	138.02	102.38	-61.49
$\Delta\text{La}^\oplus$	-0.88	3.71	-0.72	-15.02	3.53	4.23	-1.78	-19.07	9.40	13.31	20.51	5.95	-7.15	11.15	0.27
$\Delta\text{Sm}^\oplus$	-1.47	-0.45	-0.03	3.96	0.41	1.05	0.37	0.67	3.37	4.63	9.61	0.73	0.73	2.61	-0.63
$\Delta\text{Yb}^\oplus$	-2.09	-1.57	-1.85	-2.13	-1.62	-1.44	-1.64	-1.77	-1.20	-1.79	-1.68	-2.77	-2.34	-2.50	-1.87
Al	35.43	34.08	94.12	97.67	50.88	31.26	52.57	97.15	37.44	96.28	45.07	59.67	92.73	97.94	31.00
CCPI	81.15	82.17	99.56	79.34	83.31	85.81	98.49	89.54	87.49	80.22	71.61	76.18	89.79	78.48	80.45

# wt%

Al; Alteration Index =  $100 * (\text{K}_2\text{O} + \text{MgO}) / (\text{K}_2\text{O} + \text{MgO} + \text{CaO} + \text{Na}_2\text{O})$

CCPI =  $100 * (\text{Fe}_2\text{O}_3 + \text{MgO}) / (\text{Fe}_2\text{O}_3 + \text{MgO} + \text{K}_2\text{O} + \text{Na}_2\text{O})$

Least Altered samples

Table A2-2 (continued): Major element mass change based on the MacLean (1990) multiple precursor method, SWIR mineralogy, and alteration indexes.

Samples	D1411691	D1411693	D1411694	D1411695	D1411696	D1411697	D1411698	D1411700	D1410401	D1410402	D1410403	D1410405	D1410406	D1410408	D1410410
Rock Type	Int.	Int.	Felsic	Int.	Felsic	Int.	Int.	Felsic	Int.	Felsic	Int.	Felsic	Felsic	Int.	Felsic
Sub-type	1	1	A	1	A	2	1	A	2	C	1	A	Anomalous	1	A
SWIR Min 1	Epidote	FeMgChlorite	FeMgChlorite	FeMgChlorite	FeMgChlorite	Hornblende	FeMgChlorite	FeMgChlorite	-	Phengite	FeMgChlorite	Muscovite	MgChlorite	FeMgChlorite	FeMgChlorite
SWIR MIN 2	Paragonite	Muscovite	Muscovite	FeTourmaline	Muscovite	Epidote	Hornblende	-	-	FeTourmaline	Phengite	-	Muscovite	Muscovite	Muscovite
$\Delta\text{Al}_2\text{O}_3^\#$	1.24	1.24	2.04	-0.20	2.17	-0.69	-0.17	2.21	-0.79	2.17	-0.09	2.24	2.23	1.12	2.26
$\Delta\text{TiO}_2^\#$	-0.01	-0.04	-0.22	-0.25	-0.13	0.02	-0.29	-0.12	-0.45	0.13	-0.42	0.03	-0.14	0.35	-0.04
$\Delta\text{CaO}^\#$	6.89	0.36	-1.60	-2.06	-1.42	5.86	1.89	-1.29	3.75	1.44	-0.83	-0.73	-1.02	-2.03	-1.05
$\Delta\text{MgO}^\#$	-0.57	-0.63	1.87	2.92	2.80	-1.01	1.40	3.25	-1.28	1.53	-1.37	0.61	8.91	4.54	4.47
$\Delta\text{SiO}_2^\#$	-4.49	22.50	14.16	-22.23	-19.70	-5.36	-8.64	18.62	-5.24	14.53	-2.89	8.23	33.89	100.63	-4.75
$\Delta\text{Fe}_2\text{O}_3^\#$	1.89	-0.57	0.17	0.58	1.92	10.27	0.76	3.03	-2.88	0.02	-0.29	0.69	-0.94	10.74	4.72
$\Delta\text{Na}_2\text{O}^\#$	-1.05	-0.39	-2.78	-3.46	-2.88	-2.11	-2.02	-2.94	-3.06	1.36	-1.08	-3.15	-2.90	-2.98	-3.04
$\Delta\text{K}_2\text{O}^\#$	-0.66	0.23	1.49	1.76	1.22	-0.61	-0.16	1.43	-0.18	-1.48	0.31	2.12	1.13	-0.46	0.80
Total major element mass change (wt%)	3.25	22.69	15.12	-22.94	-16.03	6.37	-7.23	24.19	-10.12	19.70	-6.65	10.04	41.15	111.91	3.37
$\Delta\text{Cu}^\oplus$	-2.49	317.83	-8.17	-10.86	-4.58	919.90	0.77	13.80	-9.29	-3.09	8.74	229.26	-5.03	225.88	27.70
$\Delta\text{Zn}^\oplus$	16.34	112.06	-20.05	147.11	-14.39	81.73	116.95	37.80	49.82	28.12	47.89	-6.22	21.46	375.10	54.40
$\Delta\text{Pb}^\oplus$	9.03	727.17	-1.20	5.87	-2.46	15.13	15.59	0.48	1.23	0.29	3.06	18.17	-4.30	58.23	-4.37
$\Delta\text{Cs}^\oplus$	-0.48	1.04	0.72	0.76	0.66	-1.72	-0.50	1.12	-0.47	-0.14	-0.76	1.62	1.70	-0.03	1.35
$\Delta\text{Rb}^\oplus$	-20.01	22.97	87.14	53.03	66.01	-12.50	4.87	92.18	12.31	-40.75	23.81	92.79	52.64	-2.23	35.86
$\Delta\text{Ba}^\oplus$	-307.47	16.35	-38.81	908.36	-136.24	-215.97	-86.32	191.38	-207.39	-394.49	69.63	349.29	49.06	-150.75	133.85
$\Delta\text{Nb}^\oplus$	-4.95	3.91	6.18	-1.98	3.03	2.60	-1.74	12.52	1.34	5.53	-2.70	14.34	2.68	4.02	10.45
$\Delta\text{Zr}^\oplus$	40.97	-47.33	167.62	-28.39	163.44	117.74	-27.18	65.44	56.94	48.29	0.02	172.83	155.27	74.22	109.46
$\Delta\text{La}^\oplus$	-8.32	2.44	-11.09	-4.64	1.32	21.24	-0.25	-13.19	0.58	17.37	-2.28	17.15	-55.97	6.51	3.26
$\Delta\text{Sm}^\oplus$	0.68	-1.19	-1.68	-0.33	0.80	4.24	-0.25	-0.13	-0.02	2.69	-1.58	5.94	-7.44	0.82	2.98
$\Delta\text{Yb}^\oplus$	-2.91	-2.60	-2.71	-2.11	-2.68	-1.62	-2.11	-1.90	-1.54	-1.46	-2.23	-1.35	-2.16	-2.33	-1.58
Al	25.26	45.73	97.71	85.57	98.87	36.86	54.57	98.61	44.68	31.75	53.92	92.57	97.08	92.51	97.42
CCPI	81.87	69.48	75.29	83.70	79.48	89.30	84.58	79.65	82.98	48.99	74.99	57.43	82.41	96.30	83.58

# wt%

Al; Alteration Index =  $100 * (\text{K}_2\text{O} + \text{MgO}) / (\text{K}_2\text{O} + \text{MgO} + \text{CaO} + \text{Na}_2\text{O})$

CCPI =  $100 * (\text{Fe}_2\text{O}_3 + \text{MgO}) / (\text{Fe}_2\text{O}_3 + \text{MgO} + \text{K}_2\text{O} + \text{Na}_2\text{O})$

Least Altered samples

Table A2-2 (continued): Major element mass change based on the MacLean (1990) multiple precursor method, SWIR mineralogy, and alteration indexes.

Samples	D1410411	D1410412	D1410413	D1410415	D1410416	D1410417	D1410418	D1410419	D1410420	D1410422	D1410423	D1410424	D1410425	D1410426	D1410427
Rock Type	Int.	Felsic	Felsic	Int.	Int.	Felsic	Int.	Int.	Felsic	Int.	Int.	Felsic	Felsic	Felsic	Mafic
Sub-type	4	A	A	1	1	Anomalous	1	1	A	1	1	A	B	A	II
SWIR Min 1	MgChlorite	Muscovite	FelMgChlorite	FelMgChlorite	FelMgChlorite	FelMgChlorite	FelMgChlorite	FelMgChlorite	FelMgChlorite	FelMgChlorite	FelMgChlorite	-	-	Muscovite	FelMgChlorite
SWIR MIN 2	Muscovite	FelMgChlorite	-	Muscovite	-	-	Muscovite	Muscovite	Muscovite	-	-	-	-	MgChlorite	-
$\Delta\text{Al}_2\text{O}_3^\#$	1.16	2.02	2.25	-0.25	0.07	2.25	0.07	-0.01	1.64	-0.07	0.69	2.25	2.11	2.20	0.41
$\Delta\text{TiO}_2^\#$	0.32	0.08	-0.04	-0.25	-0.05	0.15	-0.14	-0.28	0.01	-0.32	0.79	0.00	0.05	-0.10	1.24
$\Delta\text{CaO}^\#$	-2.07	-0.51	-1.15	-3.03	-2.83	-1.08	-2.86	-2.98	-0.29	-3.01	-2.03	-0.66	-0.04	-1.26	3.74
$\Delta\text{MgO}^\#$	12.51	0.07	11.20	2.97	2.21	6.53	2.20	-0.70	0.33	3.03	6.47	2.60	-0.43	2.47	3.24
$\Delta\text{SiO}_2^\#$	-6.58	20.99	68.28	-9.33	-0.83	57.96	-9.19	-8.62	16.66	3.04	26.15	88.72	22.69	39.16	4.71
$\Delta\text{Fe}_2\text{O}_3^\#$	-4.72	-1.03	4.39	1.98	7.54	10.06	6.12	1.13	0.16	4.06	8.43	0.88	-1.63	-0.72	8.37
$\Delta\text{Na}_2\text{O}^\#$	-3.13	2.18	-3.01	-2.93	-3.91	-2.98	-3.12	-3.94	1.60	-3.99	-3.48	-0.91	2.68	-2.81	-1.58
$\Delta\text{K}_2\text{O}^\#$	0.09	-1.38	-0.49	-0.64	-0.45	-0.48	-0.57	1.25	-2.20	-0.09	-0.96	0.32	-1.40	1.78	-1.16
Total major element mass change (wt%)	-2.40	22.42	81.44	-11.48	1.76	72.40	-7.48	-14.15	17.93	2.65	36.05	93.21	24.02	40.71	18.99
$\Delta\text{Cu}^\oplus$	-15.08	-4.46	16.93	-13.76	-4.60	0.83	-14.08	-14.07	1.91	-11.69	-5.52	41.40	-1.96	-5.46	75.80
$\Delta\text{Zn}^\oplus$	-18.74	-16.54	153.68	136.87	151.50	130.11	156.74	-5.84	21.33	149.52	94.62	7.31	-27.74	-19.30	59.17
$\Delta\text{Pb}^\oplus$	-3.93	-1.45	20.75	1.11	-2.09	-0.27	5.42	-2.11	1.25	1.39	-2.75	8.60	27.72	-1.48	-2.47
$\Delta\text{Cs}^\oplus$	0.38	-0.29	1.03	-1.03	-0.94	0.53	-0.99	-0.26	-0.98	-0.60	-0.70	1.03	-0.20	0.99	-0.93
$\Delta\text{Rb}^\oplus$	13.59	-43.80	-6.65	-18.31	-7.95	-4.13	-12.22	43.79	-73.77	5.78	-23.21	28.11	-41.77	64.20	-32.67
$\Delta\text{Ba}^\oplus$	-119.86	-288.48	-244.15	-191.76	-172.38	-234.65	-198.33	186.22	-511.57	-66.85	-287.25	288.02	-336.70	612.97	-321.78
$\Delta\text{Nb}^\oplus$	0.10	10.91	13.98	0.43	2.57	14.30	0.69	-0.62	16.81	-0.06	12.24	13.44	7.88	11.72	-2.96
$\Delta\text{Zr}^\oplus$	-3.87	143.97	131.53	23.11	68.36	378.23	40.16	20.20	233.76	32.69	158.46	93.96	56.04	92.38	-62.17
$\Delta\text{La}^\oplus$	-33.43	-49.89	1.53	-0.55	14.89	17.10	2.61	4.65	-3.09	4.77	-6.97	-8.42	13.16	14.03	-11.83
$\Delta\text{Sm}^\oplus$	-5.07	-2.35	2.33	-0.38	2.07	5.45	0.22	0.42	6.05	0.36	0.97	2.65	5.82	4.79	0.16
$\Delta\text{Yb}^\oplus$	-2.77	-0.76	-1.52	-1.97	-2.00	-1.50	-2.08	-2.09	0.31	-2.09	-1.80	-1.45	-1.15	-1.90	-2.31
Al	97.17	26.40	98.93	85.51	94.85	97.37	87.64	94.89	26.63	95.99	93.15	68.97	18.42	96.51	49.40
CCPI	93.08	24.41	93.70	91.55	96.61	94.30	93.82	85.73	31.52	94.70	98.93	63.84	16.74	68.55	92.00

# wt%

Al; Alteration Index =  $100 \times (\text{K}_2\text{O} + \text{MgO}) / (\text{K}_2\text{O} + \text{MgO} + \text{CaO} + \text{Na}_2\text{O})$

CCPI =  $100 \times (\text{Fe}_2\text{O}_3 + \text{MgO}) / (\text{Fe}_2\text{O}_3 + \text{MgO} + \text{K}_2\text{O} + \text{Na}_2\text{O})$

Least Altered samples

Table A2-2 (continued): Major element mass change based on the MacLean (1990) multiple precursor method, SWIR mineralogy, and alteration indexes.									
Samples	D1410428	D1410429	D1410430	R143430					
Rock Type	Felsic	Int.	Felsic	Felsic					
Sub-type	A	3	A	Rim Granite					
SWIR Min 1	Phlogopite	FeMgChlorite	FeMgChlorite	-					
SWIR MIN 2	-	Phengite	Muscovite	-					
$\Delta\text{Al}_2\text{O}_3^\#$	-29.96	1.09	1.97	1.91					
$\Delta\text{TiO}_2^\#$	-8.95	0.47	0.04	0.03					
$\Delta\text{CaO}^\#$	-7.31	-1.97	-0.74	-0.28					
$\Delta\text{MgO}^\#$	-5.37	0.74	3.45	-0.61					
$\Delta\text{SiO}_2^\#$	114.70	-6.09	46.98	28.73					
$\Delta\text{Fe}_2\text{O}_3^\#$	2.91	-1.43	4.68	0.80					
$\Delta\text{Na}_2\text{O}^\#$	-44.17	0.00	-3.95	0.99					
$\Delta\text{K}_2\text{O}^\#$	-14.68	0.15	0.32	2.49					
Total major element mass change (wt%)	7.17	-7.05	52.75	34.06					
$\Delta\text{Cu}^\oplus$	173.91	-10.09	-0.38	-3.03					
$\Delta\text{Zn}^\oplus$	1384.31	12.59	97.27	-0.43					
$\Delta\text{Pb}^\oplus$	107.54	-1.14	-0.49	3.31					
$\Delta\text{Cs}^\oplus$	-13.62	0.15	0.80	-0.46					
$\Delta\text{Rb}^\oplus$	-624.74	20.91	24.06	56.15					
$\Delta\text{Ba}^\oplus$	-2430.29	-94.96	247.69	657.57					
$\Delta\text{Nb}^\oplus$	91.80	3.26	8.95	37.43					
$\Delta\text{Zr}^\oplus$	3778.89	16.64	142.71	151.82					
$\Delta\text{La}^\oplus$	-122.62	5.37	-9.38	36.03					
$\Delta\text{Sm}^\oplus$	64.57	3.38	4.43	12.52					
$\Delta\text{Yb}^\oplus$	40.01	-2.43	-0.77	1.06					
Al	97.35	61.99	98.13	50.24					
CCPI	80.62	69.86	79.31	24.09					

# wt%  
Al; Alteration Index =  $100 * (\text{K}_2\text{O} + \text{MgO}) / (\text{K}_2\text{O} + \text{MgO} + \text{CaO} + \text{Na}_2\text{O})$   
CCPI =  $100 * (\text{Fe}_2\text{O}_3 + \text{MgO}) / (\text{Fe}_2\text{O}_3 + \text{MgO} + \text{K}_2\text{O} + \text{Na}_2\text{O})$   
Least Altered samples

Table A2-3: Calculated best fit fractionation curves for least altered elements on element vs Th plots.

Element	Least altered fractionation curve equation
$\text{Al}_2\text{O}_3$	$= 0.0058(\text{Th})^2 - 0.2874(\text{Th}) + 16.547$
$\text{TiO}_2$	$= 0.0019(\text{Th})^2 - 0.1126(\text{Th}) + 1.8194$
$\text{CaO}$	$= 0.0022(\text{Th})^2 - 0.1726(\text{Th}) + 4.0319$
$\text{MgO}$	$= 0.0078(\text{Th})^2 - 0.4597(\text{Th}) + 7.9023$
$\text{SiO}_2$	$= -0.0278(\text{Th})^2 + 1.68464(\text{Th}) + 48.066$
$\text{Fe}_2\text{O}_3$	$= 0.0027(\text{Th})^2 - 0.3569(\text{Th}) + 10.498$
$\text{Na}_2\text{O}$	$= 0.0063(\text{Th})^2 - 0.22(\text{Th}) + 4.808$
$\text{K}_2\text{O}$	$= 0.0028(\text{Th})^2 - 0.0511(\text{Th}) + 1.4542$
$\text{Cu}$	$= -0.0228(\text{Th})^2 - 0.4331(\text{Th}) + 13.533$
$\text{Zn}$	$= -0.1756(\text{Th})^2 + 4.5704(\text{Th}) + 49.27$
$\text{Pb}$	$= -0.0143(\text{Th})^2 + 0.527(\text{Th}) + 1.0278$
$\text{Cs}$	$= 0.0061(\text{Th})^2 - 0.2415(\text{Th}) + 2.5083$
$\text{Rb}$	$= 0.1338(\text{Th})^2 - 3.1604(\text{Th}) + 49.372$
$\text{Ba}$	$= 0.2344(\text{Th})^2 + 1.71941(\text{Th}) + 333.33$
$\text{Nb}$	$= -0.0136(\text{Th})^2 + 0.5089(\text{Th}) + 10.096$
$\text{Zr}$	$= -0.568(\text{Th})^2 + 19.859(\text{Th}) + 136.71$
$\text{La}$	$= -0.0142(\text{Th})^2 + 2.5119(\text{Th}) + 13.603$
$\text{Sm}$	$= -0.0116(\text{Th})^2 + 0.4512(\text{Th}) + 4.2153$
$\text{Yb}$	$= -0.0064(\text{Th})^2 - 0.2226(\text{Th}) + 2.0568$

Figure A2-4: Principal Component Analysis eigenvalues and rescaled eigenvectors.

Initial Eigenvalues <sup>a</sup>						
Component	1	2	3	4	5	6
Total	.003	.001	.000	.000	.000	9.927E-05
% of Variance	60.761	10.938	7.526	5.778	2.827	1.886
Cumulative %	60.761	71.699	79.225	85.003	87.830	89.717
Component Matrix <sup>b</sup>						
Element	Rescaled					
	Component					
	1	2	3	4	5	6
SiO <sub>2</sub>	-.285	.027	-.036	.599	-.312	.375
Al <sub>2</sub> O <sub>3</sub>	.018	-.006	.076	-.048	.213	-.441
Fe <sub>2</sub> O <sub>3</sub>	.370	-.037	.022	-.492	.299	-.379
CaO	-.050	-.027	-.042	-.649	.433	-.347
MgO	.313	-.002	-.023	-.517	.020	-.007
Na <sub>2</sub> O	-.127	.012	.041	.057	.307	-.275
K <sub>2</sub> O	-.164	-.028	.070	.435	-.305	.333
Cr <sub>2</sub> O <sub>3</sub>	-.017	.019	-.070	-.879	.125	.413
TiO <sub>2</sub>	-.075	-.018	-.007	-.473	.406	-.531
MnO	.175	.032	-.023	-.656	.297	-.354
P <sub>2</sub> O <sub>5</sub>	-.062	-.035	-.004	-.343	.314	-.482
SrO	-.057	-.016	.005	-.242	.387	-.469
BaO	-.131	-.011	.047	.347	-.225	.219
C	-.064	.015	-.031	-.573	.145	-.084
S	.929	-.034	.281	-.028	.072	-.030
Ba	-.144	-.012	.046	.362	-.227	.216
Ce	.020	.084	.123	.402	-.101	.196
Cr	-.021	.027	-.078	-.889	.124	.397
Cs	-.059	-.019	.023	.075	-.055	.010
Dy	.015	.108	.183	.380	.094	.078
Er	.018	.124	.179	.421	.069	.131
Eu	-.117	-.015	.034	-.091	.351	-.397
Ga	.019	-.110	.031	.150	.090	-.178
Gd	.022	.077	.175	.329	.104	.039
Hf	.127	.004	.119	.564	-.091	.174
Ho	.011	.113	.177	.393	.079	.100
La	.004	.072	.109	.401	-.116	.212
Lu	.057	.131	.190	.477	.027	.201
Nb	.042	.063	.129	.464	.041	.139
Nd	.032	.090	.144	.358	-.032	.135
Pr	.023	.087	.131	.380	-.069	.172
Rb	-.152	-.028	.063	.407	-.284	.280
Sm	.043	.092	.166	.354	.032	.087
Sn	.504	-.272	-.245	.145	-.055	.012
Sr	-.079	-.010	.003	-.252	.425	-.490
Ta	.010	.065	.098	.564	-.044	.248
Tb	.021	.095	.187	.362	.096	.063
Th	.119	.056	.065	.514	-.254	.395
Tl	.004	-.034	.030	.117	-.360	.113

Figure A2-4: Principal Component Analysis eigenvalues and rescaled eigenvectors.

Initial Eigenvalues <sup>a</sup>						
Component	1	2	3	4	5	6
Total	.003	.001	.000	.000	.000	9.927E-05
% of Variance	60.761	10.938	7.526	5.778	2.827	1.886
Cumulative %	60.761	71.699	79.225	85.003	87.830	89.717
Component Matrix <sup>b</sup>						
Element	Rescaled					
	Component					
	1	2	3	4	5	6
Tm	.039	.137	.186	.444	.047	.168
U	.024	.097	.087	.505	-.207	.387
V	-.075	-.023	-.015	-.545	.355	-.477
W	.002	-.018	.067	.015	-.102	-.133
Y	-.018	.099	.156	.384	.078	.112
Yb	.042	.132	.182	.465	.041	.194
Zr	.086	-.007	.114	.475	-.036	.022
As	.152	.066	-.041	-.491	-.805	-.226
Bi	.958	.252	-.094	.020	.012	.014
Hg	.873	.143	.449	-.015	-.031	.015
Sb	.108	.019	.091	-.219	-.487	-.112
Se	.948	-.273	-.024	.004	.005	.016
Te	.485	.366	-.698	.074	.032	.005
Ag	.923	.034	-.355	.039	.014	.010
Cd	.912	-.319	.118	.004	-.017	.020
Co	.268	-.159	-.156	-.725	.293	-.253
Cu	.701	-.637	-.307	.013	-.017	-.002
Mo	-.043	.013	-.016	.196	-.134	.501
Ni	-.031	.023	-.074	-.919	.096	.220
Pb	.815	.512	-.226	.007	-.001	-.016
Zn	.951	-.148	.244	-.022	.011	.008

Extraction Method: Principal Component Analysis.

a. When analyzing a covariance matrix, the initial eigenvalues are the same across the raw and rescaled solution.

b. 6 components extracted.



Table A2-5: Principal component scores for samples and elements

Samples	PC 1	PC 2	PC 3	PC 4	PC 5	PC 6
D1425001	0.028	0.002	-0.012	-0.177	0.040	0.028
D1425002	0.031	0.003	-0.004	-0.067	-0.001	-0.010
D1425003	0.010	0.006	0.018	0.066	-0.015	0.031
D1425004	0.006	0.007	0.016	0.050	-0.005	0.020
D1425005	0.011	0.006	0.015	0.065	-0.015	0.029
D1425006	0.008	0.006	0.016	0.064	-0.013	0.030
D1425007	0.018	0.002	0.008	-0.005	0.015	-0.006
D1425008	0.028	0.000	-0.015	-0.182	0.049	0.029
D1425009	0.012	0.008	0.021	0.073	-0.011	0.031
D1425010	0.010	0.008	0.020	0.066	-0.008	0.027
D1425011	0.010	0.007	0.018	0.053	-0.005	0.023
D1425012	0.011	0.009	0.015	0.054	-0.006	0.022
D1425013	0.011	0.005	0.014	0.049	-0.007	0.022
D1425014	0.025	0.000	0.014	-0.031	0.043	-0.052
D1425015	0.026	-0.001	0.012	-0.024	0.029	-0.036
D1425016	0.016	0.001	0.010	0.010	0.011	-0.006
D1425017	0.012	0.002	0.010	0.018	0.005	-0.001
D1425018	0.014	0.002	0.009	0.014	0.007	-0.003
D1425019	0.015	0.002	0.009	0.003	0.018	-0.012
D1425020	0.020	-0.003	0.006	0.006	0.015	-0.010
D1425021	0.011	0.008	0.019	0.060	-0.004	0.022
D1425022	0.015	0.003	0.011	0.014	0.013	-0.004
D1425023	0.013	0.004	0.010	-0.003	0.021	-0.009
D1425024	0.015	0.008	0.018	0.057	0.002	0.016
D1425025	0.012	0.008	0.016	0.042	0.007	0.011
D1425026	0.014	0.002	0.010	-0.007	0.023	-0.009
D1425027	0.013	0.002	0.009	-0.012	0.026	-0.010
D1425028	0.023	0.002	0.008	-0.011	0.010	-0.012
D1425029	0.026	-0.005	0.006	0.000	-0.007	-0.001
D1425030	0.032	-0.008	0.004	0.000	-0.008	-0.001
D1425031	0.055	-0.003	0.003	-0.065	0.030	-0.014
D1425032	0.016	0.001	0.010	0.007	0.007	0.004
D1425033	0.013	0.004	0.010	0.020	0.016	-0.006
D1425034	0.011	0.005	0.014	0.051	-0.009	0.023
D1425035	0.021	0.010	0.023	0.069	-0.006	0.029
D1425036	0.028	0.002	-0.004	-0.130	0.032	0.008
D1425037	0.010	0.002	0.004	0.021	-0.005	0.015
D1425038	0.019	0.006	0.010	-0.016	0.023	0.009
D1425039	0.029	0.002	0.003	-0.070	0.034	-0.006
D1425040	0.011	0.007	0.022	0.090	-0.020	0.043
D1425041	0.014	0.002	0.012	0.016	0.006	0.003
D1425042	0.040	0.018	-0.026	0.003	0.009	0.003
D1425043	0.010	0.003	0.016	0.029	0.002	0.005
D1425044	0.016	0.011	0.018	-0.016	0.038	-0.007
D1425045	0.009	0.002	0.013	0.024	-0.004	0.011
D1425046	0.007	0.003	0.006	0.022	-0.006	0.013
D1425047	0.016	0.000	0.010	0.018	-0.001	-0.001

Table A2-5: Principal component scores for samples and elements

Samples	PC 1	PC 2	PC 3	PC 4	PC 5	PC 6
D1425048	0.013	0.008	0.019	0.069	-0.012	0.032
D1425049	0.015	0.006	0.012	0.050	-0.008	0.020
D1425050	0.014	0.007	0.012	0.052	-0.008	0.021
D1425051	0.015	0.007	0.016	0.066	-0.013	0.030
D1425052	0.022	0.002	0.004	-0.041	0.005	0.000
D1425053	0.018	0.010	0.015	0.087	-0.022	0.065
D1425054	0.018	0.008	0.014	0.060	-0.010	0.029
D1425055	0.026	0.003	0.014	-0.005	0.024	-0.020
D1425056	0.017	0.008	0.022	0.081	-0.015	0.038
D1425057	0.012	0.002	0.011	0.020	0.006	0.000
D1425058	0.011	0.002	0.011	0.022	0.001	0.006
D1425059	0.020	0.001	0.005	-0.045	0.031	-0.010
D1425060	0.011	0.003	0.009	0.010	-0.006	0.001
D1425061	0.051	-0.001	0.017	-0.011	0.004	-0.008
D1425062	0.015	0.003	0.015	0.022	0.014	-0.007
D1425063	0.015	0.003	0.015	0.023	0.015	-0.004
D1425064	0.014	0.001	0.009	-0.034	0.019	-0.004
D1425065	0.015	0.002	0.014	0.024	0.013	-0.002
D1425066	0.015	0.007	0.019	0.042	0.009	0.006
D1425067	0.007	0.005	0.013	0.047	-0.006	0.018
D1425068	0.058	-0.014	0.005	0.069	-0.024	0.034
R137251	0.027	0.005	0.018	0.037	-0.019	0.018
R137252	0.130	-0.026	0.016	0.026	-0.043	0.013
R137253	0.012	0.002	0.009	0.036	-0.013	0.018
R137254	0.040	0.008	0.000	0.014	-0.043	0.007
R137255	0.015	0.004	0.012	0.042	-0.013	0.021
R137256	0.025	0.005	0.001	-0.098	0.026	0.021
R137257	0.019	0.003	0.013	0.043	-0.022	0.020
R137258	0.067	0.022	-0.014	-0.202	-0.095	-0.011
R137259	0.106	0.004	0.017	-0.002	-0.062	0.002
R137260	0.032	0.000	0.014	0.048	-0.027	0.023
R137261	0.021	0.003	0.018	0.061	-0.035	0.031
R137262	0.012	0.004	0.014	0.053	-0.024	0.026
R137263	0.211	-0.020	0.025	-0.026	-0.029	-0.006
R137264	0.014	0.004	0.014	0.049	-0.017	0.021
R137265	0.013	0.006	0.018	0.058	-0.012	0.021
R137266	0.015	0.005	0.013	0.034	0.003	0.004
R137267	0.020	0.007	0.011	0.033	0.006	0.002
R137268	0.016	0.002	0.011	0.026	0.001	0.001
R137269	0.020	0.012	0.004	0.062	-0.014	0.029
R137270	0.022	0.014	0.000	0.062	-0.014	0.028
R137271	0.017	0.001	0.006	0.013	0.006	-0.007
R137272	0.022	0.010	0.003	0.047	-0.040	0.021
R137273	0.017	0.008	0.003	0.046	-0.013	0.023
R137274	0.023	0.006	0.002	0.016	0.000	-0.003
R137275	0.016	0.005	0.012	0.031	0.002	0.003
R137276	0.017	0.010	0.003	0.043	-0.005	0.020

Table A2-5: Principal component scores for samples and elements

Samples	PC 1	PC 2	PC 3	PC 4	PC 5	PC 6
R137277	0.021	0.001	0.007	-0.005	0.020	-0.014
R137278	0.020	0.000	0.007	-0.012	0.027	-0.020
R137279	0.022	0.007	0.016	0.063	-0.003	0.025
R137280	0.014	0.001	0.006	-0.014	0.026	-0.016
R137281	0.014	0.001	0.006	-0.020	0.026	-0.018
R137282	0.021	0.002	0.010	-0.004	0.014	-0.004
R137283	0.013	0.009	0.024	0.083	-0.010	0.031
R137284	0.053	-0.002	-0.010	-0.011	0.022	-0.012
R137285	0.017	0.003	0.008	-0.003	0.008	-0.003
R137286	0.016	0.003	0.012	0.016	0.010	-0.005
R137287	0.008	0.004	0.007	0.024	-0.004	0.012
R137288	0.021	0.002	0.002	-0.095	0.040	-0.008
R137289	0.009	0.003	0.007	0.029	-0.011	0.026
R137290	0.009	0.004	0.007	0.032	-0.010	0.023
R137291	0.012	0.006	0.016	0.005	0.013	-0.005
R137292	0.018	0.004	0.007	-0.009	0.011	-0.015
R137293	0.019	0.004	0.014	0.009	0.021	-0.013
R137294	0.015	0.012	0.025	0.075	0.005	0.019
R137295	0.018	0.017	0.034	0.098	0.005	0.026
R137296	0.022	0.009	0.020	0.074	-0.003	0.023
R137297	0.022	0.016	0.032	0.102	-0.001	0.032
R137298	0.020	0.013	0.021	0.080	-0.006	0.031
R137299	0.015	0.003	0.013	0.007	0.014	-0.003
R137300	0.012	0.003	0.009	-0.011	0.023	-0.011
D1411601	0.024	0.000	0.003	-0.037	0.019	-0.026
D1411602	0.021	0.001	0.010	-0.007	0.031	-0.027
D1411603	0.007	0.006	0.012	0.048	-0.009	0.020
D1411604	0.026	0.003	0.003	-0.023	0.018	-0.009
D1411605	0.024	0.004	0.010	0.004	0.019	-0.017
D1411606	0.020	0.004	0.008	0.017	0.003	0.005
D1411607	0.040	0.000	-0.002	-0.033	0.027	-0.033
D1411608	0.124	0.012	-0.042	-0.021	0.019	-0.011
D1411609	0.167	0.035	-0.022	-0.135	-0.043	-0.021
D1411610	1.576	0.130	0.175	0.037	0.002	0.015
D1411611	0.145	-0.018	0.030	-0.016	0.023	-0.025
D1411612	0.041	0.002	0.011	-0.006	0.020	-0.021
D1411613	0.018	-0.001	0.002	-0.034	0.016	-0.021
D1411614	0.018	0.001	0.010	-0.008	0.032	-0.030
D1411615	0.017	0.001	0.007	-0.022	0.025	-0.022
D1411616	0.022	0.001	0.006	-0.034	0.023	-0.010
D1411617	0.019	0.008	0.018	0.046	0.001	0.014
D1411618	0.020	0.004	0.014	0.011	0.017	-0.011
D1411619	0.015	0.003	0.006	-0.016	0.028	-0.023
D1411621	1.593	-0.261	-0.081	0.004	0.007	-0.001
D1411623	0.016	0.001	0.009	0.025	-0.004	0.011
D1411624	0.093	0.007	-0.013	0.002	0.036	-0.028
D1411625	0.016	0.011	0.027	0.046	0.029	-0.014

Table A2-5: Principal component scores for samples and elements

Samples	PC 1	PC 2	PC 3	PC 4	PC 5	PC 6
D1411626	0.017	0.000	0.006	-0.012	0.029	-0.022
D1411627	0.014	0.010	0.017	0.052	0.002	0.013
D1411628	0.021	0.002	0.007	-0.010	-0.011	-0.009
D1411629	0.020	0.006	0.012	0.033	-0.008	0.013
D1411630	0.011	0.003	0.009	0.004	0.011	-0.007
D1411631	0.015	0.008	0.016	0.043	0.000	0.012
D1411632	0.026	-0.001	0.007	-0.018	0.018	-0.010
D1411633	0.027	0.002	0.003	-0.063	0.032	-0.008
D1411634	0.016	0.008	0.020	0.059	-0.005	0.020
D1411636	0.011	0.001	0.008	-0.002	0.011	-0.007
D1411637	0.031	-0.001	0.000	-0.060	0.029	-0.022
D1411638	0.017	-0.001	0.010	-0.033	0.029	-0.028
D1411639	0.010	0.006	0.014	0.052	-0.015	0.030
D1411640	0.151	-0.034	-0.007	-0.009	0.004	-0.012
D1411641	0.046	0.016	0.010	0.065	-0.002	0.019
D1411642	0.014	0.003	0.008	-0.008	0.021	-0.013
D1411643	0.017	0.010	0.016	0.049	-0.005	0.016
D1411645	0.026	0.002	0.001	-0.086	0.035	-0.013
D1411646	0.024	0.011	0.022	0.053	0.004	0.016
D1411647	0.025	-0.001	-0.013	-0.202	0.045	0.043
D1411648	0.016	0.002	0.010	-0.014	0.035	-0.029
D1411649	0.019	0.001	-0.002	-0.089	0.031	0.009
D1411650	0.007	0.007	0.011	0.041	-0.001	0.015
D1411651	0.019	0.004	0.010	0.008	0.012	0.001
D1411652	0.009	0.000	0.003	-0.007	0.016	-0.014
D1411653	0.016	0.003	0.007	-0.031	0.030	-0.013
D1411656	0.664	0.230	-0.236	0.027	0.012	0.005
D1411657	0.019	0.007	0.008	0.008	0.011	-0.012
D1411658	0.009	0.007	0.015	0.044	0.004	0.011
D1411659	0.051	0.004	0.028	0.044	0.001	-0.008
D1411660	0.041	0.004	0.012	-0.018	0.042	-0.039
D1411661	0.010	0.009	0.021	0.075	-0.007	0.027
D1411662	0.033	0.000	0.010	-0.025	0.026	-0.031
D1411663	0.017	0.002	-0.004	-0.111	0.031	0.015
D1411664	0.023	0.006	0.007	-0.008	0.031	-0.028
D1411666	0.023	0.003	0.010	-0.013	0.030	-0.024
D1411667	0.024	0.000	0.009	-0.001	0.019	-0.013
D1411668	0.007	0.007	0.011	0.036	0.007	0.005
D1411669	0.018	0.001	0.003	-0.036	0.025	-0.011
D1411670	0.014	0.002	0.007	-0.009	0.024	-0.026
D1411671	0.022	0.002	0.007	-0.019	0.029	-0.033
D1411672	0.044	0.003	0.005	-0.016	0.013	-0.009
D1411674	0.030	0.019	-0.012	0.044	-0.005	0.017
D1411675	0.033	0.001	0.013	-0.024	0.024	-0.019
D1411676	0.025	0.000	0.011	-0.020	0.039	-0.038
D1411677	0.041	-0.006	0.000	-0.057	0.027	-0.017
D1411679	0.015	0.005	0.009	0.030	-0.003	0.013

Table A2-5: Principal component scores for samples and elements

Samples	PC 1	PC 2	PC 3	PC 4	PC 5	PC 6
D1411680	0.035	0.006	0.005	-0.021	0.039	-0.028
D1411682	0.013	0.007	0.015	0.051	-0.008	0.020
D1411683	0.015	0.008	0.021	0.029	0.022	0.001
D1411684	0.014	0.006	0.015	0.035	0.009	0.002
D1411687	0.069	-0.023	-0.007	0.028	-0.015	0.010
D1411688	0.013	0.007	0.015	0.057	-0.014	0.025
D1411690	0.020	-0.001	0.005	-0.032	0.039	-0.038
D1411691	0.018	0.004	0.012	0.006	0.029	-0.022
D1411693	0.117	0.045	-0.020	0.014	-0.006	-0.005
D1411694	0.010	0.004	0.013	0.046	-0.010	0.019
D1411695	0.023	0.000	0.018	0.005	-0.005	0.003
D1411696	0.016	0.010	0.020	0.070	-0.010	0.028
D1411697	0.065	-0.019	0.004	-0.028	0.039	-0.029
D1411698	0.020	0.002	0.009	-0.018	0.022	-0.015
D1411700	0.017	0.007	0.014	0.054	-0.010	0.025
D1410401	0.015	0.000	0.007	-0.021	0.020	-0.022
D1410402	0.011	0.011	0.012	0.054	-0.007	0.049
D1410403	0.025	0.002	0.005	-0.021	-0.008	-0.014
D1410405	0.043	0.006	0.018	0.078	-0.022	0.031
D1410406	0.010	0.002	0.009	0.028	-0.014	0.013
D1410408	0.027	0.002	0.006	0.009	-0.004	-0.003
D1410410	0.017	0.007	0.019	0.065	-0.011	0.025
D1410411	0.013	0.008	0.017	0.024	0.009	0.005
D1410412	0.008	0.006	0.013	0.047	-0.003	0.018
D1410413	0.018	0.006	0.011	0.029	-0.006	0.012
D1410415	0.025	0.003	0.008	-0.016	-0.007	-0.009
D1410416	0.024	0.006	0.006	0.018	-0.001	0.029
D1410417	0.017	0.006	0.015	0.038	-0.007	0.012
D1410418	0.025	0.001	0.010	0.006	0.007	-0.008
D1410419	0.016	0.003	0.011	0.010	-0.009	0.000
D1410420	0.012	0.012	0.021	0.063	-0.001	0.017
D1410422	0.022	0.002	0.010	-0.001	-0.014	-0.003
D1410423	0.021	0.005	0.012	0.006	-0.005	-0.009
D1410424	0.012	0.005	0.010	0.040	-0.006	0.016
D1410425	0.030	0.008	0.011	0.059	-0.002	0.015
D1410426	0.009	0.007	0.017	0.058	-0.009	0.023
D1410427	0.030	0.001	0.004	-0.064	0.030	-0.007
D1410428	0.015	-0.001	0.016	0.043	-0.056	0.030
D1410429	0.023	0.004	0.014	0.040	0.000	-0.002
D1410430	0.013	0.005	0.014	0.048	-0.021	0.022
R143430	0.009	0.013	0.029	0.093	-0.004	0.032
SiO <sub>2</sub>	-0.285	0.027	-0.036	0.599	-0.312	0.375
Al <sub>2</sub> O <sub>3</sub>	0.018	-0.006	0.076	-0.048	0.213	-0.441
Fe <sub>2</sub> O <sub>3</sub>	0.370	-0.037	0.022	-0.492	0.299	-0.379
CaO	-0.050	-0.027	-0.042	-0.649	0.433	-0.347
MgO	0.313	-0.002	-0.023	-0.517	0.020	-0.007
Na <sub>2</sub> O	-0.127	0.012	0.041	0.057	0.307	-0.275

Table A2-5: Principal component scores for samples and elements

Samples	PC 1	PC 2	PC 3	PC 4	PC 5	PC 6
K <sub>2</sub> O	-0.164	-0.028	0.070	0.435	-0.305	0.333
Cr <sub>2</sub> O <sub>3</sub>	-0.017	0.019	-0.070	-0.879	0.125	0.413
TiO <sub>2</sub>	-0.075	-0.018	-0.007	-0.473	0.406	-0.531
MnO	0.175	0.032	-0.023	-0.656	0.297	-0.354
P <sub>2</sub> O <sub>5</sub>	-0.062	-0.035	-0.004	-0.343	0.314	-0.482
SrO	-0.057	-0.016	0.005	-0.242	0.387	-0.469
BaO	-0.131	-0.011	0.047	0.347	-0.225	0.219
C	-0.064	0.015	-0.031	-0.573	0.145	-0.084
S	0.929	-0.034	0.281	-0.028	0.072	-0.030
Ba	-0.144	-0.012	0.046	0.362	-0.227	0.216
Ce	0.020	0.084	0.123	0.402	-0.101	0.196
Cr	-0.021	0.027	-0.078	-0.889	0.124	0.397
Cs	-0.059	-0.019	0.023	0.075	-0.055	0.010
Dy	0.015	0.108	0.183	0.380	0.094	0.078
Er	0.018	0.124	0.179	0.421	0.069	0.131
Eu	-0.117	-0.015	0.034	-0.091	0.351	-0.397
Ga	0.019	-0.110	0.031	0.150	0.090	-0.178
Gd	0.022	0.077	0.175	0.329	0.104	0.039
Hf	0.127	0.004	0.119	0.564	-0.091	0.174
Ho	0.011	0.113	0.177	0.393	0.079	0.100
La	0.004	0.072	0.109	0.401	-0.116	0.212
Lu	0.057	0.131	0.190	0.477	0.027	0.201
Nb	0.042	0.063	0.129	0.464	0.041	0.139
Nd	0.032	0.090	0.144	0.358	-0.032	0.135
Pr	0.023	0.087	0.131	0.380	-0.069	0.172
Rb	-0.152	-0.028	0.063	0.407	-0.284	0.280
Sm	0.043	0.092	0.166	0.354	0.032	0.087
Sn	0.504	-0.272	-0.245	0.145	-0.055	0.012
Sr	-0.079	-0.010	0.003	-0.252	0.425	-0.490
Ta	0.010	0.065	0.098	0.564	-0.044	0.248
Tb	0.021	0.095	0.187	0.362	0.096	0.063
Th	0.119	0.056	0.065	0.514	-0.254	0.395
Tl	0.004	-0.034	0.030	0.117	-0.360	0.113
Tm	0.039	0.137	0.186	0.444	0.047	0.168
U	0.024	0.097	0.087	0.505	-0.207	0.387
V	-0.075	-0.023	-0.015	-0.545	0.355	-0.477
W	0.002	-0.018	0.067	0.015	-0.102	-0.133
Y	-0.018	0.099	0.156	0.384	0.078	0.112
Yb	0.042	0.132	0.182	0.465	0.041	0.194
Zr	0.086	-0.007	0.114	0.475	-0.036	0.022
As	0.152	0.066	-0.041	-0.491	-0.805	-0.226
Bi	0.958	0.252	-0.094	0.020	0.012	0.014
Hg	0.873	0.143	0.449	-0.015	-0.031	0.015
Sb	0.108	0.019	0.091	-0.219	-0.487	-0.112
Se	0.948	-0.273	-0.024	0.004	0.005	0.016
Te	0.485	0.366	-0.698	0.074	0.032	0.005
Ag	0.923	0.034	-0.355	0.039	0.014	0.010

Table A2-5: Principal component scores for samples and elements

Samples	PC 1	PC 2	PC 3	PC 4	PC 5	PC 6
Cd	0.912	-0.319	0.118	0.004	-0.017	0.020
Co	0.268	-0.159	-0.156	-0.725	0.293	-0.253
Cu	0.701	-0.637	-0.307	0.013	-0.017	-0.002
Mo	-0.043	0.013	-0.016	0.196	-0.134	0.501
Ni	-0.031	0.023	-0.074	-0.919	0.096	0.220
Pb	0.815	0.512	-0.226	0.007	-0.001	-0.016
Zn	0.951	-0.148	0.244	-0.022	0.011	0.008

**Appendix3:**  
**Vertical cross-sections from Hood 10 and Hood 41A depicting SWIR-**  
**spectroscopy results, mass change, and principal component analysis**



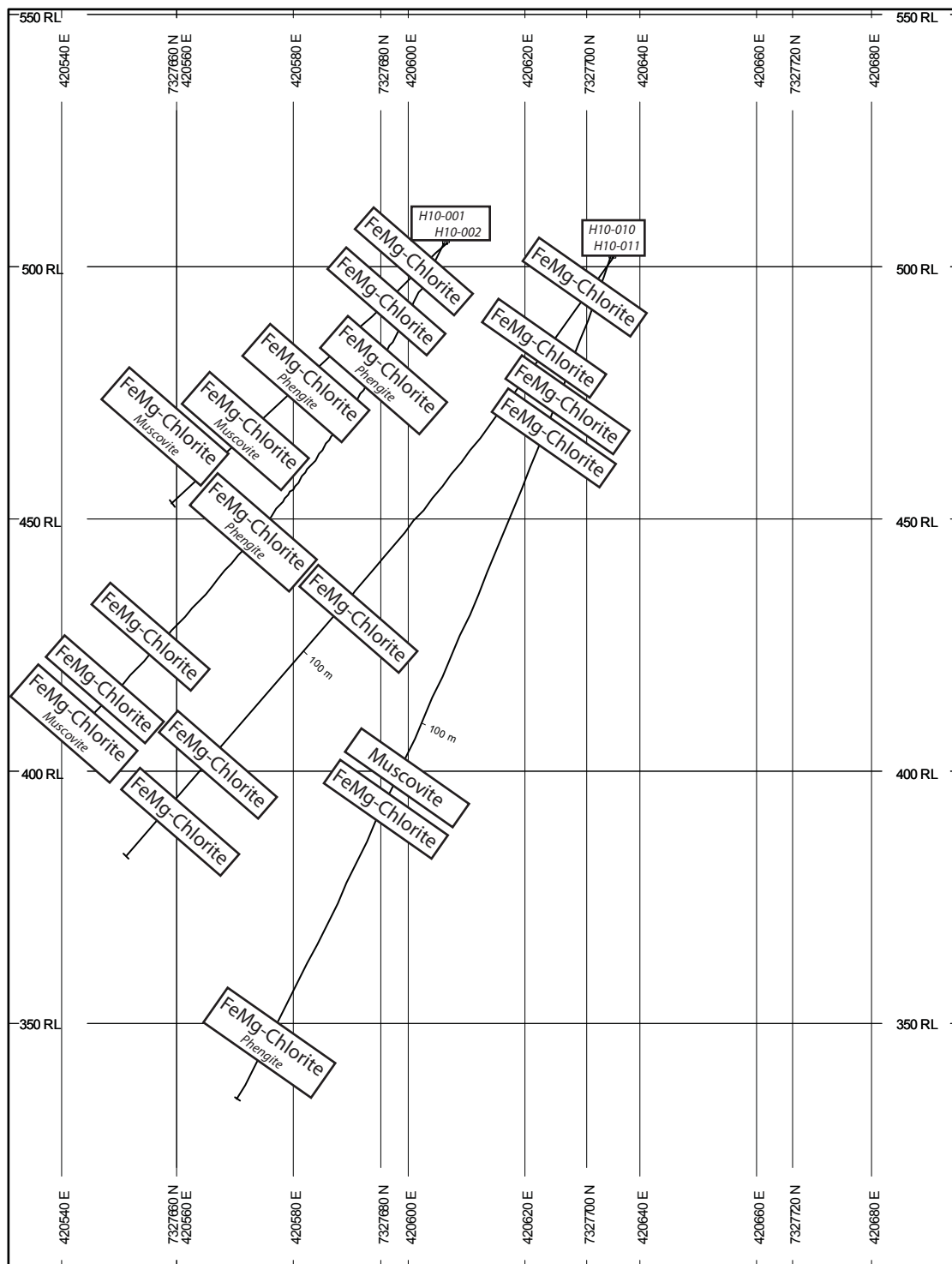


Figure A3-1: Hood 10 cross-section through the southern end of the lens demonstrating the distribution of alteration minerals based on SWIR spectroscopy.

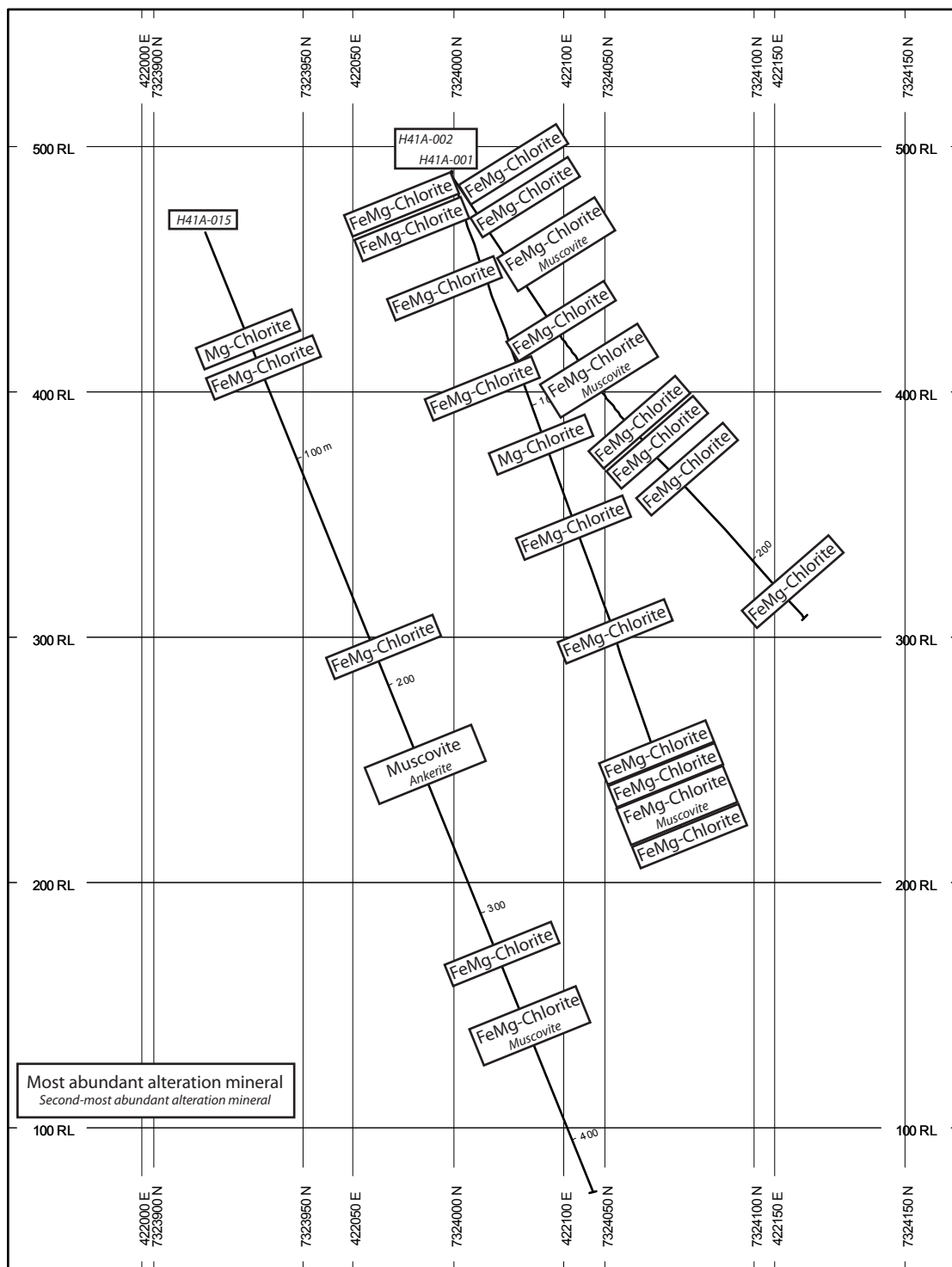


Figure A3-2: Hood 41A cross-section through the southeast end of the lens demonstrating the distribution of alteration minerals based on SWIR spectroscopy.

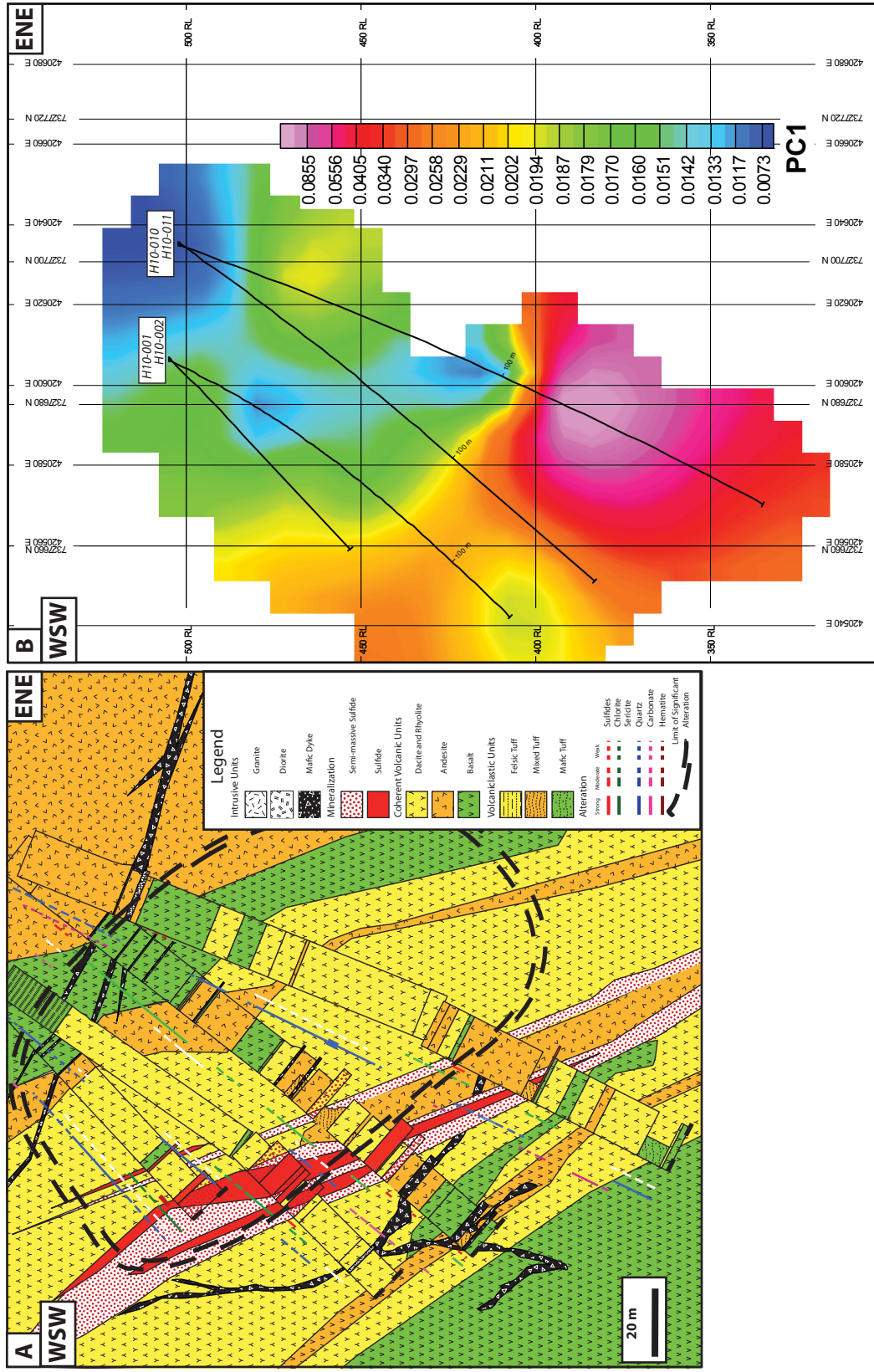


Figure A3-3: A) Hood 10 stratigraphic cross-section compared to 2-D slices of gridding of selected element mass change. B) Hood 10 cross-section slice through modeling of principal component 1 scores.

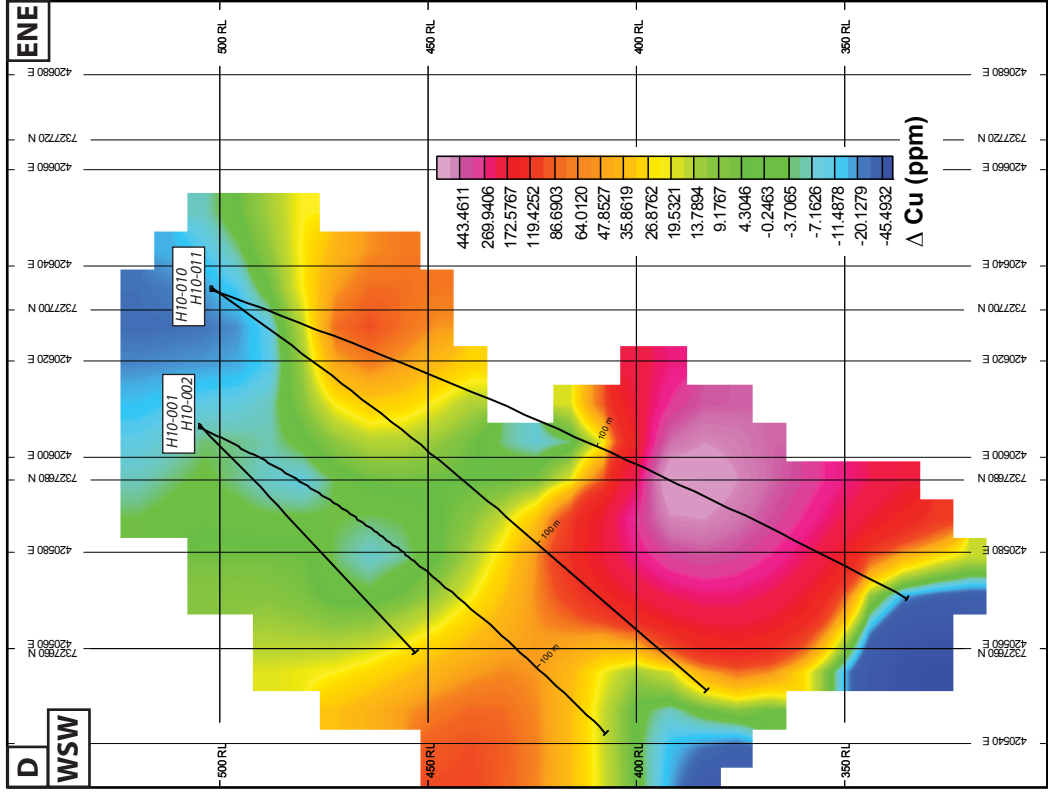
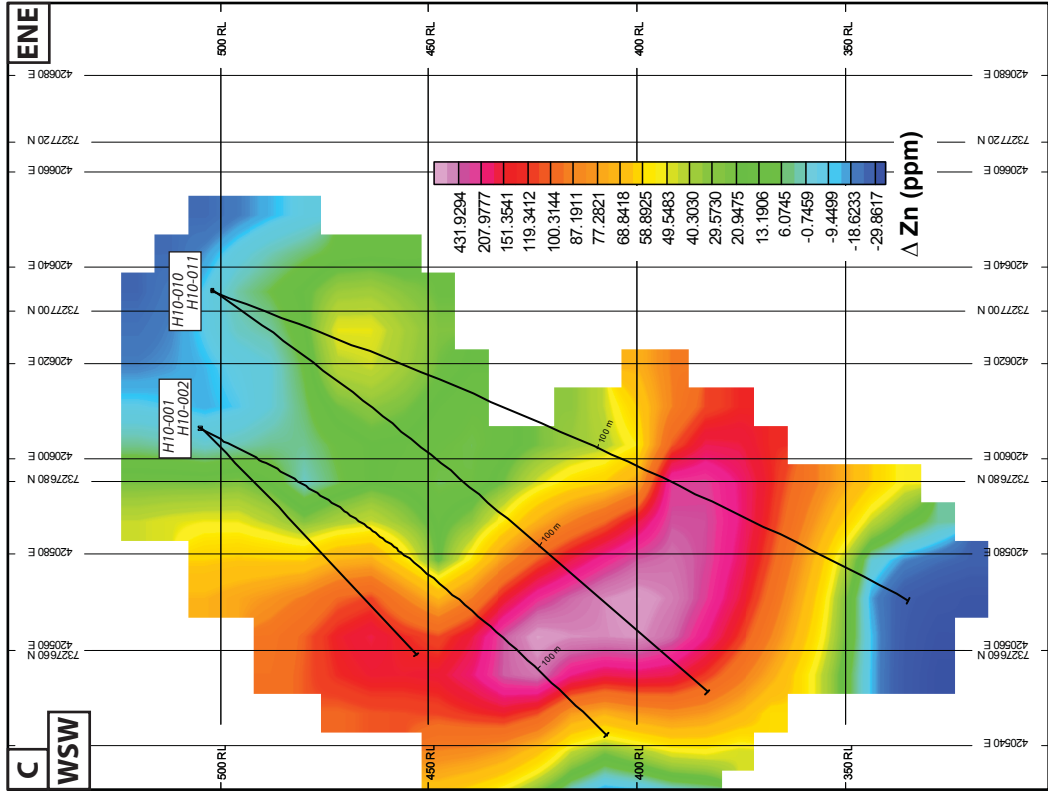


Figure A3-3 (continued): C) Hood 10 cross-section slice through modelling of  $\Delta \text{Zn}$ . D) Hood 10 cross-section slice through modelling of  $\Delta \text{Cu}$ .

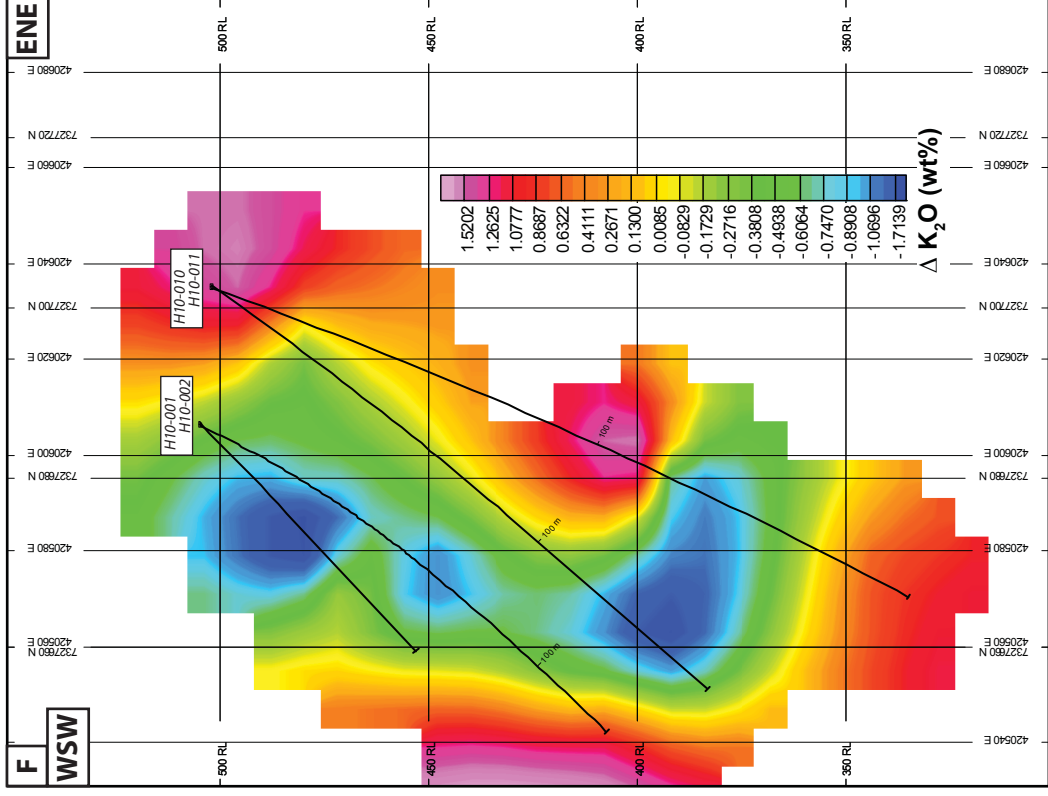
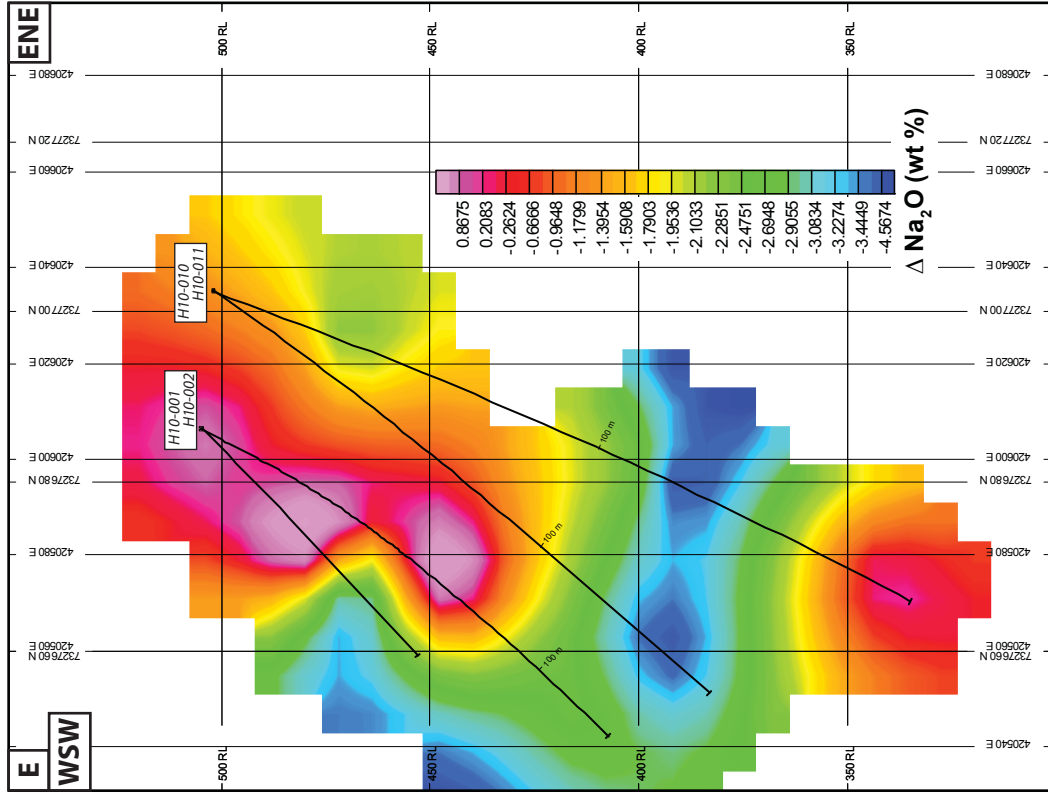


Figure A3-3 (continued): E) Hood 10 cross-section slice through modelling of  $\Delta\text{Na}_2\text{O}$ . F) Hood 10 cross-section slice through modelling of  $\Delta\text{K}_2\text{O}$ .

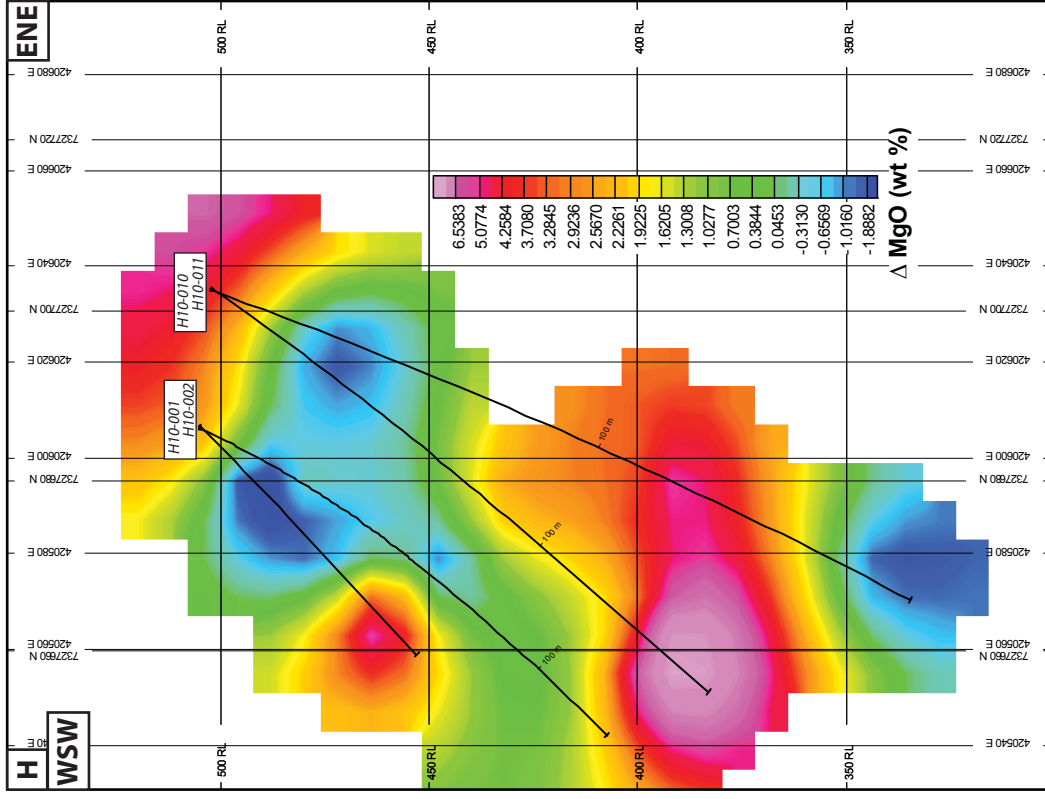
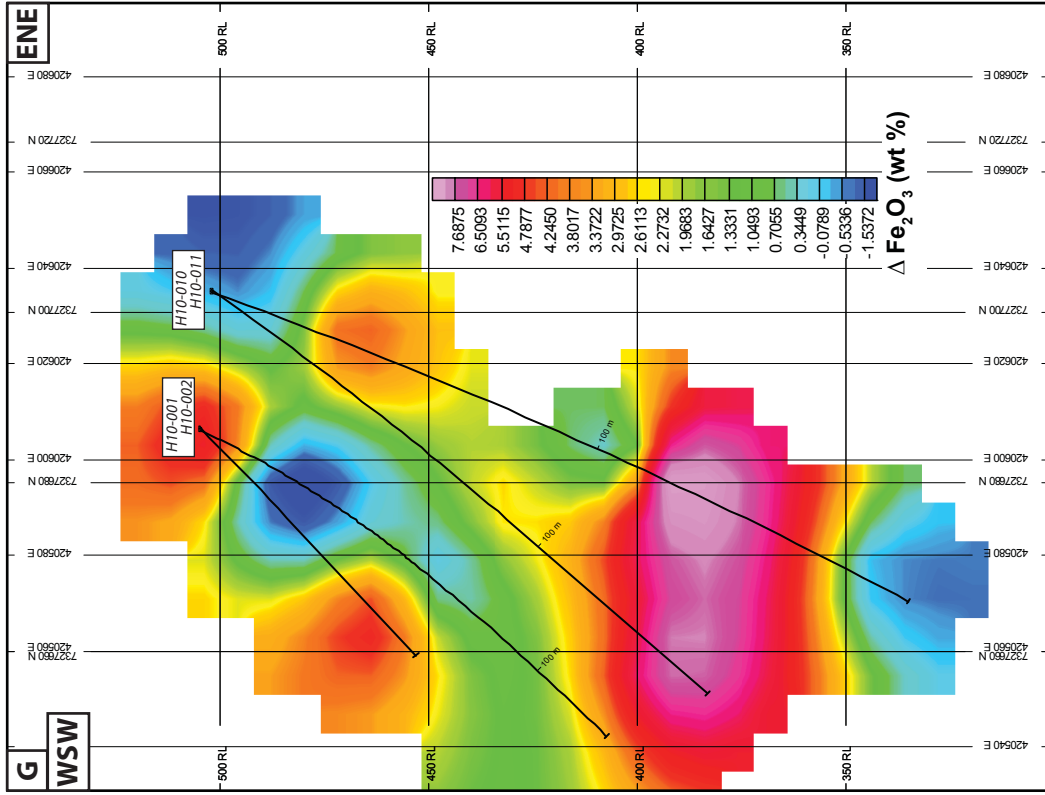


Figure A3-3 (continued): G) Hood 10 cross-section slice through modelling of  $\Delta\text{Fe}_2\text{O}_3$ . H) Hood 10 cross-section slice through modelling of  $\Delta\text{MgO}$ .



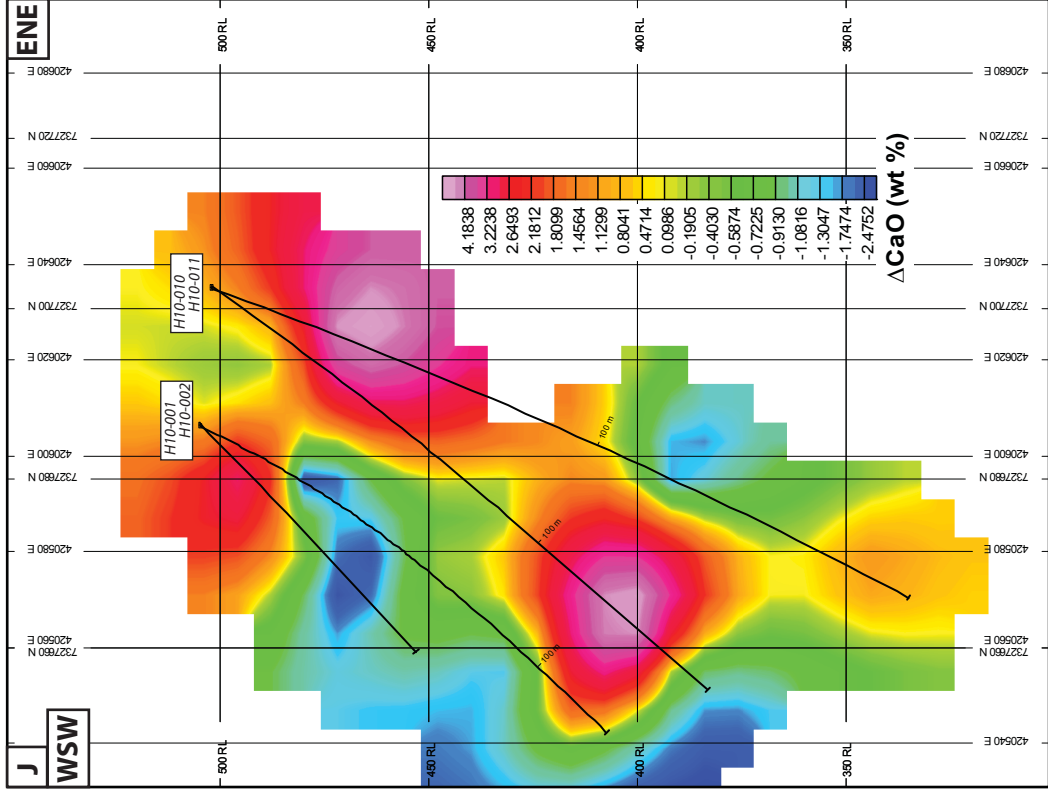
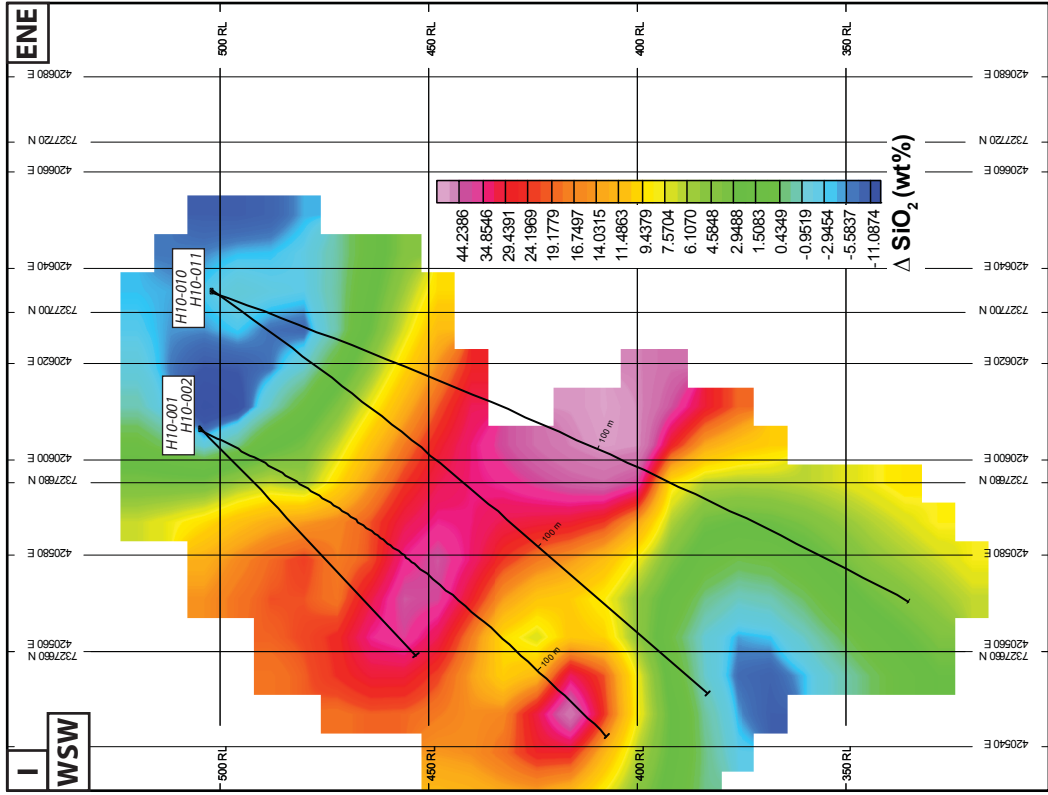


Figure A3-3 (continued): I) Hood 10 cross-section slice through modelling of  $\Delta\text{SiO}_2$ , J) Hood 10 cross-section slice through modelling of  $\Delta\text{CaO}$ .

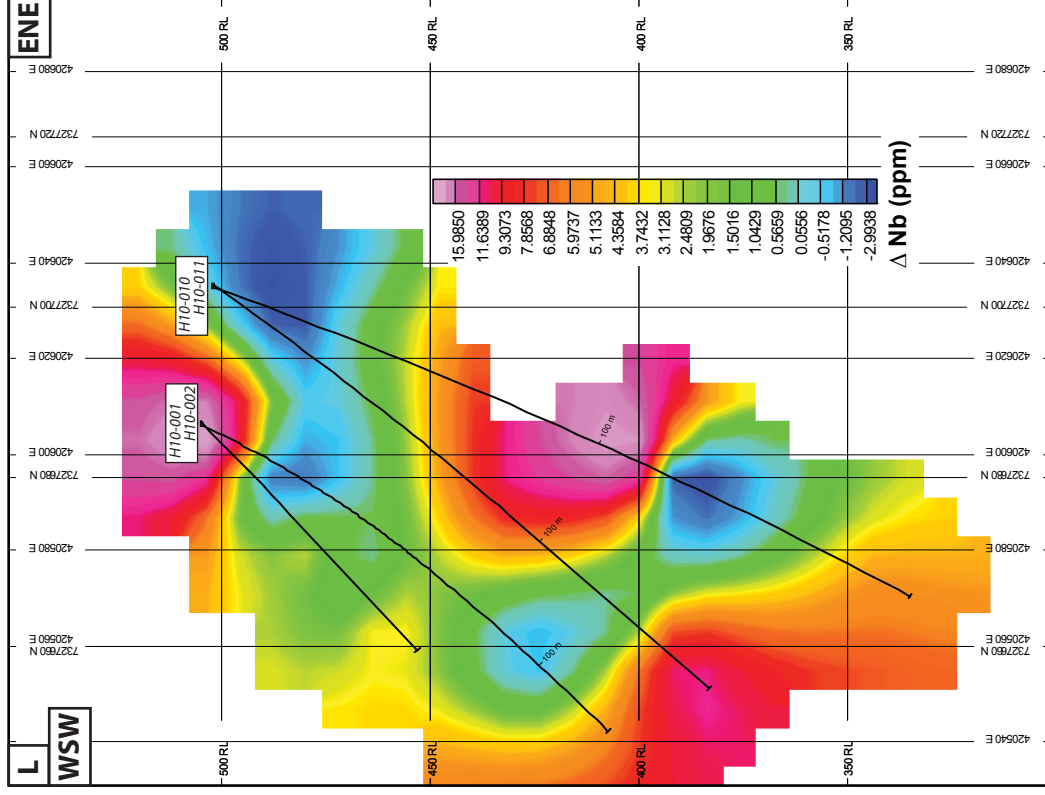
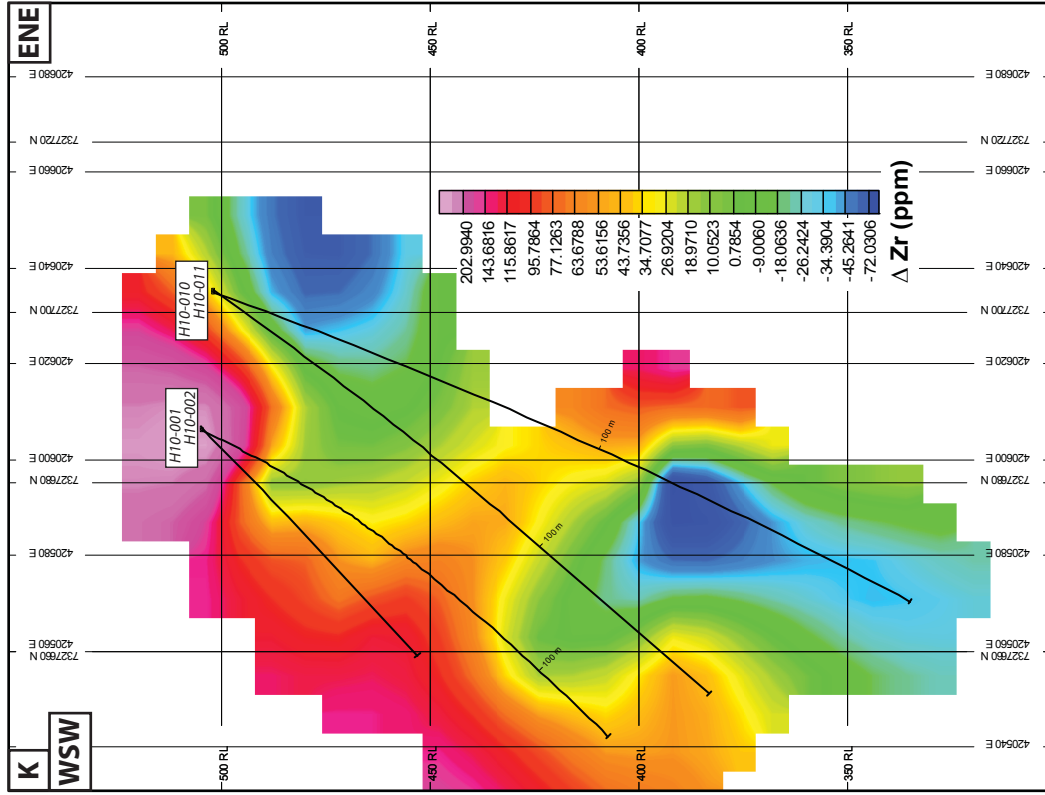


Figure A3-3 (continued): K) Hood 10 cross-section slice through modelling of  $\Delta Zr$ . L) Hood 10 cross-section slice through modelling of  $\Delta Nb$ .



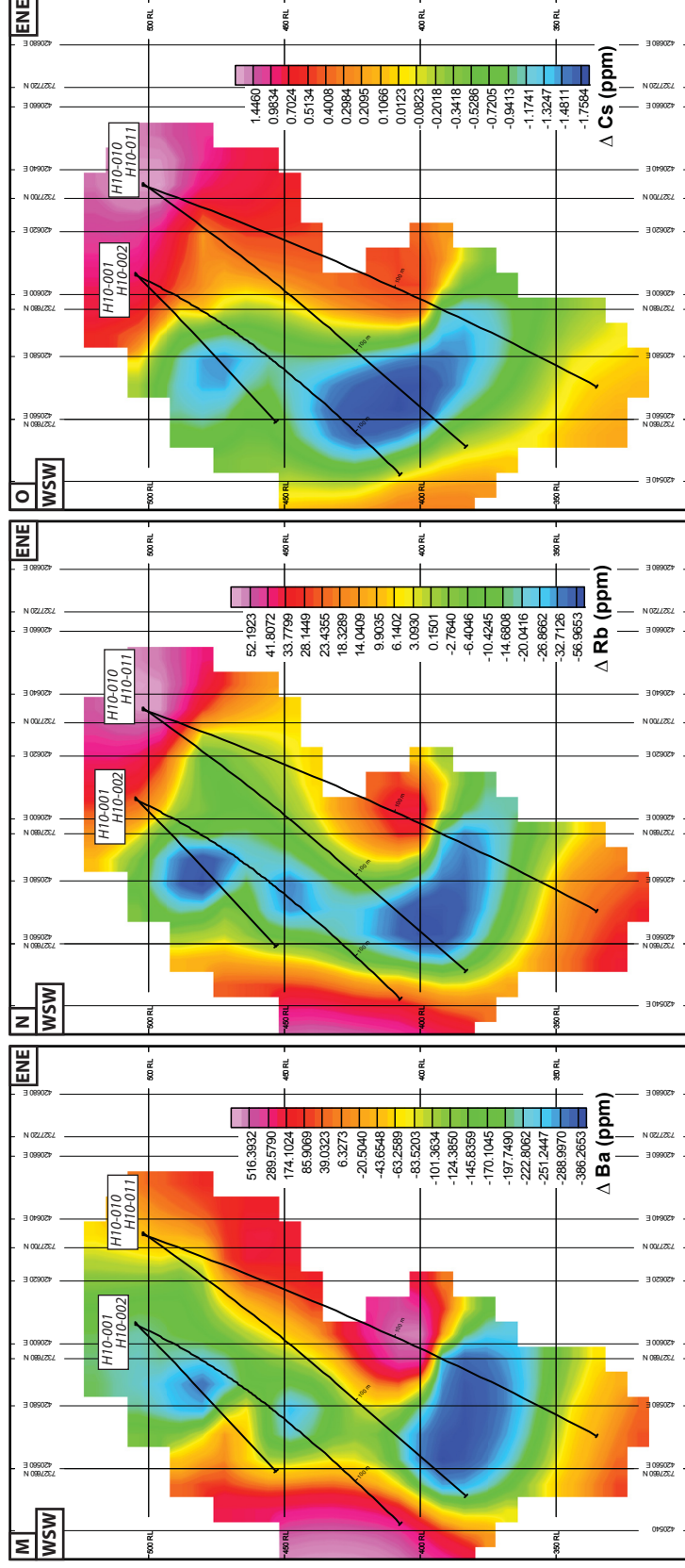


Figure A3-3 (continued): M) Hood 10 cross-section slice through modelling of  $\Delta$ Ba. N) Hood 10 cross-section slice through modelling of  $\Delta$ Rb. O) Hood 10 cross-section slice through modelling of  $\Delta$ Cs.

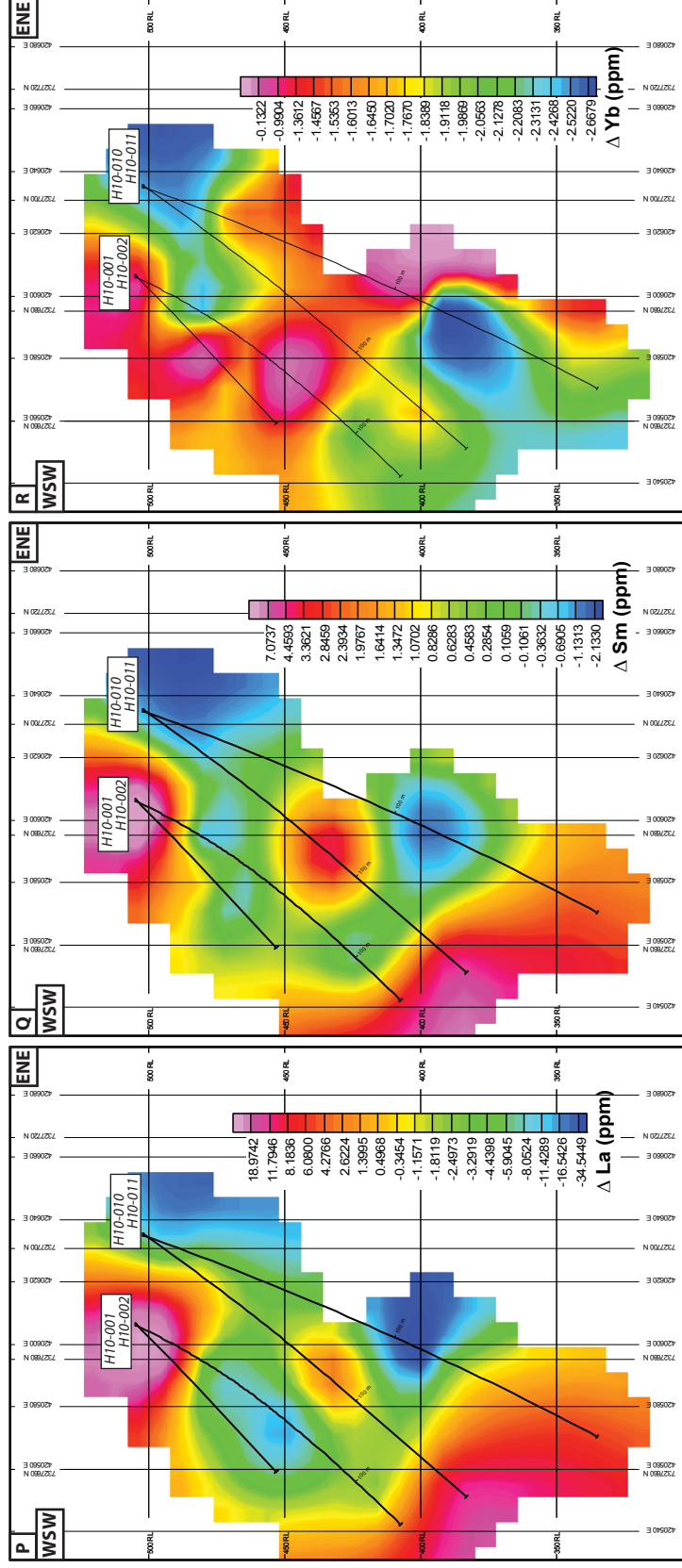


Figure A3-3 (continued): P) Hood 10 cross-section slice through modelling of  $\Delta La$ . Q) Hood 10 cross-section slice through modelling of  $\Delta Sm$ . R) Hood 10 cross-section slice through modelling of  $\Delta Yb$ .

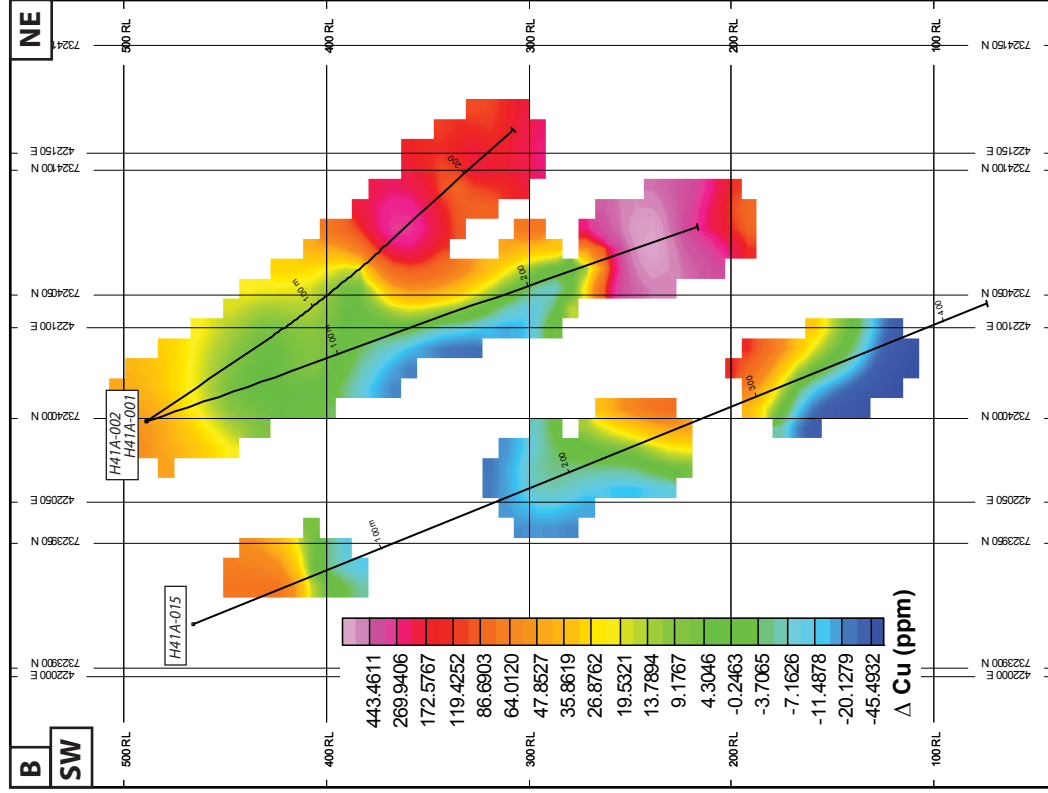
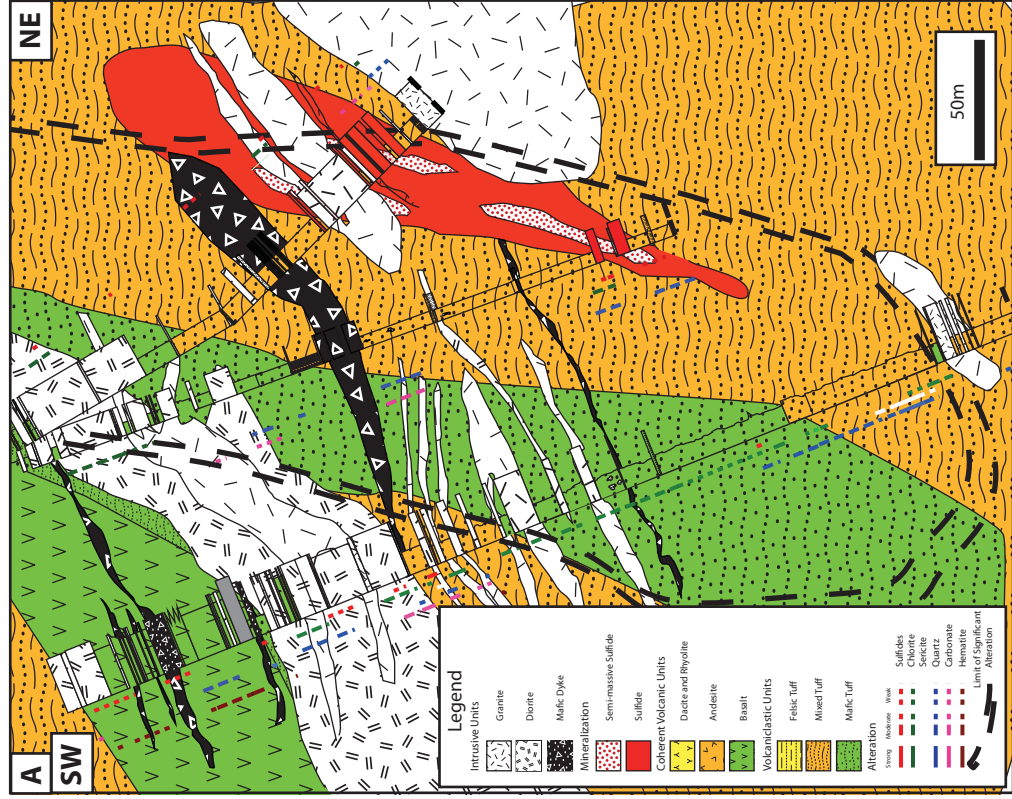


Figure A3-4: A) Hood 41A stratigraphic cross-section compared to 2-D slices of gridding of selected element mass change. B) Hood 41A cross-section slice through modelling of  $\Delta\text{Cu}$ .

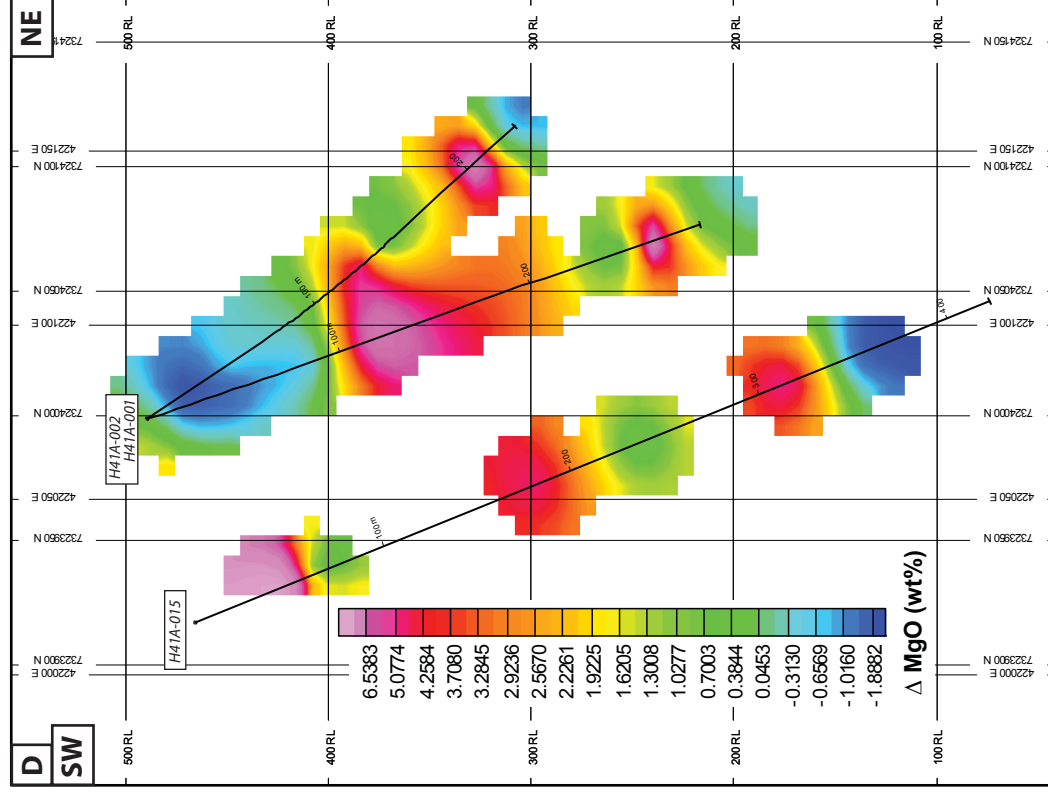
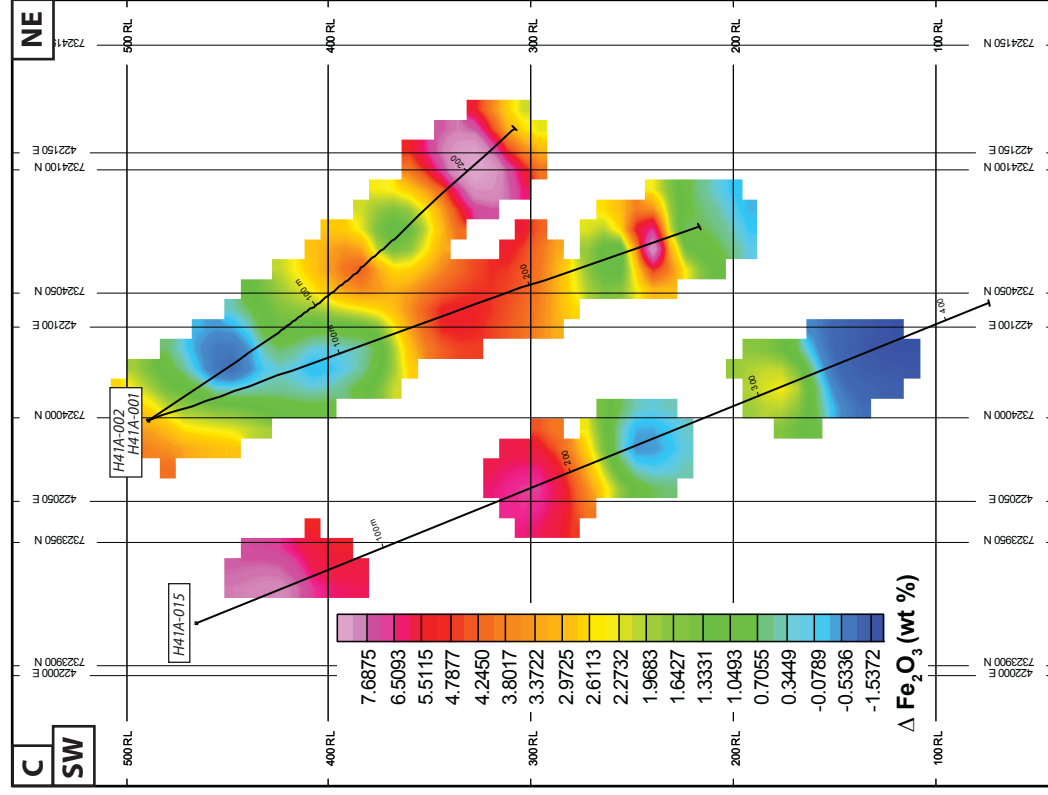


Figure A3-4 (continued): C) Hood 41A cross-section slice through modelling of  $\Delta\text{Fe}_2\text{O}_3$ ; D) Hood 41A cross-section slice through modelling of  $\Delta\text{MgO}$

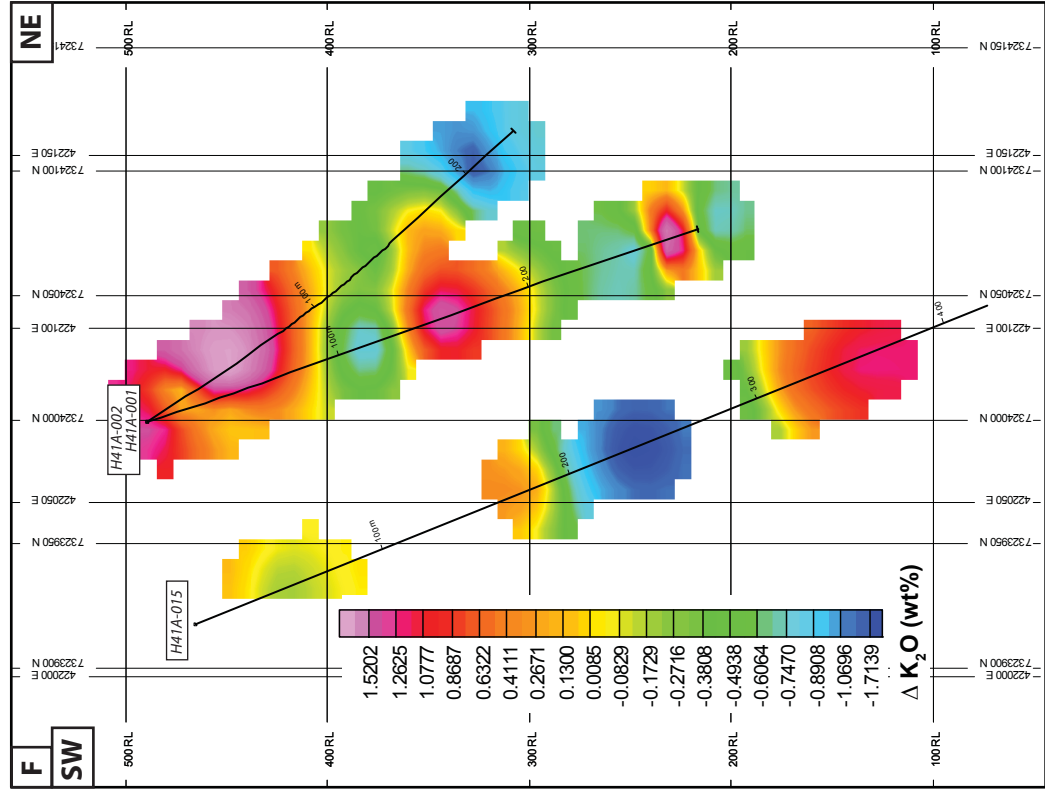
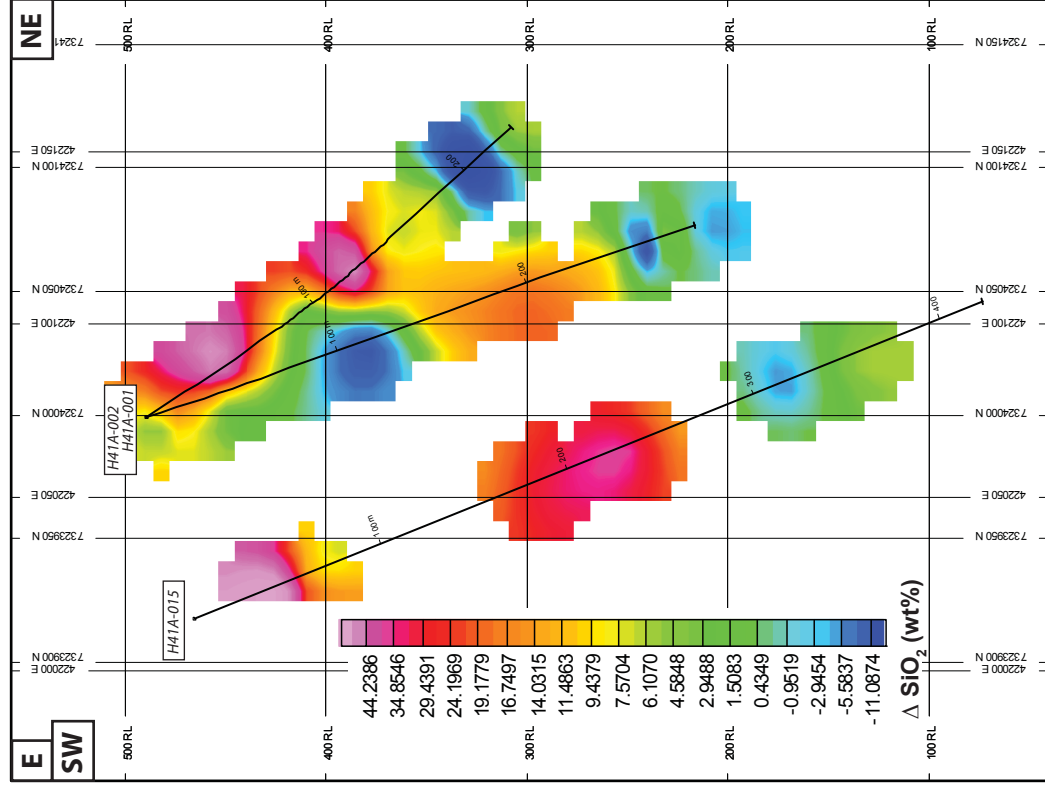


Figure A3-4 (continued): E) Hood 41A cross-section slice through modelling of  $\Delta\text{SiO}_2$ . F) Hood 41A cross-section slice through modelling of  $\Delta\text{K}_2\text{O}$ .

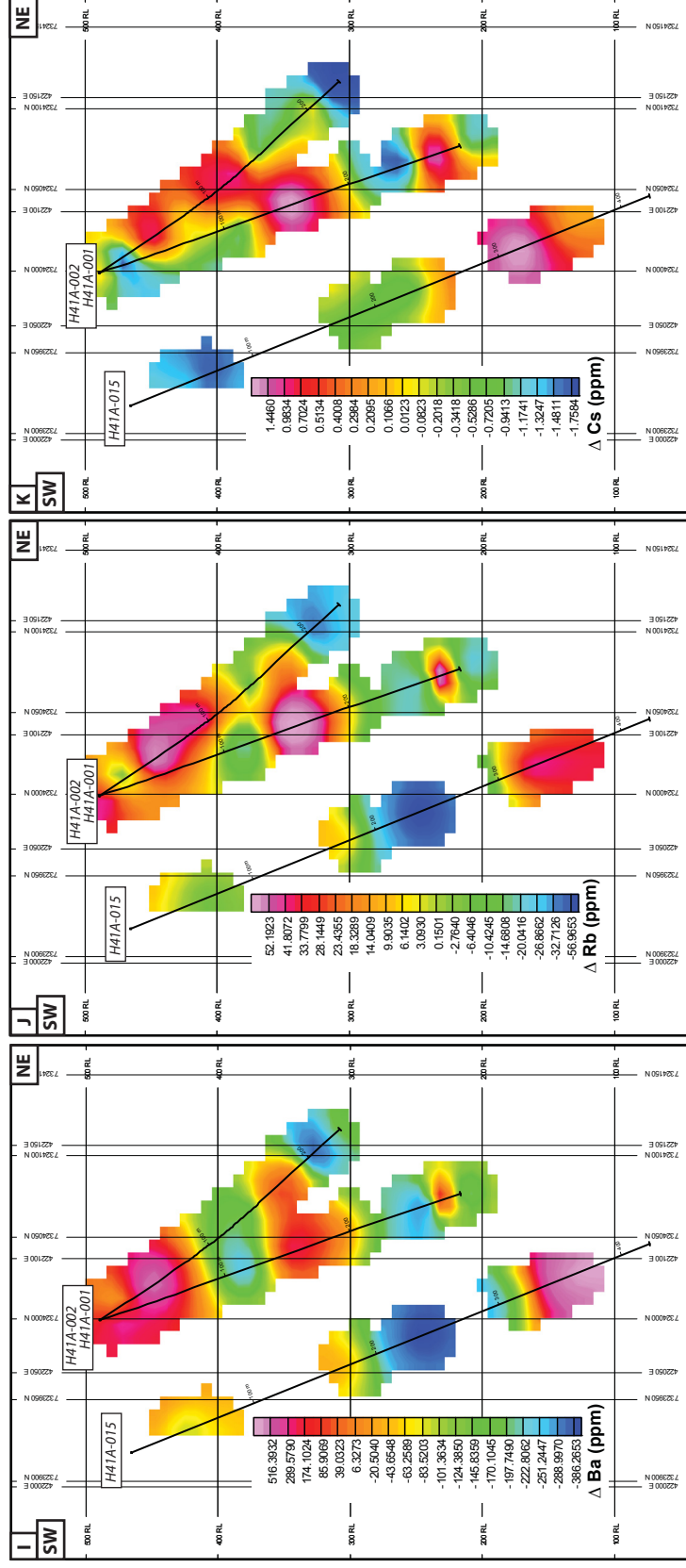


Figure A3-4 (continued): I) Hood 41A cross-section slice through modelling of  $\Delta\text{Ba}$ . J) Hood 41A cross-section slice through modelling of  $\Delta\text{Rb}$ . K) Hood 41A cross-section slice through modelling of  $\Delta\text{Cs}$ .



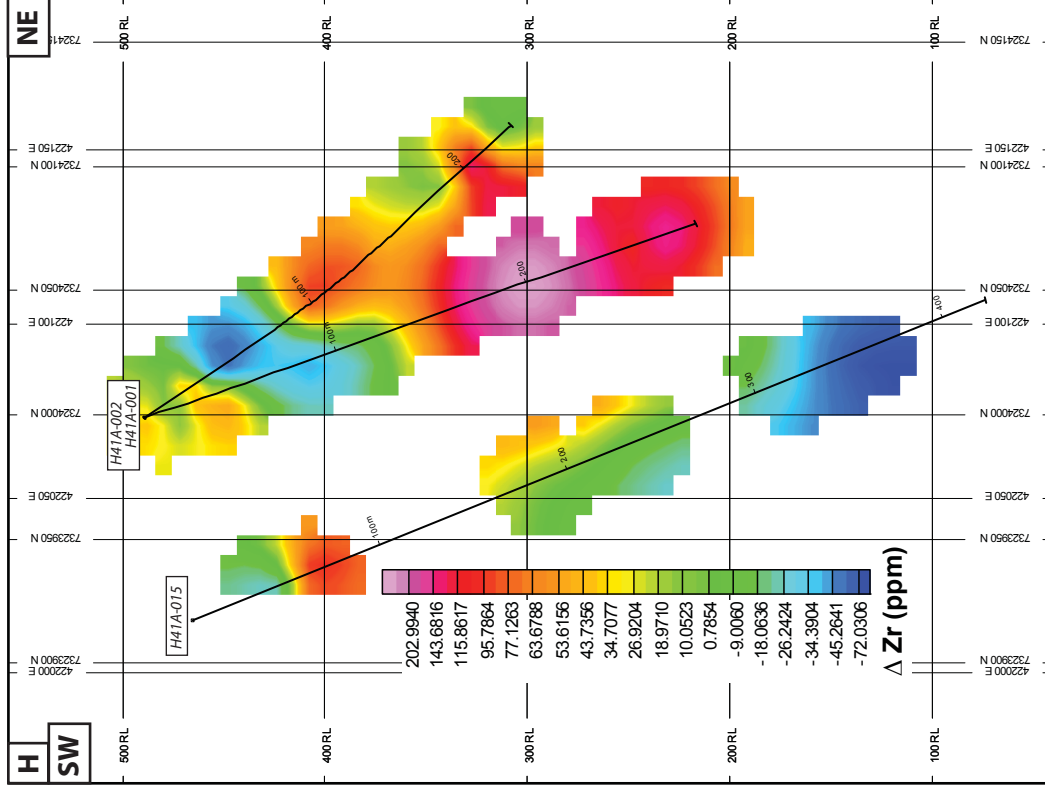
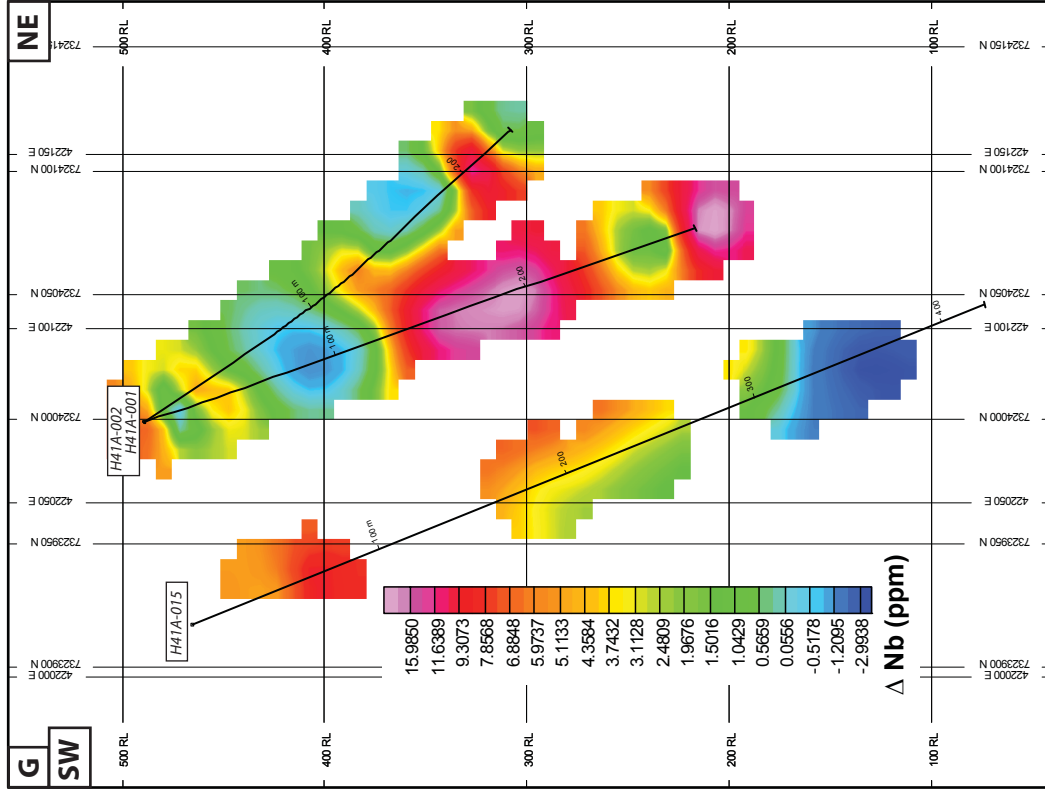


Figure A3-4 (continued): G) Hood 41A cross-section slice through modelling of  $\Delta\text{Nb}$ . H) Hood 41A cross-section slice through modelling of  $\Delta\text{Zr}$ .

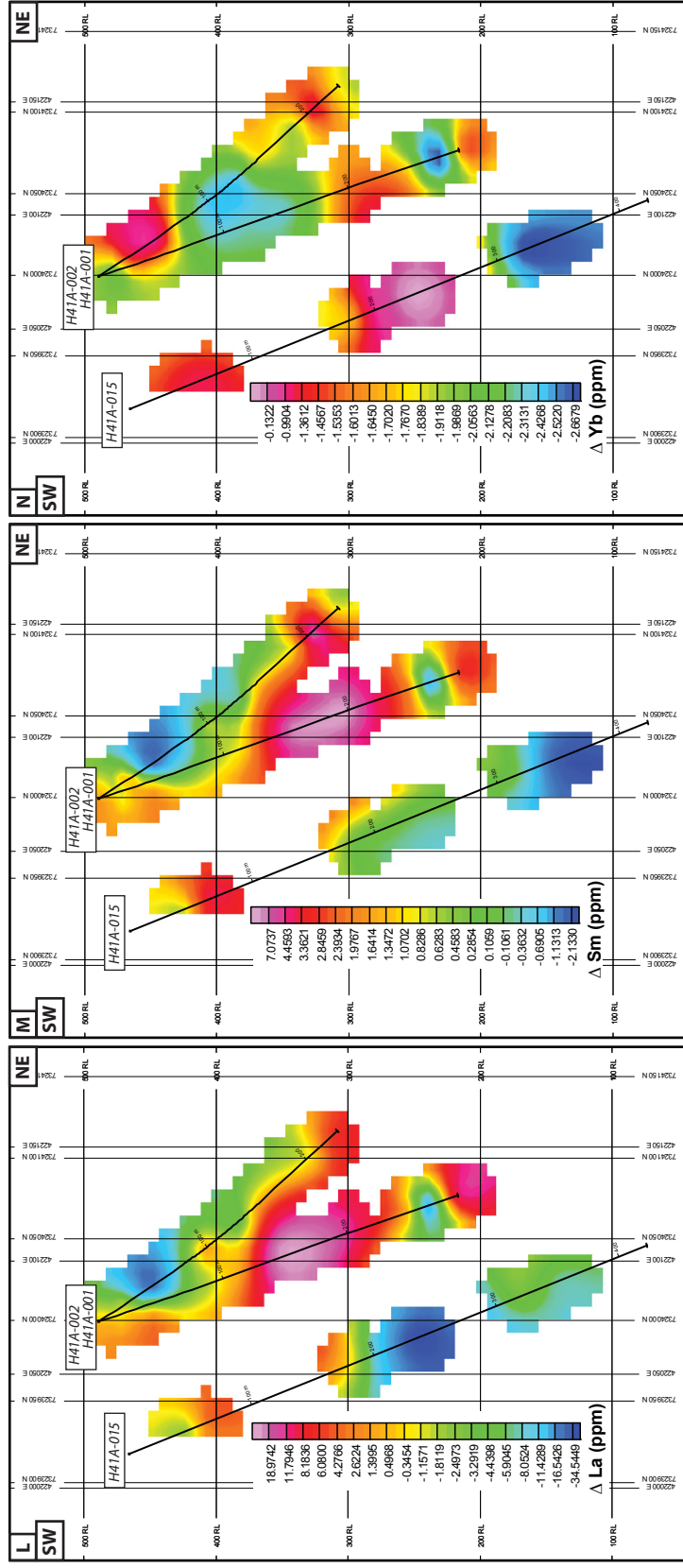


Figure A3-4 (continued): L) Hood 41A cross-section slice through modelling of  $\Delta\text{La}$ . M) Hood 41A cross-section slice through modelling of  $\Delta\text{Sm}$ . N) Hood 41A cross-section slice through modelling of  $\Delta\text{Yb}$ .